Master's thesis

NTNU
Norwegian University of Science and Technology
Faculty of Engineering
Department of Geoscience and Petroleum

Asbjørn Mong

Characterisation of alteration zones in the Skogestad- and Stabben area in the Tellnes deposit

With focus on mineralogic content, types and degree of alteration

Master's thesis in MGEOL - Bedrock and Resource Geology
Supervisor: Kurt Aasly, NTNU
Co-supervisor: Rune Berg-Edland Larsen, NTNU, Åsa E. E. Barstad, Titania AS, Marte Kristine Tøgersen, Titania AS
July 2021

NTNU
Norwegian University of Science and Technology

TITANIA
- a KRONOS Company

Asbjørn Mong

Characterisation of alteration zones in the Skogestad- and Stabben area in the Tellnes deposit

With focus on mineralogic content, types and degree of alteration

Master's thesis in MGEOL - Bedrock and Resource Geology
Supervisor: Kurt Aasly, NTNU
Co-supervisor: Rune Berg-Edland Larsen, NTNU, Åsa E. E. Barstad, Titania AS, Marte Kristine Tøgersen, Titania AS
July 2021

Norwegian University of Science and Technology
Faculty of Engineering
Department of Geoscience and Petroleum

Abstract

The Tellnes deposit is regarded as one of the largest ilmenite deposits in the world. The orebody was detected by aeromagnetic surveying supported by Titania AS in 1954, and the orebody has been mined continuously by Titania AS since 1960. The main produce is an ilmenite concentrate of 44 Wt.% TiO_2, with a magnetite and a sulphide concentrate as by-products. Currently the mixing of ore is primarily based on the amount of TiO_2 and Cr_2O_3, but there is an increasing focus on alteration zones and minerals associated with these zones, as they effect the recovery in the processing plant. In 2008 the open pit at Tellnes was expanded towards the east to include the Skogestad area, revealing new unmapped alteration zones.

Based on previous experiences with reduced recovery when processing altered ore, Titania AS wish to gain increased knowledge of the mineralogy associated with the different alteration zones in the Skogestad- and Stabben area, mapping of degree of alteration from the core zone outwards, and a detailed description of variations between the zones including mineralogy, texture, chemistry, etc.

This thesis presents a detailed study of the alteration zones in the Skogestad- and Stabben area of the Tellnes deposit with focus on mineralogical content, types and degree of alteration for zones and the associated ilmenite. Optical investigation of thin sections, X-ray diffraction, X-ray fluorescence, automated mineralogy and EPMA-analyses have been used to investigate the mineralogical and chemical content of the alteration zones. The study has used samples collected from the mining face of the alteration zones and the analytical data from the investigations have been used to determine the mineralogical and chemical content, variation in mineralogical types and establishment of two classification systems for degree of alteration.

The investigation shows that the alteration zones in the Skogestad- and Stabben area have many similarities with the previously investigated alteration zones in the Tellnes area with the carbonate mineral ankerite being the only new mineral identified. Alteration processes identified in the zones includes sericitisation, saussuritisation, kaolinisation, steatisation, chloritisation, rutilisation, carbonate and quartz precipitation and serpentinisation, indicating a complex alteration history. The lack of evidence for uralitisation and biotitisation is the primary difference compared to the previously investigated zones in the Tellnes area. The classification of the investigated alteration zones with the established classification systems has concluded that 2 out of the 8 alteration zones can be classified as ore of interest for production, while the remaining 6 zones are altered to a state where they no longer are classified as ore. The classification of the samples and zones have found that the degree of alteration is highest in distinct cores/fractures, and gradually decreases when moving outwards from these distinct cores. The alteration zones without such cores have a more stable degree of alteration from zone centres outwards, but the alteration is still of a degree that makes the rock uninteresting for production.

Sammendrag

Tellnes forekomsten regnes som en av de største ilmenitt forekomstene i verden. Forekomsten ble oppdaget ved aeromagnetiske undersøkelser støttet av Titania AS i 1954, og forekomsten har blitt utvunnet av Titania AS siden 1960. Hovedproduktet er et ilmenittkonsentrat med en konsentrasjon på 44 vekt% TiO_2, og sekundærprodukter bestående av et magnetittkonsentrat og et sulfidkonsentrat. Blanding av malm er hovedsakelig basert på mengden TiO_2 og Cr_2O_3, men det er et økende fokus på omvandlingssoner og mineraler assosiert med disse sonene som følge av at de påvirker utvinningen i oppredningsverket. I 2008 ble gruven utvidet østover til å inkludere Skogestad området og nye ukartlagte omvandlingssoner kom frem i dagen.

Basert på de tidligere erfaringene med redusert utvinning ved oppredning av omvandlet malm, ønsker Titania å øke kunnskapen om mineralogien i omvandlingssonene i Skogestad- og Stabben området, kartlegging av omvandlingsgraden fra kjernene i sonene og utover, og en detaljert beskrivelse av variasjoner mellom de ulike sonene. Beskrivelsen ønskes å inkludere mineralogi, teksturer, kjemi, etc.

Denne oppgaven presenterer en detaljert studie av omvandlingssonene i Skogestad- og Stabben området i Tellnes forekomsten og har fokus på mineralinnhold, mineraltyper og grad av omvandling for sonene og den tilhørende ilmenitten. Optisk undersøkelse av tynnslip, X-ray diffraction, X-ray fluorescence, automatisk mineralogi and EPMA-analyser er metoder brukt for å undersøke det mineralogiske og kjemiske innholdet i omvandlingssonene. Stuffprøver fra omvandlingssonene har blitt analysert og dataene har blitt brukt til å avgjøre det mineralogiske og kjemiske innholdet, variasjoner i mineraltyper og etablere to klassifikasjonssystem for grad av omvandling.

Undersøkelsene viser at omvandlingssonene i Skogestad- og Stabben området har mange likheter med de tidligere undersøkte sonene i Tellnes området, hvor bare karbonatmineralet ankeritt ikke er identifisert tidligere. Identifiserte omvandlingsprosesser i sonene inkluderer sericittisering, saussuritisering, kaolonitisering, steatisering, klorittisering, rutilisering, karbonat og kvarts avsetning og serpentinisering, som indikerer en kompleks omvandlingshistorie. Manglende spor etter uralitisering og biotittisering er den store forskjellen mellom de undersøkte sonene og sonene i Tellnes-området. Klassifiseringen av omvandlingssonene med de nyetablerte klassifikasjonssystemene konkluderer med at 2 av de 8 undersøkte sonene kan regnes som malm av produksjonsverdi, mens 6 soner ikke kan regnes som malm som følge av omvandlingen. Graden av omvandling er avgjort å være sterkest i kjernene og synker gradvis når en beveger seg bort fra kjernene. Omvandlingssonene uten utpregede kjerner viser en mer jevn grad av omvandling fra senteret av sonene og utover, men omvandlingen av sonene er fremdeles av en grad hvor sonene klassifiseres som berg som er uinteressant for produksjon.

Acknowledgements

As I now have finished this thesis, I would like to send some gratitude to some of the people that have helped me along the way!

I would start by thanking my supervisor Kurt Aasly, IGP, NTNU. I am very grateful for the help and guidance you have given me throughout this project, and your positivity and calming words when things have not gone to plan. A thanks also goes out to co-supervisor Prof. Rune Berg-Edland Larsen, IGP, NTNU.

I would like to give a special thanks to Titania AS, with co-supervisors Åsa Elisabeth Eide Barstad and Marte Kristine Tøgersen, for providing, funding, and giving me the opportunity to work on this project. A special thanks goes out to Vebjørn Røvde for assisting during the fieldwork. I wish to also thanks the rest of the personnel at Titania for the hospitality and support during my visits.

A special thanks to Torill Sørløkk and Laurentius Tijhus at the Chemical/Mineralogical Laboratory at IGP for helping me during preparation and running of the XRF and XRD analysis, and the many laughs shared during the work.

I would like to thank my fellow students for the many conversations, discussions, laughs, coffees, and hours we have shared together at the study halls at PTS. A special thanks goes out to my four best friends that been there with me throughout the three years in Sogndal and these final two years in Trondheim. Tanja, Sondre, Martin and Solveig, I could not have done this without you, and I am very lucky to have had such good friends around me on this journey. I look forward to seeing you again soon! Finally, I would like to thank my family for the support and encouragement you have given me throughout the years.

Table of contents

List of figures

List of tables

Abbreviations

AM – Automated Mineralogy

Av. – Average

BSE – Backscatter electron

EDS – Energy dispersive X-ray spectroscopy

EPMA – Electron Probe Micro Analyzer

IGP – Department of Geoscience and Petroleum

LOI – Loss on ignition

NTNU – Norwegian University of Science and Technology

PPL – Plane Polarised Light

SEM – Scanning Electron Microscope

St.Dev. – Standard deviation

Wt.% – Weight percent

XRD – X-ray Diffraction

XRF – X-ray Fluorescence

XPL – Crossed Polarized Light

1. Introduction

1.1 Titania AS

Titania AS is a Norwegian mining company, founded in 1902, which is owned by the American company Kronos Worldwide Inc. (Carstens, 2002). Titania AS is one of the world´s largest producers of ilmenite concentrate and operate the Tellnes ore deposit, which is regarded to be one of the most important ilmenite deposits in the world alongside the Lake Tio deposit in Quebec, Canada (Duchesne, 1999). The mining operations are located at Tellnes, close to Hauge i Dalane in Sokndal municipality in Rogaland county, Norway. Titania produces an ilmenite concentrate of 44% TiO_2, and two by-product concentrates of magnetite- and sulphide from the ilmenite norite ore. The products are shipped to markets in Europe and Asia from the nearby Jøssingfjord. The ilmenite concentrate is primarily used as raw material to produce white titanium oxide pigment (Carstens, 2002).

1.2 Motivation

Titania AS produces ilmenite from an ilmenite norite that comprises the ore of the Tellnes deposit. The deposit is part of the Rogaland Anorthosite Province and is situated within the Åna-Sira anorthosite massif. The ore has chemical and mineralogical variations, which can be challenging for the processing plant, resulting in a reduced recovery. Currently the mixing of ore is primarily based on the amount of TiO_2 and Cr_2O_3, but there is an increasing focus on alteration zones and minerals associated with these zones, as they effect the recovery in the processing plant. Structures and fracture systems in the open pit have previously been mapped and alteration is associated with these.

In 2008 the open pit at Tellnes was expanded towards the east to include the Skogestad area. As a result of the expansion new zones of altered ore that had not been mapped in detail was revealed. Alteration zones associated with the Ljoseskar fracture system and parallel zones between the Ljoseskar- and Tellnesvatn fracture systems are especially prominent in the Skogestad area.

Based on previous experiences with reduced recovery when processing altered ore, Titania AS wish to gain increased knowledge of the mineralogy associated with the different alteration zones, mapping of degree of alteration from the core zone outwards, and a detailed description of variations between the zones including mineralogy, texture, chemistry, etc. In addition to this it will be important to create an understanding of how ilmenite is affected by alteration with regards to mineral chemistry, texture, etc. Increased knowledge of the alteration zones with regards to geographic prevalence, chemical- and mineralogical contents and variations, provides a better basis for decision-making, increases the predictability in daily- and future production and may facilitate a better utilisation of the deposit.

1.3 Objectives of the study

This Master project was carried out at NTNU Trondheim in collaboration with Titania AS. The main objective of the project is to map and characterise selected alteration zones in the Tellnes deposit, mainly the zones associated with the Ljoseskar system and parallel zones between the Ljoseskar- and Tellnesvatn systems in the Skogestad area. The mapping will include geographic positioning and prevalence, while the characterisation will provide the chemical- and mineralogical content and variation, and degree of alteration of the different alteration zones and the associated ilmenite. This project has a heavy industrial focus to provide Titania with the desired information about alteration zones in the Tellnes deposit. This results in a very limited focus on geological features such as for example origin of the alteration zones and the minerals within.

The following sub-objectives will be completed to fulfil the main objective:

1. Develop a map that gives an overview of the deposit with respect to alteration zones in the Skogestad area (zones associated with the Ljoseskar system and parallel zones between the Ljoseskar- and Tellnesvatn systems) and the Stabben area, on the hanging wall side of the open pit.

2. Examination of characteristic differences within and between the zones and evaluation of degree of alteration, through characterisation of the mineralogy, chemistry, texture, etc. in the mapped alteration zones. A dataset that later can be incorporated into the map (described in sub-objective 1) will be developed.

3. Characterisation of ilmenite and establishment of a classification system for degree of alteration for ilmenite, based on microscopy-, X-ray diffraction and microprobe analyses.

1.4 Limitations of the study

This project is limited to being a pre-study for future processing- and process mineralogy tests that are to be conducted either at Titania AS or at IGP. Processing- and process mineralogy tests were considered to be a part of the study but were regarded as to extensive for a single thesis. This thesis will provide a basis for the future tests and extra sample materials were collected to ensure that materials that represent the investigated alteration zones are ready for the processing- and process mineralogy tests. This material is stored at Titania AS.

During the thesis work the EPMA analyses became limited due to time constraints and equipment accessibility, and the limited data were considered inadequate for use. This will be mentioned again later in the thesis and further EPMA analyses is added as an annotation for future work.

2. Geological setting

2.1 The Rogaland Anorthosite Province

The Rogaland Anorthosite Province, also called the Rogaland Igneous Province, is an igneous complex situated within an envelope of granulite facies gneisses in the south-western part of the Sveconorwegian orogenic belt in Rogaland-Agder. The province, Figure 1, covers about 1200 km^2 and consists mainly of three anorthositic massifs: the Egersund-Ogna massif, Håland-Helleren massif, and the Åna-Sira massif, and the Bjerkreim-Sokndal layered intrusion (Duchesne, 2001). There are minor units in addition to these four main units: two smaller leuconorite bodies: Hidra massif and Garsaknatt massif (Demaiffe & Hertogen, 1981), multiple jotunitic dykes (Duchesne et al., 1989), multiple Fe-Ti deposits including the Tellnes deposit (Duchesne, 1999), and three acidic intrusions: the Farsund charnockite, the Lyngdal and Kleivan granites (Maijer et al., 1987).

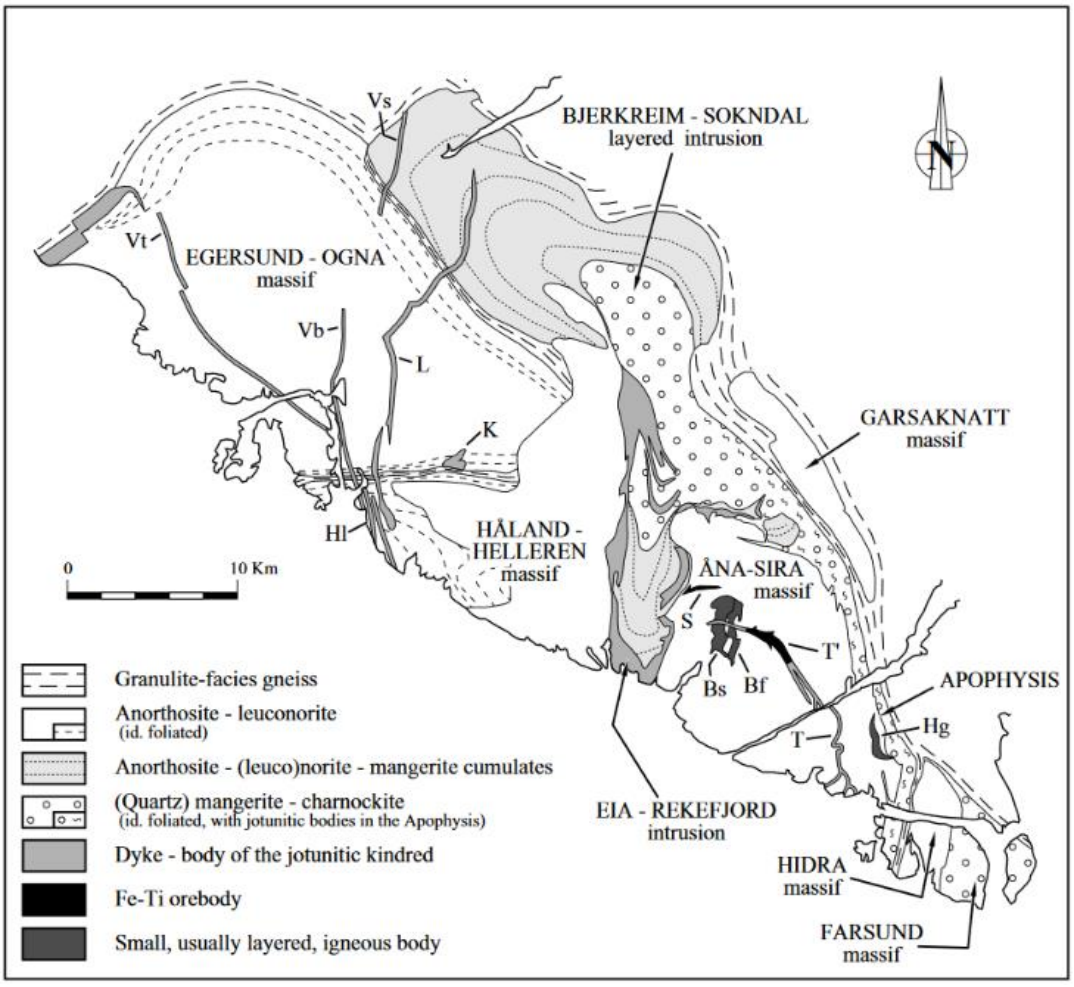

Figure 1: *Geological map of the Rogaland Anorthosite Province as presented in Duchesne (2001). The Egersund dolerite dyke swarm has not been included in the figure. Bf: Pegmatite norite of the Blåfjell deposit, Bs: Bøstølen intrusion, Hg: Hogstad layered intrusion, Hl: Håland dyke, K: Koldal intrusion, L: Lomland dyke, S: Storgangen deposit, T: Tellnes dyke, T´:Tellnes deposit, Vb: Varberg dyke, Vs: Vaersland dyke, Vt: Vettaland dyke, (Duchesne, 2001).*

2.2 The Åna-Sira Massif

Emplaced in the south-eastern part of the Rogaland Anorthosite Province (Figure 1), the Åna-Sira anorthosite massif (Figure 2) covers an area of about 200 km^2 (Krause & Pedall, 1980). The age of emplacement is estimated to 932 ± 3 Ma, by U-Pb dating (Schärer et al., 1996). The massif consists of coarse-grained andesine anorthosite and leuconorite, as well as smaller intrusions and dykes of norite, norite-ilmenite, jotunite, dolerite and mangerite (Krause et al., 1985; Krause & Pedall, 1980; Zeino-Mahmalat & Krause, 1976).

The rock association of the massif follows the temporal sequence: anorthositic-leuconoritic series, noritic series and a mangeritic series (Krause et al., 1985). The main rock is andesine anorthosite, belonging to the anorthositic-leuconoritic series, consisting of more than 90% plagioclase with an average of 45% An (range 39-50%) and 3% Or (range 1-5%) (Zeino-Mahmalat & Krause, 1976). Minor constitutes are orthopyroxene, clinopyroxene, biotite and ilmenite. Accessory minerals are apatite, K-feldspar, quartz, sulphides (pyrrhotite, pyrite, chalcopyrite and covellite) and secondary magnetite. The ilmenite shows several generations of hematite exsolution lamellas (Krause & Pedall, 1980; Zeino-Mahmalat & Krause, 1976).

The noritic series is subdivided based on the spatial relationship to the anorthosite massif of Åna-Sira. The subgroups are named internides, “conjunctive links”, and externides. The internides are located in the western and central area of the Åna-Sira massif and include some of the most significant accumulations of Fe-Ti oxides. In general, the noritic series consists of 53-84% plagioclase with an average of 49 % An (range 45-55%) and approximately 15% orthopyroxene. Minor constitutes include ilmenite, magnetite, clinopyroxene and biotite. Accessory minerals are mainly apatite, spinel, sulphides and graphite (Krause & Pedall, 1980).

The mangeritic series occurs as dikes and stocks that cut the anorthositic-leuconoritic series and the noritic series. The mineralogy is complex with plagioclase varying between 30-55% with an average of 27% An (range 20-50%). Orthopyroxene (range 7-20%) remains as a main constituent while the amount of quartz, K-feldspar and mesoperthite is increased compared to the anorthositic-leuconoritic- and the noritic series. Minor constituents are clinopyroxene, apatite, olivine, zircon, spinel, ilmenite and magnetite, with sulphides as accessories. The deficiency or total lack of amphiboles, muscovite and biotite is characteristic for the series (Krause & Pedall, 1980).

Accumulations of Fe-Ti oxides can be found locally in all the series. However, concentrations that make up deposits of economic value are exclusive to the noritic and mangeritic series and are located in the central and western part of the massif (Krause & Pedall, 1980).

The Åna-Sira massif is structurally characterised as a branchy-anticlinorium which is folded along a non-linear N-S axes. The crest of the massif is domed and is pierced by several sub-intrusions (Krause et al., 1985). This doming of the massif and emplacement of sub-intrusions at the crest are suggested by Krause and Pedall (1980) to be related to vertical movements caused by an autochthonous tectonic development following the regional N-S folding. As the deformation of the Åna-Sira massif progressed, the conditions increasingly favoured brittle deformation. This is demonstrated by the opening of fissures and the formation of the mangeritic internides. The main fractures of the internal sub-intrusions, connected to the main tension from the doming of the massif, are grouped in the crest area of the anticlinorium (Krause & Pedall, 1980).

As previously mentioned, the Åna-Sira massif contains numerous Fe-Ti deposits of both economic and non-economic value. The largest and most significant deposits include the Tellnes-, Storgangen- and Blåfjell deposits (Duchesne, 1999), of which only Tellnes is in operation today (DMF, 2021). These three deposits differ from each other with respect to their geological, petrological and mineralogical aspect (Krause et al., 1985). The Blåfjell deposit is related to a norite pegmatite and the historical ore was dominated by a coarse-grained (2-5 mm) hemoilmenite, which is characterized by two generations of exsolved hematite (Krause & Pedall, 1980; Krause & Zeino-Mahmalat, 1970). The mining operation at Blåfjell occurred in two periods, 1863-1865 and 1869-1876, and the deposit was then regarded as an iron ore. Production reached a total of 100.000 t of raw material which of 90.000 t was exported to England (Carstens, 2002). The Storgangen deposit forms a discordant dyke-system within the massive anorthosite and is foliated concordantly to the anorthosite. The historical ore is a medium-grained ilmenite norite which is massive near the footwall and gets a gradually more pronounced layering of leuconorite and norite toward the hangwall. The main target mineral was ilmenite with exsolved hematite, while titanomagnetite, spinel, sulphides and rutile were accessory opaque minerals (Duchesne, 1999; Krause et al., 1985). The mining operation at Storgangen was conducted by Titania AS and occurred from 1916-1965. An ilmenite concentrate (17-19% TiO_2) and a magnetite concentrate was produced. The total production exceeded more than 10 Mt of concentrate and mainly supplied the pigment industry (Carstens, 2002). The Tellnes deposit is trough shaped and consists of fine-grained ilmenite norite related to a late dyke structure. (Duchesne, 1999; Krause et al., 1985). The mining operation at Tellnes began in 1960 and is still ongoing. The main product is an ilmenite concentrate (44% TiO_2) and approximately 650.000 t is produced annually (Barstad, 2020). Additional products are a magnetite- and a sulphide concentrate (Carstens, 2002).

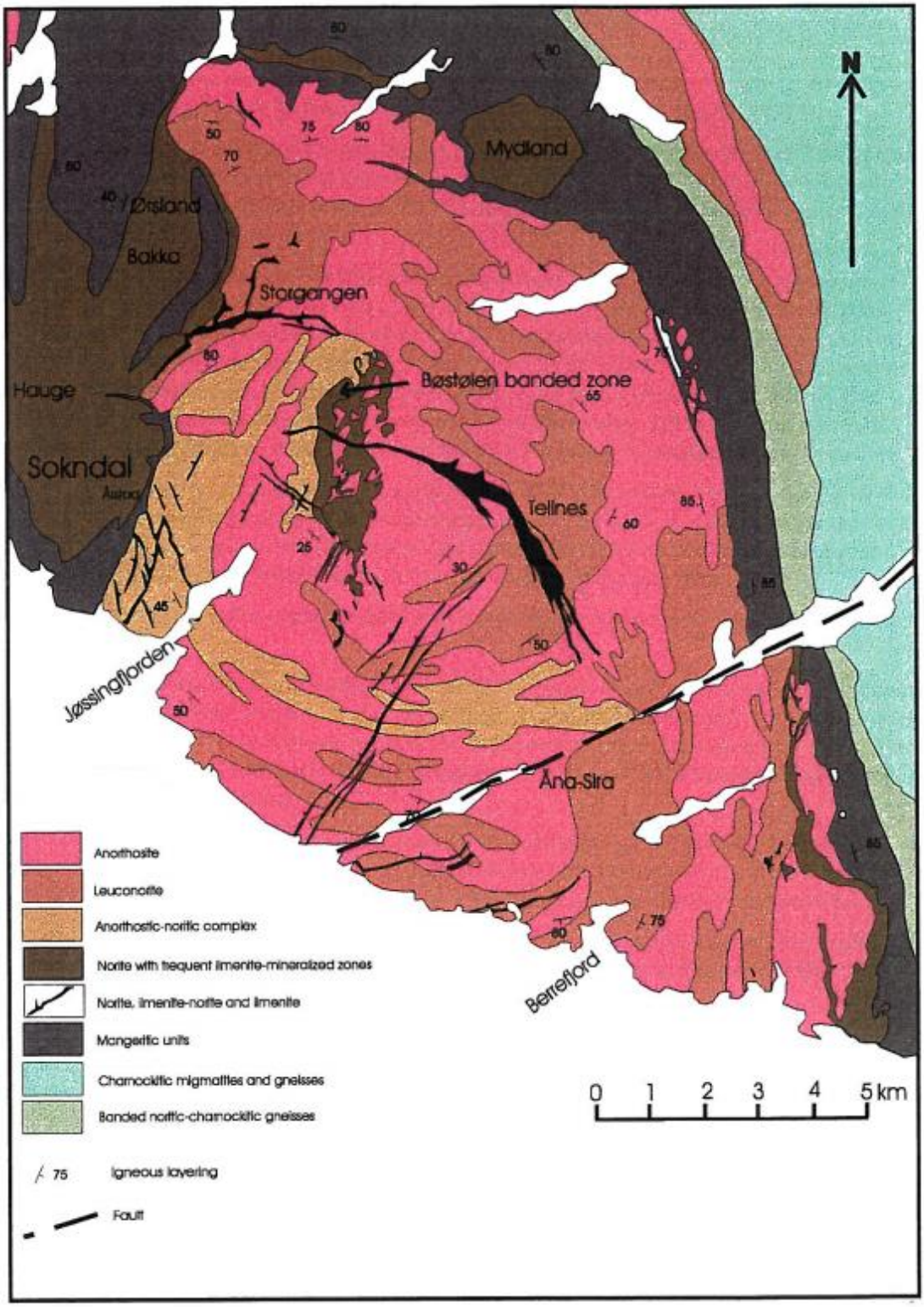

Figure 2: *Geological map of the Åna-Sira Anorthosite Massif, including the Storgangen and Tellnes Fe-Ti deposits. The map is a modified version of the map presented by Krause & Pedall (1980) presented by Karlsen (1997).*

2.3 The Tellnes deposit

2.3.1 The origin of the Tellnes deposit

The Tellnes deposit (Figure 3) is an ilmenite norite orebody, considered to be one of the most important Fe-Ti oxide deposits in the world. It is emplaced in the central part of the Åna-Sira Massif, approximately 4 km NE of Jøssingfjord. It was discovered by an aeromagnetic survey in 1954, which was part of an investigation focused on finding new ilmenite deposits that could supplement and/or replace the Storgangen deposit (Duchesne, 1999; Dybdahl, 1960). Mining operations commenced at Tellnes in 1960 by Titania AS and reserves are at 157 M tons of ore as of December 2020 (Barstad, 2020).

The ilmenite norite in the Tellnes deposit intruded into the Åna-Sira anorthosite. This is evident by sharp contacts, apophyses cutting the anorthosite, xenoliths of anorthosite and intrusive breccias (Gierth & Krause, 1973; Krause et al., 1985). The outcrop has a sickle shape and is oriented WNW-ESE to NNW-SSE, and stretches for more than 2700 m, has a width of more than 400 m in the central part and reaches a depth of at least 60 m below sea level (Dybdahl, 1960). The shape of the deposit is that of a SE-plunging elongated trough (Figure 4), where the NW contact dips 50-45° SW and the opposite contact varies from vertical to a 45° SW dip. The deposit is part of a dyke structure which extends beyond the outcrop on both sides: 4 km to the NW and more than 10 km to the SE (Krause et al., 1985). This dyke structure is referred to as the main dyke or the Tellnes dyke. The composition of the Tellnes dyke ranges from jotunite to quartz mangerite and has a thickness of 5-10 m (Gierth & Krause, 1973; Wilmart et al., 1989). The orebody is intersected by two sub-vertical, WNW-ESE striking, doleritic dikes (Figure 3) (Diot et al., 2003; Krause et al., 1985).

The two main views on the relationship between the Tellnes dyke and Tellnes deposit as well as the origin of emplacement of the deposit are the theory of Wilmart et al. (1989) and the theory of Charlier et al. (2006). Schärer et al. (1996) U-Pb dated the deposit and dyke to 920 ± 3 Ma and 931 ± 5 Ma respectively, indicating a non-comagmatic relationship between the units even though they were emplaced in the same structure. Wilmart et al. (1989), later supported by Diot et al. (2003), argued that due to differences in Sr-isotope ratio the units were non-comagmatic. With regards to the origin of emplacement they argued that the Tellnes deposit was injected into a weakness zone as sorted noritic crystal-mush, lubricated by 3 to 10 % interstitial Fe-Ti rich silicate liquid. The evidence for this origin was textural, geochemical mixing relationships (Wilmart et al., 1989), and magnetic and petrofabric evidence (Diot et al., 2003). Charlier et al. (2006) argued against this noritic cumulate origin and suggested a crystallizing trapped liquid component as the origin of the ilmenite norite. The data collected by Charlier et al. (2006) revealed more complex relationships in major element variation diagrams compared to the simple mixing line presented by Wilmart et al. (1989). Charlier et al. (2006) proposed that the ilmenite norite of the Tellnes deposit crystallized in situ in a magma chamber with a sill-shape and SE dipping floor by fractional crystallisation. The ilmenite norite then injected into the anorthosite under ductile conditions before the sill was deformed in a solid-state, forming the magnetic fabric orientation found by Diot et al. (2003) and the current trough shape of the deposit (Charlier et al., 2006).

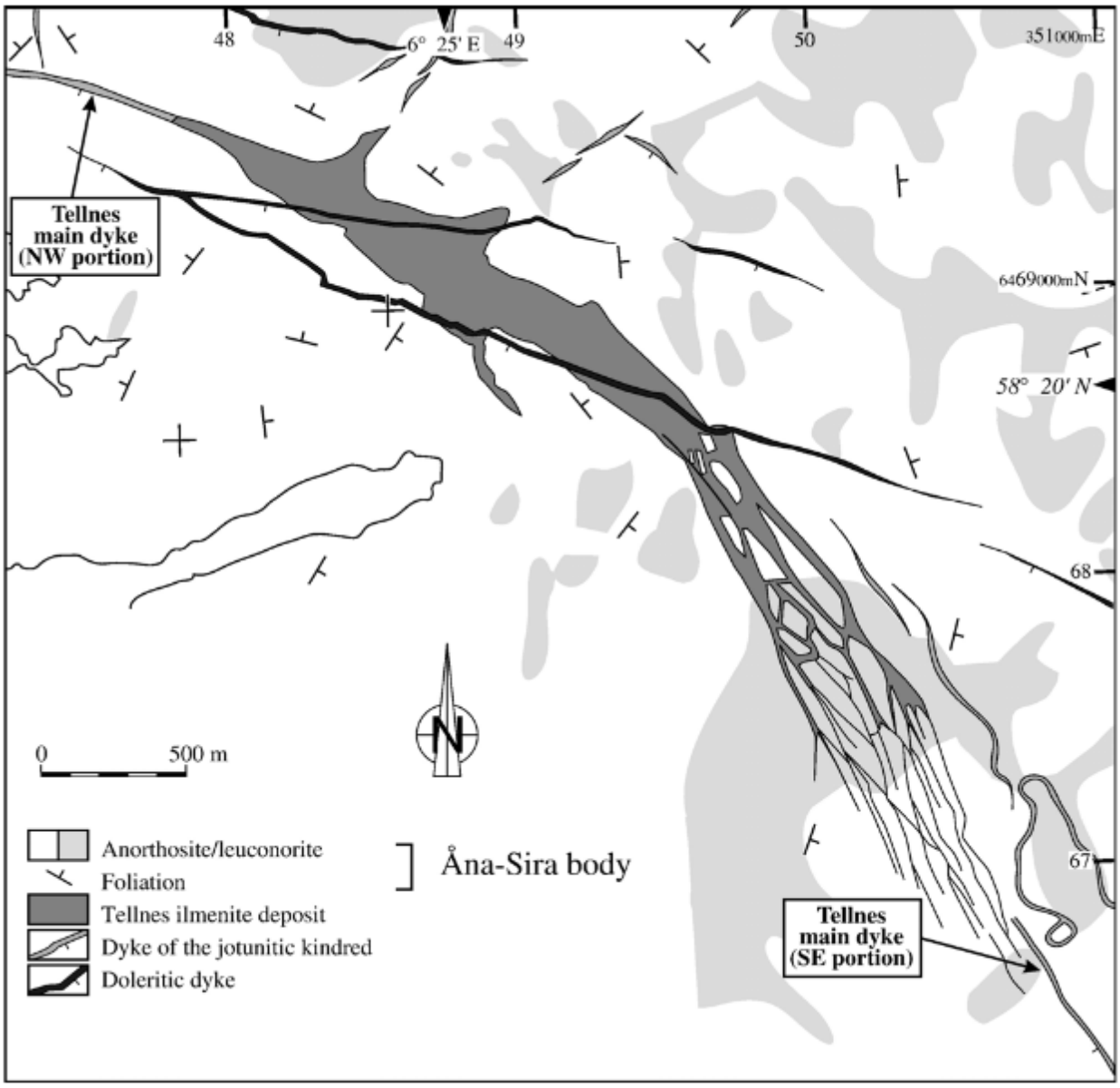

Figure 3: *Geological map of the Tellnes deposit at the level of exposure in 1985. Modified by Charlier et al. (2006) from Krause et al.(1985). The two main doleritic dykes that crosscut the deposit are figured, while minor late faults are not shown.*

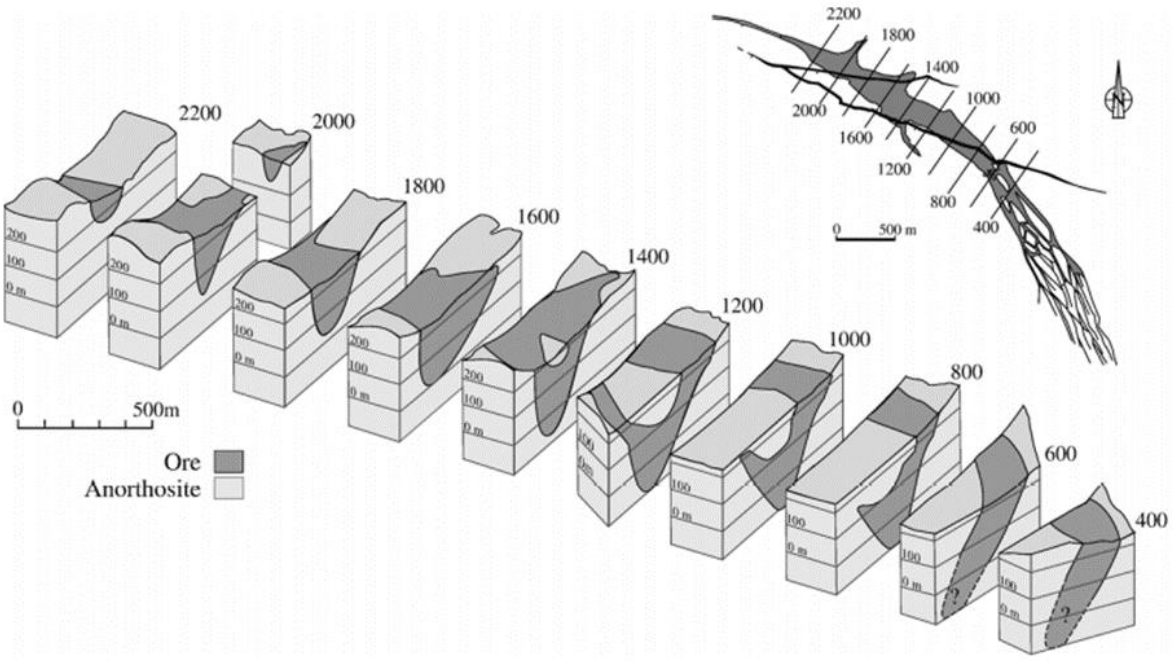

Figure 4: *3D model showing the SE-plunging elongated trough shape of the Tellnes deposit with the level of exposure before mining activity commenced. From Charlier et al. (2006) modified after Diot et al. (2003). The two doleritic dykes that crosscut the deposit are not shown in the model.*

2.3.2 Mineralogy and geochemistry of the Tellnes deposit

The Tellnes orebody is a massive, equigranular, dark coloured, medium- to fine-grained (0,5-2 mm) ilmenite norite, also referred to as ilmenite-rich norite and ilmenonorite, containing an average of approximately 18% TiO_2 (Krause et al., 1985).

The average modal mineral composition of the ore is given by Dybdahl (1960) presented in Table 1:

Table 1: *Average modal composition of the Tellnes ore (Vol.%)(Dybdahl, 1960).*

Mineral	*Vol. %*
Plagioclase	36,0 %
Ilmenite	39,0 %
Orthopyroxene	15,0 %
Biotite	3,5 %
Magnetite	2,0 %
Accessories	3,5 %
Total	100 %

Plagioclase (An_{45-42}) is the most abundant mineral in the ore and is euhedral, commonly slightly bent, locally granulated and medium- to fine-grained (0,5-2 mm) (Charlier et al., 2006; Krause et al., 1985). Very small needles of oxide minerals are commonly found within the plagioclase and some grains does also include larger equant grains of ilmenite (Charlier et al., 2006). The orthopyroxene (En_{77-75}) is abundant in the upper part of the orebody but is present throughout the entire ore (Gierth & Krause, 1973; Krause et al., 1985). Two different crystal habits of orthopyroxene are typically observed in the ore. The first variation is coarse grained, subhedral, prismatic crystals, while the other is a medium to fine grained, sub- to anhedral, tabular crystals (Opsal, 2015). A distinctive feature is the iron-oxide exsolution lamellas found in most of the orthopyroxene in the ore (Eriksen Eia, 2020). The ilmenite contains needle-shaped lenses of hematite and aluminous spinel that have a rather homogenous texture (Krause et al., 1985). Subsolidus grain boundary migration and textural equilibration during deformation and recrystallisation has severely modified the primary texture of the ilmenite. The occurrence of ilmenite is often as interstitial to the main silicate minerals (Charlier et al., 2007). Transformations of ilmenite into rutile or anatase has been observed but is not regarded as extensive (Krause et al., 1985).

The accessory minerals comprise of at least 24 minerals including: clinopyroxene, apatite, augite, olivine, aluminous spinel, hematite, zircon, rutile, baddeleyite and multiple sulphides. The sulphides include pyrite, pentlandite, phyrrhotite. bravoite, chalcopyrite, marcasite, covellite, millerite, violarite and siegenite (Charlier et al., 2006; Charlier et al., 2007; Gierth & Krause, 1973; Krause et al., 1985).

In general, the ore was considered to be fairly uniform with regards to the mineralogy as more than 90% of any ore sample is made up of plagioclase, orthopyroxene and ilmenite, and the lack of modal layering (Schiellerup et al., 2003). The modal proportions of these three minerals are varying considerably, resulting in a chemical zoning across the orebody (Gierth & Krause, 1973; Schiellerup et al., 2003). Included in this chemical zoning is a marginal zone, several meters wide, found along the margin of the deposit. This marginal zone has a lower content of ilmenite and higher amounts of plagioclase and apatite resulting in more leucocratic rocks. A small zone of coarse-grained norite-leuconorite can be observed along the sharp contact to the anorthosite (Gierth & Krause, 1973; Krause et al., 1985).

The chemical content and its variation throughout the orebody were the target of Kullerud (2003, 2005, 2007, 2008) and a sub-target of Charlier et al. (2006). The investigations of Kullerud were focused on two areas of the Tellnes orebody (Figure 7): the Tellnes area, west of profile line 6.0V, comprising the western and central part of the orebody, and the Skogestad area, east of profile line 6.0V, that comprise of the eastern part. The areas are primarily separated due to the advance of the mining operations and geographic location.

The ore beneath the Tellnes area is chemically zoned and reflect the variation in modal mineralogy. Based on these variations Kullerud (2003) divided the ore of the western and central part of the Tellnes orebody into four zones:

1. The upper marginal zone (UMZ)
2. The upper central zone (UCZ)
3. The lower central zone (LCZ)
4. The lower marginal zone (LMZ)

The differentiation of the zones is an approximate as there are a smooth transitions between them (Kullerud, 2003). The investigation of Charlier et al. (2006) analysed more than hundred samples from the three SSW-NNE sections 800, 1200 and 1600 (Figure 5), classified them based on the characteristics of the four zones established by Kullerud (2003) to get an average chemical composition for the four zones. The resulting average chemical compositions for the four zones are presented in Table 2:

Table 2: *Average whole-rock composition for major elements from the four zones of the Tellnes ore deposit (Charlier et al., 2006).*

	LCZ	*LMZ*	*UCZ*	*UMZ*
SiO_2	31,60 %	37,67 %	32,21 %	39,67 %
TiO_2	17,80 %	12,68 %	17,04 %	11,02 %
Al_2O_3	13,89 %	15,07 %	12,07 %	14,81 %
FeO_{tot}	21,18 %	18,01 %	22,51 %	17,32 %
MnO	0,13 %	0,13 %	0,15 %	0,13 %
MgO	4,14 %	4,29 %	6,79 %	5,44 %
CaO	5,21 %	5,91 %	4,49 %	5,81 %
Na_2O	3,86 %	3,99 %	3,20 %	3,90 %
K_2O	0,54 %	0,78 %	0,49 %	0,80 %
P_2O_5	0,29 %	0,46 %	0,25 %	0,39 %
Total	98,64 %	99,00 %	99,19 %	99,29 %

The UMZ is characterised by a high modal content of plagioclase and the Fe-Mg silicates: orthopyroxene, clinopyroxene and olivine, while the content of ilmenite is low. The UCZ is characterised by a high modal content of ilmenite and Fe-Mg silicates and a low plagioclase content. The LCZ is characterised as the most ilmenite rich zone. It is also characterised by the low content of Fe-Mg silicates and an intermediate content of plagioclase. The LMZ is characterised by a gradual decrease in ilmenite content and a simultaneous increase in the content of plagioclase, orthopyroxene and clinopyroxene towards the contact with the anorthosite (Kullerud, 2003).

Based on the findings during the investigations Charlier et al. (2006) concluded that the Tellnes deposit is not homogeneous, as previously believed by Gierth & Krause (1973) among others, and shows systematic variations in the cumulus assemblage.

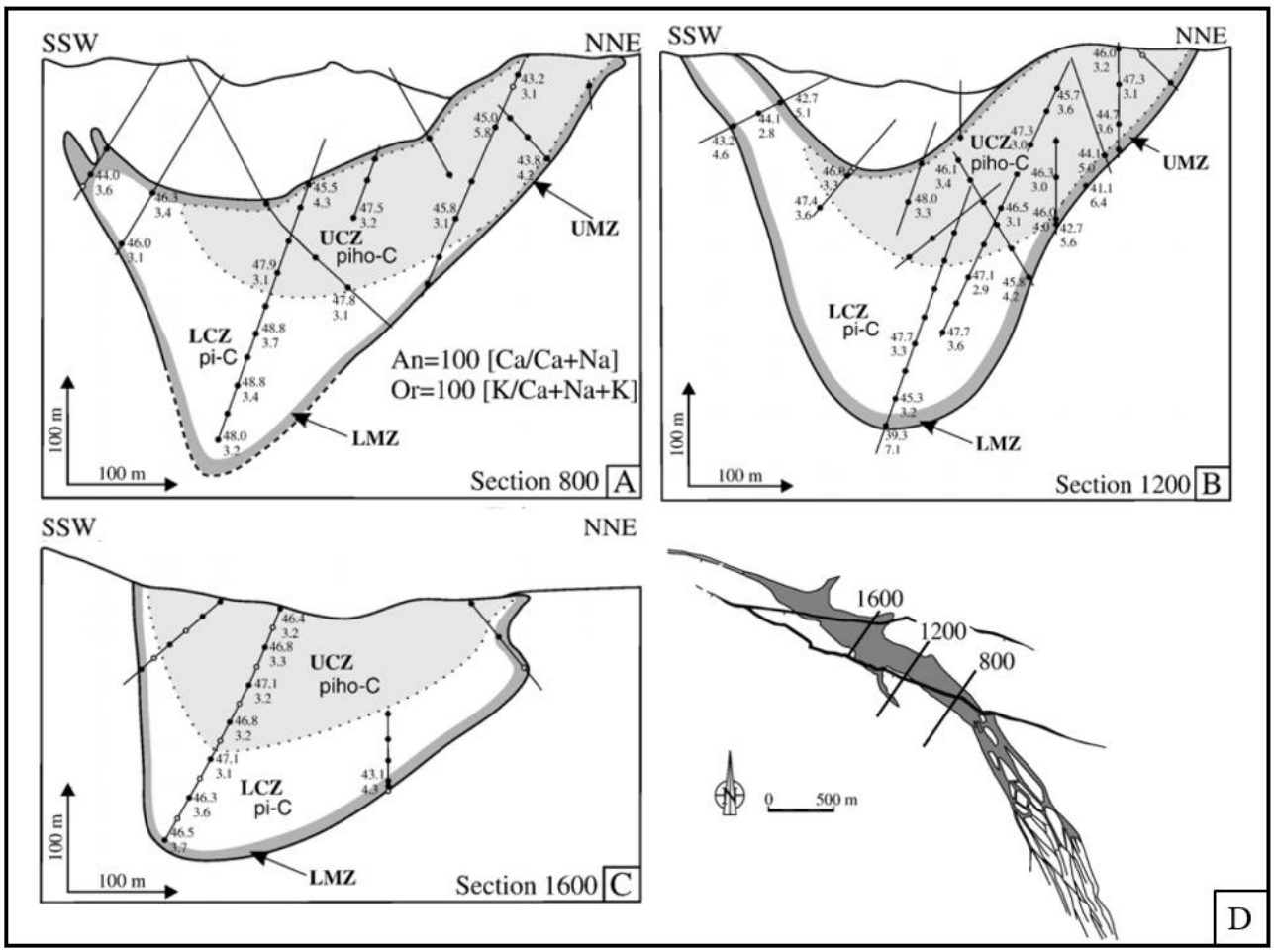

Figure 5: *Cross sections of the Tellnes orebody modified from Charlier et al. (2006). (A-C) The sections 800 (A), 1200 (B), 1600 (C) that vertically cuts the Tellnes orebody and gives an SSW-NNE profile of the orebody. The profiles shows the spatial distribution of the four zones established by Kullerud (2003) based on the results of the investigation of Charlier et al. (2006). The drill cores used to determine the extent of the different zones are figured as lines with numbers that gives the plagioclase composition (An and Or content) in selected samples. UMZ = Upper Marginal Zone, UCZ = Upper Central Zone, LCZ = Lower Central Zone and LMZ = Lower Marginal Zone. (D) Sketch of the Tellnes deposit with the 3 vertical sections, 800, 1200 and 1600 indicated.*

Further data collected between 2003 and spring 2005 presented in Kullerud (2005) supported the decision to separate the western and central part of the Tellnes orebody into 4 zones. Some samples however, from the borderline between the Tellnes- and Skogestad area, showed a distinctly different chemical content compared to the ore beneath the Tellnes area. The ore in the Skogestad area has a lower content of TiO_2 and Cr_2O_3 relative to the FeO compared to the majority of the ore in the Tellnes area (UCZ and LCZ) (Kullerud, 2005, 2007). Based on chemical analysis of 74 drill cores resulting in almost 3300 analysis, Kullerud (2008) provided a classification of the ore in the Skogestad area into 4 types. The classification is based fully on the FeO and TiO_2 content of the ore (Figure 6):

Based on the FeO and TiO_2 content in a sample, a factor F can be calculated:

$$F = TiO_2 / (FeO - 6)$$

The relationship between F and the ore type are as follows:

Type 1:	$F > 1,0$
Type 2:	$0,85 < F < 1,0$
Type 3:	$0,75 < F < 0,85$
Type 4:	$F < 0,75$

Figure 6: *The method developed and used by Kullerud (2008) to determine the ore types in the Skogestad area. Modified from Kullerud (2008).*

Type 1: The chemical composition of this ore type is equivalent to the majority of the ore in the Tellnes area.

Type 2: The ilmenite has a higher amount of MgO than type 1, but a low amount of Cr_2O_3 compared to the majority of the ore in the Tellnes area. Fe-Mg silicates, apatite and magnetite content is high. This type is considered the middle ground between Type 1 and Type 3 and the borders are diffuse.

Type 3: The chemical composition of this ore type is distinctly different than the ore from the Tellnes area. The ilmenite has a high amount of MgO, low amount of Cr_2O_3. The content of magnetite and Fe-Mg silicates is high, while the amount of Ni- and Cu-sulphides is lower.

Type 4: The concentration of TiO_2 is < 13 Wt.% and this ore type is considered to be uninteresting with regards to production.

The occurrence of the ore types within the Skogestad area is not consistent. In the western part of the Skogestad area Type 4 is emplaced at the upper part, followed by Type 3, then 2 and finally Type 1. Towards the east Type 1 is emplaced in both the upper and lower part, with Type 2 and 3 in the middle. The Type 4 is not present at a significant extent towards the east. In summary the Type 2, 3 and 4 have a lower concentration of Al_2O_3, CaO, Na_2O and Sr than Type 1, which is mainly controlled by the plagioclase content. The amount of magnetite is on the other hand generally higher for Type 2, 3 and 4 than Type 1. Most of the samples of Type 2, 3 and 4 have a resemblance to that of the ore from the UMZ (Kullerud, 2008).

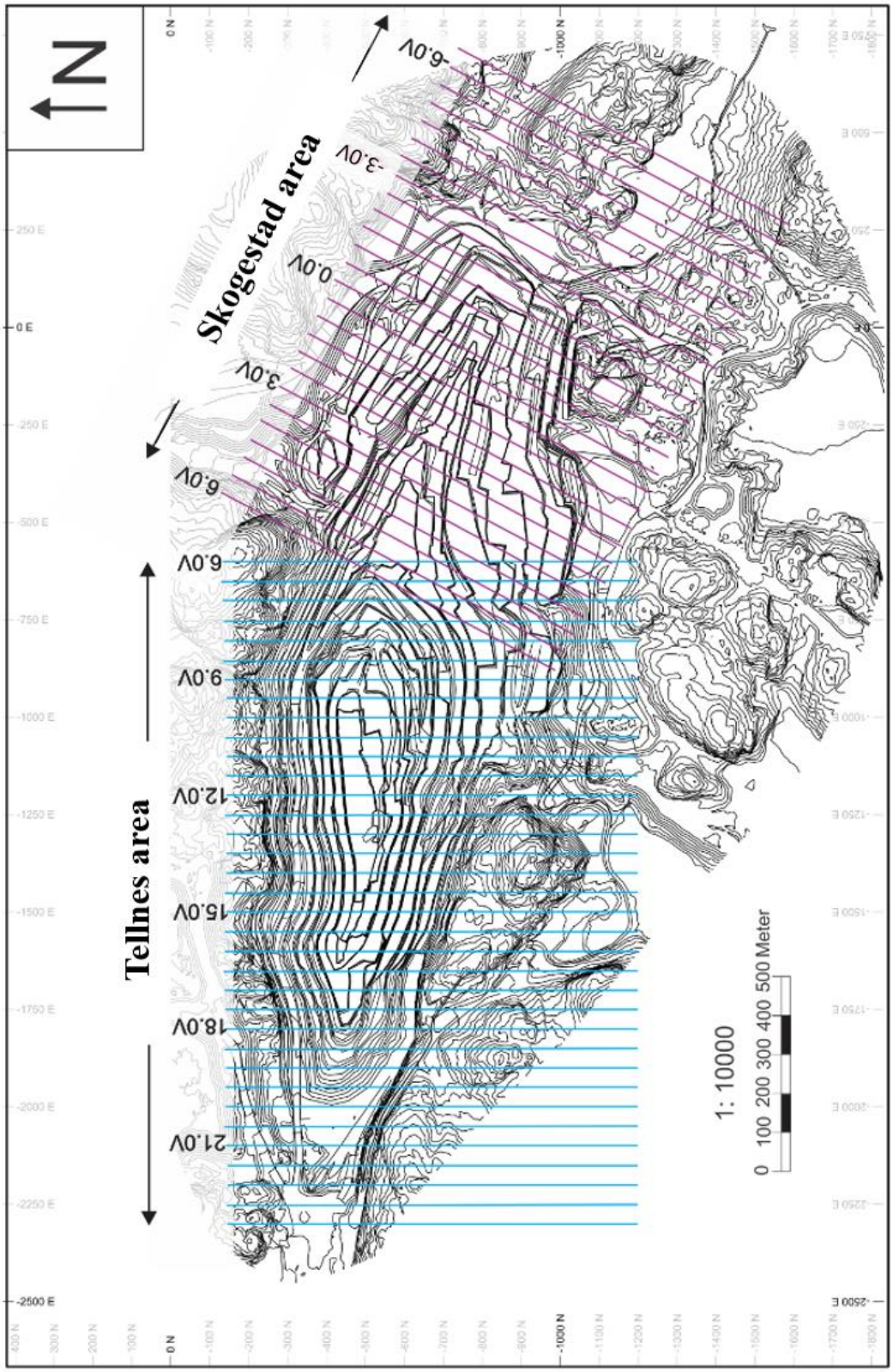

Figure 7: *Map of the open pit at Tellnes. The Tellnes area (Blue lines) stretches from profile line 23.0V to 6.0V, while the Skogestad area (Purple lines) stretches from profile line 6.0V to -6.0V. Modified from Opsal (2015).*

2.3.3 Faults and fracture zones in the Tellnes deposit

Two major faults belonging to a major regional structural trend cut through the orebody: the Tellnesvatn fault, NE-SW trending from Ljosevatn to Tellnesvatn and dips approximately 60° to the NW, and the Hommedal fault, N-S trending and dipping 70° W. The faults have caused a vertical displacement in the order of 80-100 m (Krause et al., 1985; Schenk, 1987). In addition to these two major faults, numerous planar discontinuities occur in the deposit. Some of them are high angle faults with some movement, while others show no signs of movement and are therefore interpreted as fractures. Based on trend plots of the dip directions the general conception is that each of the regional faults are composed of a system of subordinate faults and joints. These faults and joints are generally conjugated or parallel to the main fault direction, but it is usually not possible to designate one main fault plane (Schenk, 1987).

Karlsen (1997) and Karlsen et al. (2000) mapped and characterized lineaments and fracture systems on regional and local scale from aerial photos and field mapping in the open pit. The detailed mapping of the fracture systems was limited to those systems that intersected the open pit in 1996 and 1999, and positional references must therefore be seen against maps of the open pit at that time. Fracture systems outside the pit, during the fieldwork in 1996 and 1999 are interpreted mainly by the lineament mapping (Karlsen, 1997). Karlsen (1997) found that the correlation between the lineament mapping and the fracture mapping was good. As a result, the lineament mapping gives a decent general description of fracture systems outside of the open pit. A general description of the most prominent fracture systems will follow:

- **Åna – Sira fracture system:** The Åna-Sira fracture system is defined by WSW-ENE striking fractures that dip gently (50-65°), most commonly towards the SSE, but also towards the NNW. Some of the fractures are interpreted as faults due to field observations and slickenside striae indicate that the movement is normal. The three major structures that belong to this system are the Tellnesvatn fault (dips NNW), Porsmyra fault (dips SSE) and Leirviken fault (dips SSE). This fracture system is especially common in the south-eastern half of the pit (Karlsen, 1997).

- **Jøssingfjord fracture system:** The Jøssingfjord fracture system is defined by NE-SW to NNE-SSW striking fractures that dip steeply (~75°) towards the SE or NW. The system is abundant in the south-easternmost part of the pit and further SE of the pit. Some of the SE dipping fractures show indications of normal faulting. The Ljoseskard fracture is the major structure and is found SE of the pit together with parallel fractures (Karlsen, 1997). The Ljoseskard fracture was not investigated in detail by Karlsen (1997) and Karlsen et al. (2000) as it was located outside the pit during the fieldwork in 1996 and 1999.

- **Hommedal fracture system:** The Hommedal fracture system is defined by N-S striking fractures that dips almost vertically. The system consists of the most common small-scale structures and fractures in the Tellnes area, and the Hommedal fault is the most distinct structure (Karlsen, 1997).

- **Crusher fracture system:** The Crusher fracture system is defined by NNW-SSE striking fractures that dip gently (45-65°) towards the ENE or WSW. The system is abundant in the south-western part of the pit and has caused stability problems in the area where Titania's old crusher was situated (Karlsen, 1997).

- **Tellnesmyra fracture system:** The Tellnesmyra fracture system is defined by NW-SE striking fractures with gentle dips. The main fracture is the Tellnesmyra fracture which is interpreted to go through the entire ore body. The system is difficult to distinguish from the Crusher- and the WNW-ESE fracture system (Karlsen, 1997).

- **WNW-ESE fracture system:** The system is defined by WNW-ESE striking fractures, that dips both gently towards the SSW (45-70°) and steeply (75-85°) towards the NNE. The gently dipping fractures are the most common and the system occurs frequently S-E of the pit (Karlsen, 1997).

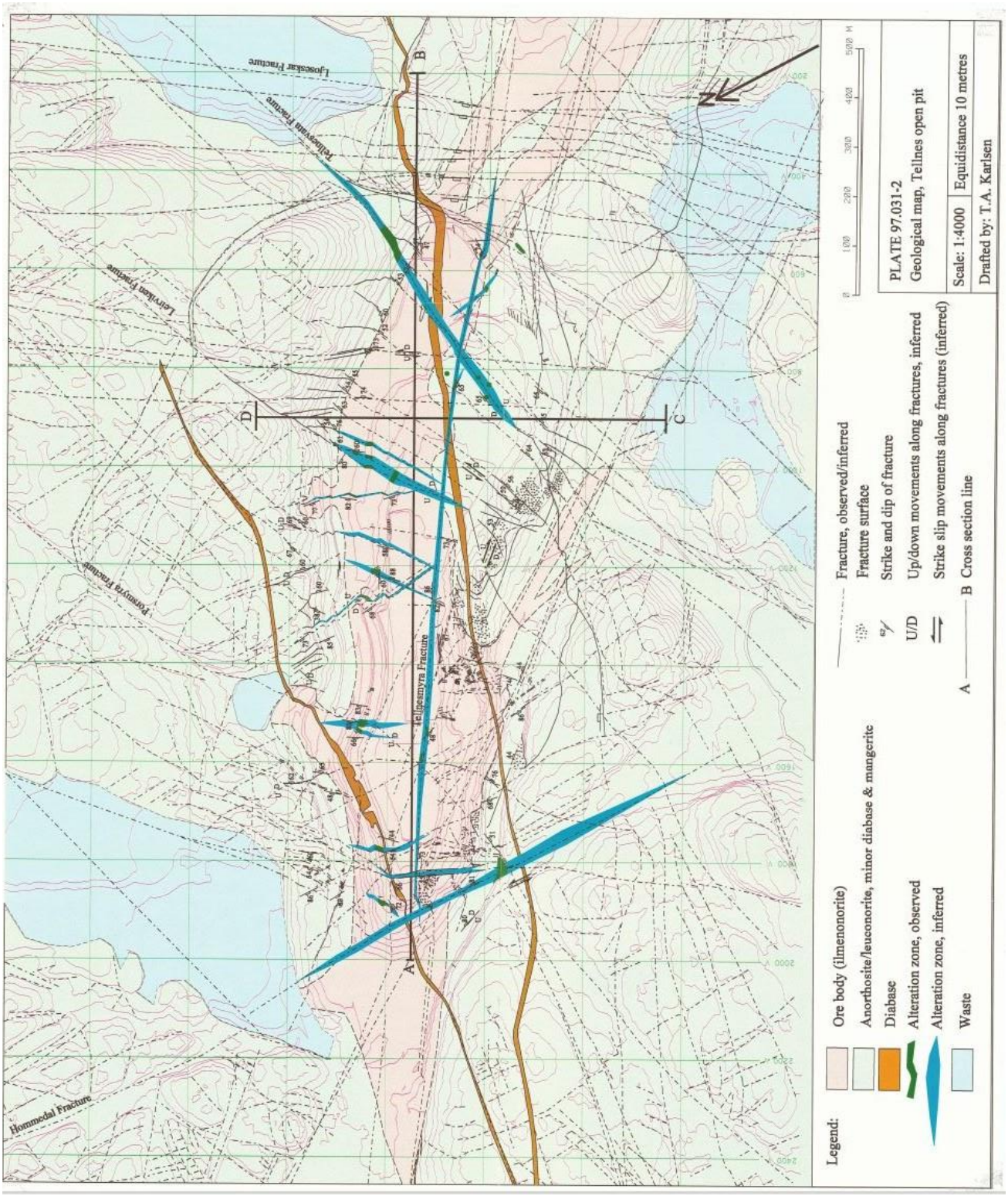

Figure 8: *Geological map showing the major fractures, both observed and inferred, and alteration zones associated with the fractures, both observed and inferred, in the Tellnes deposit from Karlsen (1997). The Ljoseskar fracture, in the eastern part of the map, was interpreted by lineament mapping from aerial photos.*

2.4 Previous studies of alteration in the Tellnes deposit

Alteration has been the primary or secondary target of the studies and investigations of Malvik (1978, 1985), Schenk (1987), Hagen (1995) and Karlsen (1997). Alteration in the Tellnes deposit is related to faults and fractures, section *2.3.3 Faults and fracture zones in the Tellnes deposit*, and appear in both the ore and the surrounding anorthosite.

Malvik (1978) investigated the mineralogical composition of filled joints and zones of weakness related to alteration by XRD. Most of the material was fine grained and ranged from a pale green to dark green colour. The following secondary minerals was identified to be present in the ore: montmorillonite, chlorite, talc, mica, calcite, dolomite and tremolite. Traces of nontronite and an unidentified Mg-Al-silica-hydroxide occurred in a few samples.

Malvik (1985) investigated rutilisation of ilmenite by microscopic investigation. The investigation found that rutilisation normally relates to fractures, but also occurs along and out from grain boundaries and micro cracks in individual grains. In addition to rutile other secondary Ti-phases, one of which was regarded as likely to be anatase, were found in the samples but not identified in detail.

Schenk (1987) investigated the alteration effects on ilmenite-norite along faults and fracture zones by optical microscopy, XRD, XRF and wet chemical methods. The investigation found two critical zones of alteration and a continuous alteration series starting with sericitisation of plagioclase, through alteration of ortho- and later clinopyroxene to complete replacement of ilmenite, plagioclase and pyroxene mainly by carbonates, sericite and rutile. Multiple secondary and accessory minerals were identified including siderite, sericite, albite, zoisite, uralite, olivine, chabazite, natrolite and stilbite.

The results of Malvik (1978, 1985) and Schenk (1987) was compiled and evaluated by Hagen (1995), and summarized into a list of the alteration reactions found in the ore. Furthermore, the list also gives an approximate chronological order for time of reaction:

- Plagioclase alters to epidote (sausseritisation)
- Pyroxene alters to amphibole, uralite (uralitisation)
- Plagioclase alters to fine grained mica (sericitisation)
- Plagioclase and sericite alter to kaolin
- Pyroxene alters to chlorite and talc
- Sulphides dissolves and precipitate as fine-grained adhesions with other secondary minerals
- Altered silica minerals further alter to montmorillonite and other clay minerals
- Carbonates and quartz precipitate as coating in fractures and fissures
- Ilmenite, with hematite lamellas, alters to rutile and magnetite

The secondary minerals have a fine-grained texture, often with intricate adhesion relationships. Commonly the minerals occur as coating in fractures but also in whole rock (Hagen, 1995).

Karlsen (1997) conducted an extensive investigation of the geometry of fractures, fracture zones and lineaments and how they influence the ore quality at Tellnes by field observations, mapping from aerial photos, XRD and, to a very limited degree, optical microscopy. Six types of alteration were observed in the anorthosite, where chloritisation and sericitisation are the two most extensive types. Five types of alteration were observed in the ore including:

- Chloritisation
- Biotitisation
- Carbonate formation
- Sulphide enrichment
- Grain size reduction

A common feature for the observed alteration in the ore is the green colour caused by the high chlorite content. Secondary minerals found in the alteration zones include rutile, talc, epidote, serpentine, carbonates, zeolite, and clay minerals. The types of alteration did not favour any fracture system and all alteration types were found in all the observed systems. The mapped fractures and alteration zones are presented in Figure 8.

3. Theory

3.1 Alteration

3.1.1 Definitions

Autometamorphism is the process of which secondary mineral reactions occur in igneous rocks as they are cooled down, instead of a product of a metamorphic event. The process is distinguished from metamorphism as it is a natural part of igneous cooling. Autometamorphic processes are more commonly found in plutonic rocks as they remain at elevated temperatures for an extended amount of time compared to volcanic rocks (Winter, 2010).

Deuteric alteration is a low temperature magmatic alteration, considered a subset of autometamorphism, which involves hydration, H_2O, either introduced externally or liberated from residual melt (Hékinian, 1982; Winter, 2010). The reactions termed deuteric involve, and is restricted to, changes in primary mineral phases during magmatic crystallisation. The minerals or amorphous compounds are formed where the hydrous fluids interact with the rock, including the interstices of the matrix minerals, lining the walls of veins and/or cavities and in vesicles (Hékinian, 1982).

Metasomatism is a metamorphic process that alter the chemical composition of a solid-state rock or rock portion in a pervasive manner by the introduction and/or removal of chemical components due to interaction between the rock and aqueous fluids (Harlov, 2013).

3.1.2 Types of alteration

Distinguishing minerals that formed during late magmatic reactions, deuteric alteration, from minerals formed by later penetration of fluids in a pre-existing rock may be difficult (Hékinian, 1982). Alteration is therefore often divided into types based on what main mineral(s) the alteration produces. Some of the principal alteration processes are listed below, including those previously found at Tellnes:

- Biotitisation – is the alteration process of which biotite is produced commonly from amphibole (hornblende) or directly from pyroxene. Secondary minerals like epidote may be produced because of the release of Ca^{2+} when the hornblende alters to biotite (Winter, 2010).

- Chloritisation – is the alteration process of which mafic minerals alters to chlorite. The very hydrous phyllosilicate chlorite commonly replaces the less hydrous mafic minerals at low temperatures. Chloritisation is often found along the mineral rims of pyroxene, hornblendes and biotite altering from the rim inwards (Winter, 2010).

- Uralitisation – is the deuteric alteration process of which pyroxene alters to actinolitic amphibole and is commonly a late magmatic alteration process at modest temperatures (Winter, 2010).

- Saussuritisation – is the alteration process of which Ca-rich plagioclase alters to epidote and albite (± calcite and/or sericite). This type of alteration is especially prominent in gabbro and when diabase develops from dolerite. Saussuritisation is often accompanied by both uralisation and chloritisation (Winter, 2010).

- Sericitisation – is the alteration process of which felsic minerals, commonly feldspars, alters to fine-grained, white sericite mica. Sericitisation of plagioclase requires access to K^+ ions and are therefore often associated with chloritisation of biotite which release potassium (Winter, 2010).

- Rutilisation – is the alteration process of which ilmenite alters to rutile by oxidation and leaching of iron from the mineral structure (Temple, 1966).

- Serpentinisation – is the alteration process of which Fe-Mg-silicates in primarily ultramafic rocks such as olivine, amphibole and pyroxene alters to serpentine ± magnetite (Pinti, 2011).

- Steatisation – is the hydrothermal alteration process of which mafic minerals such as pyroxene, serpentine and amphibole alter to talc in the presence of CO_2 and water (Nesse, 2012b; Strekeisen, n.d-b). Is also known as talc carbonation (Strekeisen, n.d-b).

3.2 Ilmenite

3.2.1 General

Ilmenite is a black, ferrous titanite mineral, $FeTiO_3$, often occurring as an accessory mineral in a broad variety of both igneous and metamorphic rocks. The occurrence is often as separate grains or as exsolved lamellae in magnetite. Larger concentrations of ilmenite are typically associated with magmatic bodies of gabbro, norite, anorthosite and mafic and ultramafic rocks related to these, but also in detrital sands. Ilmenite is the most important ore mineral for extraction of titanium either metallic or as an oxide, TiO_2, used in a wide range of products and industries (Nesse, 2012a).

Compositionally the ideal chemical composition of ilmenite is $FeTiO_3$. The composition can still often depart from this by containing variable amounts of manganese or magnesium, which are trace elements that substitute for iron while in a complete solid solution. The result is two solid solution series that exist between ilmenite ($FeTiO_3$) and geikielite ($MgTiO_3$) and pyrophanite ($MnTiO_3$). At high temperatures a third solid solution series between ilmenite and hematite (Fe_2O_3) exist and naturally occurring ilmenite often include hematite exsolution lamellas (King, n.d).

3.2.2 Alteration of ilmenite

The alteration of ilmenite is an important subject due to its, often negative, effect on the pigment processing from TiO_2 concentrates. The alteration of ilmenite involves the process of oxidation and leaching of iron from the mineral structure (Temple, 1966). The investigations of Temple (1966), Gray & Reid (1975) and Mücke & Bhadra Chaudhuri (1991) found that the ilmenite alteration series is a continuous reaction series where ilmenite alter to rutile or leucoxene, a mixture of primarily rutile and anatase, through pseudorutile. The following reaction series was established by Mücke & Bhadra Chaudhuri (1991) (Figure 9).

$$6Fe^{2+}TiO_3 + 3H_2O + 1.5O_2 \longrightarrow 2Fe_2^{3+}Ti_3O_9 + 2Fe(OH)_3 \quad (1)$$

$$Fe_2^{3+}Ti_3O_9 + 3H_2O \longrightarrow Fe^{3+}Ti_3O_6(OH)_3 + Fe(OH)_3 \quad (2)$$

$$Fe^{3+}Ti_3O_6(OH)_3 \longrightarrow 3TiO_2 + Fe(OH)_3 \quad (3)$$

Figure 9: *The continuous reaction series established by Mücke & Bhadra Chaudhuri (1991) where ilmenite alters to rutile or leucoxene through pseudorutile. (1) Alteration of ilmenite to pseudorutile by oxidation and leaching. (2) Alteration of pseudorutile to leucoxene by leaching and hydrolysis. (3) Alteration of leucoxene to rutile by disintegration and dehydration.*

This model of which Fe is completely oxidized and partly removed from the crystal lattice by diffusion is the accepted model for alteration of ilmenite (Gray & Reid, 1975; Mücke & Bhadra Chaudhuri, 1991; Temple, 1966).

The experimental study of ilmenite alteration in high pH conditions and hydrochloric acid, conducted by Janssen et al. (2010) found indications that implied a direct replacement of pure ilmenite by rutile without any intermediate reaction product. The study showed that the rutile precipitated as an inwardly moving reaction front in ilmenite with a finger-like alteration structure at a scale of hundreds of µm, similar to the structures found in naturally weathered ilmenite. The alteration mechanism was determined to be a dissolution-reprecipitation process rather than a solid-state diffusion mechanism (Janssen et al., 2010). As ilmenite often occur with hematite exsolution lamellas in nature, Wengorsch et al. (2019) tried the same experiment as Janssen et al. (2010) with ilmenite with hematite exsolution lamellas instead of pure ilmenite. The resulting alteration of ilmenite with hematite exsolution lamellas by rutile also occurred by a dissolution-reprecipitation process. The texture and extent of alteration differed as the finger -like texture and the extent of alteration was limited to ~100 µm. The conclusion was that the hematite might have a negative impact on the alteration of ilmenite by rutile as the hematite limits the change in porosity and therefore limits the area of interaction between the fluid and the ilmenite (Wengorsch et al., 2019).

3.2.3 Ilmenite alteration in other deposits than Tellnes

The Lac Tio orebody is a massive hemo-ilmenite deposit with an average ore composition of 70 Wt.% ilmenite and 30 Wt.% hematite. The other minerals identified in the deposit are all regarded as accessory or trace minerals and include magnetite, rutile and anatase, among others. The rutile in the Lac Tio orebody mainly occur near the main faults found in the orebody. Investigations of polished thin sections indicate that rutile invade the hemo-ilmenite crystals along borders zones of spinel grains. Anatase is, like rutile, present only in trace amounts in the orebody. The microscopic examination of the anatase found that it preferentially occurs along cracks and twin planes and confirmed it to be an alteration product of ilmenite. Both the rutile and anatase is often found in association with secondary magnetite and the anatase is always surrounded by an iron rich rim. The hematite lamellas in the ilmenite remain untouched during the alteration from ilmenite to anatase. No local concentrations of rutile and anatase grains were found to be important as the quantities are too small to have a noticeable influence on the TiO_2 content (Bergeron, 1980).

The Manavalakurichi beach placer has ilmenite as the predominant mineral, grade of 24 % in the raw sand, and ilmenite alteration products rutile, up to 8 %, and leucoxene, ~1%. The ilmenite in the beach placer is gradually converted to leucoxene and pseudorutile under oxidising conditions leaving an enriched residue of TiO_2 and SiO_2, among others. This results in the formation of porous grains of ilmenite where the pores may remain open or get filled with secondary minerals that affect their quality/grade. EPMA data indicate a solid solution between ilmenite, pyrophanite and geikielite, and alteration that leads to a loss of FeO, MnO and ZnO while causing an enrichment of TiO_2, MgO, Al_2O_3, Cr_2O_3, SiO_2, K_2O, V_2O_5, BaO, CaO, and Na_2O. The alteration of the ilmenite is proposed to be caused by exogenic processes after it was released from the parent rocks. The study further indicated a non-uniform alteration of ilmenite (Bhaskar et al., 2005).

3.3 Norite

3.3.1 General

Norite is a mafic igneous rock, commonly coarse grained, consisting mainly of calcic plagioclase and orthopyroxene. Norite is termed a gabbroic rock as it is closely related to gabbro both when it comes to appearance and occurrence, and may be essentially indistinguishable when viewed as hand specimens (Streckeisen, 1974; Strekeisen, n.d-a). The two rock types are classified, and therefore separated, based on the dominant type of pyroxene in the rock, orthopyroxene in norite and clinopyroxene in gabbro, see Figure 10 (Streckeisen, 1974). The occurrence of norite include a wide range of settings from oceanic crust and ophiolites, to layered mafic intrusions such as the Bushveld Complex, to impact melt sheets such as the Sudbury Complex (Pedro et al., 2020).

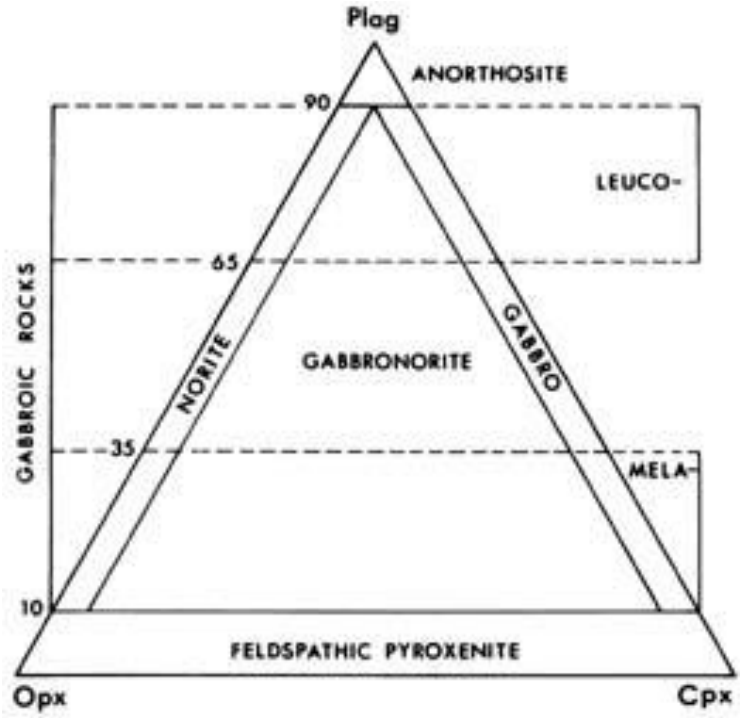

Figure 10: *The schematic classification of gabbroic rocks after Streckeisen (1974). The dominant pyroxene type determines the classification between norite and gabbro. Plag = Plagioclase, Opx = Orthopyroxene and Cpx = Clinopyroxene.*

3.3.2 Alteration of norite

In norite a wide range of alteration can occur based on the primary minerals and further alteration of the secondary alteration minerals. The types of alteration found in norite include the alteration types presented earlier, *2.4 Previous studies of alteration in the Tellnes deposit* and *3.1.2 Types of alteration*, and are found in other complexes with gabbroitic rocks like in The Sudbury Igneous Complex (Oliver, 1951), The Archan Mayurbhanj Mafic Complex (Bhattacharjee & Mondal, 2021) and The Lac Des Iles Palladium Deposit (Boudreau et al., 2014).

The Sudbury Igneous Complex located in Ontario, Canada, is regarded as one of the world's most important nickel deposits. The norite here is affected by uralitisation of pyroxene, which is widespread, and saussuritisation of plagioclase which is less common. Evidence of serpentinisation of olivine is also found in the Sudbury norite but is not regarded as extensive compared to the uralitisation and saussuritisation (Oliver, 1951).

The Archan Mayurbhanj Mafic Complex in Singhbhum Craton, India, consists of gabbroic rocks and multiple types of alteration have been identified. Among the identified alteration types are uralitisation of pyroxene, sericitisation of plagioclase and some small amounts of biotitisation and chloritisation (Bhattacharjee & Mondal, 2021).

The Lac Des Iles Palladium Deposit in Ontario, Canada has extensive alteration as all rocks show some degree of alteration. Orthopyroxene is altered to talc and amphibolite caused by uralitisation. The alteration of plagioclase ranges from the moderate sericitisation, through saussuritisation (epidote), to strongly altered plagioclase where an almost complete replacement by chloritisation occurs (Boudreau et al., 2014).

3.4 Analytical methods

3.4.1 X-ray diffraction (XRD)

X-ray diffraction analysis is a method that is based on the diffraction of X-rays caused by the interaction with a crystal lattice resulting in an X-ray diffraction pattern. By analysing the X-ray diffraction pattern, information about the crystal parameters of the sample, such as the lattice parameter, the crystallographic axis direction, the shape of unit cells, and the dislocation density (Kovalev et al., 2017). When analysing minerals, X-ray powder diffraction is often used as it is a rapid method used for phase identification of crystalline materials and can therefore determine an average bulk mineral composition of a finely grained, homogenised material (Dutrow & Clark, n.d.).

The X-ray diffractometers are compiled of three main elements: an X-ray tube, a sample holder and an X-ray detector. The X-rays are generated by heating a filament in a cathode ray tube to produce electrons, that are accelerated towards a target material by applying a voltage. The bombardment of the target material with electrons will dislodge the inner shell electrons in the target material, producing characteristic X-ray spectra. The X-ray spectra from the target material is subsequently filtered, by foils or a crystal monochromator, to produce monochromatic X-rays that are required for diffraction. The monochromatic X-rays are collimated and directed at the sample material. While the X-rays are directed at the sample material, the sample and detector are rotated to record the intensity of the reflected X-rays. The sample is set to rotate in the path of the collimated X-ray beam at an angle θ while the detector rotates at an angle of 2θ (Dutrow & Clark, n.d.).

An important part of the X-ray diffractometers is the target material of which the X-rays are generated. The material used should be compatible to the sample composition to insure a diffractogram of good quality. The most commonly applied material is copper, but this can lead to difficulties and/or misinterpretation of phase identification when analysing minerals containing Fe. The cause of this is a high background signal caused by fluorescence and is especially prominent in combination with low peak intensity. These difficulties can be solved by using cobalt as the target material. The cobalt with its lower fluorescence has a superior high peak to noise ratio that leads to high quality diffractograms and an unambiguous phase identification (Mos et al., 2018). A secondary factor that affects the peak to noise ratio is absorption. Samples with high content of Fe/Co will strongly absorb and fluorescence when exposed to copper radiation, while samples that contain high amounts of Mn/Ti/Ca will strongly absorb and fluorescence when exposed to cobalt radiation. The absorption cease diffraction resulting in a lower diffraction peak intensity and subsequent lower peak to noise ratio (Proto, 2021).

3.4.2 Automated Mineralogy (AM)

Automated mineralogy, often referred to as AM or SEM-AM, is a scanning electron microscopy (SEM) based analytical tool designed for the characterisation of ores and mineral processing products. All SEM based AM systems are a combination of a hardware platform, a specific image analysis and a processing software. The hardware platform, the SEM, requires a high vacuum operation mode with a pressure range in the order of 10^{-5} to 10^{-7} Pa. The automated measurements also require an electron beam with a long-term stability. Tungsten cathodes or field emission guns are therefore recommended as electron sources. The AM firstly measures, collects, and assesses backscattered electron (BSE) images to subsequently direct the steering of the electron beam for energy dispersive X-ray spectroscopy (EDS) for the various AM measurement routines. The measured EDS spectra is then classified up against a list of approved reference EDS spectra (Bernhard et al., 2020).

The principal AM measurement routines include the following (Bernhard et al., 2020):

1. Point counting modal analysis
2. Particle analysis
3. Sparse phase search
4. EDS spectral mapping

The point counting modal analysis provides an estimation of the modal contents of the different phases in the analysed sample but lacks further information about the particle geometry and properties. The particle analysis is used for quantification of the modal mineralogy, calculated assay, sizes and geometries of particles and grains. The routine also allows quantification of associations and liberation of particles with a differing chemical composition. The sparse phase search finds rare phases in the sample like small grains of gold and platinum group minerals which would be highly time-consuming in a manual search. The EDS spectral mapping routine provides information about intra-particle details, chemical zonation, and phase relationships in particles. The measurement routines are applied and combined in different analysis modes that varies from software to software based on the target of the analysis (Bernhard et al., 2020).

4. Materials and methods

4.1 Materials

The materials used for this study consists of hand specimen samples collected from 8 localities found on bench level 155, 170, 180 and 200 on the hangingwall side of the open pit at Tellnes (Figure 12). A total of 29 primary samples were collected from the 8 localities, and the number of samples collected from each locality is presented in Table 3. All samples were marked with a designation code containing the following information:

- Initials of sampler
- Area of the open pit
- Side of the open pit
- The bench level of the locality
- Location number to separate localities on same bench level
- Sample number at location to separate samples from same location

An example of the designation code is presented in Figure 11:

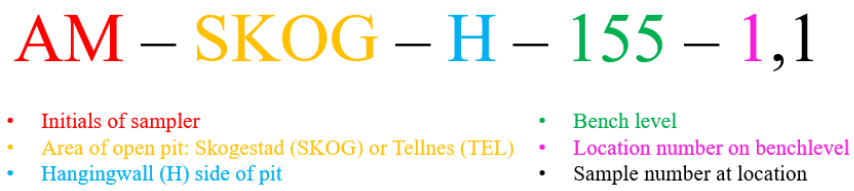

Figure 11: *Example of the designation code used during sampling. Red = Initials of sampler, Yellow = Area of sample location, Blue = Side of pit, Green = Bench level of sample locality, Pink = Location number on given bench level, Black = sample number at location.*

The designation code is shortened to only include bench level, location number and sample number when mentioned for easier reading.

Table 3: *The number of samples collected from each field locality.*

Field locality	***Number of samples***
AM-SKOG-H-155-1	6
AM-SKOG-H-170-1	2
AM-SKOG-H-170-2	2
AM-SKOG-H-170-3	3
AM-SKOG-H-185-1	3
AM-SKOG-H-185-2	4
AM-SKOG-H-200-1	4
AM-TEL-H-155-2	5

As a result of production- and time limitations a maximum of 24 thin sections could be produced for this study. A priority list (Table 4) was therefore made at Titania, based on the field locality descriptions and the appearance of the collected samples, before the samples were sent to NTNU Trondheim. After arriving at NTNU, 2 of the 29 primary samples were split resulting in a total of 31 samples and one change to the priority list.

The 24 highest prioritised samples, Batch 1 and Batch 2, were prepared thin section production by marking a section of the hand specimen. The samples were then delivered to the personnel at the Thin Section Laboratory at IGP which produced 24 polished thin sections.

Table 4: *Sample priority list for thin section production.*

Priority list for thin section production		
Batch 1	**Batch 2**	**Batch X**
AM-SKOG-H-170-2,1	AM-SKOG-H-200-1,2-2 *	AM-SKOG-H-170-1,1-1 **
AM-SKOG-H-170-2,2	AM-SKOG-H-185-2,1	AM-SKOG-H-170-1,1-2 **
AM-SKOG-H-170-3,1	AM-SKOG-H-185-2,2	AM-SKOG-H-155-1,6
AM-SKOG-H-185-1,1	AM-SKOG-H-185-2,3	AM-SKOG-H-170-1,2
AM-SKOG-H-185-1,2	AM-SKOG-H-185-2,4	AM-SKOG-H-155-1,4
AM-SKOG-H-185-1,3	AM-SKOG-H-170-3,2	AM-SKOG-H-155-1,3
AM-SKOG-H-200-1,1	AM-SKOG-H-170-3,3	AM-SKOG-H-155-1,5
AM-SKOG-H-200-1,2-1 *	AM-TEL-H-155-2,1	
AM-SKOG-H-200-1,3	AM-TEL-H-155-2,2	
AM-SKOG-H-200-1,4	AM-TEL-H-155-2,3	
AM-SKOG-H-155-1,1	AM-TEL-H-155-2,4	
AM-SKOG-H-155-1,2	AM-TEL-H-155-2,5	

** Sample AM-SKOG-H-200-1,2 was split into two sub-samples when prepared for thin section production.*

*** Sample AM-SKOG-H-170-1,1 was split into two sub-samples when prepared for XRD/XRF.*

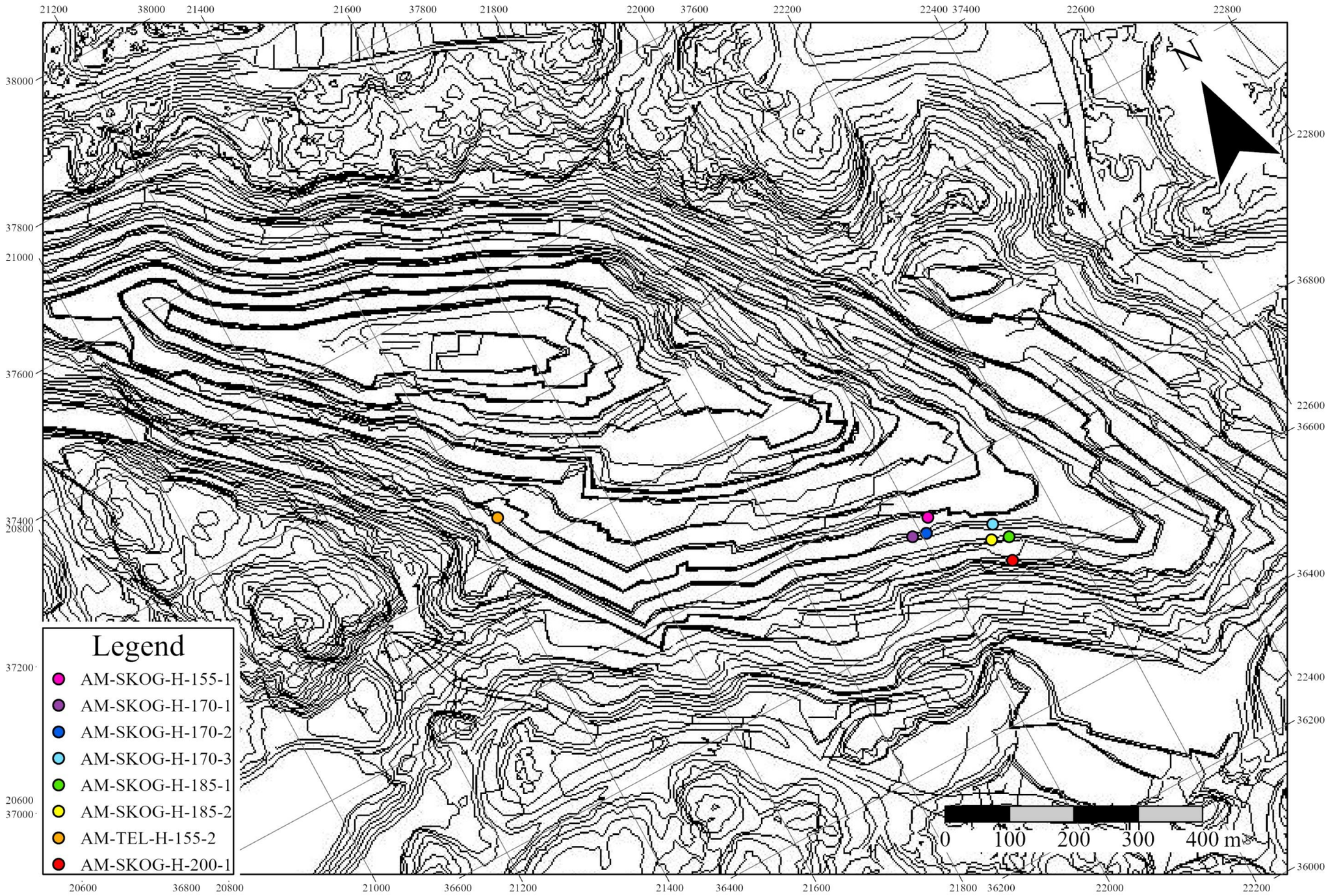

Figure 12: *Map of the localities in open pit. The topography is that of the open pit during the fieldwork.*

4.2 Methods

4.2.1 Fieldwork and sampling

Fieldwork was conducted in the open pit mine at Tellnes during August and September 2020. As the mine would be in production for most of the fieldwork, the mine was visited to limit the extent of the field area, get an initial impression of the amount of alteration zones and the availability of the bench levels of the mine. Based on the observations and future production plans the field area was limited to only include the hanging wall side of the mine and the bench levels 200, 185, 170 and 155. The name of a bench is based on the height above sea-level.

The fieldwork consisted of identifying alteration zones, describing the appearance of the identified alteration zones, extracting samples and registering the locations with GNSS. The sample locations were registered with a Leica Viva GS14 GNSS RTK Rover and a Leica Viva CS15 Controller with an accuracy of 5 cm. Sampling consisted of extracting hand specimens, representative of the sample location, from the mining face with a geological hammer. More than one hand specimen was extracted for each sample.

4.2.2 Preparation of materials for XRD and XRF

The first stage of preparation for XRD and XRF is equal for both analytical methods and includes crushing and grinding of the hand specimens down to μm-scale. For the samples in Batch X a hand specimen was taken to the preparation stage, while for the samples in Batch 1 and 2 the remains of the hand specimen after thin section production were taken to preparation for XRD and XRF. All tools used in the preparation were cleaned thoroughly before a new sample was introduced to the stage to prevent contamination.

Coarse crushing was conducted with sledgehammer at the Coarse Crushing Laboratory at IGP. The hand specimens were placed on the wooden surface in the designated sledgehammer area and then repeatedly hit with the sledgehammer until the fractionations reach a grain size of <50 mm.

Fine crushing was conducted with a RETCH Jaw Crusher BB 100 at the Fine Crushing Laboratory at IGP. All samples went through 3 stages of crushing in the jaw crusher, with a gradually smaller gap width between the crushing arms, resulting in a gradual grain size reduction. During the last stage of crushing the crushing arms touch each other, making a distinctive sound, and reach a grain size of <5 mm.

Sample splitting was conducted with a RETSCH PT8 Sample Divider and a feeder driven by an AEG KF 1-2 vibrator at the Preparation Laboratory at IGP. The splitting of the samples had two purposes: getting at least two parallel samples and reduce the sample sizes to match the requirements of the equipment at the next preparation stage. At least two parallel samples were needed as one sample was to be analysed at the Chemical/Mineralogical Laboratory at IGP and one at the laboratory at Titania. Each bulk sample is put into the feeder, which was put to feeding speed 4 out of 10, to get a steady flow of material and a low risk of jamming the entrance to the sample divider. The bulk sample is then divided into 8 parallel samples where each sample has a composition that correspond to the original bulk sample. 1 sample was then put

into a small plastic bag and was then weighed. Further sample preparation requires at least 40 g of sample material, and if the sample weighed less than 42 g (plastic bag = 1,8-2 g) another parallel sample was put into the plastic bag. The bag was then marked as the IGP bag and the same procedure was done for another bag marked as the Titania bag. The IGP bags were taken to the grinding stage while the Titania bags were sent for transport to Titania.

Grinding was conducted with a RETSCH Vibratory Disc Mill RS 200 at the Fine Crushing Laboratory at IGP. The grinding tools consisted of a tungsten carbide chamber and disc. The grinding jar has a capacity of 50 ml. Samples that still exceeded this capacity limit after the previous splitting was split once more with a standard splitting tool (minimum 40 g after splitting). The sample is put into the chamber together with the grinding disc, the chamber is sealed and placed into the disc mill. The disc mill is then set to 1200 rpm and grinding time of 90 sec. The chamber is then opened to evaluate if additional grinding is required. This is done by taking some material and rub it between two fingers. If individual grains can be sensed, the chamber is sealed, and grinding commences for an additional 30 sec. After grinding the grain size will be <30 μm. A more accurate grain size estimation cannot be done without a grain distribution analysis which was regarded as unnecessary.

4.2.3 Optical microscopy

The 24 polished thin sections were studied in both transmitted and reflected light using a Leica DM750P polarizing microscope, at the student microscopy lab at IGP at NTNU, a Nikon OPTIHOT – POL polarizing microscope, at the laboratory at Titania, and a Nikon Eclipse E600 polarizing microscope fitted with the Spot 5.3 programme for photography of minerals in the sections, at the microscopy lab at IGP at NTNU.

Examination of isotropic and anisotropic minerals was done in transmitted light applying both plane- (PPL) and cross polarization (XPL) while the opaque minerals were examined in reflected light. The examination was focused on mineral identification, observation and description of mineral associations, textures, and microstructures. The thin section descriptions were essential when selecting thin sections for AM- and EPMA-analyses. Thin section descriptions can be found in Appendix E.

All the thin sections were scanned in PPL, XPL and reflected light, using an Olympus BX51 microscope equipped with an Olympus UC90 camera and controlled by the Olympus Stream software. The scans were used to determine modal mineralogy and support the thin section examination and preparation for EPMA-analyses. The thin section scans can be found in Appendix A.

4.2.4 X-ray diffraction (XRD) at IGP

Preparation for XRD was conducted at the Chemical/Mineralogical Laboratory at IGP. All equipment was cleaned thoroughly before preparing a new sample to prevent contamination.

The preparation for XRD starts with a rounding and grain size reduction stage. A spoonful of sample material and 10 ml of ethanol is put into a container with 48 cylindrical agate grinding elements. The container is placed into a a McCrone Micronizing Mill and grinding commences for 2 minutes to get rounded grains. The sample material, now rounded and with < ~10 µm grain size, is then poured into a petri dish and the grinding elements and container is sprayed with ethanol over the petri dish to obtain as much of the sample material as possible. The petri dish is then placed into a MEMMERT 2 heating cabinet at 60°C until all the ethanol has evaporated (minimum of ~ 4 hours). This procedure is repeated for all the samples. After the ethanol has evaporated, the sample material is put into sample holders. The surface of the samples is smoothed out with a glass plate to increase the accuracy of the analysis. The sample holders are marked with the journal number and the samples are analysed with a BRUKER D8 ADVANCE Series II X-ray Diffractometer. The diffractometer is equipped with a cobalt target material and uses X-rays with a wavelength of 1,79 Å during the analysis. During the analysis, the sample and detector is rotating from 3 - 80° (2θ) with a step size of 0,01° analysing for 0,6 s/step size.

4.2.5 X-ray fluorescence (XRF) at IGP

Preparation for XRF was conducted at the Chemical/Mineralogical Laboratory at IGP and is separate for main- and trace element analysis. All equipment was cleaned thoroughly before preparing a new sample to prevent contamination.

Preparation for XRF main element analysis consists of making the sample materials (<30 µm) into glass pellets. The first stage of preparation is an LOI test where 2,5 g ± 0,0002 g of sample material is placed into pre-weighed ceramic crucibles. The crucibles are subsequently placed into a desiccator and burnt at 1000°C for 60 minutes in a Nabertherm Muffle B180 Furnace. The crucibles are then weighed, the LOI is calculated, and the sample material is placed into glass containers. The second stage of preparation follows where 5,0000 g ± 0,0002 g of flux, lithium tetraborate/metaborate (66/34) and 0,5 g ± 0,0002 g of sample material is put into platina/gold (95/5) crucibles. All the weighing procedures conducted during these two preparation stages are done with a Mettler Toledo AG285 Analytical Scale. The platina/gold crucibles are placed on a MU-XRF-Mixer for 5 seconds to mix the flux and sample material before 120 µl of lithium iodide is put into each crucible. The crucibles are subsequently placed into a Malvern Panalytical Claisse TheOX Advanced where the samples are melted at 1050°C for 20 minutes. After the 20 minutes the melt is poured into the lid of the crucible where is solidifies to a glass pellet. The glass pellets are then marked with their designated journal number, are removed from the lid with a suction cup and placed into holders. The glass pellets are then analysed with a Malvern Panalytical Zetium Minerals Edition XRF machine equipped with a rhodium target material. The method/setup when analysing trace elements at IGP is the WROXI, quantitative method for main element analysis, developed and distributed by Malvern Panalytical.

Preparation for XRF trace element analysis consists of making the sample materials (<30 µm) of each sample into powder pellets. The crushed sample material is stirred, and 9,6 g of material is placed into a mixing container with 2,4 g of Licowax and a Polamide 9 mm mixing ball. The sample material and wax are weighed using an Ohaus Scout Pro Balance SP202 scale. The mixing container is placed into a MU-XRF-Mixer where the sample is mixed for minimum 2 minutes at intensity level 7/10. After mixing the mixing ball is removed with forceps. The mixed sample is then pressed into powder pellets with a Herzog TP40/2D Manual Pellet Press under a load of 200 kN for minimum 2 minutes. The pellets are then marked with their designated journal number and analysed with a Malvern Panalytical Zetium Minerals Edition XRF machine equipped with a rhodium target material. The method/setup when analysing trace elements at IGP is the Pro-Trace, quantitative method for trace element analysis, developed and distributed by Malvern Panalytical.

4.2.6 X-ray diffraction (XRD) and x-ray fluorescence (XRF) at TITANIA

At Titania the samples were prepared in accordance with the methods used by Titania when analysing whole rock samples from the daily operation. This includes the following:

- Fine crushing of samples with Herzog HP-MA automatic pulverizing mill with pre-set programs that crush the samples for both XRF and XRD for 70 seconds. Before fine crushing the XRF samples, two Holger Hartman PE190 grinding aid pellets are added to each sample container to aid in the grinding and act as binder during pellet pressing.
- Pressing of powder pellets in steel rings for XRF-analysis using a Herzog HTP 40 Semi-automatic Pellet Press under a load of 200 kN.
- Manual pressing of powder pellets for XRD-analysis.

The XRD-analysis was conducted with a BRUKER D4 Endeavor, series number: 206791, equipped with a copper target material. The software used is Bruker Diffrac plus.

The XRF-analysis was conducted with a Panalytical Axios Max advanced, series number: DY5112, equipped with a rhodium target material. The software used is Panalytical SuperQ 5.3.

4.2.7 Automated mineralogy (AM)

Automated mineralogy (AM) was conducted at the Microscopy Laboratory at IGP using a Zeiss Sigma 300 field emission SEM, equipped with the Mineralogic software from Zeiss. AM was conducted on 7 thin sections: 170-3,1, 170-3,2, 170-3,3, 200-1,1, 200-1,2-1, 200-1,3 and 200-1,4. The AM was used to identify and map mineral phases with more precision than what is possible by optical microscopy.

The sections were coated with carbon using a Cressington 208C carbon coater to increase the conductive ability. Increasing the conductive ability is done to avoid charging the thin sections which can affect the measured data. A layer of carbon with a thickness of 15-20 nm are applied to each of the thin sections.

When investigating the samples, an accelerating voltage of 20 kV was used at a working distance of 8,5 mm and 120 µm aperture. The sections were mapped with a resolution of 20 µm with an 89,3X magnification. Two smaller areas of section 170-3,1 were mapped with a resolution of 2 µm with an 223X magnification.

4.2.8 Electron Probe Micro Analysis (EPMA)

Electron Probe Micro Analysis (EPMA) were performed at the Microscopy Laboratory at IGP using a JEOL JXF-8530F PLUS Hyper Probe with a Schottky-type field emitter. The analysis aims to get high precision quantitative chemical analyses of selected minerals in 3 thin sections: 155-1,1, 155-1,2 and 200-1,1. The minerals selected for analysis are ilmenite, talc, and serpentine.

The sections were coated with carbon using a Cressington 208C carbon coater to increase the conductive ability. Increasing the conductive ability is done to avoid charging the thin sections which can affect the measured data. A layer of carbon with a thickness of 15-20 nm are applied to each of the thin sections.

Ilmenite was analysed with a beam current of 20 nA, an acceleration voltage of 15 kV and a defocused beam diameter of 1 µm. The reference materials used to determine the chemical composition included diopside (Mg), sanidine (Al), hematite (Fe), willemite (Mn), rutile (Ti) pentlandite (Ni) and pure metal references (Co, V, Cr and Zn).

Talc and serpentine were analysed with a beam current of 20 nA, an acceleration voltage of 15 kV and a defocused beam diameter of 1 µm. The reference materials used to determine the chemical composition included albite (Na, Al), diopside (Mg, Ca), fluorite (F), sanidine (Si, K), hematite (Fe), willemite (Mn), rutile (Ti), tugtupite (Cl), pentlandite (Ni), chromite (Cr) and pure metal reference (Zn).

5. Results

5.1 Appearance of alteration zones in the open pit

5.1.1 Alteration zones in the Skogestad area

5.1.1.1 AM-SKOG-H-155-1

Alteration zone 155-1 (Figure 13) is a ~15 m wide, near vertical zone of alteration that transect the height of the bench. The zone is dominated by 4 distinct, water-conducting, fractures filled with heavily fractured material. The rock masses between the four distinct fractures are massive, with few fractures that decrease in frequency when moving away from main fractures. At the edges of the formation green slickensides are visible, but no signs of movement were recorded at the 4 main fractures.

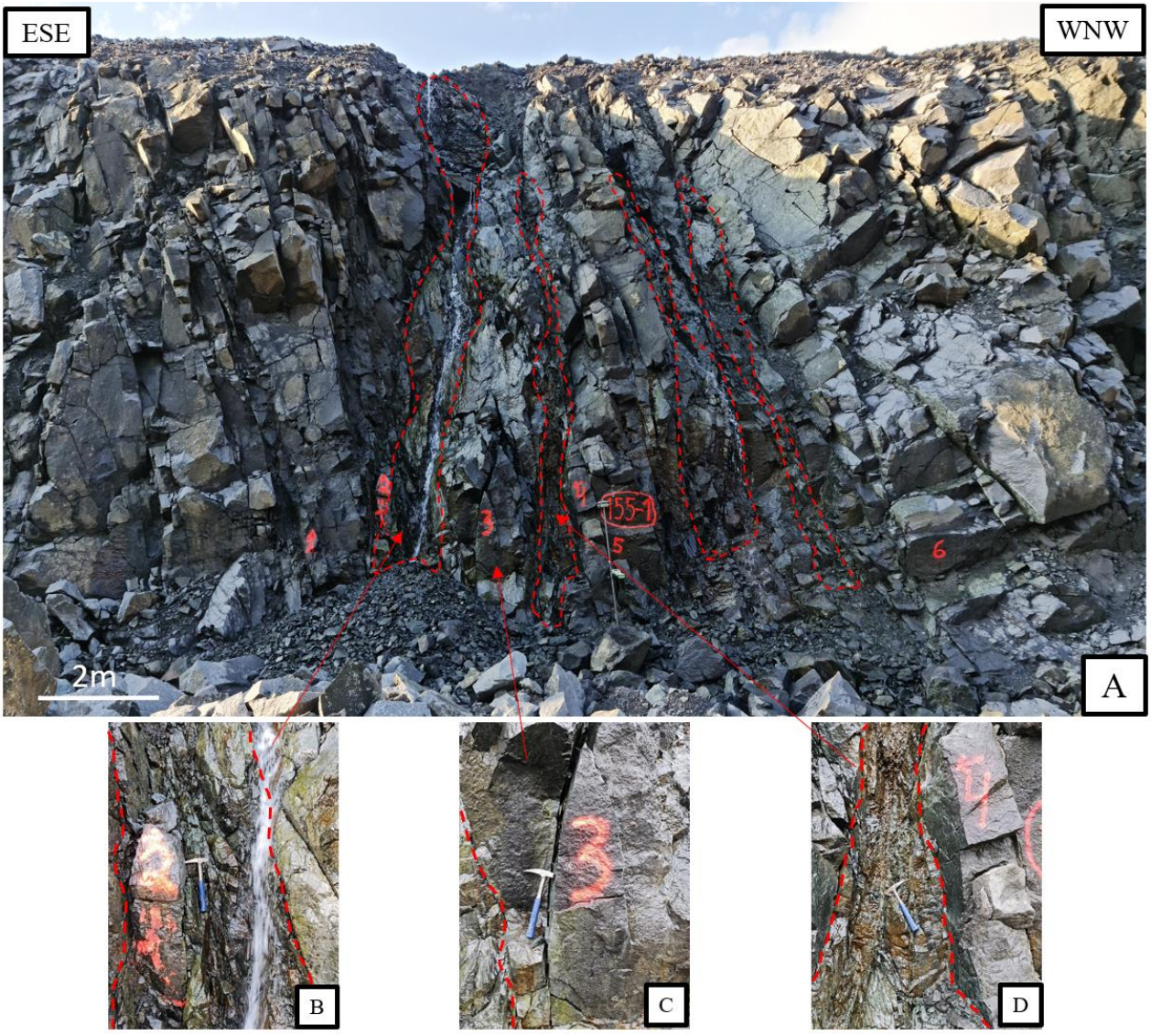

Figure 13: *Appearance of alteration zone 155-1. (A) Alteration zone 155-1 with the four distinct fractures (within stippled, red lines) that transect the bench height. (B) The distinct fracture at 155-1,2 (within stippled, red lines) is heavily fractured, a stream of water runs in and along the fractured rock. (C) The area of 155-1,3 is massive with some fractures. (D) The distinct fracture at 155-1,4 (within stippled, red lines) has very distinct boundaries to the neighbouring massive rock mass. Geological hammer for scale.*

5.1.1.2 AM-SKOG-H-170-1

Alteration zone 170-1 (Figure 14) is a 23,5 m long fracture dipping at 45° that diagonally transect the height of the bench. The fracture has damage zone that varies from 20 cm – 1 m thickness and has a 1- 3 cm core that is filled with very fine-grained gauge. The damage zone is filled with smaller parallel fractures and the rock mass has a slightly greenish tint. The zone is connected to zone 170-2 at the top of the bench at the SE side of the locality.

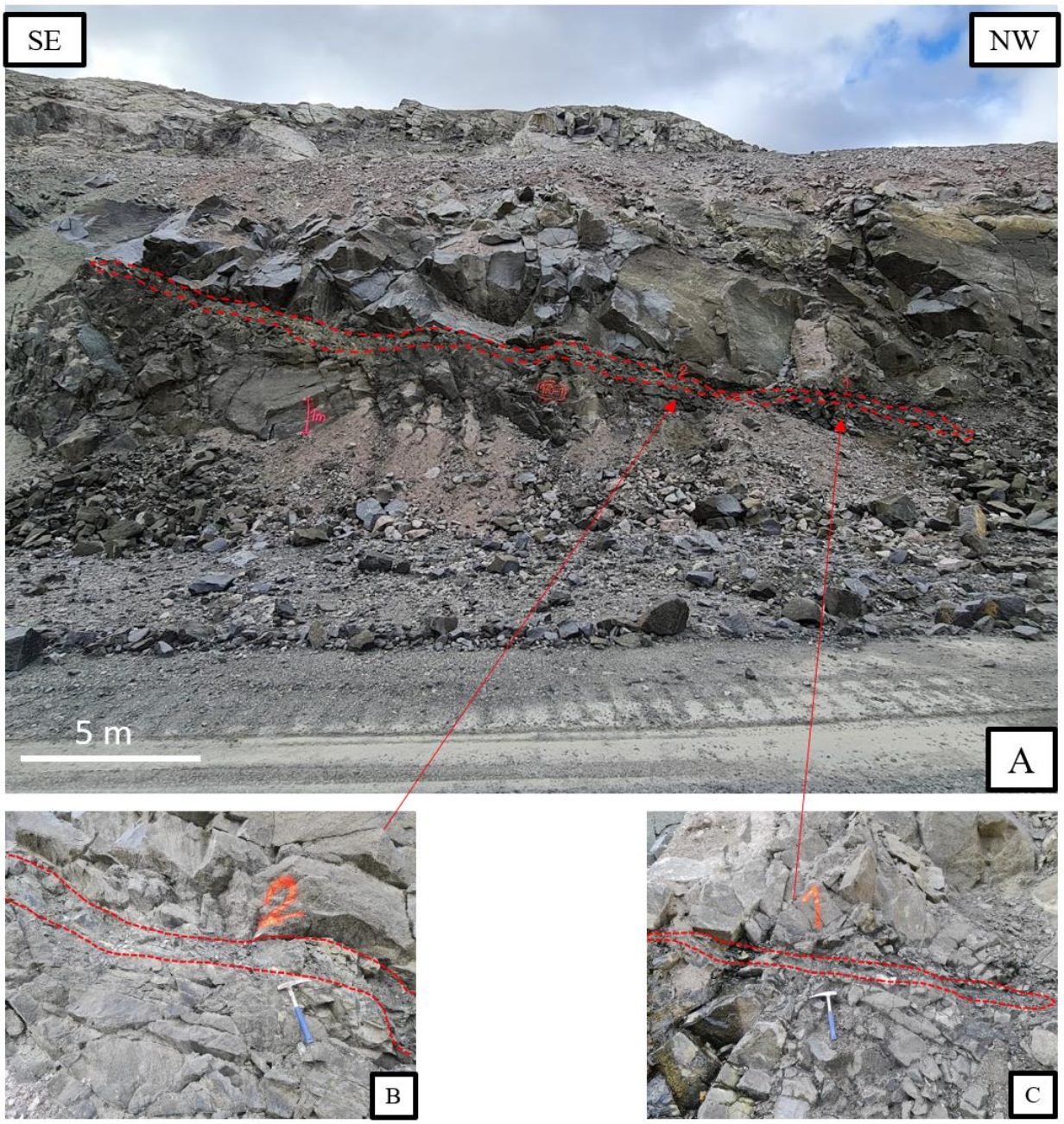

Figure 14: *Appearance of alteration zone 170-1. (A) Alteration zone 170-1 with the distinct, 23,5 m long fracture and associated damage zone (within stippled, red lines). (B) The core zone at 170-1,2 (within stippled, red lines) is filled with very fine-grained gauge. (C) The core zone at 170-1,1 (within stippled red lines) is filled with very fine-grained gauge. Geological hammer for scale.*

5.1.1.3 AM-SKOG-H-170-2

Alteration zone 170-2 (Figure 15), located just SE of 170-1, is a near vertical zone of alteration with a trapezoid shape. The zone is as tall as the bench and has a base width of 9,5 m. The zone consists of a cluster of smaller fractures, 20+, with no pronounced main fracture. The central part of the zone has a greater frequency of fractures than towards the edges where sections of massive rock remain between the fractures. Some of the fractures are filled with a white mineral assemblage and the rock mass generally has a greenish tint.

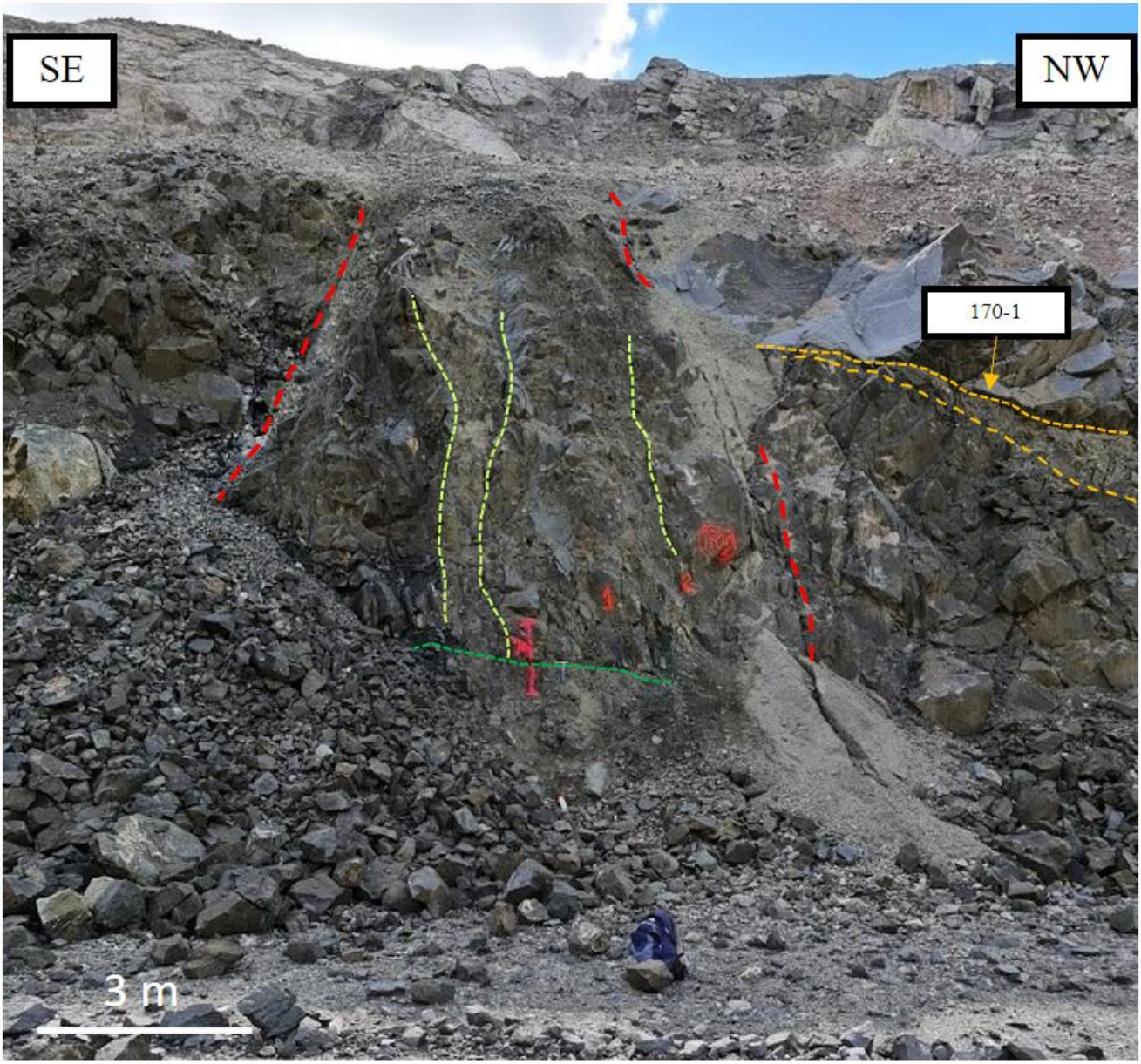

Figure 15: *Alteration zone 170-2 (defined by stippled red lines) has no distinct main fracture(s) but is a zone of heavily fractured rock. Near vertical fractures (some represented by light green stippled lines) are a characteristic feature of the zone. One near horizontal fracture transect the zone at the lower part of the bench. The SE part of alteration zone 170-1 (defined by stippled, orange lines) is visible to the right and appears to be connect to zone 170-2.*

5.1.1.4 AM-SKOG-H-170-3

Alteration zone 170-3 (Figure 16A) is a near vertical zone with no pronounced, large scale core zone. The zone transects the entire bench height and has a width of 4-6 m. Some sectors of the zone are more fractured and could probably be damage zones. A further indicator for this is a banded, ~2 cm wide core zone, filled with a solid, fine grained, mineral assemblage, that stretches towards a more fractured sector (Figure 16C). The more fractured sector is in the upper part of the bench, while the smaller core stretches down to the lower part of the bench. The rock mass has a coating, that resembles that of phyllites, but seems more healthy underneath. (Figure 16B and 16D)

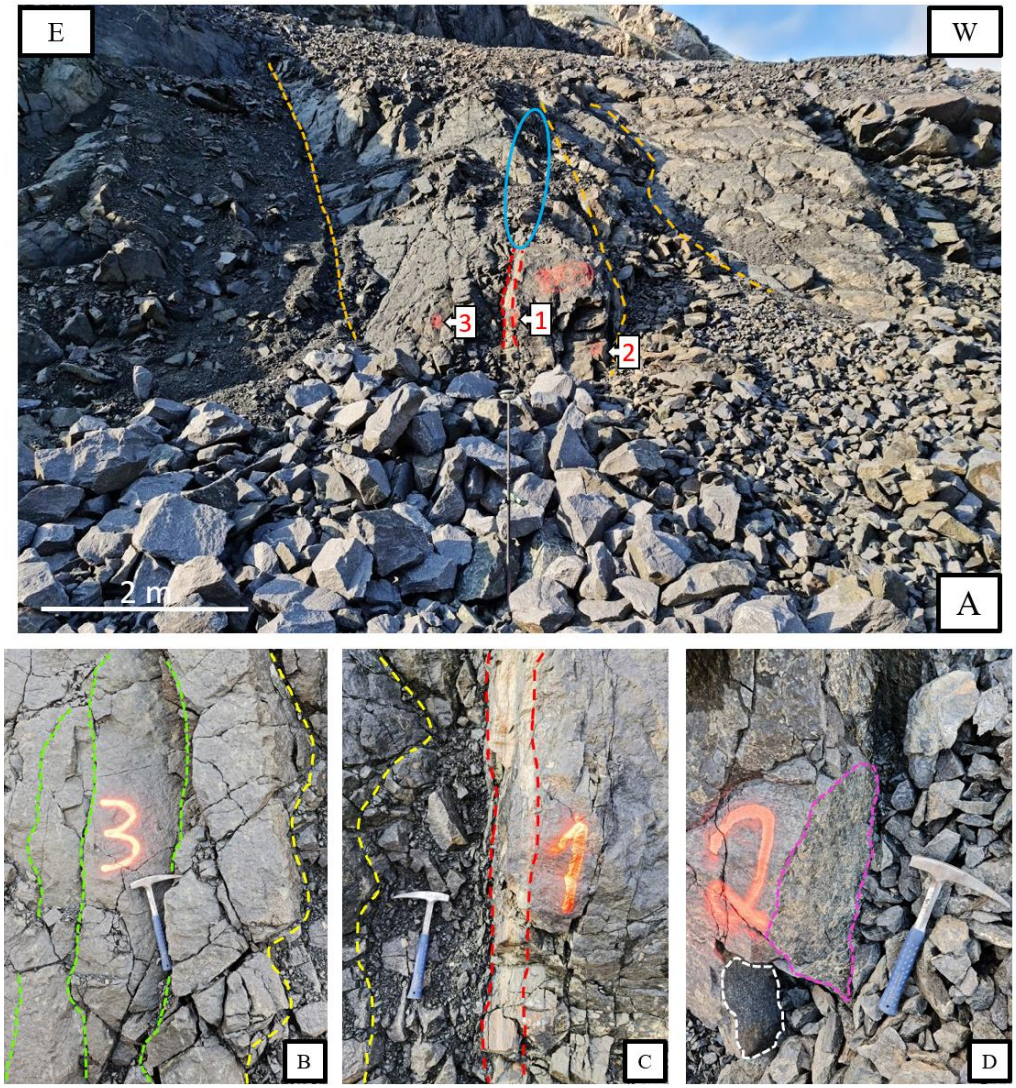

Figure 16: *Appearance of alteration zone 170-3. (A) Alteration zone 170-3, defined by stippled, orange lines. The western boundary is difficult to determine due to loose rocks that covers the rock mass. The banded core is located in the central part of the zone (within stippled, red lines) an a more fractured area is located above this core (within blue circle). (B) At 170.3,3 multiple near vertical fractures are present (stippled, green lines) and the rock has a green coating that resembles that of phyllite. (C) Closeup of the mineralised core at 170-3,1 (within stippled, red lines). To the left of the core a heavily fractured area is present (limited by the stippled, yellow line to the E). (D) At 170-3,2 both the green coating (encircled by stippled purple line) and more healthy underlying rock (encircled by stippled, white line) is visible. Geological hammer for scale.*

5.1.1.5 AM-SKOG-H-185-1

Alteration zone 185-1 (Figure 17A) is located at a contact between anorthosite, to the E, and norite, to the W. The zone is near vertical, 4-5 m wide, and a pronounced fracture with associated damage zone is found in the norite at the contact (Figure 17B). The damage zone stretches primarily into the norite while the anorthosite remains massive. Smaller parallel fractures are found 1 m from the damage zone and some are filled with white mineral assemblage that react to HCl (Figure 17D)

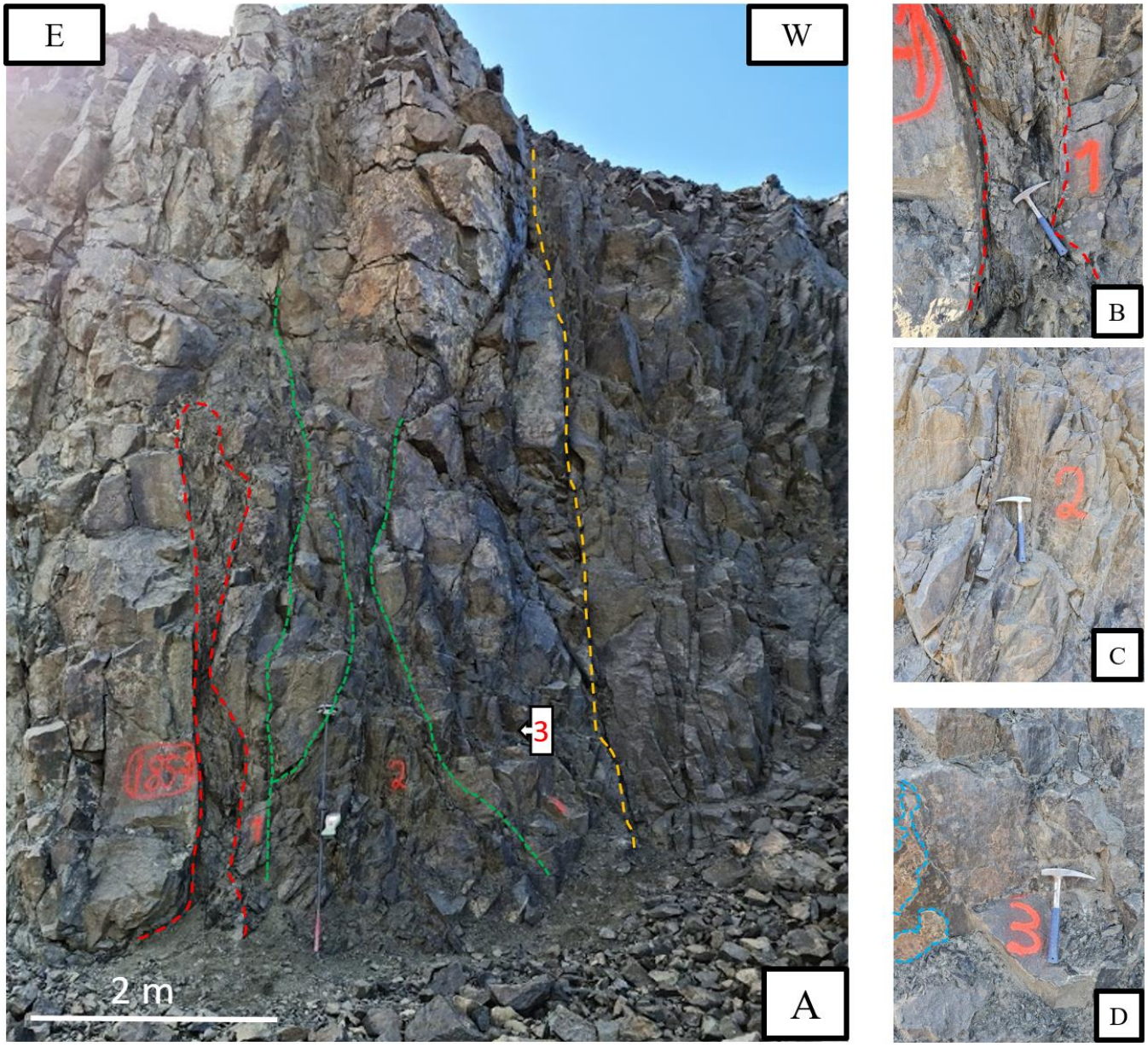

Figure 17: *Appearance of alteration zone 185-1. (A) Alteration zone 185-1 is defined by the stippled, orange line to the W and the anorthosite contact to the E with a fracture with an associated damage zone (within stippled, red line). Fractures are near vertical outside the damage zone (stippled, green lines). (B) A closeup of the damage zone by the contact (within stippled, red lines). (C) Closeup of the area by 185-1,2. (D) Closeup of the area 185-1,3. Examples of the white mineral assemblage coating is visible to the left (defined by stippled, blue lines). Geological hammer for scale.*

5.1.1.6 AM-SKOG-H-185-2

Alteration zone 185-2 (Figure 18A) is a 6 m wide, moderately dipping zone of alteration that transect the bench. The alteration zone is moderately to heavily fractured and have multiple colours due to being partially covered by coating of white/orange and grey/green colours, especially to the W (Figure 18B-D). The white/orange coating is reacting to HCl, while the grey/green coating do not respond to the HCl. No distinct main fracture was detected.

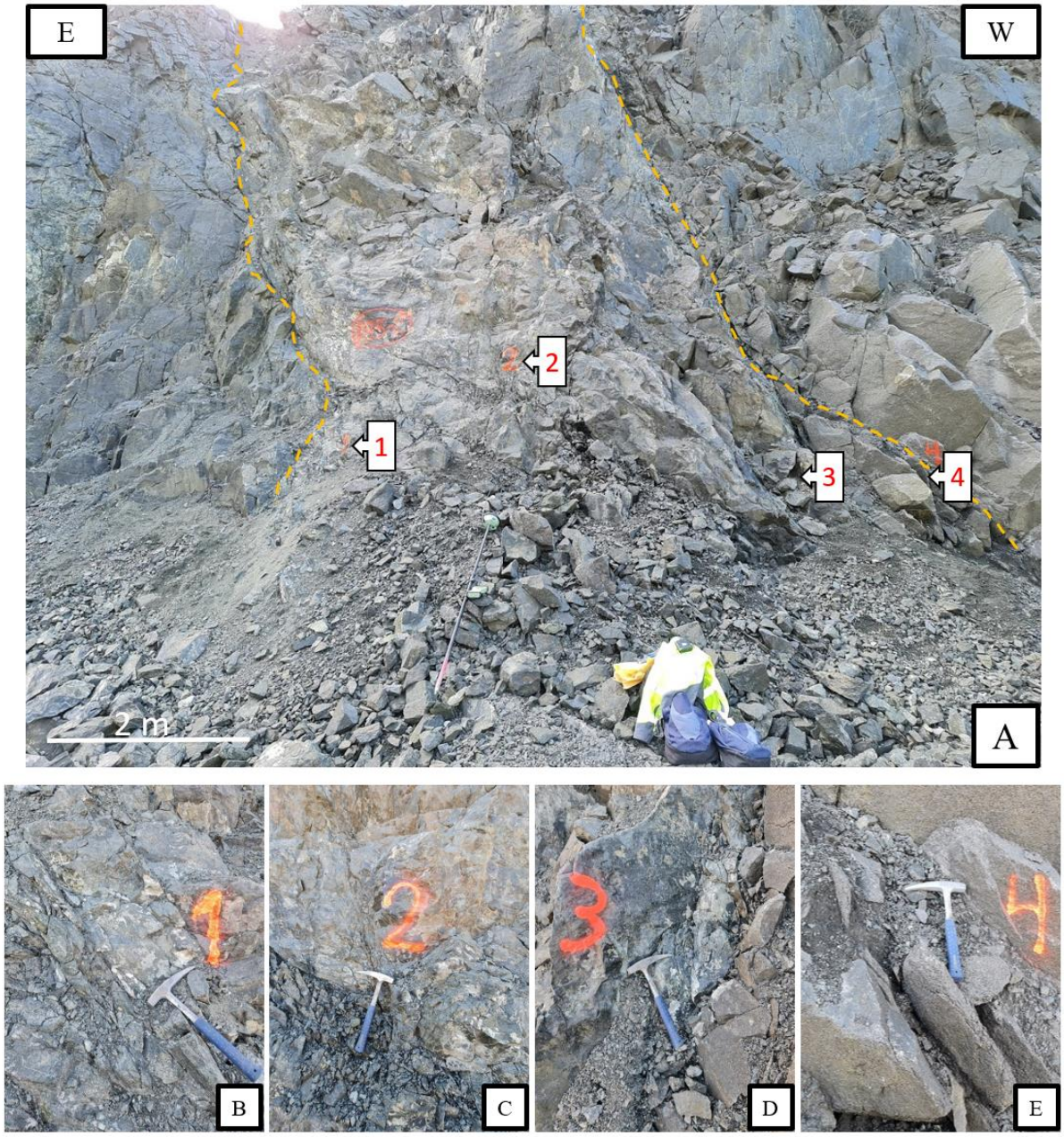

Figure 18: *Appearance of alteration zone 185-2. (A) Alteration zone 185-2 (defined by stippled, orange lines) is a moderately to heavily fractured rock mass with changing colours. (B-E) The 4 sample locations at 185-2 shows changing colours in the rock mass and coatings. Geological hammer for scale.*

5.1.1.7 AM-SKOG-H-200-1

Alteration zone 200-1 (Figure 19A) is a ~7,5m wide, near vertical alteration zone located at a contact between anorthosite, to the NW, and norite, to the SE. A pronounced, water-conducting, fracture with an associated core, varying from 20-40 cm in width, is located at the contact (Figure 19E). From the core outwards (SE-direction) parallel fractures occur with a gradually reducing fracture frequency (Figure 19B-D). Between the fractures the rock mass remains massive and the fractures closest to the core contains a white mineral assemblage.

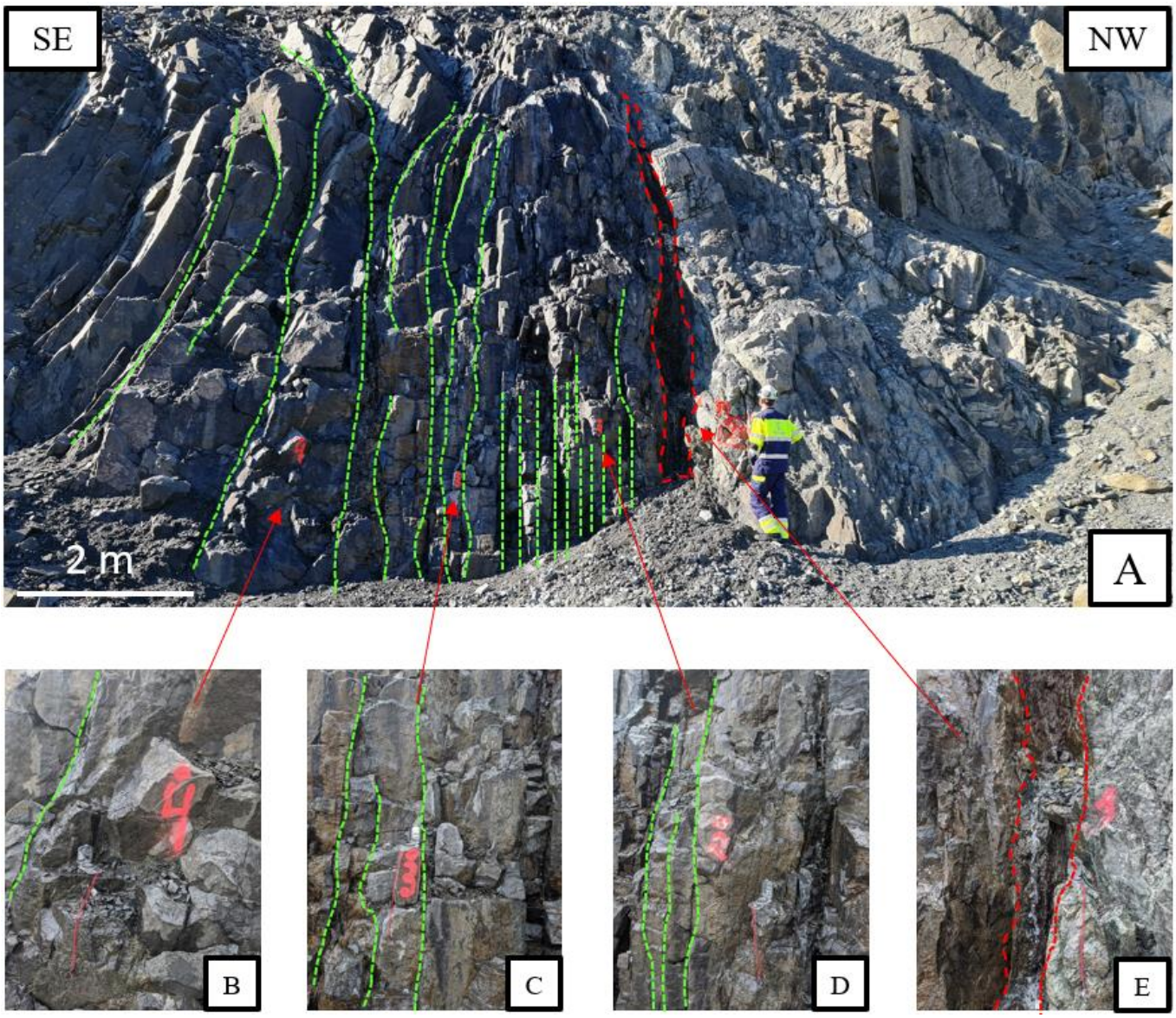

Figure 19: *Appearance of alteration zone 200-1. (A) Alteration zone 200-1 has a distinct fracture with a 20-40 cm wide core/damage zone (within stippled, red lines). The fracture frequency is decreasing when moving away from the main fracture (visualised by stippled, light green lines). (B-D) closeups of sample locations 200-1,2, 200-1,3 and 200-1,4, where the fracture frequency is gradually decreasing from 200-1,2 towards 200-1,4. (Visualized by stippled, light green lines). (E) Closeup of the main fracture and associated, very heavily fractured, core/damage zone (within stippled, red lines). Water can be seen running along the main fracture. Compass for scale.*

5.1.2 The Stabben alteration zone in the Tellnes area

The Stabben alteration zone, AM-TEL-H-155-2, (Figure 20A) is a 40-50 m wide zone of altered rock mass, limited by an anorthosite contact to the SE and a fault/fracture in the NW. The rock in the alteration zone has a coating with a shining gloss of green colour. The central part of the zone is porous and crumbles by the touch of hand, while the flanks are more massive underneath the skin, withstanding heavy strikes by hammer during sampling. An area with similar green colour is located further down in the open pit (Figure 20B) but was not sampled due to accessibility and HMS guidelines.

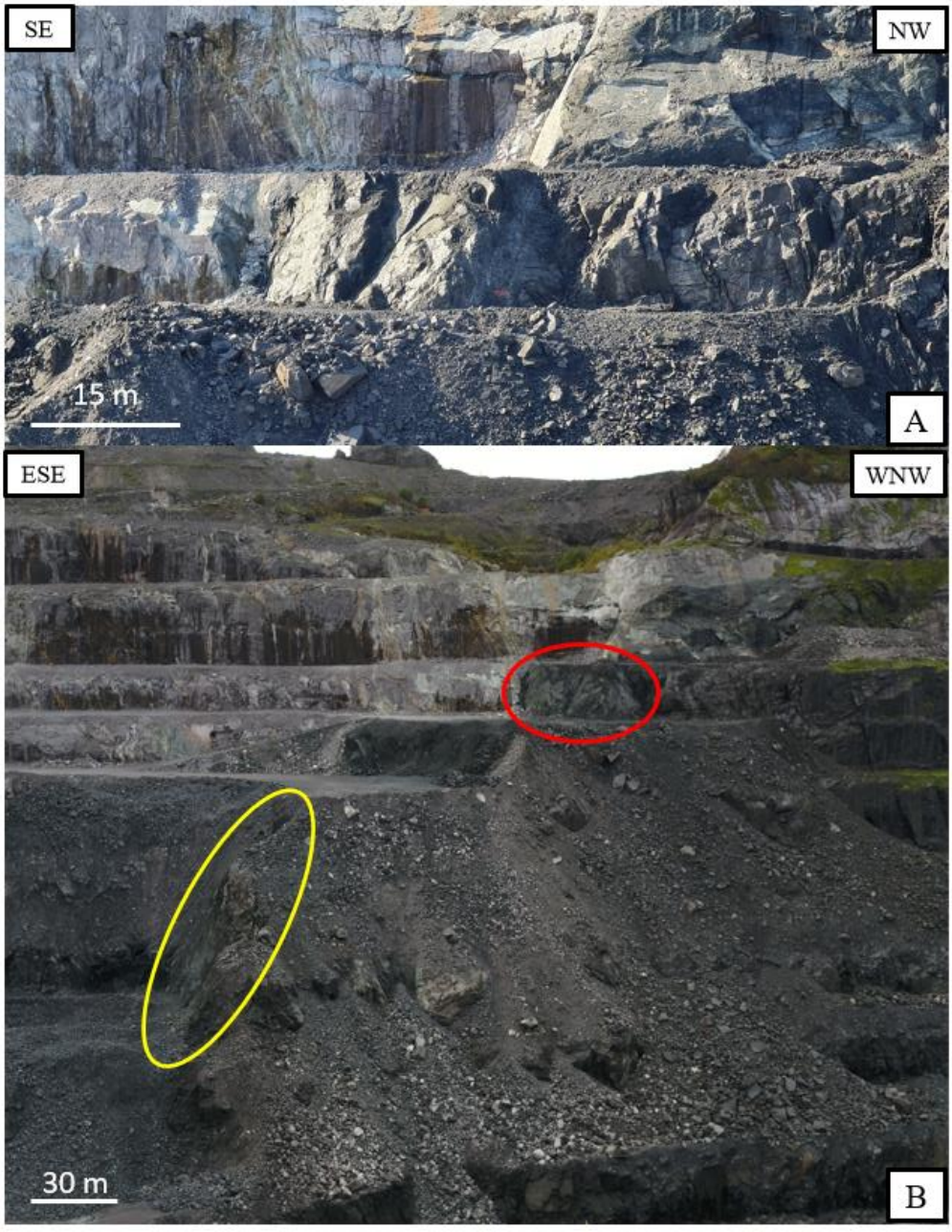

Figure 20: *Appearance of alteration zone 155-1. (A) The Stabben alteration zone (155-2) is a large, 40-50 m wide, zone of altered rock. (B) An area with similar green colour (within yellow circle) as the Stabben alteration zone (within red circle) is located further down in the pit, but was not investigated due to accessibility. Bench for scale.*

5.1.3 The placement of the samples in relation to the zone appearance

At alteration zone 155-1 (Figure 13) the samples are collected from following areas: 155-1,1 is retrieved from massive rock mass at the ESE edge of the zone, 155-1,2 is retrieved from the distinct damage zone furthest to the ESE, 155-1,3 is retrieved the area of massive rock between the two distinct damage zones furthest to the ESE, 155-1,4 is retrieved from the damage zone to the right of 155-1,3, 155-1,5 is retrieved from the area of massive rock to the right of 155-1,4, and 155-1,6 is retrieved from the area of massive rock at the WNW edge of the zone.

At alteration zone 170-1 (Figure 14) the samples are collected from the following areas: 170-1,1-1 is retrieved from the rock underlying the gauge towards the NW edge of the zone, 170-1,1-2 is retrieved from the gauge overlying 170-1,1-1, and 170-1,2 is retrieved from the rock underlying the gauge approximately 5 m SE of 170-1,1.

At alteration zone 170-2 (Figure 15) the samples are collected from the following areas: 170-2,1 is retrieved from the centre of the damage zone and 170-2,2 is retrieved from approximately 1 m NW of the centre of the damage zone.

At alteration zone 170-3 (Figure 16) the samples are collected from the following areas: 170-3,1 is retrieved from the banded zone in the centre of the zone, 170-3,2 is retrieved from massive rock approximately 1 m W of the centre, and 170-3,3 is retrieved from massive, fractured rock approximately 1 m E of the centre.

At alteration zone 185-1 (Figure 17) the samples are collected from the following areas: 185-1,1 is retrieved from the distinct damage zone at the western edge of the zone, 185-1,2 is retrieved from approximately 2 m E of the distinct damage zone, and 185-1,3 is retrieved from approximately 2 m E of 185-1,2.

At alteration zone 185-2 (Figure 18) the samples are collected from the following areas: 185-2,1 is retrieved from the eastern edge of the zone, 185-2,2 is retrieved from the eastern part of the zone centre, 185-2,3 is retrieved from the western part of the zone centre, and 185-2,4 is retrieved from the western edge of the formation.

At alteration zone 200-1 (Figure 19) the samples are collected from the following areas: 200-1,1 is retrieved from the distinct damage zone at the north-western edge of the zone, 200-1,2-1 is retrieved from massive, fractured rock approximately 1 m SE of the distinct damage zone, 200-1,2-2 is retrieved from the thin Ca-bearing sheets filling vertical fractures at 200-1,2, 200-1,3 is retrieved from massive rock approximately 2 m SE of 200-1,2, and 200-1,4 is retrieved from massive rock approximately 2 m SE of 200-1,3.

At alteration zone 155-2 (Figure 20) the samples are collected from the following areas: 155-2,1 is retrieved from the NW edge of the zone, 155-2,2 is retrieved from the NW side of the centre, 155-2,3 is retrieved from the SE side of the centre, 155-2,4 is retrieved approximately 10 m NW of the SE edge of the zone, 155-2,5 is retrieved from massive rock approximately 1 m NW of the NW edge of the zone.

5.1.4 The map of the alteration zones in the Skogestad- and Stabben area

The map of the alteration zones in the Skogestad- and Stabben area, Figure 21, is based on field observations.

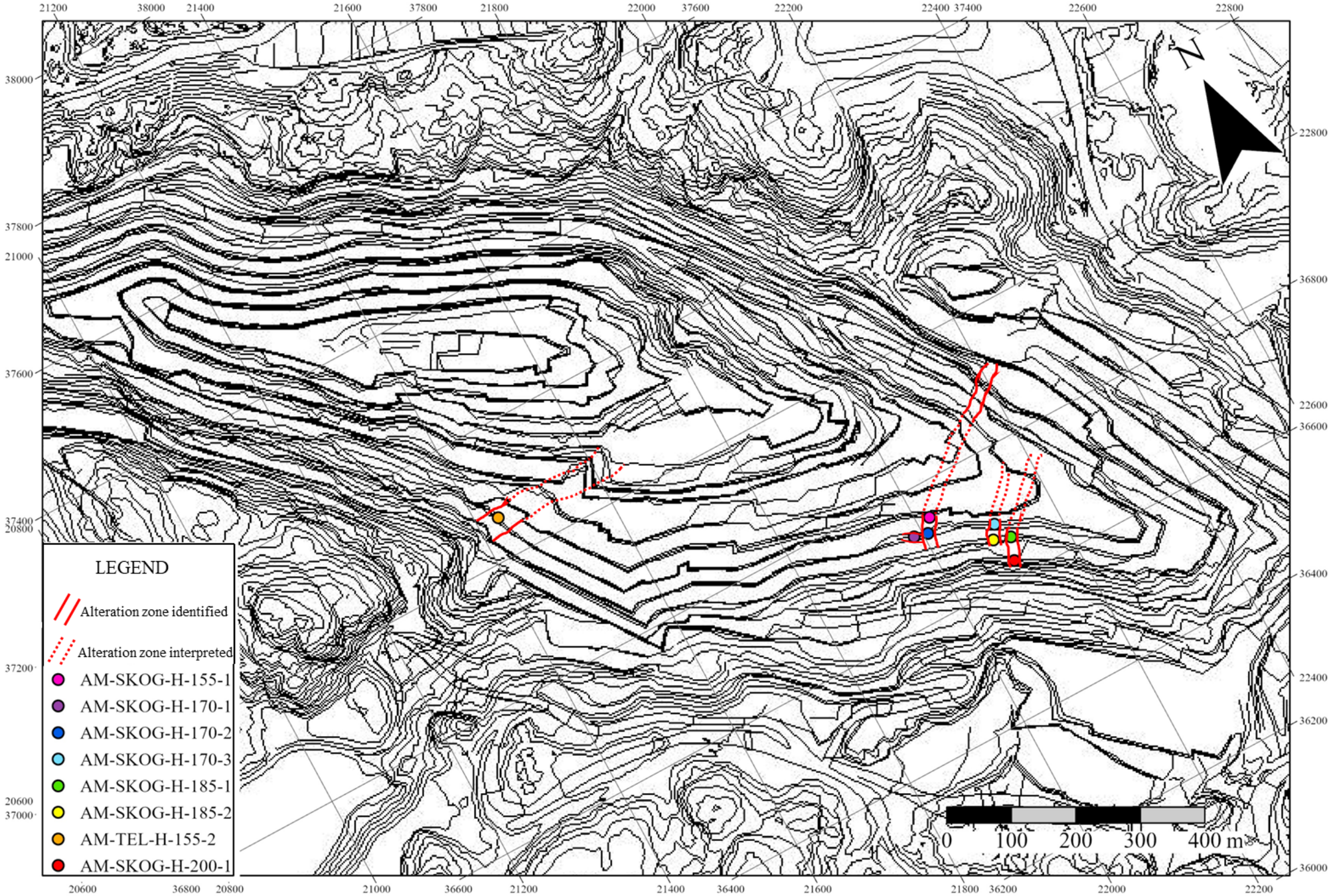

Figure 21: *The map showing the location and prevalence of alteration zones in the Skogestad- and Stabben area with identified and interpreted boundaries. Map is also found in Appendix G.*

5.2 Whole rock chemistry (XRF)

5.2.1 Main elements (IGP)

The WROXI main element analysis at IGP provides analytical data on a range of oxides commonly found as main elements in rocks. The entire analytical results can be found in Appendix B. The oxides that generally make up more than 1 Wt.% of the bulk composition are regarded as the main elements and include: TiO_2, MgO, Na_2O, SiO_2, Al_2O_3, CaO and Fe_2O_3. These oxides are presented in Table 5 and boxplots for each main element oxide is presented in Figure 22 to check for outliers.

Table 5: *The XRF main element analysis at IGP. The main elements are oxides that make up at least 1 Wt.% of the bulk composition of the sample.*

	TiO_2 (Wt.%)	**MgO (Wt.%)**	**Na_2O (Wt.%)**	**SiO_2 (Wt.%)**	**Al_2O_3 (Wt.%)**	**CaO (Wt.%)**	**Fe_2O_3 (Wt.%)**
AM-SKOG-H-155-1,1	17,52	9,22	1,41	29,20	9,67	3,06	26,88
AM-SKOG-H-155-1,2	17,55	8,82	1,38	30,31	9,90	2,46	26,28
AM-SKOG-H-155-1,3	18,36	7,63	1,56	28,76	9,69	3,30	27,58
AM-SKOG-H-155-1,4	14,21	6,81	2,35	34,31	12,72	3,76	22,22
AM-SKOG-H-155-1,5	19,16	6,30	1,80	27,96	10,05	3,83	28,46
AM-SKOG-H-155-1,6	17,17	7,56	1,95	30,88	10,49	4,22	25,50
AM-SKOG-H-170-1,1-1	15,43	5,13	2,49	33,31	13,02	4,59	23,42
AM-SKOG-H-170-1,1-2	6,63	9,57	1,71	42,46	10,64	3,57	16,49
AM-SKOG-H-170-1,2	14,89	5,48	2,16	34,65	11,75	4,94	22,92
AM-SKOG-H-170-2,1	11,07	6,08	2,79	38,17	13,19	5,29	19,68
AM-SKOG-H-170-2,2	11,96	5,91	2,82	37,77	12,80	4,86	20,77
AM-SKOG-H-170-3,1	12,79	8,88	0,42	32,31	8,65	5,80	18,95
AM-SKOG-H-170-3,2	16,18	7,97	1,58	31,35	9,61	3,37	25,77
AM-SKOG-H-170-3,3	16,84	8,07	1,84	32,64	9,61	3,45	25,19
AM-SKOG-H-185-1,1	16,48	8,17	0,54	28,11	9,16	1,65	29,59
AM-SKOG-H-185-1,2	16,32	8,85	1,30	30,38	9,01	2,67	27,21
AM-SKOG-H-185-1,3	6,41	3,36	4,18	46,15	18,66	5,87	11,70
AM-SKOG-H-185-2,1	19,27	6,36	1,55	29,09	10,44	2,86	26,24
AM-SKOG-H-185-2,2	17,50	5,65	1,95	30,48	11,16	4,24	24,70
AM-SKOG-H-185-2,3	15,64	6,27	1,13	34,89	9,11	6,20	18,20
AM-SKOG-H-185-2,4	24,67	5,69	1,44	22,74	8,35	3,11	33,06
AM-SKOG-H-200-1,1	0,43	6,50	4,34	52,76	20,15	0,60	8,47
AM-SKOG-H-200-1,2-1	17,21	6,76	1,89	30,60	10,35	3,82	26,61
AM-SKOG-H-200-1,2-2	0,69	7,06	0,01	31,99	2,80	27,12	5,18
AM-SKOG-H-200-1,3	16,19	7,58	1,88	31,51	10,44	4,27	25,45
AM-SKOG-H-200-1,4	16,22	8,26	1,95	33,69	9,94	3,92	24,66
AM-TEL-H-155-2,1	12,52	3,55	2,77	37,60	15,25	5,62	18,16
AM-TEL-H-155-2,2	17,26	3,90	2,52	32,27	13,72	4,65	22,32
AM-TEL-H-155-2,3	14,70	3,66	2,89	35,64	14,98	5,57	19,98
AM-TEL-H-155-2,4	11,77	5,43	2,76	38,37	14,68	5,01	17,50
AM-TEL-H-155-2,5	12,99	4,18	3,19	38,13	15,21	5,61	19,03

Table 6: *The average main element concentration (Av.), standard deviation (Std.Dev.), highest measured concentration (High) and lowest measured concentration (Low) for each sample location and the zones combined.*

	TiO2				MgO				Na2O				SiO2				Al2O3			
	Av.	**Std.Dev.**	**High**	**Low**	**Av.**	**Std.Dev.**	**High**	**Low**	**Av.**	**Std.Dev.**	**High**	**Low**	**Av.**	**Std.Dev.**	**High**	**Low**	**Av.**	**Std.Dev.**	**High**	**Low**
AM-SKOG-H-155-1	17,33	1,54	19,16	14,21	7,72	1,03	9,22	6,30	1,74	0,34	2,35	1,38	30,24	2,06	34,31	27,96	10,42	1,07	12,72	9,67
AM-SKOG-H-170-1	12,31	4,03	15,43	6,63	6,73	2,01	9,57	5,13	2,12	0,32	2,49	1,71	36,81	4,04	42,46	33,31	11,80	0,97	13,02	10,64
AM-SKOG-H-170-2	11,51	0,45	11,96	11,07	5,99	0,08	6,08	5,91	2,81	0,02	2,82	2,79	37,97	0,20	38,17	37,77	13,00	0,20	13,19	12,80
AM-SKOG-H-170-3	15,27	1,77	16,84	12,79	8,31	0,41	8,88	7,97	1,28	0,62	1,84	0,42	32,10	0,55	32,64	31,35	9,29	0,45	9,61	8,65
AM-SKOG-H-185-1	13,07	4,71	16,48	6,41	6,79	2,44	8,85	3,36	2,01	1,56	4,18	0,54	34,88	8,02	46,15	28,11	12,28	4,51	18,66	9,01
AM-SKOG-H-185-2	19,27	3,37	24,67	15,64	5,99	0,32	6,36	5,65	1,52	0,29	1,95	1,13	29,30	4,35	34,89	22,74	9,77	1,10	11,16	8,35
AM-SKOG-H-200-1	10,15	7,84	17,21	0,43	7,23	0,63	8,26	6,50	2,01	1,38	4,34	0,01	36,11	8,39	52,76	30,60	10,74	5,52	20,15	2,80
AM-TEL-H-155-2	13,85	1,96	17,26	11,77	4,14	0,68	5,43	3,55	2,83	0,22	3,19	2,52	36,40	2,28	38,37	32,27	14,77	0,56	15,25	13,72
ALL ZONES	14,39	5,04	24,67	0,43	6,60	1,73	9,57	7,97	2,02	0,94	4,34	0,01	33,82	5,72	52,76	22,74	11,46	3,25	20,15	2,80

Table 7: *Continuation of* *Table 6.*

	CaO				Fe_2O3			
	Av.	**Std.Dev.**	**High**	**Low**	**Av.**	**Std.Dev.**	**High**	**Low**
AM-SKOG-H-155-1	3,44	0,58	4,22	2,46	26,15	1,99	28,46	22,22
AM-SKOG-H-170-1	4,37	0,58	4,94	3,57	20,94	3,16	23,42	16,49
AM-SKOG-H-170-2	5,07	0,21	5,29	4,86	20,22	0,55	20,77	19,68
AM-SKOG-H-170-3	4,21	1,13	5,80	3,37	23,30	3,09	25,77	18,95
AM-SKOG-H-185-1	3,40	1,80	5,87	1,65	22,83	7,93	29,59	11,70
AM-SKOG-H-185-2	4,11	1,32	6,20	2,86	25,55	5,28	33,06	26,24
AM-SKOG-H-200-1	7,95	9,68	27,12	0,60	18,08	9,26	26,61	5,18
AM-TEL-H-155-2	5,29	0,39	5,62	4,65	19,40	1,68	22,32	17,50
ALL ZONES	4,82	4,27	27,12	0,60	22,20	5,98	33,06	26,24

Calculations of the average composition with standard deviation, median composition, and the highest and lowest measured concentration for each main element at all 8 localities (Table 6 and Table 7) provides a general representation of the chemical composition in each alteration zone.

TiO_2 is the main element of highest interest for the production at Titania as it is the most important element in the ilmenite concentrate. The measured TiO_2 values range from 0,43 – 24,67 Wt.% where 3 outliers are determined by the boxplot (Figure 22). Two of the three outliers have a value below 1 Wt.% at 0,43 and 0,69 Wt.% both found at zone 200-1. The third outlier is found at zone 185-2 with a value of 24,67 Wt.% TiO_2. The range of the remaining measurements are from 6,41 – 19,27 Wt.%. The average TiO_2 composition is at 14,39 Wt.% with a standard deviation of 5,04 Wt.%, while the median concentration is at 16,18 Wt.%.

The average composition of TiO_2 for individual zones ranges from 10,15 – 19,27 Wt%, with standard deviation ranging from 0,45 – 7,84 Wt.%. The median concentration for individual zones ranges from 11,51 – 18,38 Wt.%.

For the remaining main elements, the outliers determined in the boxplots (Figure 22) will be presented in detail, while the remaining information can be found in Table 6, Table 7 and Figure 22. The SiO_2 measurements have one high outlier at 52,76 Wt.% found at zone 200-1. The Al_2O_3 measurements have one low outlier, at 2,80 Wt.%, and two high outliers, at 18,66 and 20,15 Wt.%. The low outlier and the high outlier at 20,15 Wt.% Al_2O_3 are found at 200-1, while the other high outlier at 18,66 Wt.% is found at 185-1. The CaO measurements have one high outlier at 27,12 Wt.% found at zone 200-1. The Fe_2O_3 measurements have one low outlier at 5,18 Wt.% found at 200-1. No outliers are found in the MgO and Na_2O.

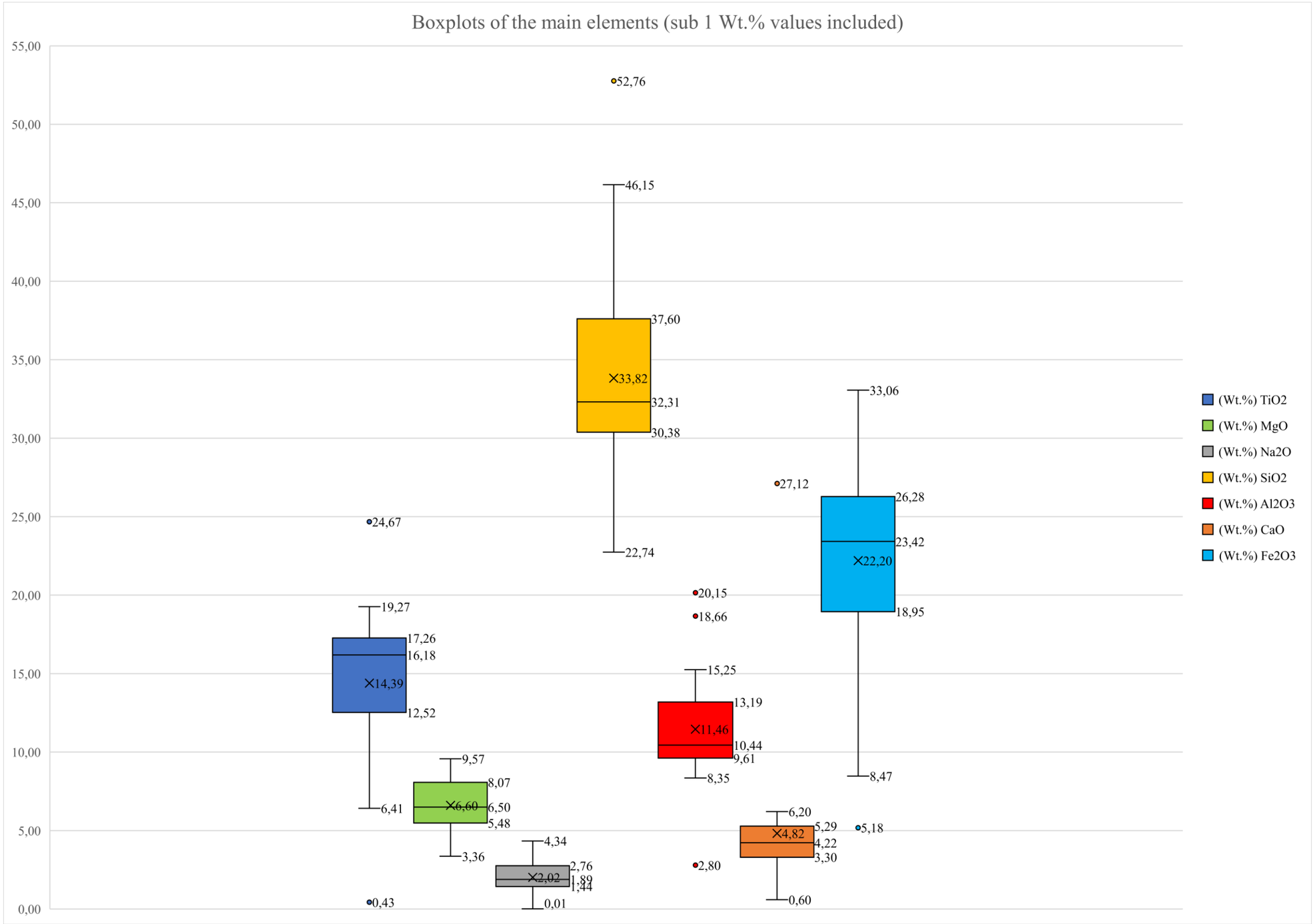

Figure 22: *Boxplots for the main elements. The boxplots give the mean (x), median (line inside box), range of 50% of the samples (the upper and lower part of the box), the sample range (upper and lower horizontal lines) and identifies statistical outliers (dots).*

5.2.2 Bivariate diagrams for the main elements

In the alteration zones the TiO_2 content varies from 0,43 – 24,67 Wt.% (Table 6). The other main elements are plotted against TiO_2 (Wt.%) in bivariate diagrams to get an overview of changes in the chemical composition as TiO_2 varies. The bivariate diagrams (Figure 23) indicate which elements that have a negative or positive correlation with the TiO_2 content. The main element that has a positive correlation with the TiO_2 content is Fe_2O_3. The main elements that have a negative correlation with the TiO_2 content are SiO_2, Al_2O_3, Na_2O and CaO. The main element MgO does not show a clear positive nor negative correlation.

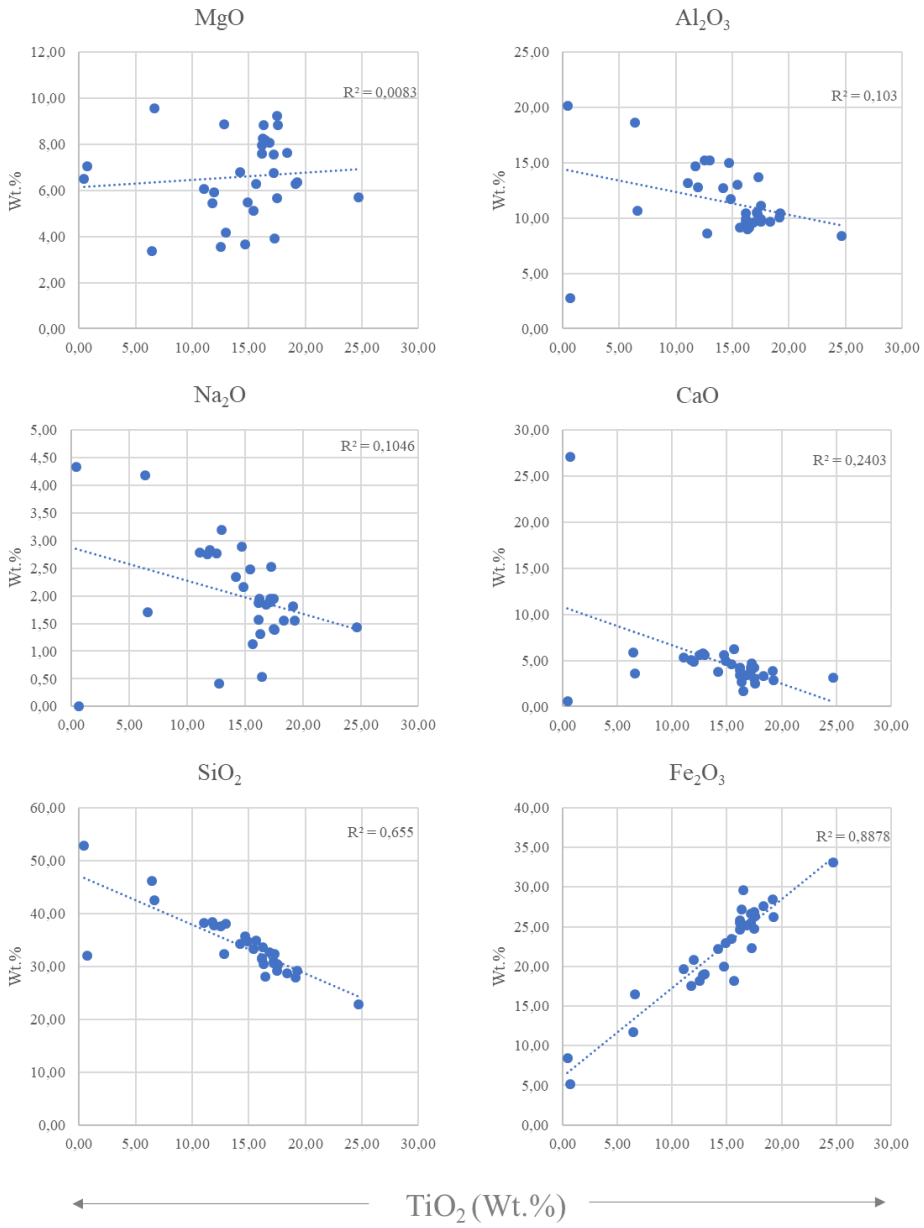

Figure 23: *Bivariate diagrams showing the chemical variation of main elements plotted against TiO_2 for the 31 samples from the 8 alteration zones.*

5.2.3 Trace elements (IGP)

The trace elements are the elements that make up less than 1 Wt.% of the bulk composition. The trace elements are not presented in detail as they will not be used in the discussion. The XRF trace element analysis can be found in Appendix B.

5.3 Mineral chemistry from EPMA

Time limitations on the EPMA instrument resulted in a limited analysis of ilmenite, talc and serpentine grains. The mineral chemistry data provided by the EPMA are therefore very limited and considered insufficient for use in the discussion. Based on this evaluation the mineral chemistry data retrieved from the EPMA are placed in Appendix F.

5.4 Mineralogical content and description

Identification, description and quantification of the mineral content in the alteration zones was done with a combination of optical microscopy, XRD and AM. Description of minerals are primarily based on optical microscope observations and aided by AM for the section at 170-3 and 200-1.

Quantification of the mineral content in each sample is conducted by XRD analysis from both IGP and Titania. The analysis at IGP provides the wider identification archive and is therefore preferred over the XRD analysis at Titania. The analysis from Titania is favoured for the minerals: rutile, orthopyroxene, clinopyroxene, olivine, hematite and spinel. This is due to the advantage of a copper target material when analysing a TiO_2 dominated mineral such as rutile, the ability to separate ortho- and clinopyroxene from each other and quantification of minerals identified in the sections that was not identified by the analysis at IGP. AM aids in quantification of the sections from 170-3 and 200-1 but does not provide a quantification to an entire sample like the XRD. It is important to emphasize that XRD provides quantification of minerals with a margin of ± 1 Wt.%, and always normalize to 100%. Sub 1 Wt.% values during the quantification should be seen with caution.

The optical microscope description of the thin sections can be found in its entirety in Appendix E. The XRD analysis from IGP and Titania can be found in its entirety in Appendix C. The AM analysis can be found in its entirety in Appendix D.

5.4.1 AM-SKOG-H-155-1

5.4.1.1 Silicates

Plagioclase: Plagioclase is present in both sections at 155-1. The plagioclase is identified easily by distinct twinning features, with examples of albite-, pericline and Carlsbad twinning occurring in all sections. The plagioclase is affected by alteration by chlorite/serpentine, sericite and saussurite at varying degrees at 155-1 altering along boundaries fractures and in grain centres. At 155-1,1 the grain size is fine to medium grained with subhedral to anhedral equant grain shapes. The grains are heavily fractured and are partially affected by alteration. At 155-1,2 the grain size is medium to fine grained with subhedral to anhedral, tabular and equant grain shapes. The grains are heavily to very heavily fractured with most grains being heavily affected by alteration. Plagioclase grains in both sections contains inclusions of ilmenite and biotite and grain boundaries varies from straight to lobate. The plagioclase content in the six samples at 155-1 is determined by the XRD analysis at IGP, and is given in Figure 24.

Biotite: Biotite is identified in both sections and are easily visible with varying pleochroism of brown colours. The grain size is fine with subhedral to anhedral, tabular, laths and equant grains in both sections. The grains are partially fractured and at 155-1,2 some alteration by chlorite/serpentine are identified along a couple of boundaries. The biotite often occurs in aggregates with ilmenite, magnetite, and rutile and as inclusions in plagioclase. The biotite content in the six samples at 155-1 is determined by the XRD analysis at IGP, and is given in Figure 24.

Chlorite/Serpentine: Chlorite and serpentine are identified in both sections and often occurs in a mix with each other, with an indistinguishable grain size making it difficult to differentiate between the two minerals. The minerals occur in fractures and as reaction rims especially along plagioclase and pseudomorph orthopyroxene. The chlorite/ serpentine content in the six samples at 155-1 is determined by the XRD analysis at IGP, and is given in Figure 24. Serpentine is identified as antigorite in the XRD analysis.

Talc: Talc is identified in both sections with equal properties. The talc occurs as the main alteration product in altered, pseudomorph orthopyroxene. The grain size is very fine to fine grained with subhedral fibrous/laths grain shapes with no visible fractures. The talc content in the six samples at 155-1 is determined by the XRD analysis at IGP, and is given in Figure 24.

Clinopyroxene: Clinopyroxene is identified in both sections as alteration/replacement product of altered orthopyroxene. The grain size is fine to very fine grained with anhedral to subhedral equant grains. The grains are partially to moderately fractured with straight and lobate borders. The replacement of orthopyroxene occurs both along grain boundaries and within grain centres. The clinopyroxene content in the six samples at 155-1 is determined by the XRD analysis at Titania, and is given in Figure 24.

Muscovite: Muscovite occurs as alteration product of plagioclase in all sections at 155-1. The grain size is very fine grained with indistinguishable grain shape. The muscovite is identified based on high interference colours. The muscovite content in the six samples at 155-1 is determined by the XRD analysis at IGP, and is given in Figure 24.

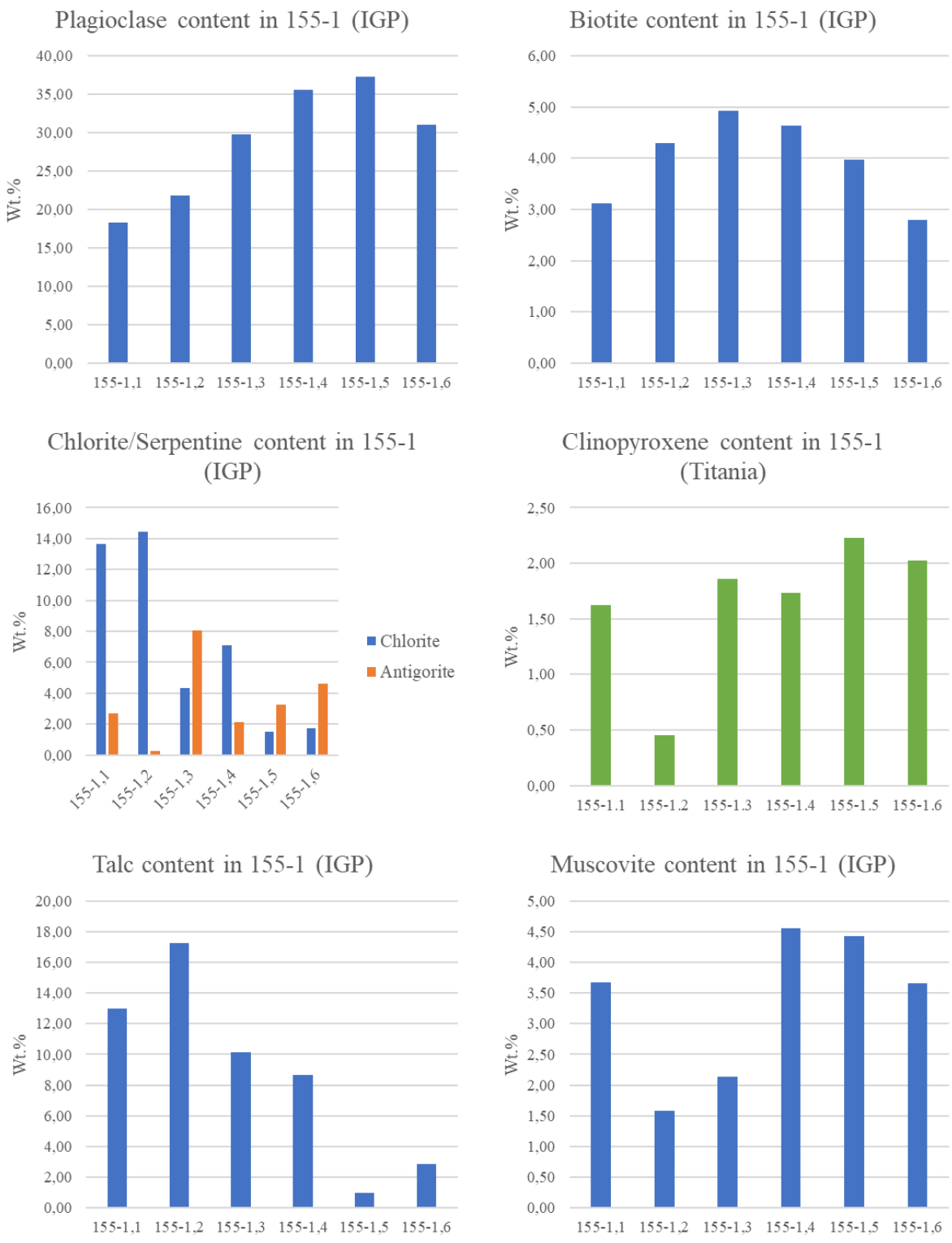

Figure 24: *The plagioclase, biotite, chlorite/serpentine, clinopyroxene, talc and muscovite content in alteration zone 155-1 determined by the XRD analyses from IGP and Titania.*

5.4.1.2 Oxides

Ilmenite: Ilmenite is identified in both sections. The grains have anhedral, equant grain shapes with varying straight and lobate boundaries in both sections. In section 155-1,1 the grain size is fine to very fine grained. The grains are partially fractured and is partially affected by alteration by rutile. In section 155-1,2 the grain size is fine to medium grained. The grains are moderately to heavily fractured and are partially affected by alteration to rutile along borders, fractures and in grain centres. In both sections the ilmenite contains hematite exsolution lamellas. The ilmenite often appears in aggregates with magnetite ± biotite ± rutile ± sulphides. Some grains appear as inclusions in plagioclase. The ilmenite content in the six samples at 155-1 is determined by the XRD analysis at IGP, and is given in Figure 25.

Magnetite: Magnetite is identified in both sections. The grain size is fine grained with subhedral to anhedral, equant grain shapes in both sections. In section 155-1,1 the grains are moderately fractured with cryptocrystalline inclusions and spinel lamellas. In section 155-1,2 the grains are heavily to very heavily fractured and contains multiple cryptocrystalline inclusions. Grains in both sections have straight and lobate borders and often occur in aggregates with ilmenite ± biotite ± rutile ± sulphides. The magnetite content in the six samples at 155-1 is determined by the XRD analysis at IGP, and is given in Figure 25.

Rutile: Rutile is identified in both sections at 155-1 and occur as an alteration product of ilmenite along boundaries, fractures and in some grain centres. The grain size is fine to very fine grained with anhedral, equant grain shapes. The grain boundaries vary between straight and lobate with the grains being partially to moderately fractured. The rutile often occurs in aggregates with ilmenite ± magnetite ± biotite ± sulphides. The rutile content in the six samples at 155-1 is determined by the XRD analysis at Titania, and is given in Figure 25.

Hematite: Hematite occurs as exsolution lamellas in ilmenite in both sections. The hematite content in the six samples at 155-1 is determined by the XRD analysis at Titania, and is given in Figure 25.

Spinel: Spinel is only identified in section 155-1,1. The grain size is fine to very fine grained with acicular grain shape. The borders vary from straight to lobate and the grains are partially fractured. The spinel occurs exclusively as inclusions in magnetite. The spinel content in the six samples at 155-1 is determined by the XRD analysis at Titania, and is given in Figure 25.

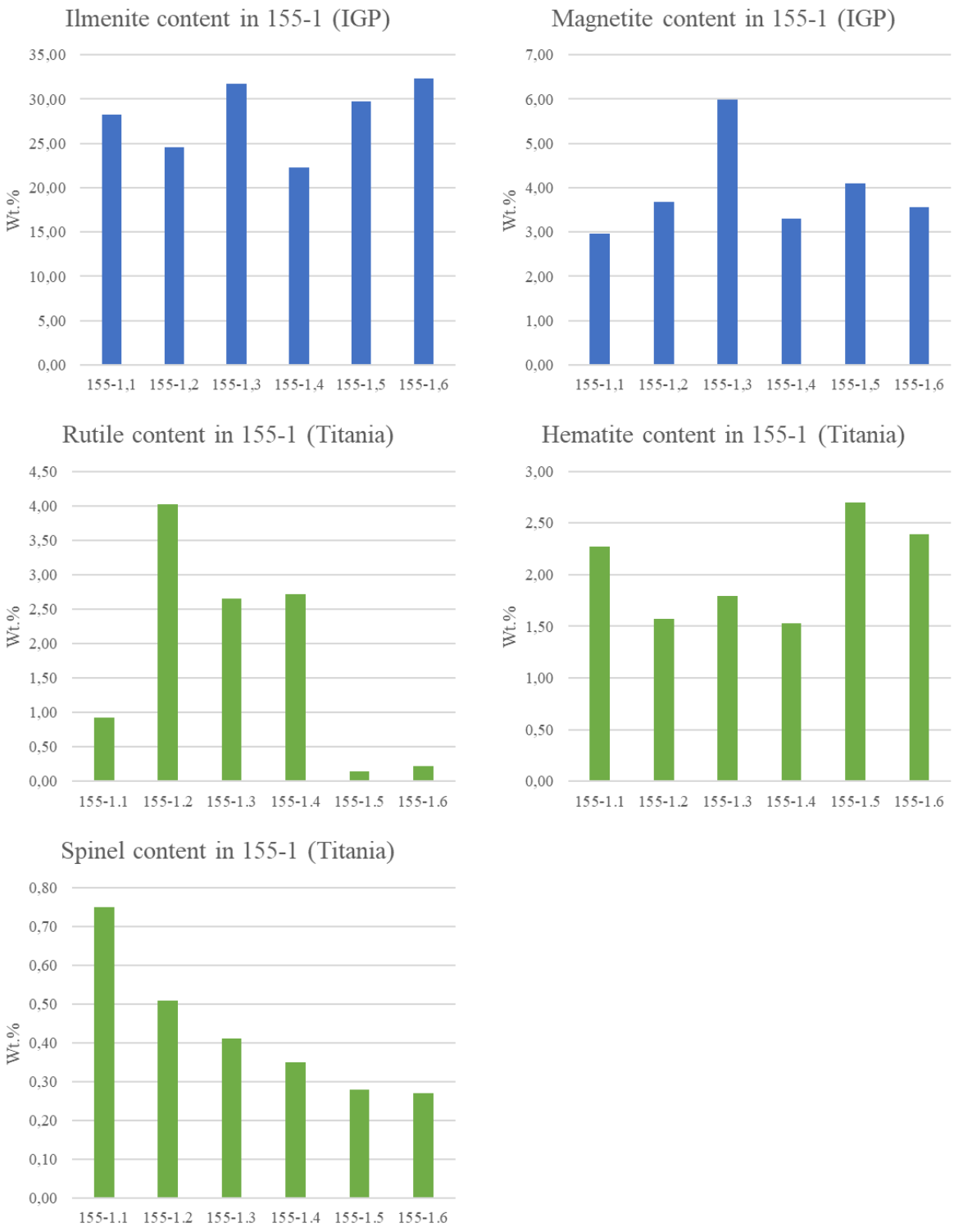

Figure 25: *The ilmenite, magnetite, rutile, hematite and spinel content in alteration zone 155-1 determined by the XRD analyses from IGP and Titania.*

5.4.1.3 Sulphides

The sulphides were not a main target during the investigation and a differentiation between different sulphide phases was not conducted. Sulphides are identified in both sections at 155-1. The sulphides are dominated by a pyrite phase and have a fine to very fine grain size. The grains have subhedral to anhedral, equant grain shapes, and have straight and lobate borders. The grains are partially fractured and occurs sporadically throughout the sections. The pyrite content in the six samples at 155-1 is determined by the XRD analysis at IGP, and is given in Figure 26.

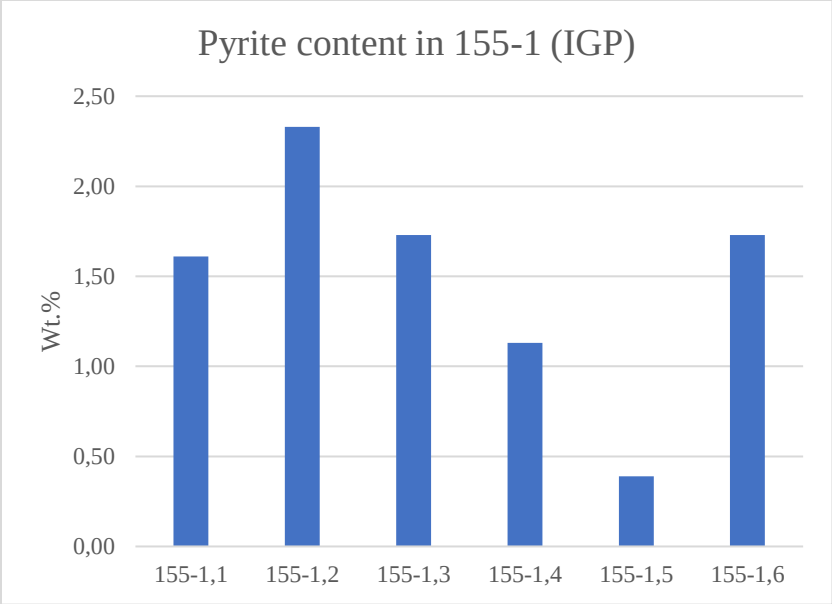

Figure 26: *The pyrite content in alteration zone 155-1. The pyrite content represents the sulphide content of the samples. Pyrite is identified in all samples by XRD and ranges from 0,39 – 2,33 Wt.%.*

5.4.1.4 Identification and quantification of additional mineral phases at AM-SKOG-H-155-1

The XRD at Titania identified and quantified the minerals shown in Figure 27. Some of the minerals identified by the XRD were not found in the thin sections from 155-1,1 and 155-1,2 during the optical investigation, and includes: orthopyroxene (0,37 – 12,03 Wt.%), olivine (0 – 2,33 Wt.%), quartz (0,36 – 0,87 Wt.%), calcite (0 – 0,21 Wt.%) and apatite (0 – 0,07 Wt.%).

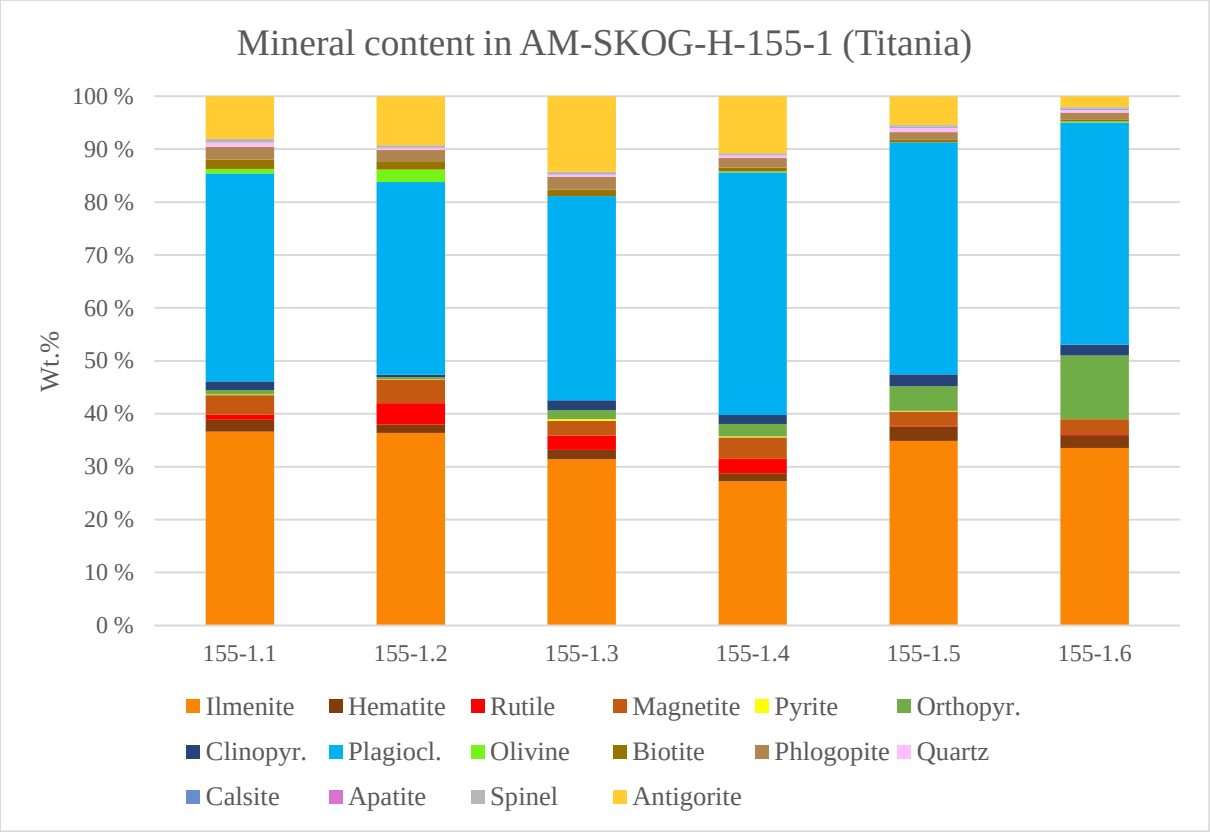

Figure 27: *The XRD analysis at Titania provided the following mineral identification and quantification for the samples in alteration zone 155-1. Mineral phases that were identified by XRD but not in the thin sections includes: orthopyroxene (0,37 – 12,03 Wt.%), olivine (0 – 2,33 Wt.%), quartz (0,36 – 0,87 Wt.%), calcite (0 – 0,21 Wt.%) and apatite (0 – 0,07 Wt.%). The analysis at Titania also provides two types of biotite: biotite and phlogopite.*

The XRD at IGP identified and quantified the minerals shown in Figure 28. Some of the minerals identified by the XRD were not found in the thin sections from 155-1,1 and 155-1,2 during the optical investigation, and includes: calcite (0 – 0,94 Wt.%), pyroxene (0 – 14,44 Wt.%), quartz (0 – 1,43 Wt.%), hornblende (0 – 5,68 Wt.%), zoisite (0 – 5,03 Wt.%), sphalerite (0 – 0,07 Wt.%) and olivine (0 – 1,71 Wt.%).

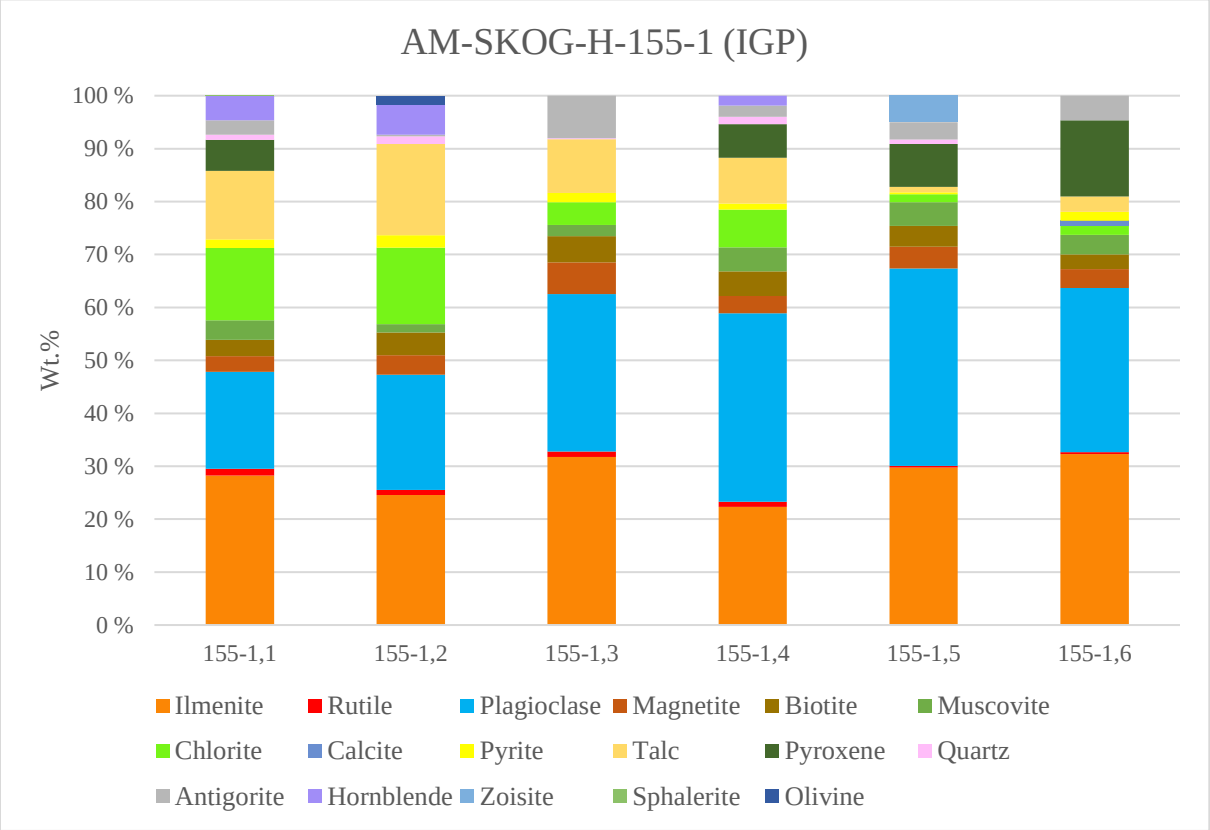

Figure 28: *The XRD analysis at IGP provided the following mineral identification and quantification for the samples in alteration zone 155-1. Mineral phases that were identified by XRD but not in the thin sections includes: calcite (0 – 0,94 Wt.%), pyroxene (0 – 14,44 Wt.%), quartz (0 – 1,43 Wt.%), hornblende (0 – 5,68 Wt.%), zoisite (0 – 5,03 Wt.%), sphalerite (0 – 0,07 Wt.% and olivine (0 – 1,71 Wt.%)*

5.4.2 AM-SKOG-H-170-1

Alteration zone 170-1 was only analysed by XRD for mineral identification and quantification. The XRD analysis at IGP (Figure 29) identified the following minerals in alteration zone 170-1: plagioclase, biotite, muscovite, chlorite, calcite, talc, ilmenite, rutile, magnetite and pyrite in all samples. Dolomite in sample 170-1,1-1, pyroxene in sample 170-1,1-2, quartz in sample 170-1,1-2 and 170-1,2 and siderite in sample 170-1,1-2. Montmorillonite was identified in sample 170-1,1-2 but not quantified.

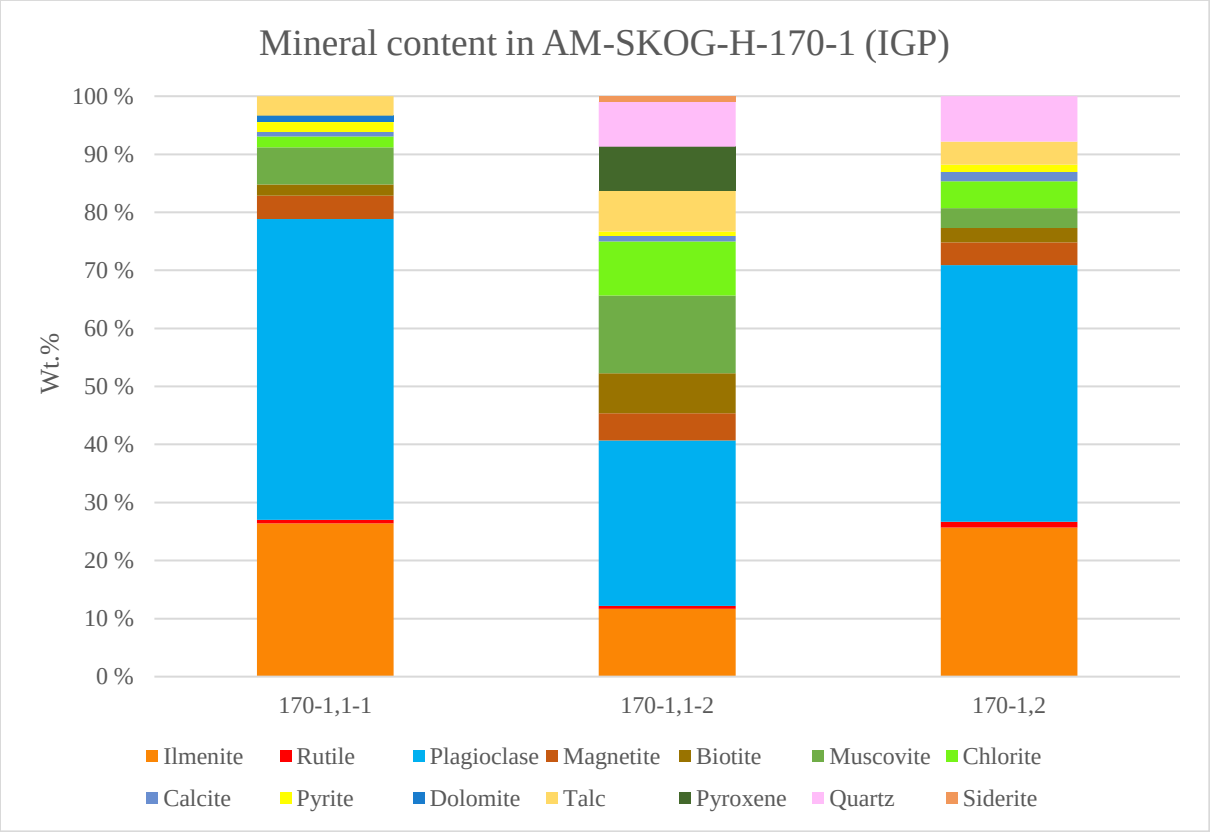

Figure 29: *The XRD analysis at IGP provided the following mineral identification and quantification for the samples in alteration zone 170-1. Montmorillonite was identified in sample 170-1,1-2 but was not quantified.*

The XRD analysis at Titania (Figure 30) identified the following minerals in alteration zone 170-1: ilmenite, hematite, rutile, magnetite, pyrite, orthopyroxene, clinopyroxene, plagioclase, olivine, biotite, phlogopite, quartz, calcite, spinel and antigorite in all samples. Apatite was identified in sample 170-1,2.

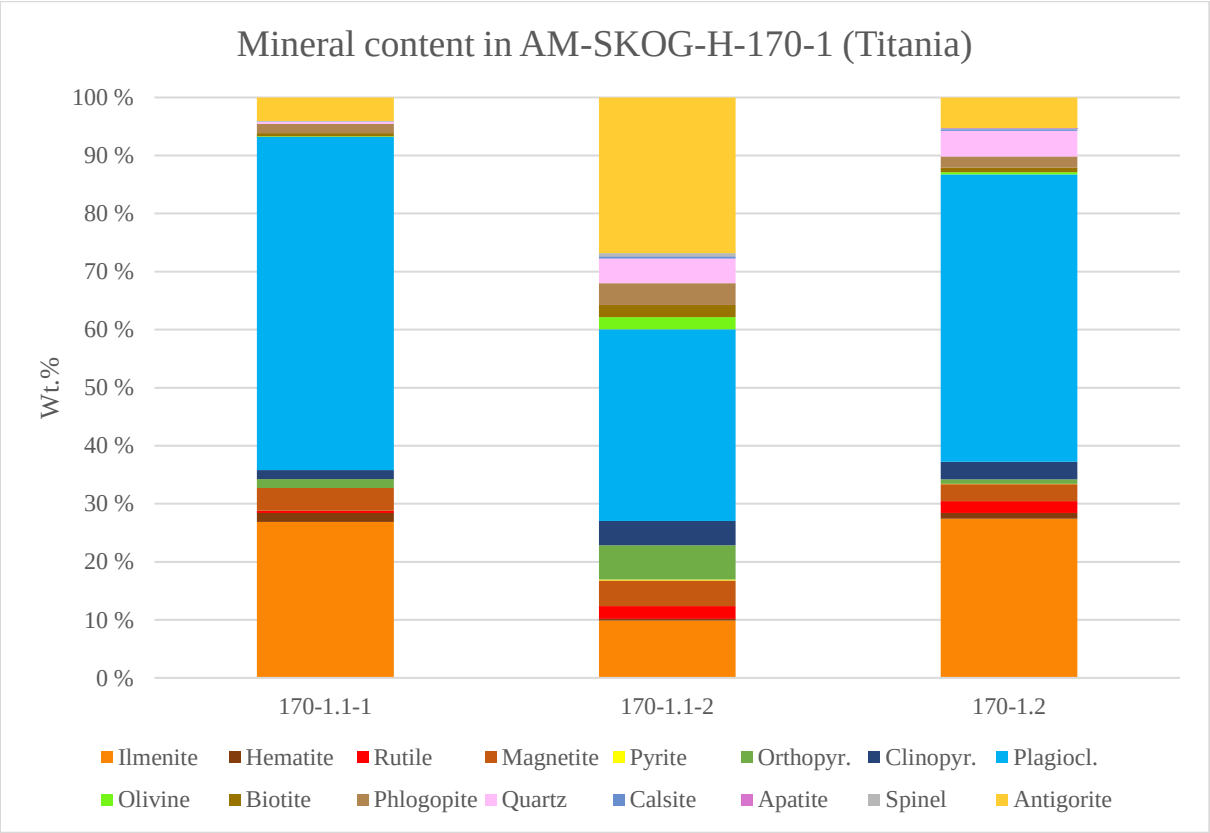

Figure 30: *The XRD analysis at Titania provided the following mineral identification and quantification for the samples in alteration zone 170-1.*

5.4.3 AM-SKOG-H-170-2

5.4.3.1 Silicates

Plagioclase: Plagioclase is identified in both sections at 170-2. The plagioclase is identified easily by distinct twinning features, with examples of albite-, pericline and Carlsbad twinning occurring in both sections. The grains have a subhedral to anhedral, tabular and equant grain shapes in both sections and are heavily fractured. Boundaries vary between straight and lobate. The plagioclase often contains ilmenite and biotite inclusions. Most grains are moderately to heavily affected by alteration by chlorite/serpentine, sericite and saussurite along grain boundaries, fractures and in grain centres in both sections. In 170-2,1 the grain size is primarily medium grained with a range from medium to fine grained. In 170-2,2 the grain size is primarily medium grained with a range from coarse to fine grained. The plagioclase content in the two samples at 170-2 is determined by the XRD analysis at IGP, and is given in Figure 31.

Orthopyroxene: Non-pseudomorph grains only identified in 170-2,2. All grains are completely pseudomorph at 170-2,1. Unaltered and pseudomorph grains contains Fe-Ti-oxide lamellas. At 170-2,2 the grain size is fine to medium grained with subhedral to anhedral, equant grain shapes. The grains are moderately to heavily fractured and partially to heavily affected by alteration by talc and clinopyroxene along boundaries, fractures and in grain centres. The boundaries vary between straight and lobate. The orthopyroxene content in the two samples at 170-2 is determined by the XRD analysis at Titania, and is given in Figure 31.

Biotite: Biotite is identified in both sections at 170-2. The biotite is identified by varying pleochroism of brown colours. The grains have euhedral to subhedral, tabular, laths and equant grain shapes with mostly straight and some lobate borders. The grains are partially fractured in both sections. The biotite often occurs in aggregates with ilmenite ± magnetite ± sulphides, or as inclusions in plagioclase. Some biotite grains contain ilmenite inclusions. In 170-2,1 the grain size is fine grained while the grains in 170-2,2 are fine to medium grained. The biotite content in the two samples at 170-2 is determined by the XRD analysis at IGP, and is given in Figure 31.

Talc: Talc is identified in both sections at 170-2 and appears as the main alteration product in altered and pseudomorph orthopyroxene. The grain size is very fine with single grains being indistinguishable from each other. The talc content in the two samples at 170-2 is determined by the XRD analysis at IGP, and is given in Figure 31.

Chlorite/Serpentine: Chlorite and serpentine are identified in both sections and often occurs in a mix with each other, with an indistinguishable grain size making it difficult to differentiate between the two minerals. The minerals occur in fractures and as reaction rims especially along plagioclase and pseudomorph orthopyroxene. The chlorite/ serpentine content in the two samples at 170-2 is determined by the XRD analysis at IGP, and is given in Figure 31. Serpentine is identified as antigorite in the XRD analysis.

Muscovite: Muscovite occurs as alteration product of plagioclase in both sections, often related to dusty, cryptocrystalline aggregates in the plagioclase. The grain size is very fine grained with indistinguishable grain shapes. The muscovite content in the two samples at 170-2 is determined by the XRD analysis at IGP, and is given in Figure 31.

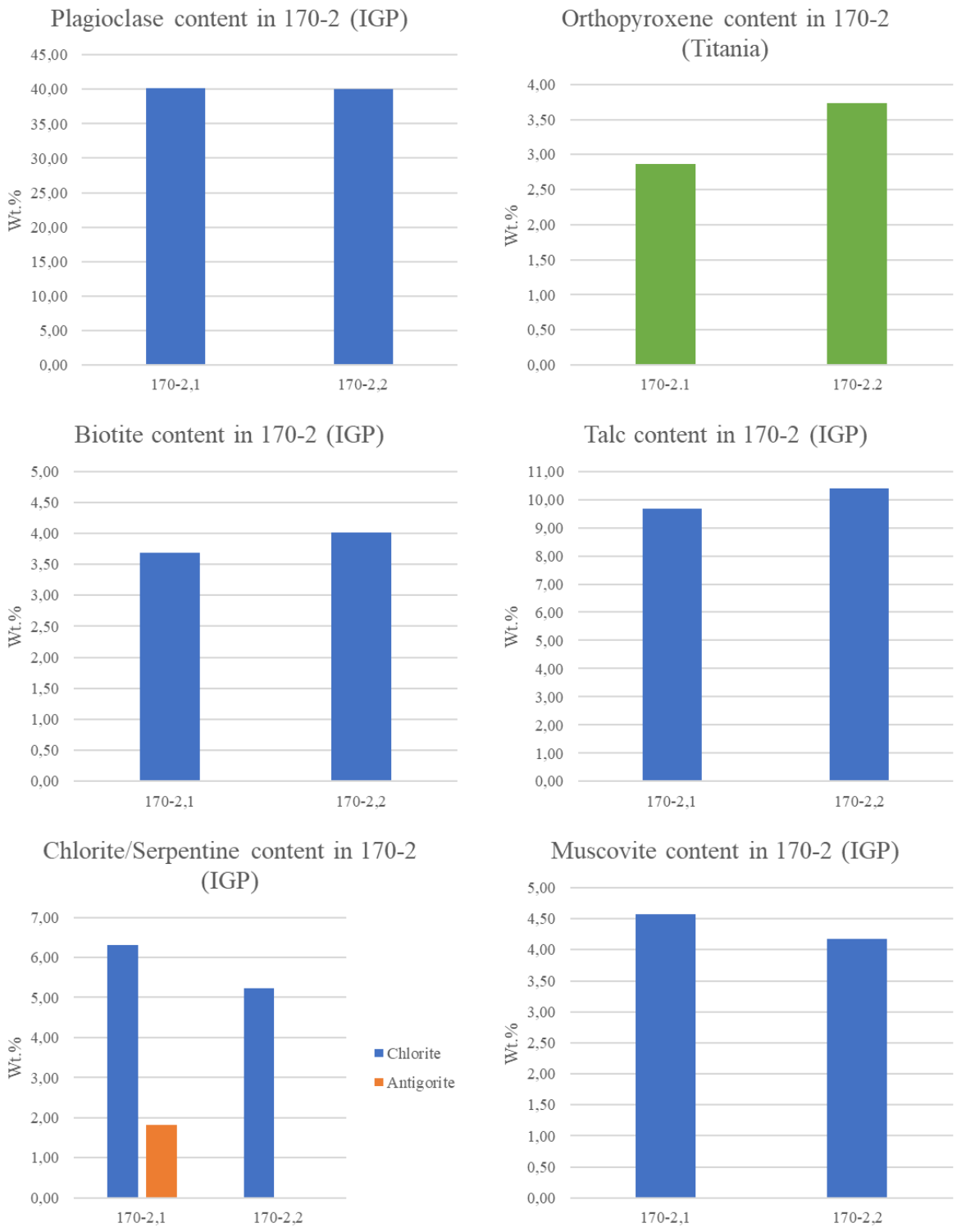

Figure 31: *The plagioclase, orthopyroxene, biotite, talc, chlorite/serpentine and muscovite content in alteration zone 170-2 determined by the XRD analyses from IGP and Titania.*

Olivine: Olivine is identified in both sections at 170-2. The grain size is medium to fine grained with subhedral to euhedral, equant grain shapes. The grains are heavily fractured, with straight and lobate boundaries in both sections. The olivine often occurs in aggregates with ilmenite or as inclusions in pyroxene. A cryptocrystalline mineral(assemblage) fills in the fractures in the olivine. The olivine content in the two samples at 170-2 is determined by the XRD analysis at Titania, and is given in Figure 32.

Quartz: Quartz is only identified in section 170-2,2. The grain size is fine grained with anhedral to subhedral, equant grain shapes. The grains have straight and lobate boundaries and contains few to no fractures. No sign of undulate extinction is registered. The quartz content in the two samples at 170-2 is determined by the XRD analysis at IGP, and is given in Figure 32.

Clinopyroxene: Clinopyroxene is only identified in 170-2,2 and occur as an alteration product in pseudomorph orthopyroxene. The grain size is fine grained with subhedral to anhedral, equant grain shapes. The boundaries vary between straight and lobate, and the grains are partially fractured. The clinopyroxene content in the two samples at 170-2 is determined by the XRD analysis at Titania, and is given in Figure 32.

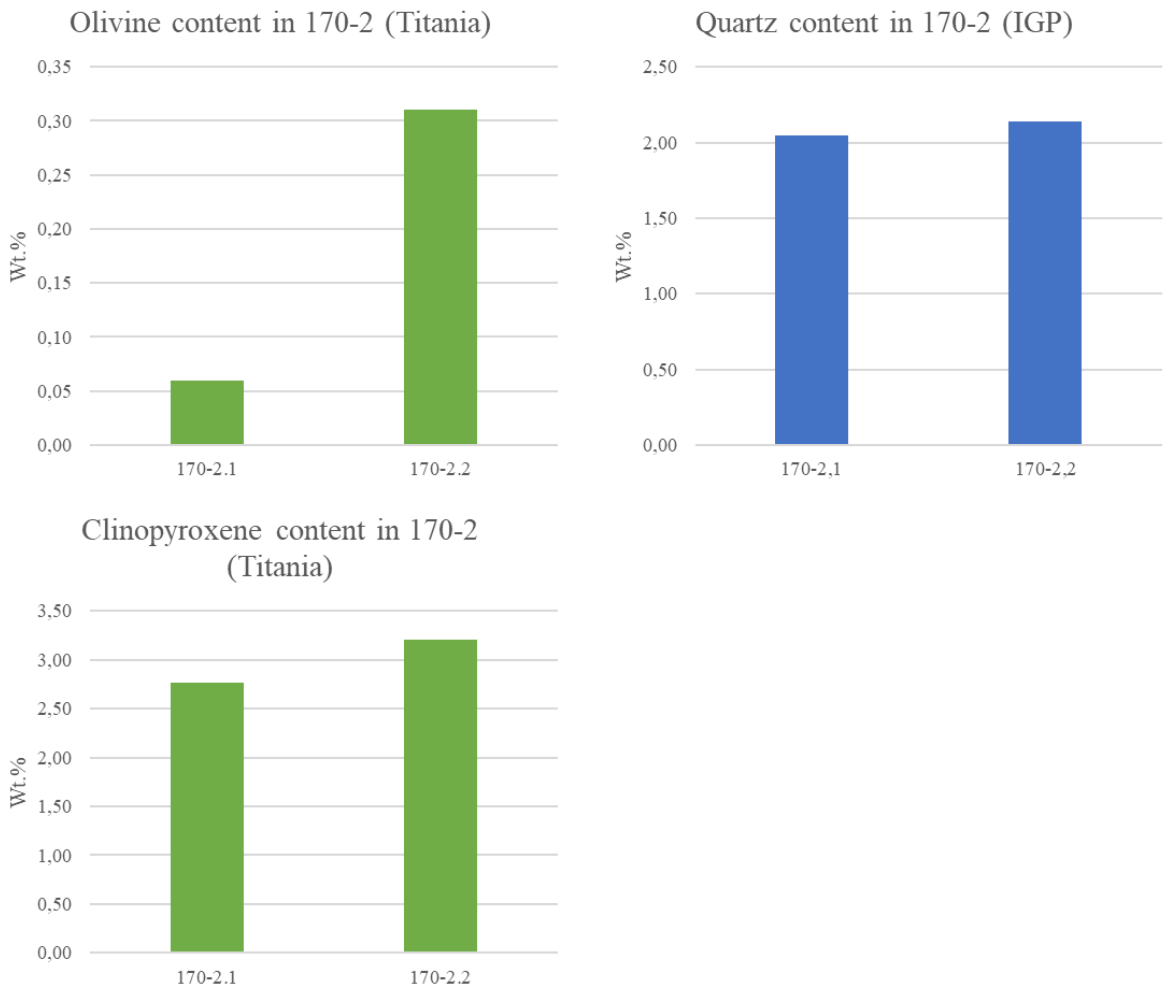

Figure 32: *The olivine, quartz and clinopyroxene content in alteration zone 170-2 determined by the XRD analyses from IGP and Titania.*

5.4.3.2 Oxides

Ilmenite: Ilmenite is identified in both sections at 170-2. The grain size is fine to medium grained with subhedral to anhedral, equant grain shapes. The boundaries vary between straight and lobate, and the grains are partially to moderately fractured. The ilmenite is partially affected by alteration by rutile along boundaries, fractures and in some grain centres in both sections. The ilmenite often occurs as inclusions in plagioclase, orthopyroxene and biotite, and in aggregates with magnetite ± biotite ± sulphides ± rutile. The ilmenite contains hematite exsolution lamellas. The ilmenite content in the two samples at 170-2 is determined by the XRD analysis at IGP, and is given in Figure 33.

Rutile: Rutile is identified in both sections at 170-2 and occur as an alteration product of ilmenite along boundaries, fractures and in some grain centres. The grain size is fine to very fine grained with anhedral, equant grain shapes. The grain boundaries vary between straight and lobate with the grains being partially fractured. The rutile often occurs in aggregates with ilmenite ± magnetite ± biotite ± sulphides. The rutile content in the two samples at 170-2 is determined by the XRD analysis at Titania, and is given in Figure 33.

Magnetite: Magnetite is identified in both sections at 170-2. The magnetite often occurs in aggregates with ilmenite ± biotite ± rutile ± sulphides. The boundaries vary between straight and lobate, and the magnetite contains cryptocrystalline inclusions in both sections. At 170-2,1 the grain size is fine grained with subhedral, equant grain shapes. The grains are moderately fractured with cryptocrystalline mineral appearing along some of the boundaries. At 170-2,2 the grain size is fine to medium grained with subhedral to anhedral, equant shapes. The grains are moderately to heavily fractured and contains spinel inclusions. The magnetite content in the two samples at 170-2 is determined by the XRD analysis at IGP, and is given in Figure 33.

Hematite: Hematite occur as exsolution lamellas in ilmenite in both sections. The hematite content in the two samples at 170-2 is determined by the XRD analysis at Titania, and is given in Figure 33.

Spinel: Spinel is only identified in section 170-2,2. The grain size is fine to very fine grained with acicular grain shapes. The borders vary from straight to lobate and the grains are partially fractured. The spinel occurs exclusively as inclusions in magnetite. The spinel content in the two samples at 170-2 is determined by the XRD analysis at Titania, and is given in Figure 33.

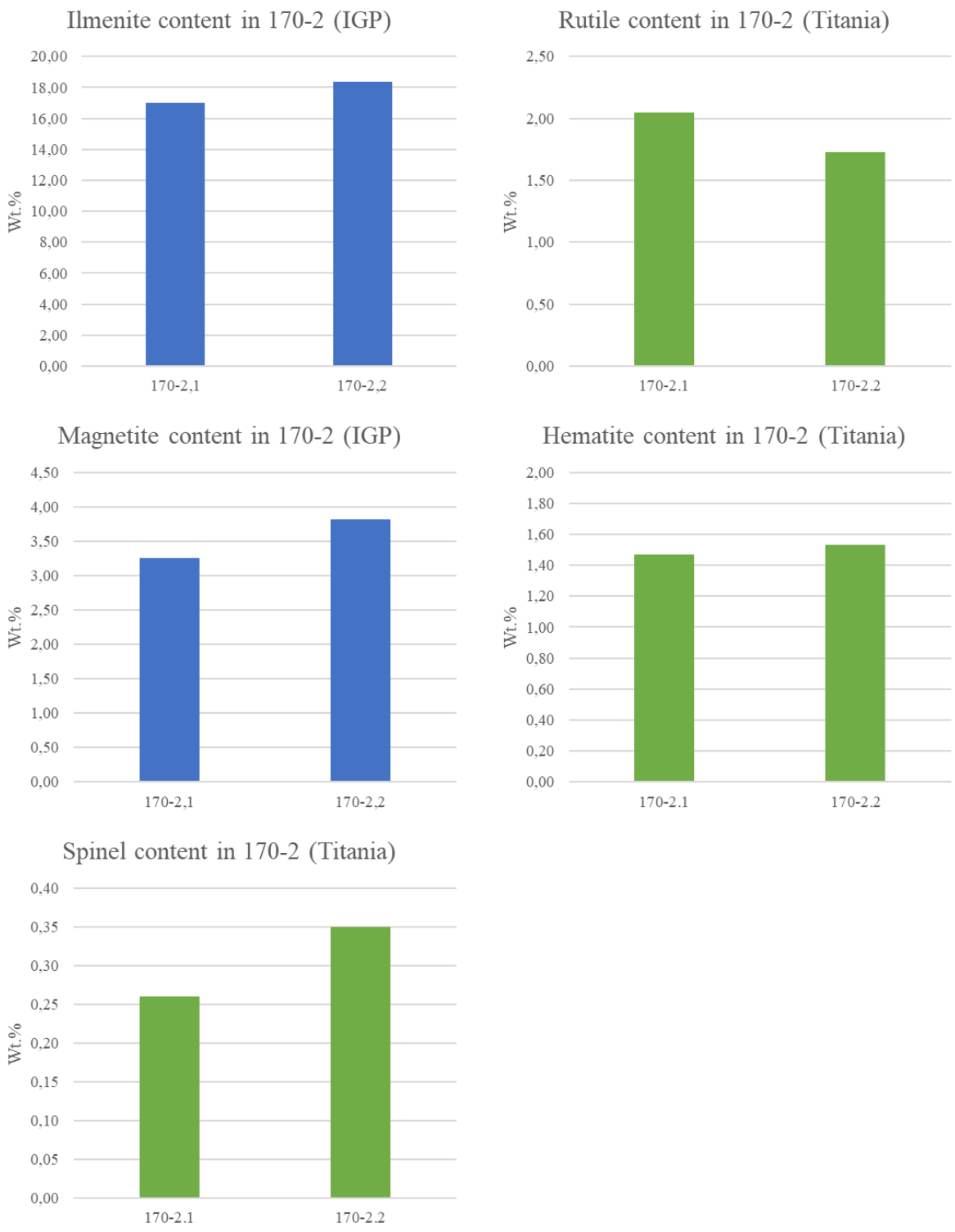

Figure 33: *The ilmenite, rutile, magnetite, hematite and spinel content in alteration zone 170-2 determined by the XRD analyses from IGP and Titania.*

5.4.3.3 Sulphides

The sulphides were not a main target during the investigation and a differentiation between different sulphide phases was not conducted. Sulphides are only identified in 170-2,1. The sulphides are dominated by a pyrite phase and have a fine to very fine grain size. The grains have subhedral to anhedral, equant grain shapes, and have straight and lobate borders. The grains are partially fractured and occurs sporadically throughout the section often in aggregates with ilmenite ± magnetite ± biotite. The pyrite content in the two samples at 170-2 is determined by the XRD analysis at IGP, and is given in Figure 34.

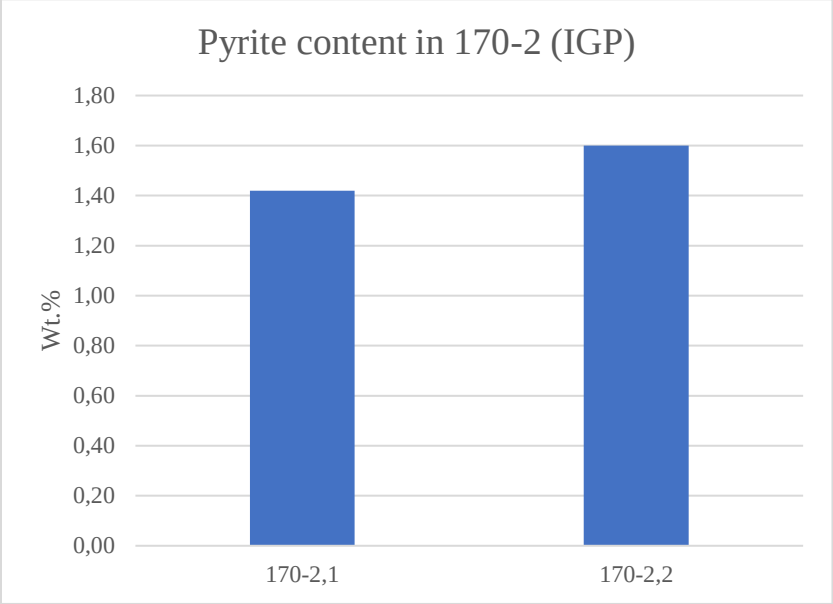

Figure 34: *The pyrite content in alteration zone 170-2. Pyrite is identified in both samples by XRD at 1,42 and 1,60 Wt.%.*

5.4.3.4 Identification and quantification of additional mineral phases at AM-SKOG-H-170-2

The XRD at Titania identified and quantified the minerals shown in Figure 35. Some of the minerals identified by the XRD were not identified in the thin sections from 170-2,1 and 170-2,2 during the optical investigation, and includes: calcite (0,15 and 0,16 Wt.%) and apatite (0,02 and 0 Wt.%).

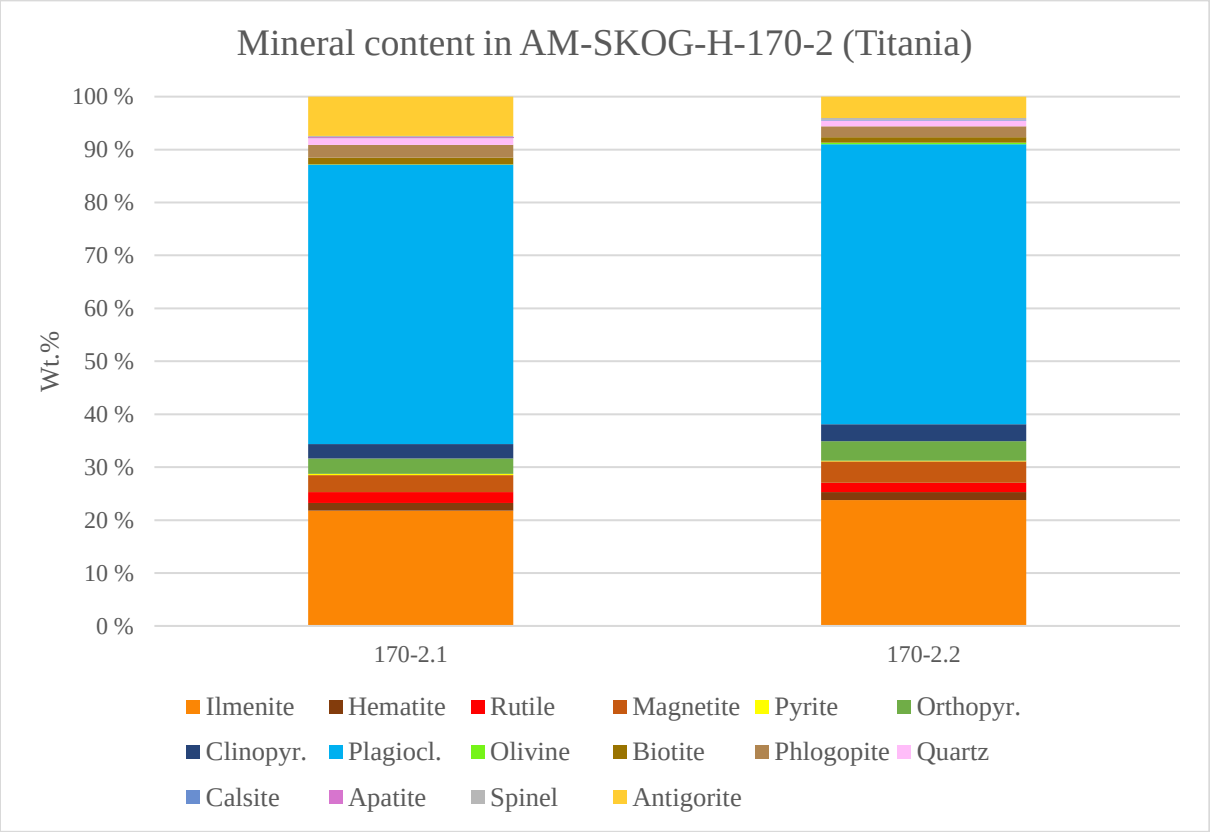

Figure 35: *The XRD analysis at Titania provided the following mineral identification and quantification for the samples in alteration zone 170-2. Mineral phases that were identified by XRD but not in the thin sections includes: calcite (0 ,15 and 0,16 Wt.%) and apatite (0,02 and 0 Wt.%). The analysis at Titania also provides two types of biotite: biotite and phlogopite.*

The XRD at IGP identified and quantified the minerals shown in Figure 36. Some of the minerals identified by the XRD were not found in the thin sections from 170-2,1 and 170-2,2 during the optical investigation, and includes: hornblende (2,70 and 2,43 Wt.%), calcite (0,09 and 0,08 Wt.%) and siderite (0,82 and 0,85 Wt.%). Pyroxene is identified in both the XRD and the thin sections but is not separated into ortho- and clinopyroxene. The pyroxene is quantified to 5,70 Wt.% at 170-2,1 and 6,59 Wt.% at 170-2,2.

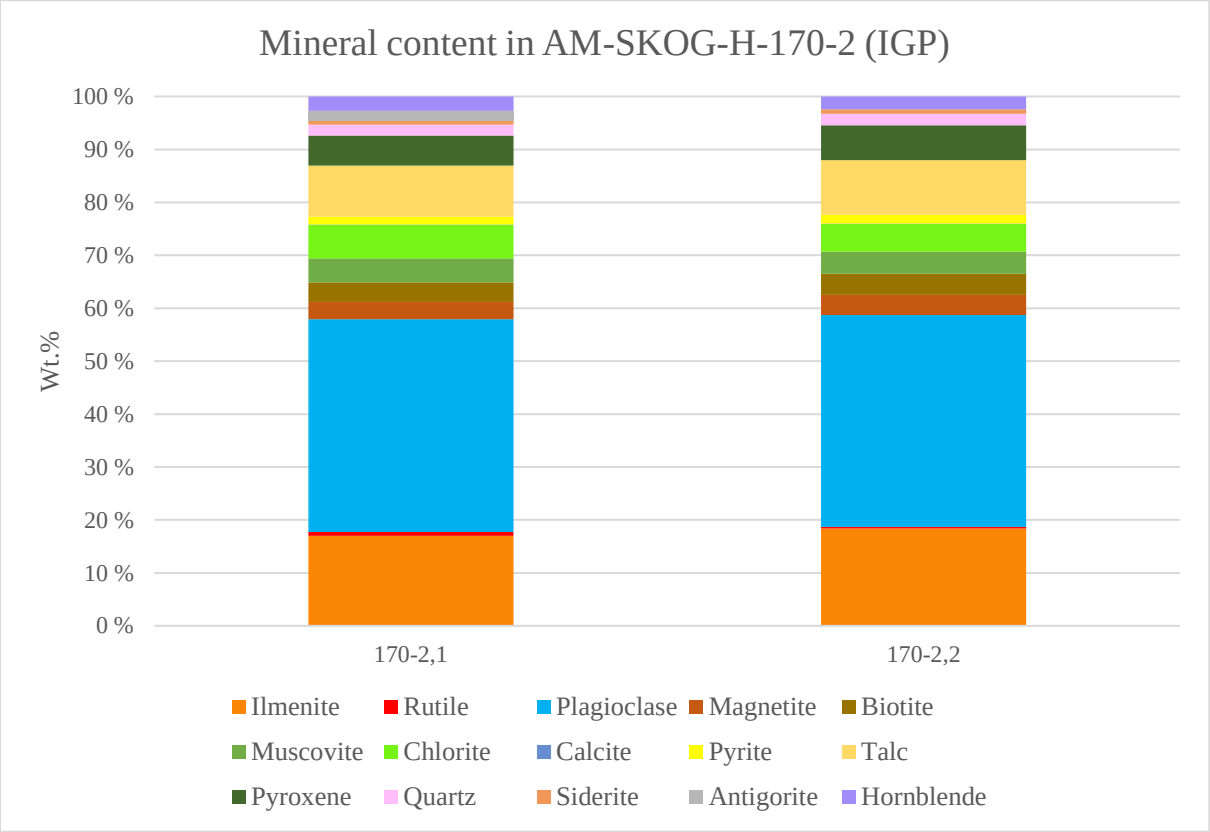

Figure 36: *The XRD analysis at IGP provided the following mineral identification and quantification for the samples in alteration zone 170-2. Mineral phases that were identified by XRD but not in the thin sections includes: hornblende (2,70 and 2,43 Wt.%), calcite (0,09 and 0,08 Wt.%) and siderite (0,82 and 0,85 Wt.%). Pyroxene is identified but not separated into ortho- and clinopyroxene.*

5.4.4 AM-SKOG-H-170-3

5.4.4.1 Silicates

Plagioclase: Plagioclase is identified in all sections at 170-3. The plagioclase contains examples of albite-, pericline and Carlsbad twinning in all sections. The plagioclase is altered by chlorite/serpentine, sericite, saussurite and kaolinite at varying degrees. Grains in all sections contains inclusions primarily ilmenite and biotite with some inclusions of rutile and pyroxene. In 170-3,1 the grain size is very fine to medium grained, with subhedral, tabular and anhedral, equant grain shapes. The grains are heavily fractured and heavily affected by alteration. In 170-3,2 the grain size is medium to fine grained with euhedral to subhedral, tabular and subhedral to anhedral equant grain shapes. The grains are partially to heavily fractured and partially to heavily altered. In 170-3,3 the grain size is medium to fine grained with subhedral to euhedral, tabular and equant grains. The grains are partially fractured and partially altered. The plagioclase content in the samples at 170-3 is determined by the XRD analysis at IGP, and is given in Figure 37.

Biotite: Biotite is identified in all sections at 170-3 and is easily identified by varying pleochroism of brown colours. At 170-3,1 the grains are fine to very fine grained with anhedral, equant and laths grain shapes. The grains are heavily fractured. At 170-3,2 the grains are fine grained with subhedral to anhedral, tabular/laths grain shapes. The grains are partially fractured with mostly straight boundaries. At 170-3,3 the grains are fine grained with subhedral to anhedral, tabular/laths grain shapes. The grains are partially fractured with mostly straight boundaries. The biotite content in the samples at 170-3 is determined by the XRD analysis at IGP, and is given in Figure 37.

Talc: Talc is identified in section 170-3,2 and 170-3,3. The talc occurs as an alteration product of altered orthopyroxene altering both along boundaries and in grain centres. In 170-3,2 the grains are very fine to fine grained with subhedral, fibrous/laths grain shapes. The boundaries are mostly straight, and the grains are generally not fractured. In 170-3,2 the grains are very fine grained with indistinguishable grain shapes. The talc content in the samples at 170-3 is determined by the XRD analysis at IGP, and is given in Figure 37.

Chlorite/Serpentine: Chlorite/serpentine is identified in all sections at 170-3. The grain size is very fine grained with often indistinguishable shape. The chlorite/serpentine alter plagioclase and some orthopyroxene, and appears in larger section cutting fractures. In 170-3,1 AM identifies serpentine in what is likely pseudomorph plagioclase and generally throughout the section. The grains have anhedral, equant/laths shapes. In 170-3,2 and 170-3,3 the serpentine is very fine grained with indistinguishable shapes. The chlorite/serpentine content in the samples at 170-3 is determined by the XRD analysis at IGP, and is given in Figure 37. Serpentine is identified as antigorite in the XRD analysis.

Orthopyroxene: Orthopyroxene is identified in section 170-3,3. The grain size is fine to medium grained with subhedral, tabular and equant grain shapes. The boundaries are mostly straight with some lobate. The grains are moderately to heavily fractured and some grains are affected by alteration by talc and serpentine along grain boundaries and in grain centres. The orthopyroxene contains Fe-Ti-oxide and biotite exsolution lamellas. The AM identifies very fine-grained remains of orthopyroxene among the talc in near pseudomorph orthopyroxene grains in section 170-3,2. The orthopyroxene content in the samples at 170-3 is determined by the XRD analysis at Titania, and is given in Figure 37.

Clinopyroxene: Clinopyroxene is identified in section 170-3,3. The grain size is fine grained with subhedral to anhedral, equant grain shapes. The grains are heavily to very heavily fractured and have irregular boundaries. The orthopyroxene content in the samples at 170-3 is determined by the XRD analysis at Titania, and is given in Figure 37.

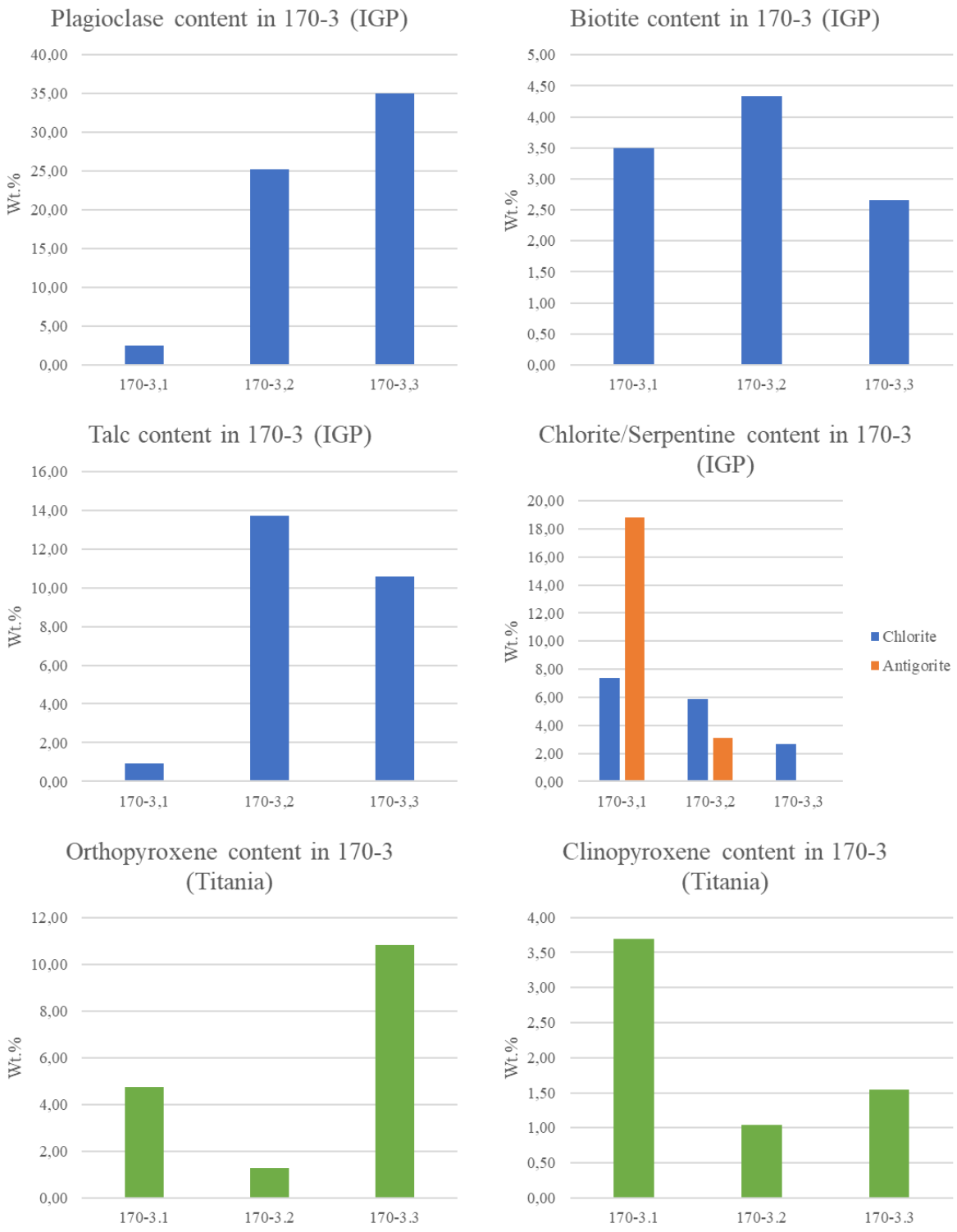

Figure 37: *The plagioclase, biotite, talc, chlorite/serpentine, orthopyroxene and clinopyroxene content in alteration zone 170-3 determined by the XRD analyses from IGP and Titania.*

Calcite/Ankerite: Calcite/ankerite are identified in section 170-3,1 and calcite is identified in section 170-3,2. The AM identified ankerite in 170-3,1 while the XRD identifies it as dolomite. In 170-3,1 the calcite and ankerite have a fine to very fine grain size, with subhedral to anhedral prismatic/equant grain shapes. The calcite/ankerite contains few fractures and appears sporadically throughout the section and in fractures with a vein like texture. In 170-3,2 the calcite has a very fine grain size, with indistinguishable shapes. The calcite contains few fractures and occurs in larger section cutting fractures. The calcite/ankerite content in the samples at 170-3 is determined by the XRD analysis at IGP, and is given in Figure 38.

Quartz: Quartz is identified in section 170-3,1. The grain size is very fine to fine grained with anhedral, equant grain shapes. The grains are not fractured and have straight and lobate boundaries. The quartz occurs sporadically throughout the section and often occurs in vein like textures in larger fractures. The quartz content in the samples at 170-3 is determined by the XRD analysis at IGP, and is given in Figure 38.

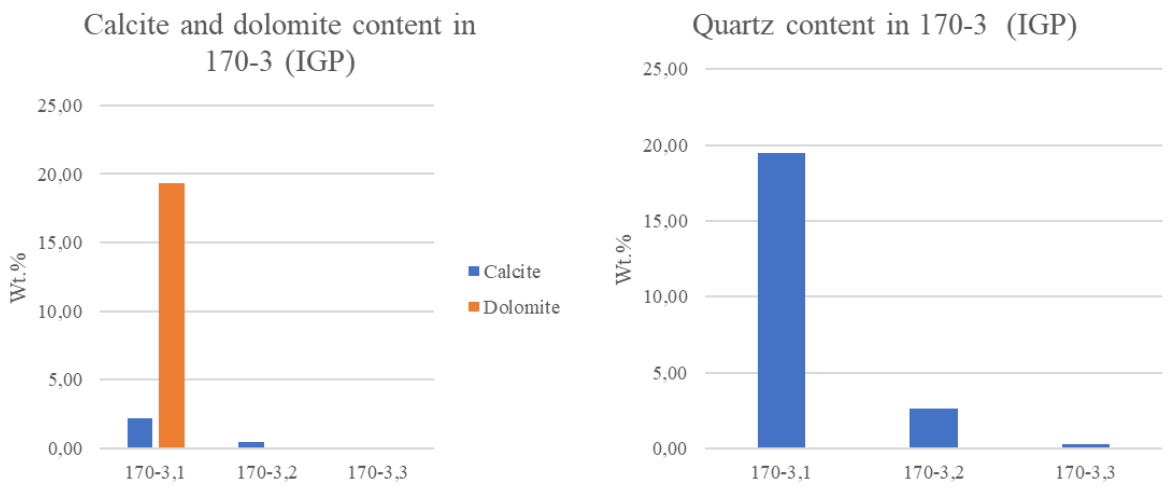

Figure 38: *The calcite/dolomite and quartz content in alteration zone 170-3. The dolomite is identified as ankerite in the AM analysis.*

5.4.4.2 Oxides

Ilmenite: Ilmenite is identified in all sections at 170-3. The ilmenite often occurs in aggregates with magnetite ± biotite ± sulphides ± rutile. The grain size is fine to very fine grained with straight and lobate boundaries in all sections. At 170-3,1 the grains have anhedral, equant shapes, are heavily fractured and heavily altered by rutile. At 170-3,2 the grains have anhedral, equant shapes, are partially to moderately fractured and partially to moderately affected by alteration. At 170-3,3 the grains have subhedral to anhedral, equant grain shapes, are partially fractured and not affected by alteration. The ilmenite contains hematite exsolution lamellas in section 170-3,2 and 170-3,3. The ilmenite content in the samples at 170-3 is determined by the XRD analysis at IGP, and is given in Figure 39.

Magnetite: Magnetite is identified in section 170-3,2 and 170-3,3. The magnetite contains acicular spinel lamellas and often occurs in aggregates with ilmenite ± biotite ± sulphides. The grain size is fine to very fine grained and the boundaries vary from straight to lobate in both sections. At 170-3,2 the grains have anhedral, equant grain shapes, and the grains are moderately to heavily fractured. At 170-3,3 the grains have anhedral to subhedral, equant shapes, and the grains are partially to moderately fractured. The magnetite content in the samples at 170-3 is determined by the XRD analysis at IGP, and is given in Figure 39.

Rutile: Rutile is identified in section 170-3,1 and 170-3,2. The rutile appear as an alteration product of ilmenite and as singular grains. The rutile alters ilmenite from the boundaries and fractures inwards, often forming a corona texture. The grain size is very fine to fine grained with anhedral to subhedral, equant grain shapes. The grains are partially fractured, and the grain boundaries vary from straight to lobate. The rutile content in the samples at 170-3 is determined by the XRD analysis at Titania, and is given in Figure 39.

Hematite: Hematite is identified in section 170-3,2 and 170-3,3. The hematite occurs as exsolution lamellas in ilmenite. The lamellas are acicular with a very fine grain size. The hematite content in the samples at 170-3 is determined by the XRD analysis at Titania, and is given in Figure 39.

Spinel: Spinel is identified in section 170-3,2 and 170-3,3. The spinel occurs as inclusions in magnetite and are fine grained with acicular shape. The boundaries are straight and lobate and are partially fractured. The spinel content in the samples at 170-3 is determined by the XRD analysis at Titania, and is given in Figure 39.

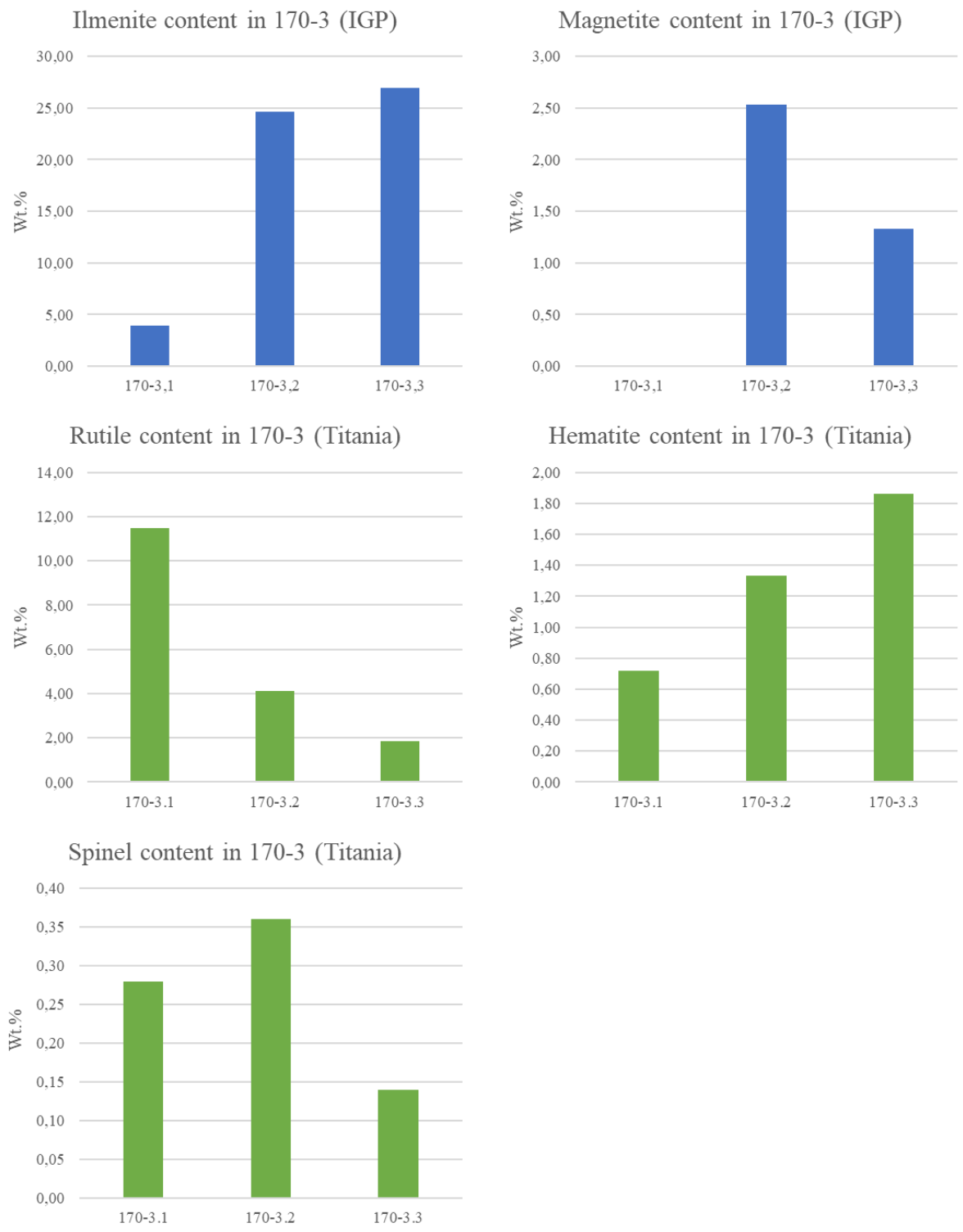

Figure 39: *The ilmenite, magnetite, rutile, hematite and spinel content in alteration zone 170-3 determined by the XRD analyses from IGP and Titania.*

5.4.4.3 Sulphides

The sulphides were not a main target during the investigation and a differentiation between different sulphide phases was not conducted. Sulphides are identified in all sections. The sulphides are dominated by a pyrite phase and have a fine to very fine grain size. The grains have anhedral, equant grain shapes with straight and lobate boundaries. The grains are partially to heavily fractured and occurs sporadically throughout the sections often associated with Fe-Ti- oxides. The pyrite content in the samples at 170-3 is determined by the XRD analysis at Titania, and is given in Figure 40.

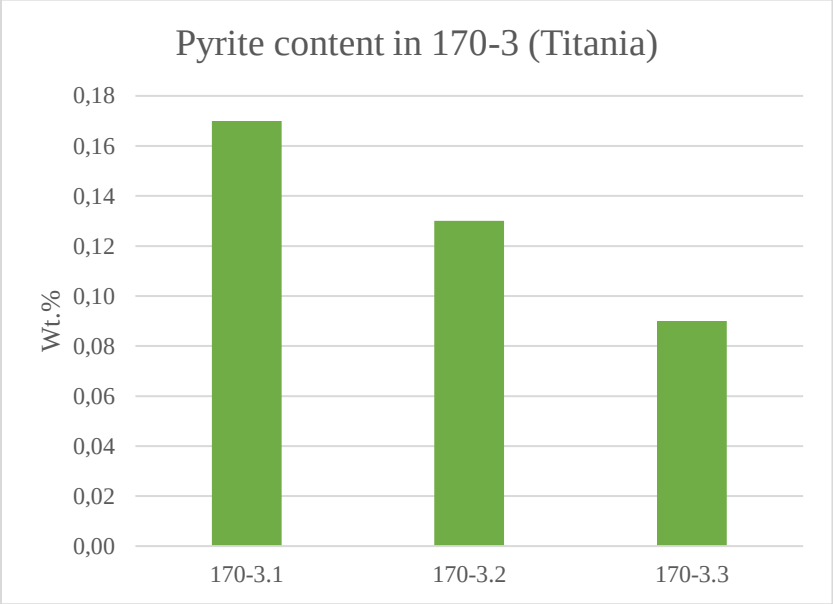

Figure 40: *The pyrite content in alteration zone 170-3. The XRD analysis at Titania identified pyrite in all samples with a range from 0,09 – 0,17 Wt.%.*

5.4.4.4 Identification and quantification of additional mineral phases at AM-SKOG-H-170-3

From the AM analysis additional mineral phases above 1 Wt.% will be presented. The entire AM analysis is presented in Appendix D. The only additional mineral phase above 1 Wt.% is the clay mineral kaolinite, which is found as an alteration product of plagioclase in the three analysed sections. Figure 41 shows the amount of kaolinite in the sections.

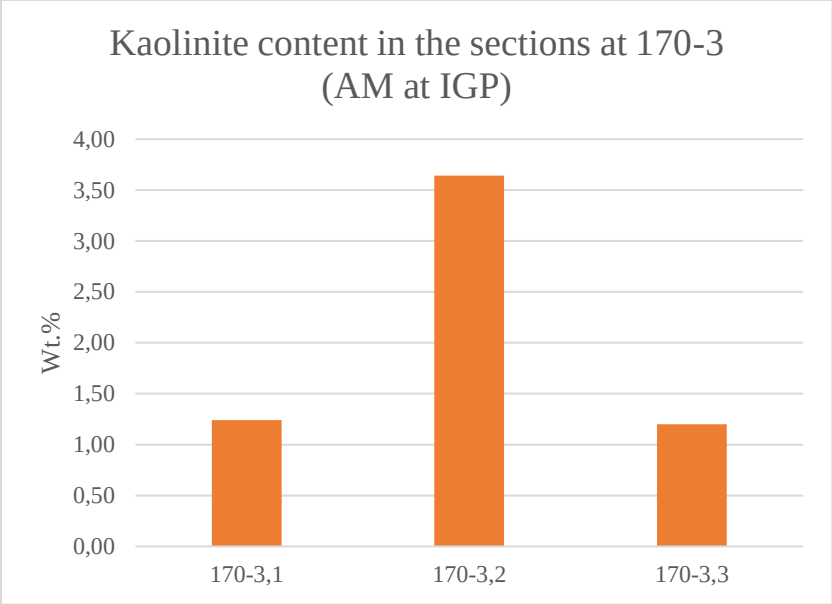

Figure 41: *The kaolinite content in the three analysed sections at 170-3 quantified by the AM at IGP.*

The XRD analysis at Titania identified and quantified the minerals shown in Figure 42. Some of the minerals identified by the XRD analysis were not identified in the thin sections during the optical investigation, and includes: olivine (0 – 1,70 Wt.%) and apatite (0 – 0,85 Wt.%).

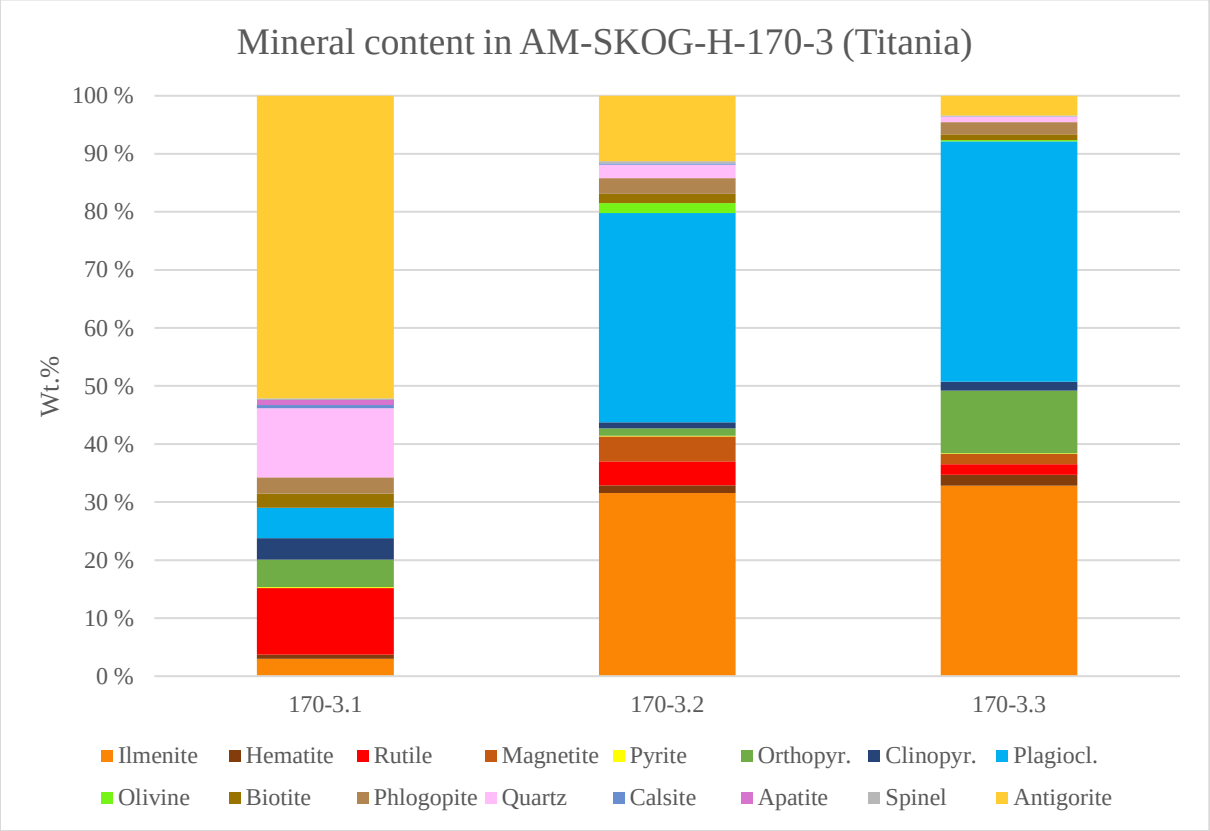

Figure 42: *The XRD analysis at Titania provided the following mineral identification and quantification for the samples in alteration zone 170-3. Mineral phases that were identified by XRD but not in the thin sections includes: olivine (0 – 1,70 Wt.%) and apatite (0 – 0,85 Wt.%).*

The XRD analysis at IGP identified and quantified the minerals shown in Figure 43. Some of the minerals identified by the XRD analysis were not identified in the thin sections during the optical investigation, and includes: muscovite (3,37 – 4,95 Wt.%) and hornblende (0 – 3,23 Wt.%).

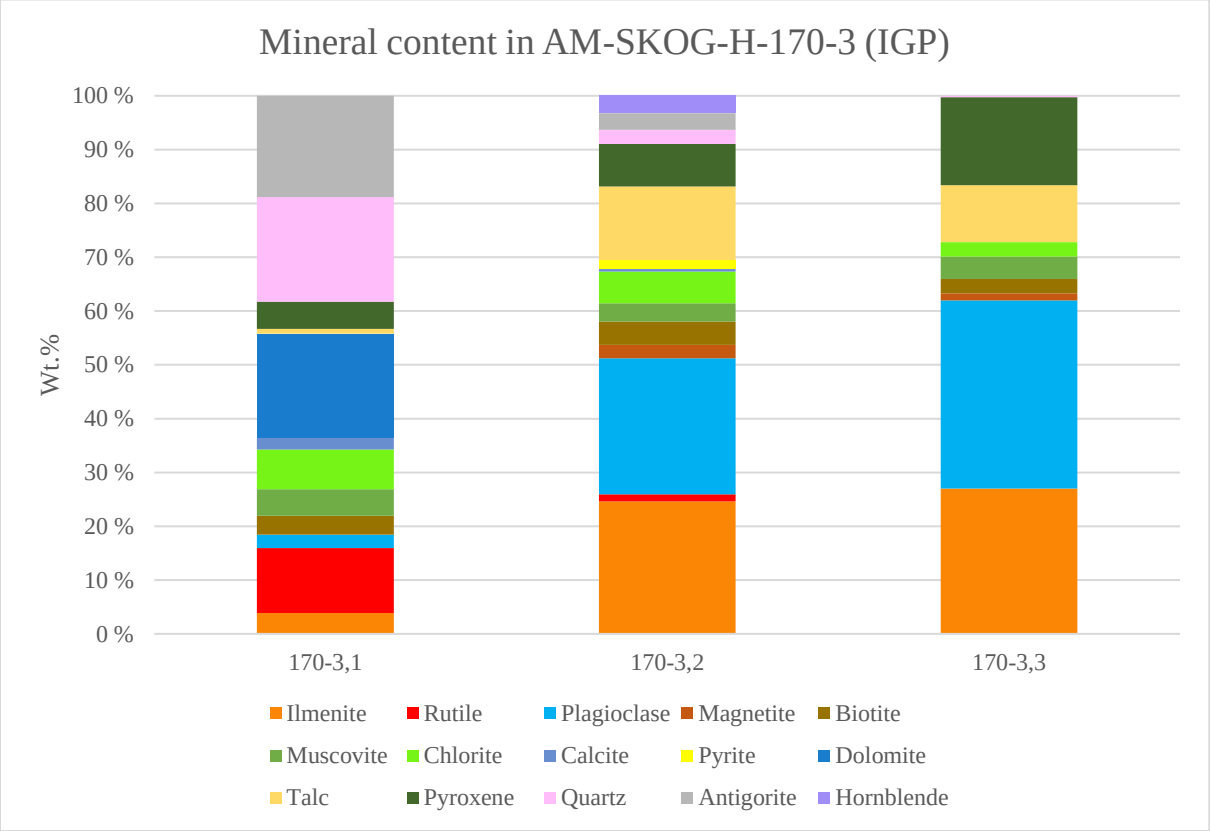

Figure 43: *The XRD analysis at IGP provided the following mineral identification and quantification for the samples in alteration zone 170-3. Mineral phases that were identified by XRD but not in the thin sections includes: muscovite (3,37 – 4,95 Wt.%) and hornblende (0 – 3,23 Wt.%).*

5.4.5 AM-SKOG-H-185-1

5.4.5.1 Silicates

Plagioclase: Plagioclase is identified in all sections and is identified by distinct twinning features with examples of albite-, pericline and Carlsbad twinning occurring in all sections. Some of the plagioclase grains contains inclusions of ilmenite and biotite and the grain boundaries vary between straight and lobate in all sections. The plagioclase is affected by alteration by chlorite/serpentine, sericite and saussurite at varying degrees in the three sections along boundaries, fractures and in grain centres. At 185-1,1 the grain size is fine to medium grained with anhedral to subhedral, equant shapes. The grains are heavily fractured and heavily affected by alteration primarily by chlorite/serpentine that covers most grain centres and fractures. Many grains are pseudomorph. At 185-1,2 the grain size is medium to fine grained with subhedral to anhedral, tabular and equant grain shapes. The grains are moderately to heavily fractured and moderately affected by alteration. At 185-1,3 the grain size is medium to fine grained with euhedral to subhedral, tabular and equant grain shapes. The grains are partially fractured and partially affected by alteration. The plagioclase content in the three samples at 185-1 is determined by the XRD analysis at IGP, and is given in Figure 44.

Orthopyroxene: Orthopyroxene appears only in 185-1,3 in non-pseudomorph form. The grain size is fine grained with subhedral, equant grain shapes. The grain boundaries vary from straight to lobate. The grains are heavily to very heavily fractured, and contain Fe-Ti oxide and biotite lamellas. In all the section original orthopyroxene grains had a fine to medium grain size and have been heavily affected by alteration by primarily talc and partially by clinopyroxene, chlorite/serpentine and quartz. All grains in 185-1,1 and 185-1,2 are pseudomorph and most grains in 185-1,3 are heavily affected along boundaries, fractures and grain centres. The pseudomorph orthopyroxene grains retains the Fe-Ti-oxide lamellas from the primary orthopyroxene. The orthopyroxene content in the three samples at 185-1 is determined by the XRD analysis at Titania, and is given in Figure 44.

Biotite: Biotite is present in all sections at 185-1. The grain size is fine grained with subhedral to euhedral, tabular, laths and equant grain shapes. Grain boundaries are mostly straight, with some lobate boundaries. The grains vary from being partially to moderately fractured and show a varying pleochroism of brown colours. The biotite grains often occur in aggregates with ilmenite ± magnetite ± sulphides. Biotite also appears as inclusions in plagioclase and pseudomorph orthopyroxene. The biotite content in the three samples at 185-1 is determined by the XRD analysis at IGP, and is given in Figure 44.

Chlorite/Serpentine: Chlorite/Serpentine is identified in all sections. The chlorite/serpentine have an indistinguishable grain size making it difficult to separate the two minerals with optical microscope. The minerals appear as an alteration product of altered plagioclase and orthopyroxene primarily in fractures and along borders of other minerals. In section 185-1,1 the chlorite/serpentine also dominates in the grain centres, completely altering entire plagioclase grains and almost entire pyroxene grains, causing a greenish tint to the entire section. In 185-1,2 and 185-1,3 the chlorite/serpentine mixture is limited to fractures and borders and only partially alters pseudomorph orthopyroxene. The chlorite/serpentine content in the three samples at 185-1 is determined by the XRD analysis at IGP, and is given in Figure 44. Serpentine is identified as antigorite in the XRD analysis.

Talc: Talc is identified in all sections at 185-1 and appear as an alteration product in altered orthopyroxene. The grain size is very fine grained and single grains are often indistinguishable in all sections. The distinguishable grains have euhedral, tabular/laths shapes and have straight and lobate boundaries. The talc is often found in association with other alteration products such as clinopyroxene (185-1,2 and 185-1,3) and quartz (185-1,1 and 185-1,2). The talc surrounds the Fe-Ti- oxide lamellas found in primary orthopyroxene. The talc content in the three samples at 185-1 is determined by the XRD analysis at IGP, and is given in Figure 44.

Quartz: Quartz is identified in 185-1,1 and 185-1,2. The grain size is fine to very fine grained. The grains have subhedral, equant shapes with straight and lobate borders. The grains are little to partially fractured and often occurs in fractures or in grain centres of pseudomorph orthopyroxene. The quartz content in the three samples at 185-1 is determined by the XRD analysis at IGP, and is given in Figure 44.

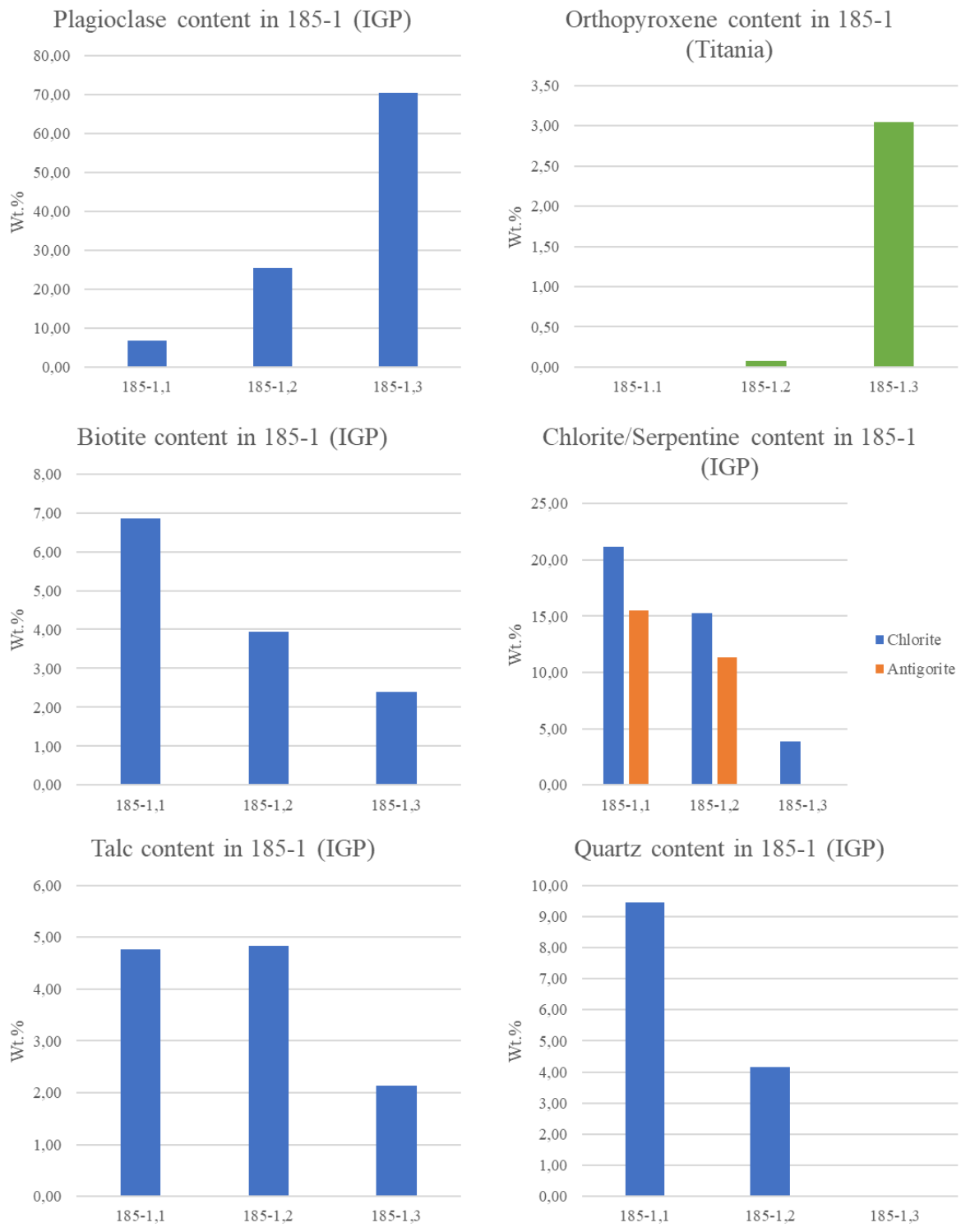

Figure 44: *The plagioclase, orthopyroxene, biotite, chlorite/serpentine, talc and quartz content in alteration zone 185-1 determined by the XRD analyses from IGP and Titania.*

Muscovite: Muscovite occurs as alteration product of plagioclase in all sections at 185-1. The muscovite is often related to dusty, cryptocrystalline aggregates in the plagioclase. The grain size is very fine grained with single grains being indistinguishable from each other. The muscovite content in the three samples at 185-1 is determined by the XRD analysis at IGP, and is given in Figure 45.

Clinopyroxene: Clinopyroxene is identified in 185-1,2 and 185-1,3 as it replaces altered primary orthopyroxene. The grains are fine grained with a subhedral to anhedral equant grain shapes. Grain boundaries varies from straight to lobate and the grains are moderately to heavily fractured. Occurs with other alteration products of altered orthopyroxene: talc ± quartz (in 185-1,2) ± chlorite/serpentine (in 185-1,3). The clinopyroxene content in the three samples at 185-1 is determined by the XRD analysis at Titania, and is given in Figure 45.

Olivine: Olivine is only identified in 185-1,3 with a medium to fine grain size. The grains have a subhedral to anhedral equant shape with straight and lobate borders. The olivine is heavily fractured with characteristic microfractures and high green interference colours. The olivine appears sporadically in the section. The olivine content in the three samples at 185-1 is determined by the XRD analysis at Titania, and is given in Figure 45.

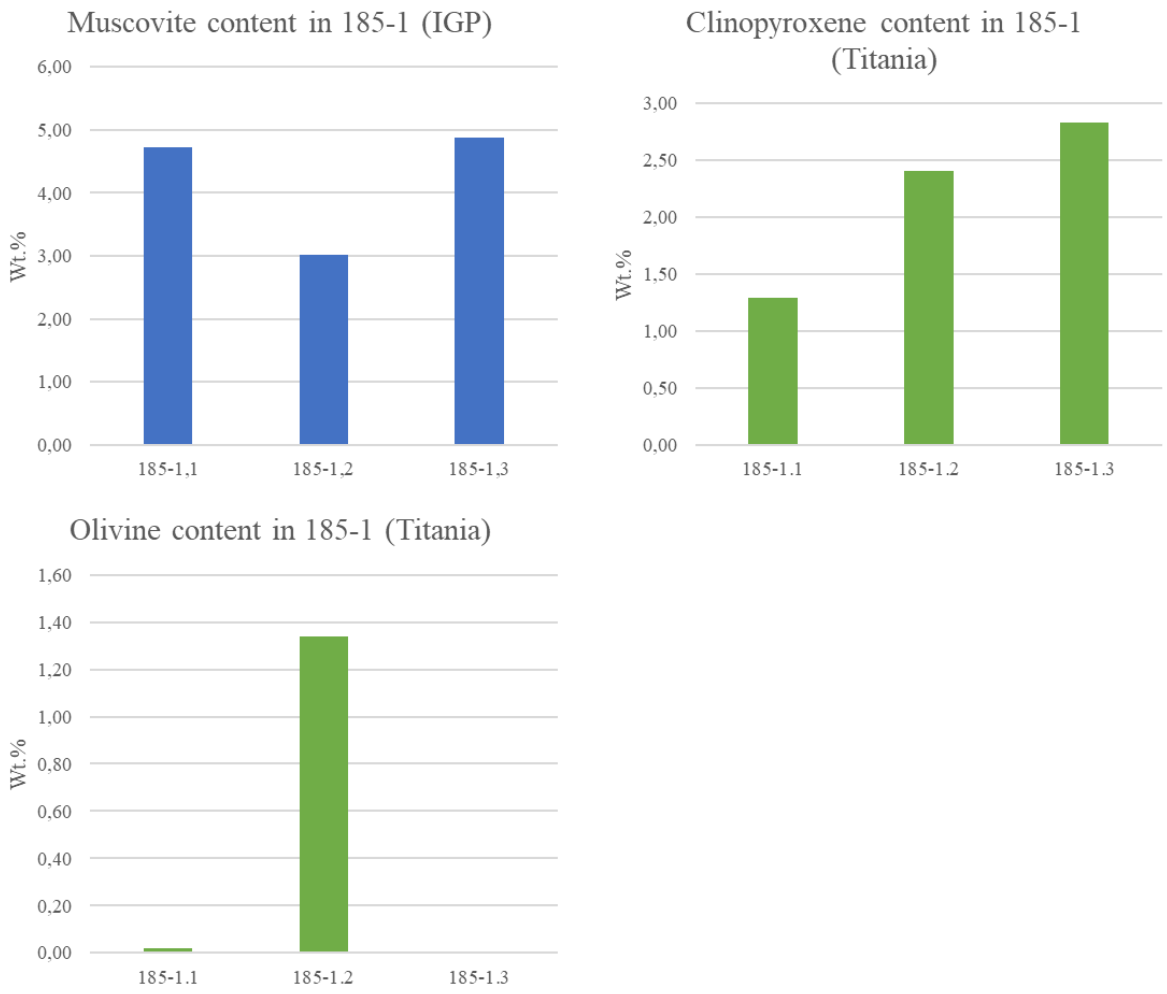

Figure 45: *The muscovite, clinopyroxene and olivine content in alteration zone 185-1 determined by the XRD analyses from IGP and Titania.*

5.4.5.2 Oxides

Ilmenite: Ilmenite is identified in all sections at 185-1. The grains have subhedral to anhedral, equant grain shapes, with boundaries that vary between straight and lobate in all sections. The ilmenite contains hematite exsolution lamellas in all sections. The ilmenite often occurs in aggregates with biotite ± rutile ± magnetite ± sulphides, and as inclusions in plagioclase and orthopyroxene. At 185-1,1 the grain size is fine to very fine grained. The grains are moderately to heavily fractured and moderately affected by alteration by rutile. At 185-1,2 the grain size is fine to medium grained. The grains are partially to moderately fractured and partially affected by alteration by rutile. At 185-1,3 the grain size is fine to very fine grained. The grains are heavily fractured and partially to moderately affected by alteration. Most to all grains contains < 25 µm inclusions creating a similar texture to that of magnetite. The mineral content in the inclusions are difficult to determine due to the size of the inclusions, but likely to be rutile. The ilmenite content in the three samples at 185-1 is determined by the XRD analysis at IGP, and is given in Figure 46.

Rutile: Rutile is present in all sections as an alteration product of ilmenite along boundaries, fractures and in grain centres. The grain size is very fine to fine grained with anhedral, equant grain shapes in all sections. The grains have no visible fractures and grain boundaries that vary between straight and lobate. The rutile content in the three samples at 185-1 is determined by the XRD analysis at Titania, and is given in Figure 46.

Magnetite: Magnetite is only identified in section 185-1,3. The grain size is fine to very fine grained with anhedral, equant grain shapes. The grains are heavily to very heavily fractured and contains a large number of cryptocrystalline inclusions. The magnetite often occurs in aggregates with ilmenite. Boundaries vary between straight and lobate. The magnetite content in the three samples at 185-1 is determined by the XRD analysis at IGP, and is given in Figure 46.

Hematite: Hematite occur as exsolution lamellas in ilmenite in all three sections. The hematite content in the three samples at 185-1 is determined by the XRD analysis at Titania, and is given in Figure 46.

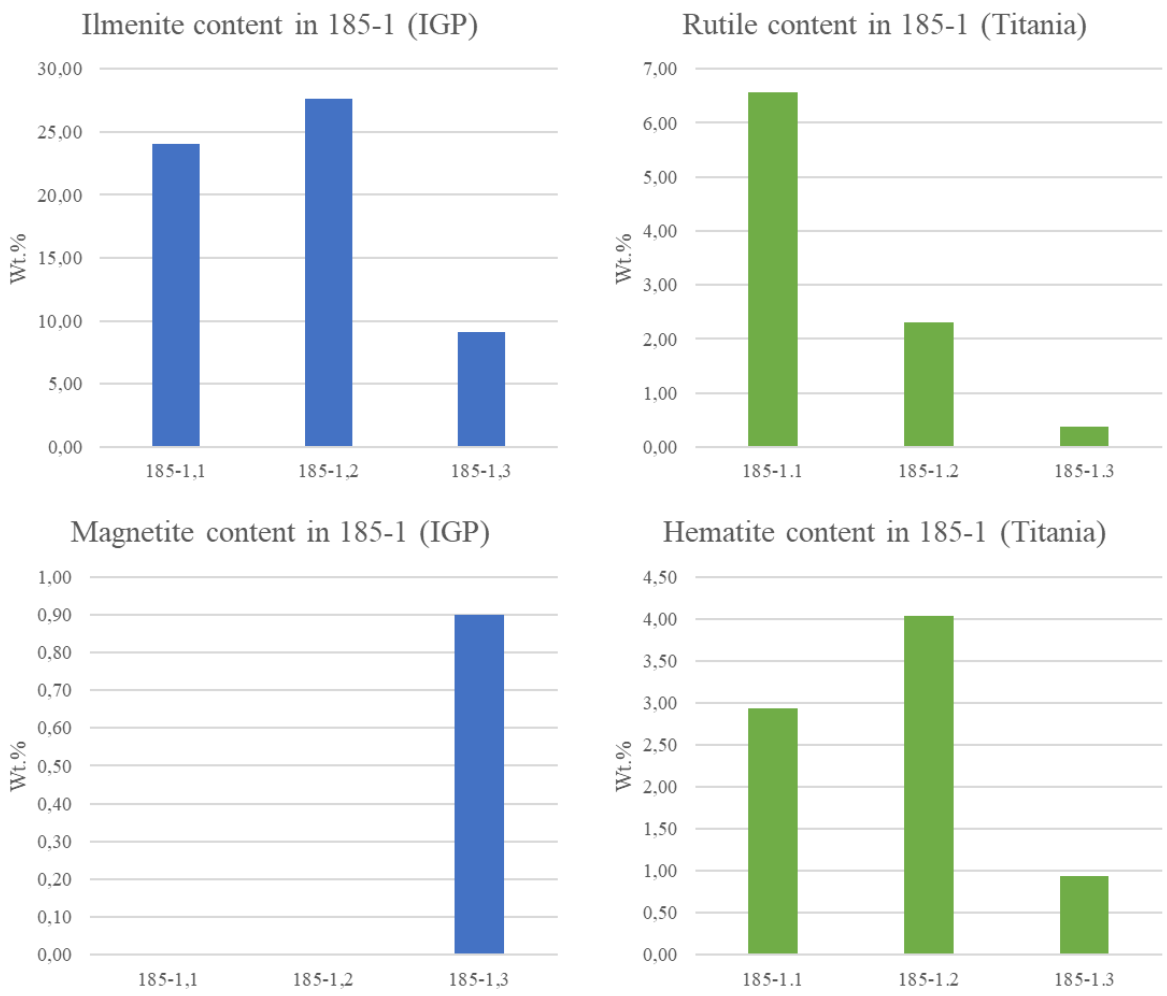

Figure 46: *The ilmenite, rutile, magnetite and hematite content in alteration zone 185-1 determined by the XRD analyses from IGP and Titania.*

5.4.5.3 Sulphides

The sulphides were not a main target during the investigation and a differentiation between different sulphide phases was not conducted. Sulphides are identified in all sections. The sulphides are dominated by a pyrite phase and have a fine to very fine grain size. The grains have anhedral and equant grain shapes with straight and lobate boundaries. The grains are heavily fractured in all sections except from 185-2,4 where they are moderately fractured. The sulphides occur sporadically throughout the sections. The pyrite content in the samples at 185-1 is determined by the XRD analysis at IGP, and is given in Figure 47.

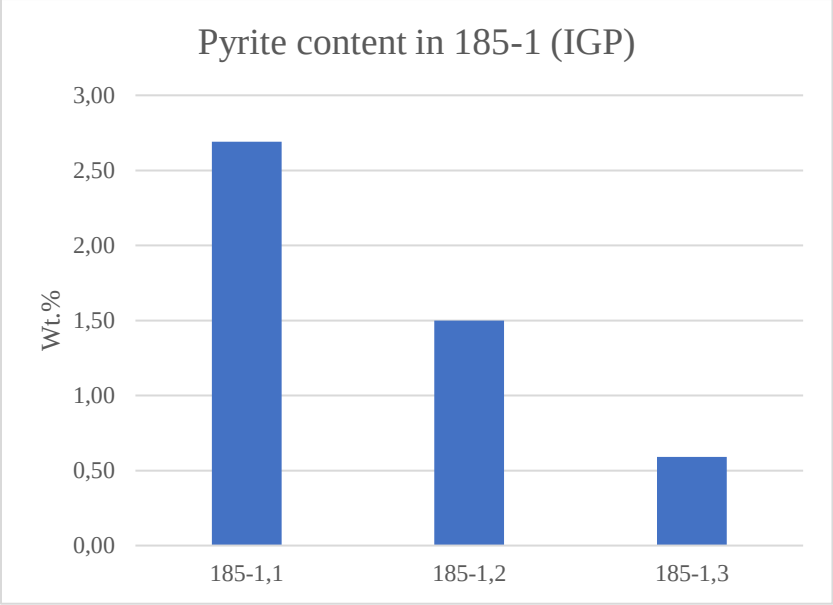

Figure 47: *The pyrite content in alteration zone 185-1. XRD identified pyrite in all samples with a range from 0,59 – 2,69 Wt.%.*

5.4.5.4 Identification and quantification of additional mineral phases at AM-SKOG-H-185-1

The XRD at Titania identified and quantified the minerals shown in Figure 48. Some of the minerals identified by the XRD were not identified int the thin sections from 185-1 during the optical investigation, and includes: apatite (0 – 0,02 Wt.%) and spinel (0,05 – 0,35 Wt.%).

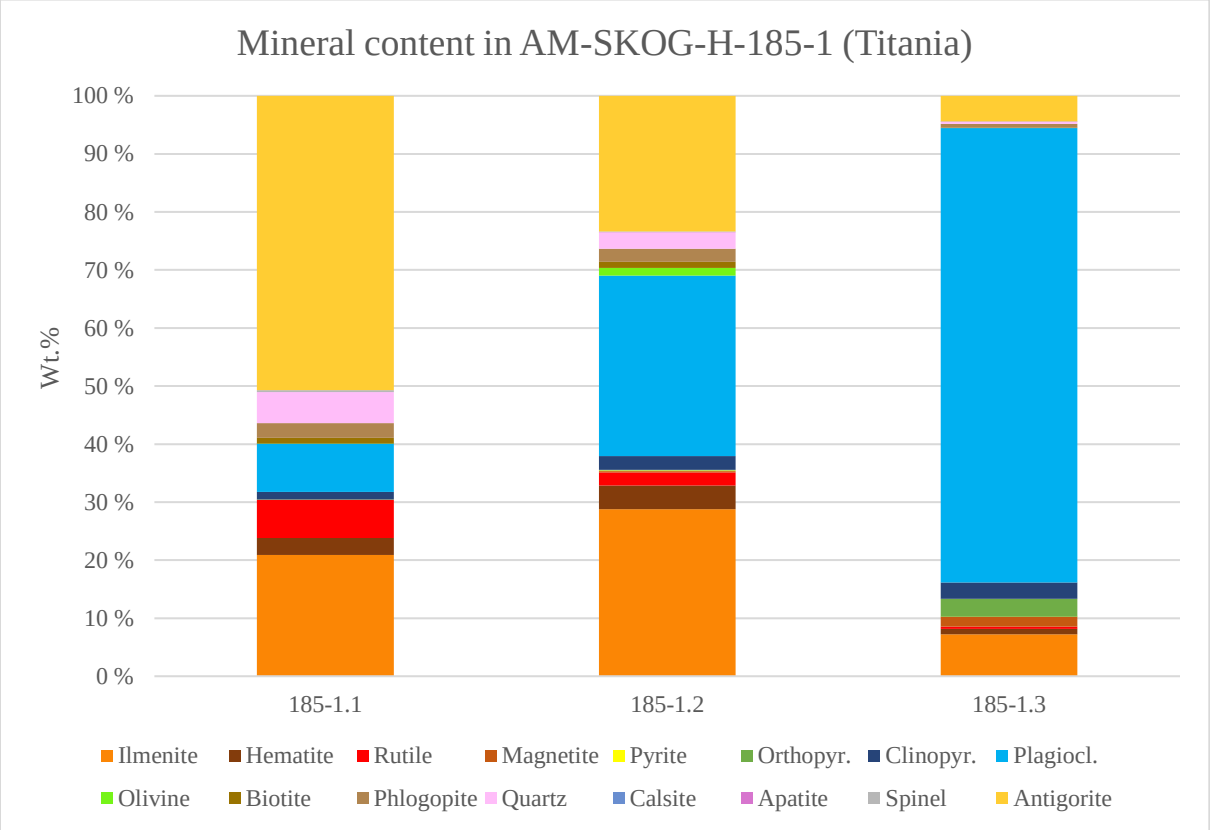

Figure 48: *The XRD analysis at Titania provided the following mineral identification and quantification for the samples in alteration zone 185-1. Mineral phases that were identified by XRD but not in the thin sections includes: apatite (0-0,02 Wt.%) and spinel (0,05 – 0,35 Wt.%).*

The XRD analysis at IGP identified and quantified the minerals shown in Figure 49. All minerals identified in the XRD analysis were identified in the sections.

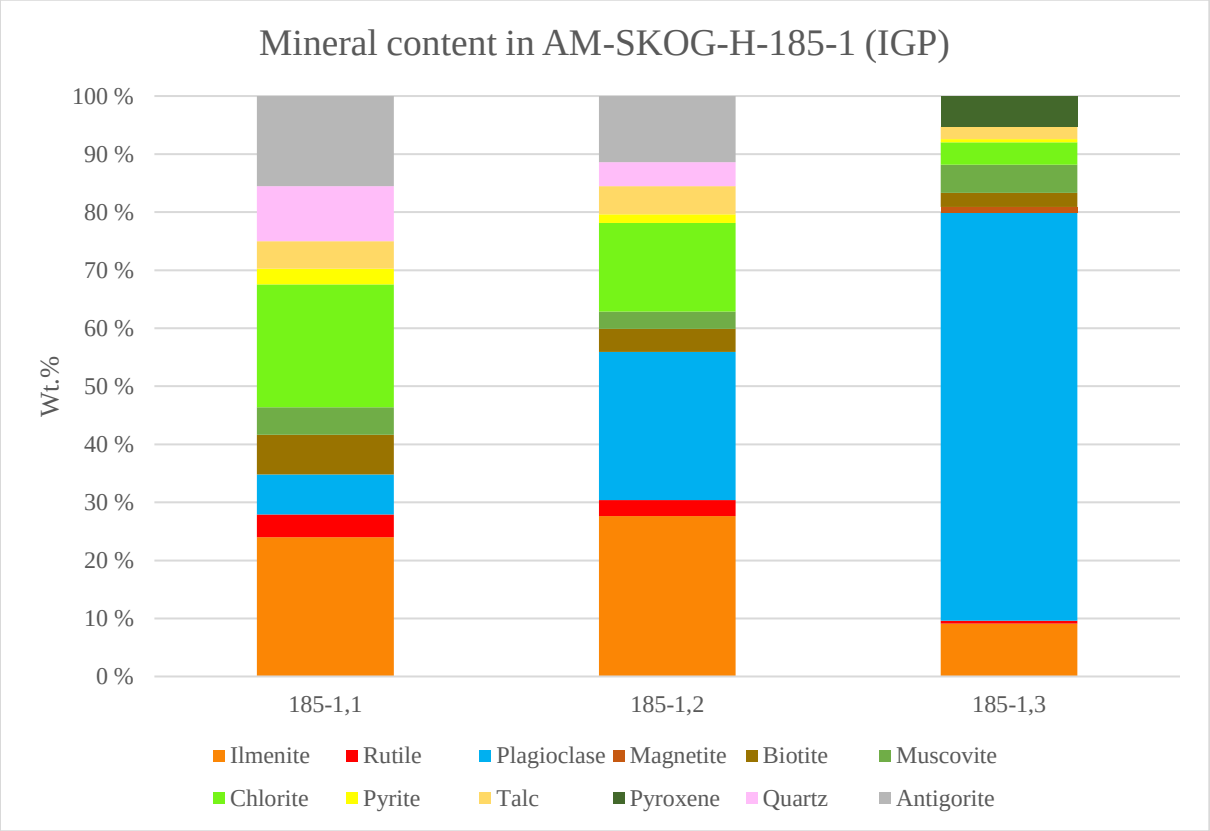

Figure 49: *The minerals identified and quantified in alteration zone 185-1 by the XRD at IGP.*

5.4.6 AM-SKOG-H-185-2

5.4.6.1 Silicates

Plagioclase: Plagioclase is identified in all sections at 185-2. The plagioclase is identified easily by distinct twinning features, with examples of albite-, pericline and Carlsbad twinning occurring in all sections. The boundaries vary between straight and lobate in all sections. The plagioclase contains inclusions of ilmenite ± biotite ± magnetite. At 185-2,1 the grain size is fine to medium grained with anhedral, equant grain shapes. The grains are heavily to very heavily fractured and are heavily affected by alteration by chlorite/serpentine along fractures, boundaries and in grain centres. At 185-2,2 the grain size is medium to fine grained with subhedral to anhedral, equant and tabular grain shapes. The grains are heavily fractured and moderately to heavily affected by alteration by chlorite/serpentine, sericite and saussurite along fractures, boundaries and in grain centres. At 185-2,3 the grain size is fine to medium grained with anhedral, equant grain shapes. The grains are heavily to very heavily fractured and are heavily to very heavily affected by alteration by chlorite/serpentine, sericite and saussurite along boundaries, fractures and in grain centres. At 185-2,4 the grain size is medium to fine grained with subhedral to euhedral, tabular and equant grain shapes. The grains are generally partially fractured with some examples of heavy fracturing. Grains are generally not to partially affected by alteration, but the more heavily fractured grains are moderately to heavily affected by alteration by chlorite/serpentine, sericite and saussurite along boundaries, fractures and in grain centres. The plagioclase content in the four samples at 185-2 is determined by the XRD analysis at IGP, and is given in Figure 50.

Biotite: Biotite is identified in all sections at 185-2. The biotite shows varying pleochroism of brown colours. The grain size is fine grained, with mostly straight and some lobate boundaries. The biotite often occurs in aggregates with ilmenite ± magnetite ± rutile, and appear as inclusions in plagioclase. Some biotite grains contain ilmenite inclusions. At 185-2,1 the grains have an anhedral, equant and laths grain shape, and are partially fractured. At 185-2,2 the grains have subhedral to euhedral, laths and equant grain shapes, and are partially fractured. At 185-2,3 the grains have subhedral, laths and equant grain shapes, and are heavily fractured. At 185-2,4 the grains have subhedral, tabular, equant and laths grain shapes, and are partially fractured. The biotite content in the four samples at 185-2 is determined by the XRD analysis at IGP, and is given in Figure 50.

Orthopyroxene: Orthopyroxene is only identified in section 185-2,3 and 185-2,4. In 185-2,3 the grain size is fine grained with anhedral, equant grain shapes. The grain boundaries are straight and lobate, and the grains are heavily fractured. The primary, medium grained, orthopyroxene are pseudomorph to heavily altered by chlorite/serpentine. The orthopyroxene grains found in 185-2,3 are only a fraction of the original grains. In 185-2,4 the grain size is medium grained with a range down to very fine grained. The grains have subhedral, equant shapes with straight and lobate boundaries. The grains are moderately to very heavily fractured and is partially to very heavily affected by alteration by chlorite/serpentine, clinopyroxene and talc, with some grains being almost pseudomorph. The alteration occurs from boundaries and fractures inwards. The orthopyroxene contains Fe-Ti-oxide and biotite lamellas, that remains after the orthopyroxene is altered. The orthopyroxene content in the four samples at 185-2 is determined by the XRD analysis at Titania, and is given in Figure 50.

Chlorite/Serpentine: Chlorite/serpentine occurs in all sections at 185-2. The chlorite to serpentine ratio is undetermined with the optical microscope. The chlorite/serpentine occur as an alteration product in orthopyroxene and plagioclase. Single grains are indistinguishable. The chlorite/ serpentine content in the four samples at 185-2 is determined by the XRD analysis at IGP, and is given in Figure 50. Serpentine is identified as antigorite in the XRD analysis.

Talc: Talc is identified in section 185-2,1, 185-2,2 and 185-2,4 and appear as an alteration product in altered and pseudomorph orthopyroxene. In 185-2,1 the grain size is very fine to fine grained with subhedral, fibrous/laths grain shapes. The boundaries are straight and lobate and the grains are partially fractured. The talc is found together with chlorite/serpentine and Fe-Ti-oxide lamellas that originates from primary orthopyroxene. In 185-2,2 the grain size is very fine to fine grained with subhedral to euhedral, fibrous/laths grain shapes. The boundaries are straight and the grains have few to no fractures. The talc often occurs with other alteration products like chlorite/serpentine ± quartz ± clinopyroxene and Fe-Ti-oxide lamellas from primary orthopyroxene. In 185-2,4 single grains are indistinguishable from each other. The talc content in the four samples at 185-2 is determined by the XRD analysis at IGP, and is given in Figure 50.

Quartz: Quartz is identified in section 185-2,1, 185-2,2 and 185-2,3. The grain size is fine to very fine grained with subhedral, equant grain shapes in all sections. The boundaries vary between lobate and straight and the grains are not to partially fractured. In 185-2,1 the quartz often occurs in or close to larger fractures often together with chlorite/serpentine. In 185-2,2 the quartz occurs in grain centres of pseudomorph orthopyroxene together with talc ± clinopyroxene. In 185-2,3 the quartz occurs as filling in larger fractures often surrounded by chlorite/serpentine. The quartz content in the four samples at 185-2 is determined by the XRD analysis at IGP, and is given in Figure 50.

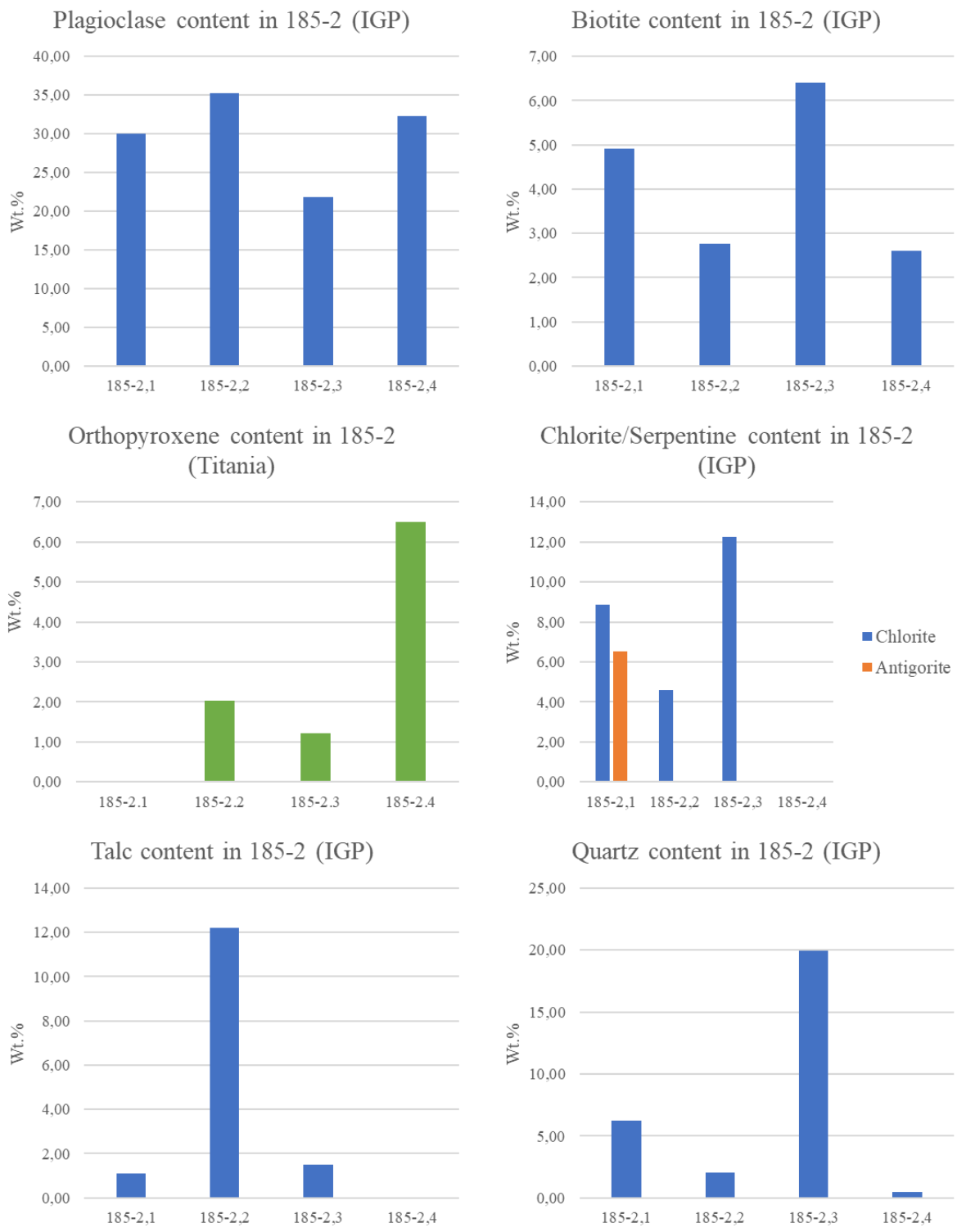

Figure 50: *The plagioclase, biotite, orthopyroxene, chlorite/serpentine, talc and quartz content in alteration zone 185-2 determined by the XRD analyses from IGP and Titania.*

Calcite: Calcite is identified in section 185-2,1, 185-2,2 and 185-2,3. The grain size is very fine to fine grained where single grains often are indistinguishable. The fine-grained grains have anhedral, equant grain shapes and contains little to no fractures. The boundaries vary between straight and lobate. The calcite occurs as fracture filling in larger, section transecting fractures in the three sections. The calcite content in the four samples at 185-2 is determined by the XRD analysis at IGP, and is given in Figure 51.

Clinopyroxene: Clinopyroxene is identified in section 185-2,2 and 185-2,4 as an alteration product in orthopyroxene. The grain size is fine to very fine grained with anhedral, equant grain shapes. The grain boundaries are straight and lobate on both sections. In 185-2,2 the grains are heavily fractured and often appear with talc ± quartz ± chlorite/serpentine in altered orthopyroxene. In 185-2,4 the grains are partially fractured and often found with chlorite/serpentine ± talc in altered orthopyroxene. Often retains the Fe-Ti-oxide lamellas from the orthopyroxene. The clinopyroxene content in the four samples at 185-2 is determined by the XRD analysis at Titania, and is given in Figure 51.

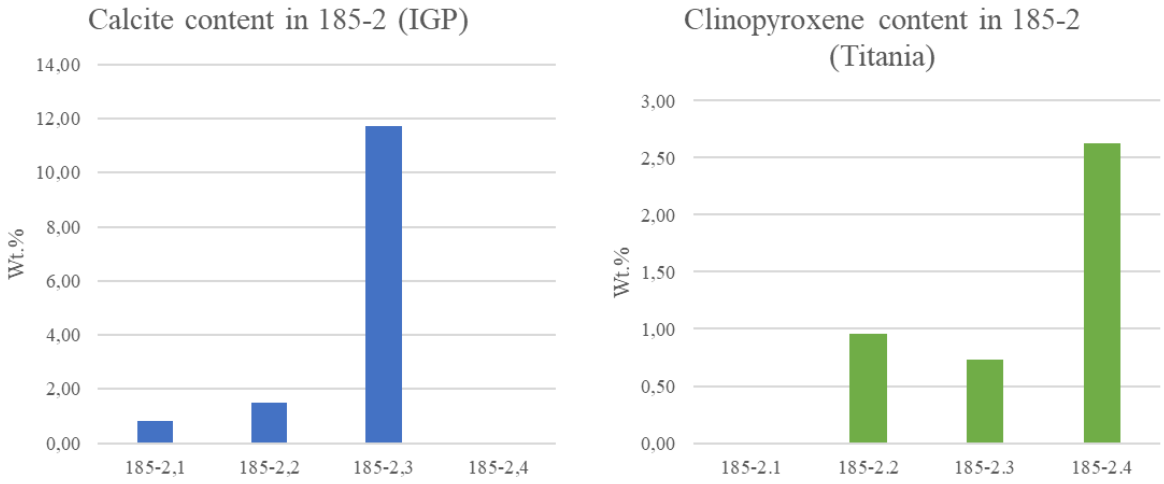

Figure 51: *The calcite and clinopyroxene content in alteration zone 185-2 determined by the XRD analyses from IGP and Titania.*

5.4.6.2 Oxides

Ilmenite: Ilmenite is identified in all sections. The grains have boundaries that vary between straight and lobate in all sections. The ilmenite is often found in aggregates with magnetite ± biotite ± rutile ± sulphides, and appear as inclusions in plagioclase ± biotite. At 185-2,1 the grain size is fine to very fine grained with subhedral to anhedral, equant grain shapes. The grains are moderately to very heavily fractured and partially affected by alteration by rutile from boundaries and fractures inwards. The ilmenite grains contain hematite exsolution lamellas. At 185-2,2 the grain size is fine to medium grained with subhedral to anhedral, equant grain shapes. The grains are partially to heavily fractured and are partially affected by alteration from boundaries and borders inwards. The ilmenite grains contain hematite exsolution lamellas. At 185-2,3 the grain size is fine to very fine grained with anhedral, equant grain shapes. The grains are moderately to very heavily fractured and are moderately to heavily affected by alteration by rutile from borders and fractures inwards with a sometimes finger like texture. Lacks hematite exsolution lamellas. At 185-2,4 the grain size is fine to medium grained with subhedral, equant grain shapes. The grains not to partially fractured with some grains being partially affected by alteration by rutile. The ilmenite contains hematite exsolution lamellas. The ilmenite content in the four samples at 185-2 is determined by the XRD analysis at IGP, and is given in Figure 52.

Rutile: Rutile is identified in all sections at 185-2 and occur as an alteration product of ilmenite from boundaries and fractures inwards. The boundaries vary between straight and lobate in all sections. The rutile often occurs in aggregates with ilmenite ± magnetite ± biotite ± sulphides. In 185-1 the grain size is fine to very fine grained with subhedral to anhedral, equant grain shapes. The grains are partially to moderately fractured. In 185-2,2 the grain size ranges from very fine to medium grained, dominated by fine grained grains. The grains have anhedral to subhedral, equant shapes and are partially fractured. In 185-2,3 the grain size is fine to very fine grained with subhedral to anhedral, equant shapes. The grains are moderately fractured. In 185-2,4 the grain size is fine to very fine grained with anhedral, equant grain shapes. The grains contain little to no fractures. The rutile content in the four samples at 185-2 is determined by the XRD analysis at Titania, and is given in Figure 52.

Magnetite: Magnetite is identified in all sections and often appear with multiple cryptocrystalline inclusions. The magnetite often occurs in aggregates with ilmenite ± biotite ± rutile ± sulphides and contains inclusions of spinel. The grain boundaries vary between lobate and straight in all sections. In 185-2,1 the grain size is fine to very fine grained with subhedral to anhedral, equant grain shapes. The grains are heavily to very heavily fractured. In 185-2,2 the grain size is fine to very fine grained with anhedral, equant grain shapes. The grains are moderately to heavily fractured, where the heavy fracturing occurs in grains found near larger, section cutting, fractures. In 185-2,3 the grain size is dominated by the fine-grained fraction, but has a range from very fine to medium grained. The grains have anhedral, equant grain shapes and are heavily to very heavily fractured. In 185-2,4 the grain size is dominated by the fine-grained fraction, but has a range from very fine to medium grained. The grains have subhedral, equant grain shapes and are partially to moderately fractured. The magnetite content in the four samples at 185-2 is determined by the XRD analysis at IGP, and is given in Figure 52.

Hematite: Hematite is identified in section 185-2,1, 185-2,2 and 185-2,4 and occurs as exsolution lamellas in ilmenite. The hematite content in the four samples at 185-2 is determined by the XRD analysis at Titania, and is given in Figure 52.

Spinel: Spinel is identified in all sections. The grain size is fine to very fine grained with acicular grain shapes. The borders vary from straight to lobate and the grains are partially fractured. The spinel occurs exclusively as inclusions in magnetite. The spinel content in the four samples at 185-2 is determined by the XRD analysis at Titania, and is given in Figure 52.

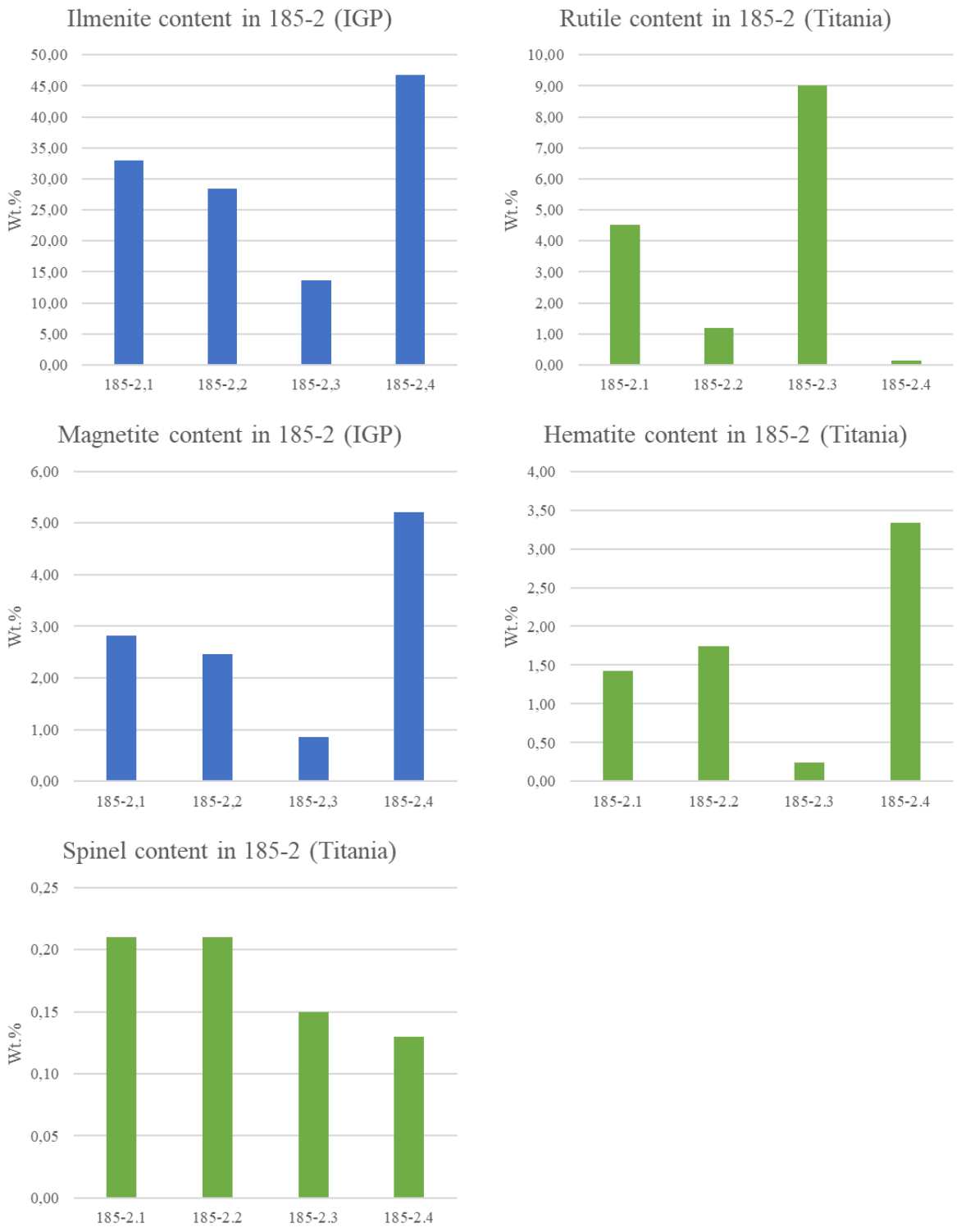

Figure 52: *The ilmenite, rutile, magnetite, hematite and spinel content in alteration zone 185-2 determined by the XRD analyses from IGP and Titania.*

5.4.6.3 Sulphides

The sulphides were not a main target during the investigation and a differentiation between different sulphide phases was not conducted. Sulphides are identified in all sections. The sulphides are dominated by a pyrite phase and have a fine to very fine grain size. The grain shapes are anhedral and equant grain shapes with straight and lobate boundaries. The grains are heavily fractured in all sections except from 185-2,4 where they are moderately fractured. The sulphides occur sporadically throughout the sections. The pyrite content in the four samples at 185-2 is determined by the XRD analysis at IGP, and is given in Figure 53.

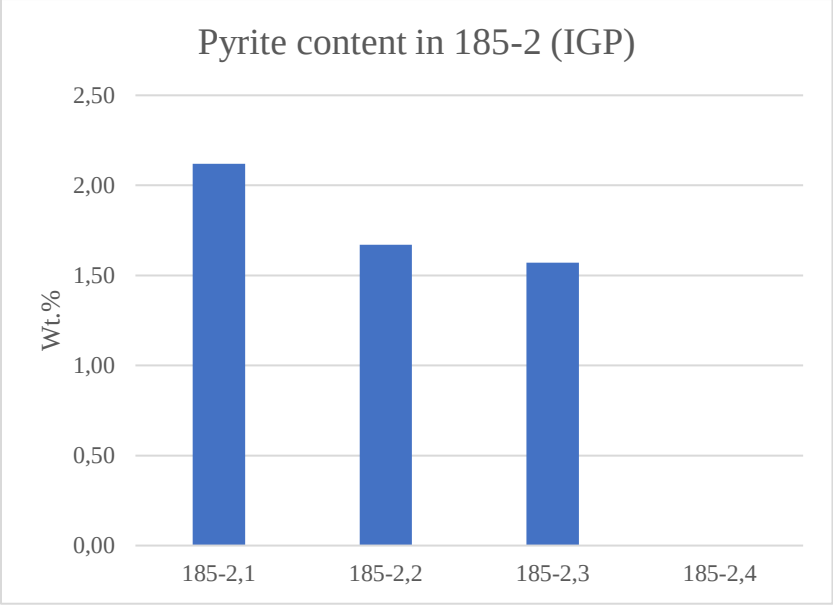

Figure 53: *The pyrite content in alteration zone 185-2. Pyrite was identified in all sections except 185-2,4 by XRD with a range of (1,57 – 2,12 Wt.%).*

5.4.6.4 Identification and quantification of additional mineral phases at AM-SKOG-H-185-2

The XRD at Titania identified and quantified the minerals shown in Figure 54. Some of the minerals identified by the XRD were not identified in the thin sections during the optical investigation, and includes: olivine (0 – 0,73 Wt.%) and apatite (0 – 0,05 Wt.%).

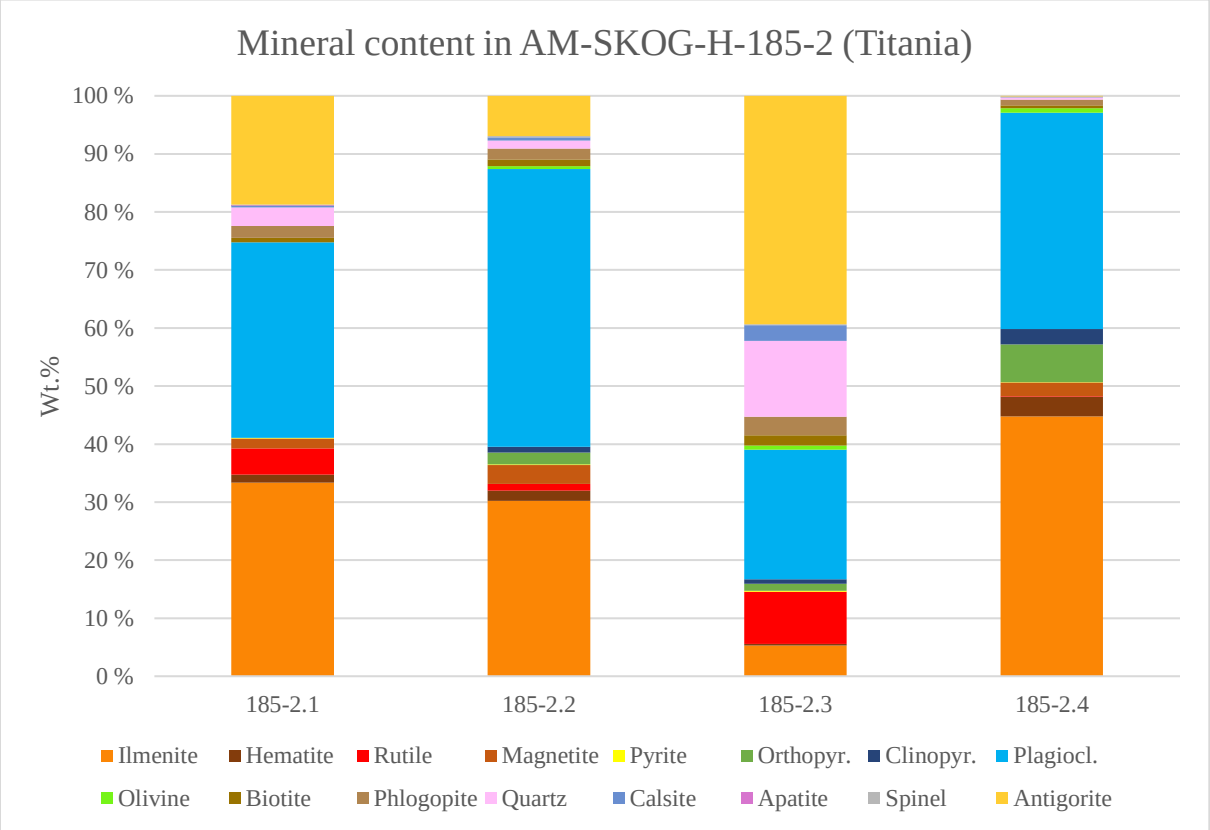

Figure 54: *The XRD analysis at Titania identified and quantified the following minerals in the samples in alteration zone 185-2. Mineral phases which were identified by XRD but not in the thin sections includes: olivine (0 – 0,73 Wt.%) and apatite (0 – 0,05 Wt.%.*

The XRD analysis at IGP identified and quantified the minerals shown in Figure 55. All minerals identified in the XRD analysis were identified in the sections from 185-2.

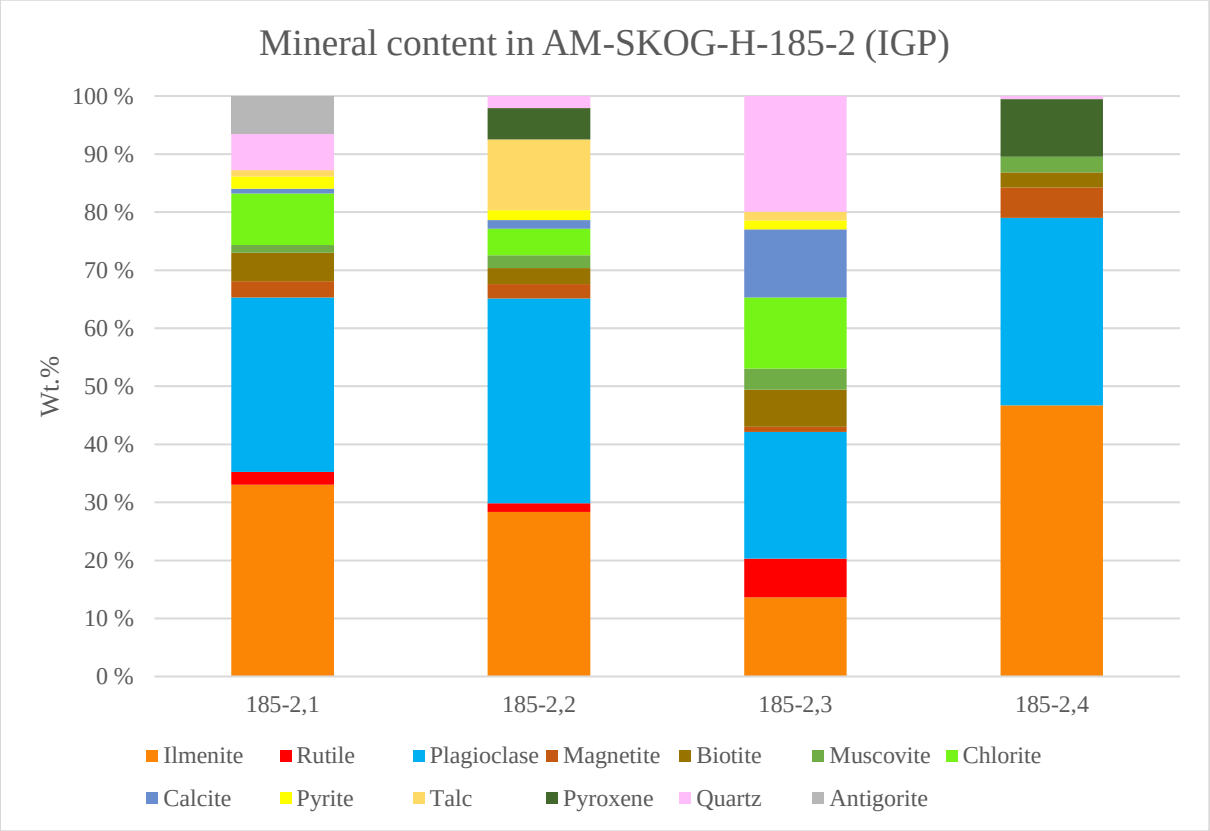

Figure 55: *The minerals identified and quantified in alteration zone 185-2 by the XRD at IGP.*

5.4.7 AM-SKOG-H-200-1

5.4.7.1 Silicates

Plagioclase: Plagioclase is identified in all sections except 200-1,2-2. At 200-1,1 the grain size is fine to very fine grained with anhedral, equant grain shapes. The grains are very heavily fractured and heavily affected by alteration by chlorite/serpentine and sericite. At 200-1,2-1, 200-1,3 and 200-1,4 the grain size is medium grained with euhedral, tabular and subhedral, tabular to equant grain shapes. The grains are partially fractured and partially affected by alteration by chlorite/serpentine, sericite and saussurite. The boundaries are mostly straight with some lobate examples in equant grains. The plagioclase contains inclusions of ilmenite and biotite. The plagioclase content in the samples at 200-1 is determined by the XRD analysis at IGP, and is given in Figure 56.

Orthopyroxene: Orthopyroxene is identified in section 200-1,3 and 200-1,4. The grain size is medium to very fine grained with subhedral, equant and prismatic grain shapes. The grains are moderately to very heavily fractured. The orthopyroxene grains contain Fe-Ti oxide and biotite lamellas that remains as the orthopyroxene is altered. The grains also contain ilmenite and biotite inclusions. At 200-1,3 the grains are partially to very heavily affected by alteration by talc and chlorite/serpentine. At 200-1,4 the grains are partially to moderately affected by alteration by talc, chlorite/serpentine and clinopyroxene. The orthopyroxene content in the samples at 200-1 is not separated from clinopyroxene, and determined by the XRD analysis at IGP as pyroxene (Figure 56).

Clinopyroxene: Clinopyroxene is identified in section 200-1,2-1 and 200-1,4. The grain size is fine grained with anhedral, equant grain shapes. The boundaries are often straight with some lobate. The clinopyroxene often occurs along boundaries of unaltered and pseudomorph orthopyroxene and is often associated with talc and chlorite/serpentine. The orthopyroxene content in the samples at 200-1 is not separated from orthopyroxene, and is determined by the XRD analysis at IGP as pyroxene (Figure 56).

Biotite: Biotite is identified in section 200-1,2-1, 200-1,3 and 200-1,4. The grain size is fine grained with subhedral to euhedral, laths and equant grain shapes. The boundaries are mostly straight with some lobate boundaries. The biotite is partially fractured and sometimes contains ilmenite inclusions. The biotite often occurs in aggregates with ilmenite and as inclusions in plagioclase and orthopyroxene. The biotite content in the samples at 200-1 is determined by the XRD analysis at IGP, and is given in Figure 56.

Chlorite/Serpentine: Chlorite/serpentine are identified in all sections at 200-1. In all sections except 200-1,1 the grain size is very fine grained with indistinguishable shape. At 200-1,1 the grain size is fine to very fine grained with anhedral, equant and subhedral, tabular grain shapes. The boundaries are straight with some irregularities and the grains are partially fractured. Chlorite/serpentine occurs as an alteration product of plagioclase and orthopyroxene in all sections except 200-1,2-2. In 200-1,2-2 the chlorite/serpentine occur in larger fractures. The chlorite/ serpentine content in the samples at 200-1 is determined by the XRD analysis at IGP, and is given in Figure 56. Serpentine is identified as antigorite in the XRD analysis.

Talc: Talc is identified in section 200-1,2-1, 200-1,2-2, 200-1,3, 200-1,4. At 200-1,2-1 single grains are indistinguishable from each other and occurs as an alteration product of primary orthopyroxene. At 200-1,2-2 the grains are indistinguishable from each other, and the talc occurs with serpentine/chlorite, quartz and calcite. At 200-1,3 the grain size varies from very fine to fine grained with subhedral to euhedral tabular/laths grain shapes. The boundaries are straight, and the grains have little to no fractures. The talc occurs as an alteration product of primary orthopyroxene. At 200-1,4 the single grains are indistinguishable from each other and occurs as an alteration product of primary orthopyroxene. The talc content in the samples at 200-1 is determined by the XRD analysis at IGP, and is given in Figure 56.

Muscovite: Muscovite is identified in all sections at 200-1. Muscovite occurs as an alteration product of plagioclase in all sections, except from 200-1,2-2 where it appears sporadically in the section among calcite. The grain size is very fine grained in all sections. Grain shape is only identifiable in 200-1,2-2 where subhedral, tabular/laths grain shapes are present. The muscovite content in the samples at 200-1 is determined by the XRD analysis at IGP, and is given in Figure 56.

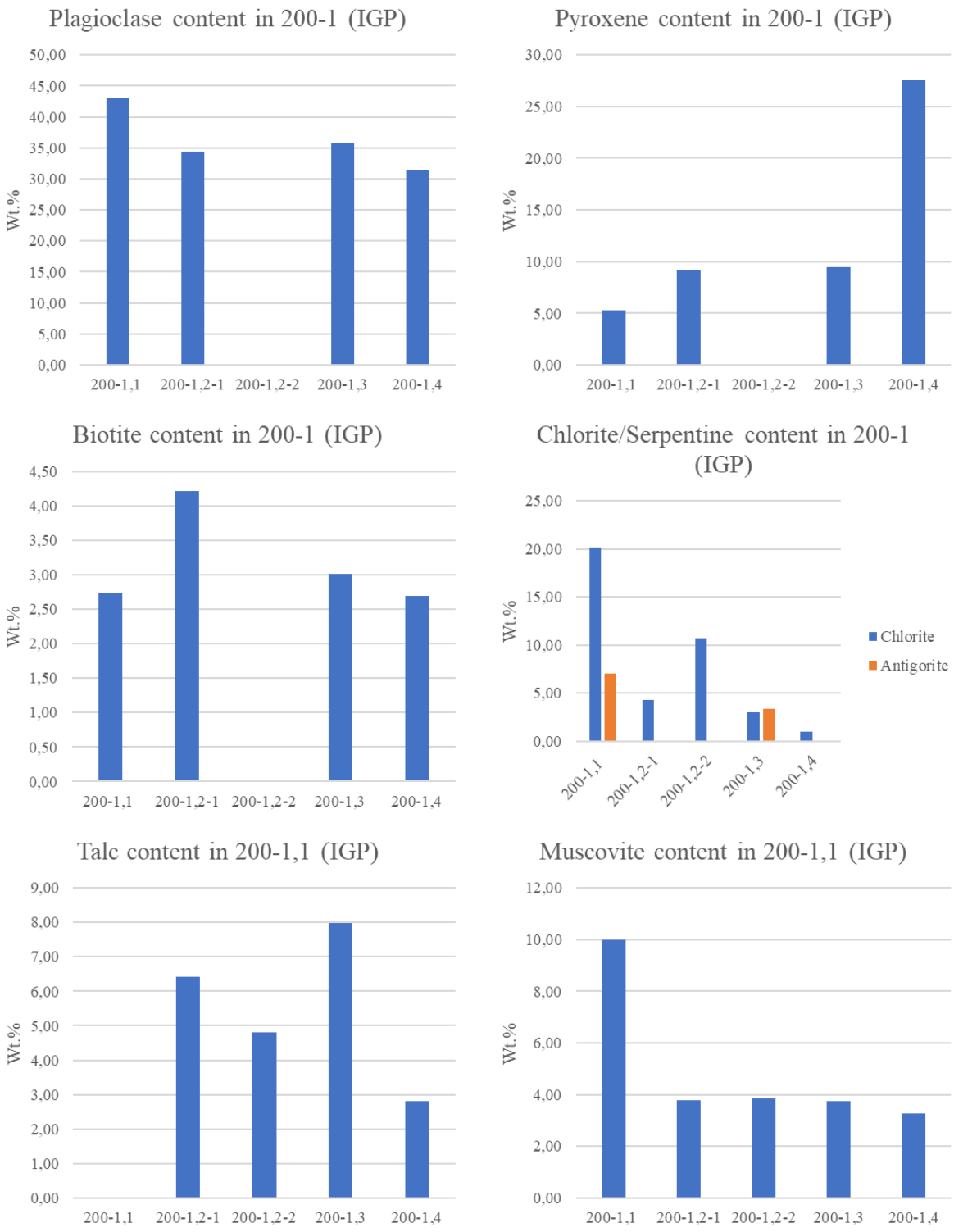

Figure 56: *The plagioclase, pyroxene, biotite, chlorite/serpentine, talc and muscovite content in alteration zone 200-1 determined by the XRD analysis at IGP.*

Quartz: Quartz is identified in section 200-1,1, 200-1,2-2 and 200-1,3. The grain size is very fine grained with anhedral, equant grain shapes. The boundaries are lobate with few to no fractures. The quartz often appears in fractures, forming long vein textures, often in association with calcite. The quartz content in the samples at 200-1 is determined by the XRD analysis at IGP, and is given in Figure 57.

Calcite: Calcite is identified in section 200-1,2-2 and 200-1,3. The grain size is very fine to fine grained with mostly straight and some lobate boundaries. At 200-1,2-2 the grains have subhedral, tabular and equant grain shapes. The grains are partially fractured and often contains characteristic twinning features. At 200-1,3 the grains have anhedral and equant shapes, with no fractures. Some of the grains show characteristic twinning features. The calcite often occurs in thicker layers and as filling in larger fractures. The calcite content in the samples at 200-1 is determined by the XRD analysis at IGP, and is given in Figure 57.

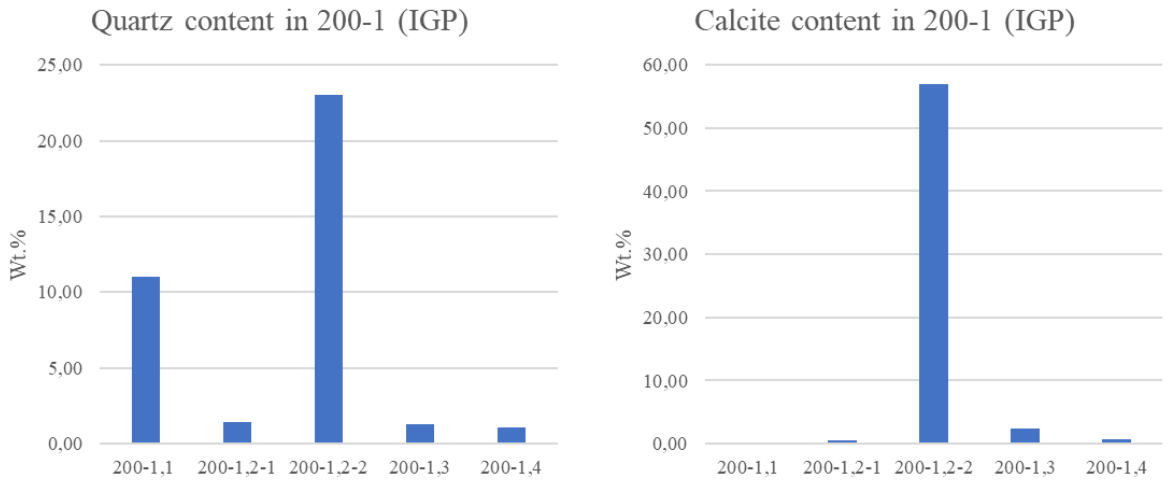

Figure 57: *The quartz and calcite content in alteration zone 200-1 determined by the XRD analysis at IGP.*

5.4.7.2 Oxides

Ilmenite: Ilmenite is identified in section 200-1,2-1, 200-1,3 and 200-1,4. The grain size range from very fine to medium grained, and is dominated by fine to medium grained. The grains have anhedral to subhedral, equant grain shapes with straight and lobate boundaries. The grains are partially fractured and some grains are partially affected by alteration by rutile from boundaries and fractures inwards in the three sections. The ilmenite is often found in aggregates with magnetite ± biotite ± sulphides ± rutile. The ilmenite also appears as inclusions in plagioclase and biotite, and as lamellas in pyroxene. The ilmenite contains hematite exsolution lamellas. The ilmenite content in the samples at 200-1 is determined by the XRD analysis at IGP, and is given in Figure 58.

Magnetite: Magnetite is identified in all sections except 200-1,2-2. The grain size is fine grained and the grains have anhedral, equant shapes in the four sections. The boundaries are straight and lobate in all sections. At 200-1,1 the grains are heavily fractured. At 200-1,2-1, 200-1,3 and 200-1,4 the grains are moderately to heavily fractured and contains spinel inclusions. The magnetite content in the samples at 200-1 is determined by the XRD analysis at IGP, and is given in Figure 58.

Rutile: Rutile is identified in all sections except 200-1,2-2 and appear as alteration product of ilmenite or as singular grains. The boundaries are straight and lobate in all sections. At 200-1,1 the grain size is fine grained, with anhedral, equant grain shapes. The grains are partially fractured. At 200-1,2-1 the grain size is very fine grained with anhedral, equant grain shapes. The grains are not fractured. At 200-1,3 the grain size is very fine to fine grained with anhedral, equant grain shapes. The grains are not fractured. At 200-1,4 the grain size is very fine grained with indistinguishable grain shape. The rutile content in samples at 200-1 is determined by the XRD analysis at Titania, and is given in Figure 58.

Hematite: Occurs in all sections except 200-1,2-2 as needle shaped exsolution lamellas. The hematite content in the samples at 200-1 is determined by the XRD analysis at Titania, and is given in Figure 58.

Spinel: Spinel is identified in section 200-1,2-1, 200-1,3 and 200-1,4 and occurs as inclusions in magnetite. The spinel is fine grained with acicular grain shape. The grains have straight and lobate boundaries and are partially fractured. The spinel content in samples at 200-1 is determined by the XRD analysis at Titania, and is given in Figure 58.

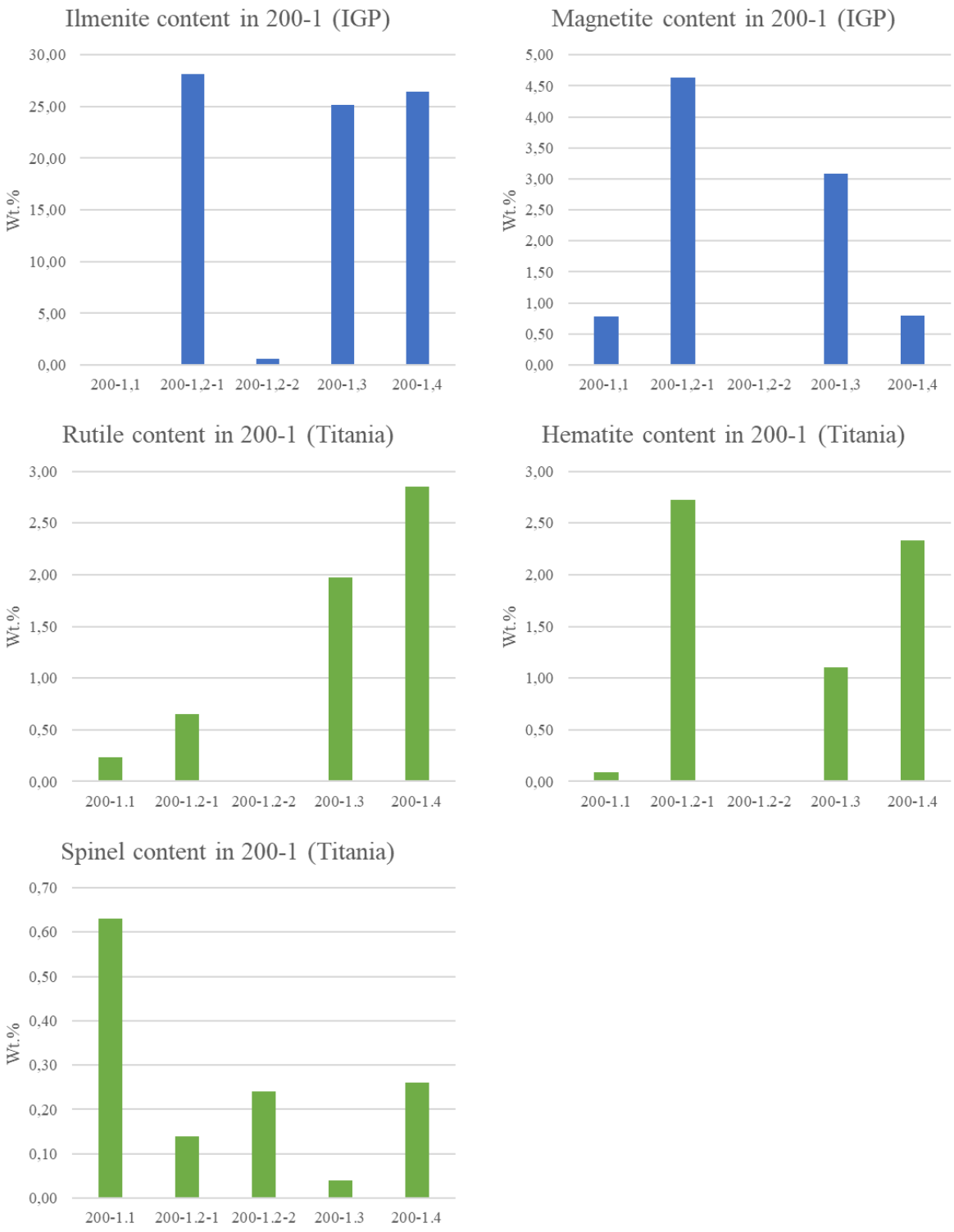

Figure 58: *The ilmenite, magnetite, rutile, hematite, and spinel content in alteration zone 200-1 determined by the XRD analyses at IGP and Titania.*

5.4.7.3 Sulphides

The sulphides were not a main target during the investigation and a differentiation between different sulphide phases was not conducted. Sulphides are identified in all sections except 200-1,1. The sulphides have a fine to very fine grain size. The grain shapes are anhedral and equant grain shapes with straight and lobate boundaries. The grains are moderately to heavily fractured in all sections. The sulphides occur sporadically throughout the sections. The pyrite content in the samples at 200-1 is determined by the XRD analysis at IGP, and is given in Figure 59.

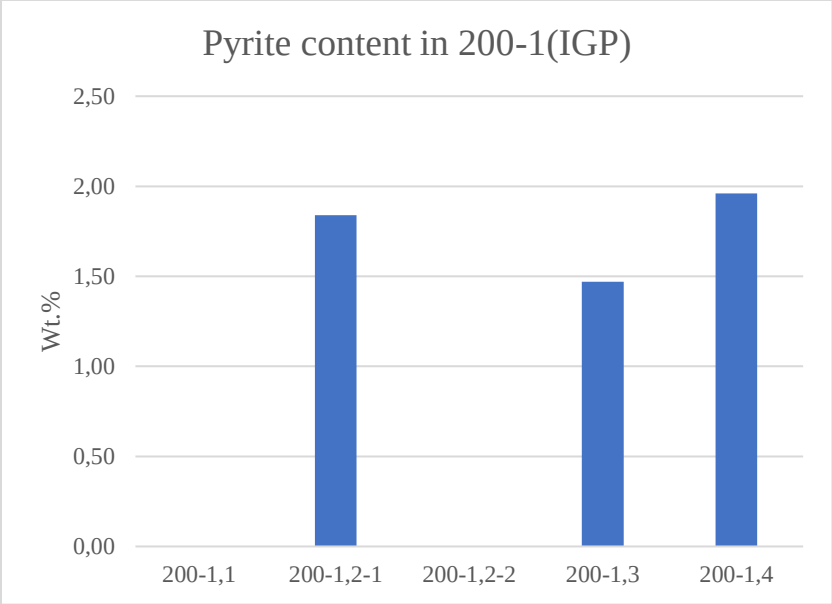

Figure 59: *The pyrite content in alteration zone 200-1. Pyrite was identified in 200-1,2-1, 200-1,3 and 200-1,4 by XRD with a range of 1,47 – 1,96 Wt.%. Sulphides were identified optically in very small quantity in section 200-1,2-2 and is not detected as pyrite in the XRD analysis.*

5.4.7.4 Identification and quantification of additional mineral phases at AM-SKOG-H-200-1

From the AM analysis additional mineral phases above 1 Wt.% will be presented. The entire AM analysis is presented in Appendix D. The only additional mineral phase above 1 Wt.% is the clay mineral kaolinite, which is found as an alteration product of plagioclase in the four analysed sections. Figure 60 shows the amount of kaolinite in the sections.

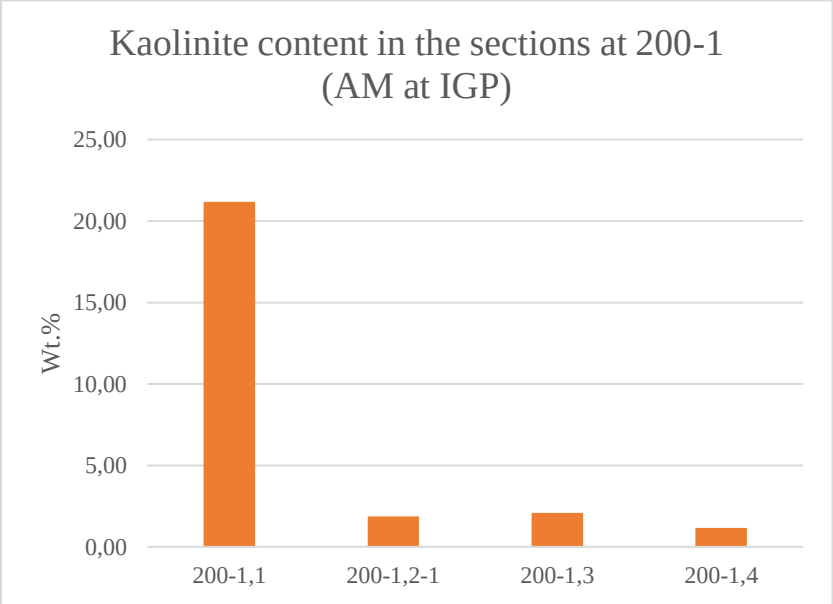

Figure 60: *The kaolinite content in the four analysed sections at 200-1 quantified by the AM at IGP.*

The XRD analysis at Titania identified and quantified the minerals shown in Figure 61. Some of the minerals identified by the XRD analysis were not identified in the thin sections during the optical investigation, and includes: olivine (0 – 0,69 Wt.%) and apatite (0 – 0,08 Wt.%).

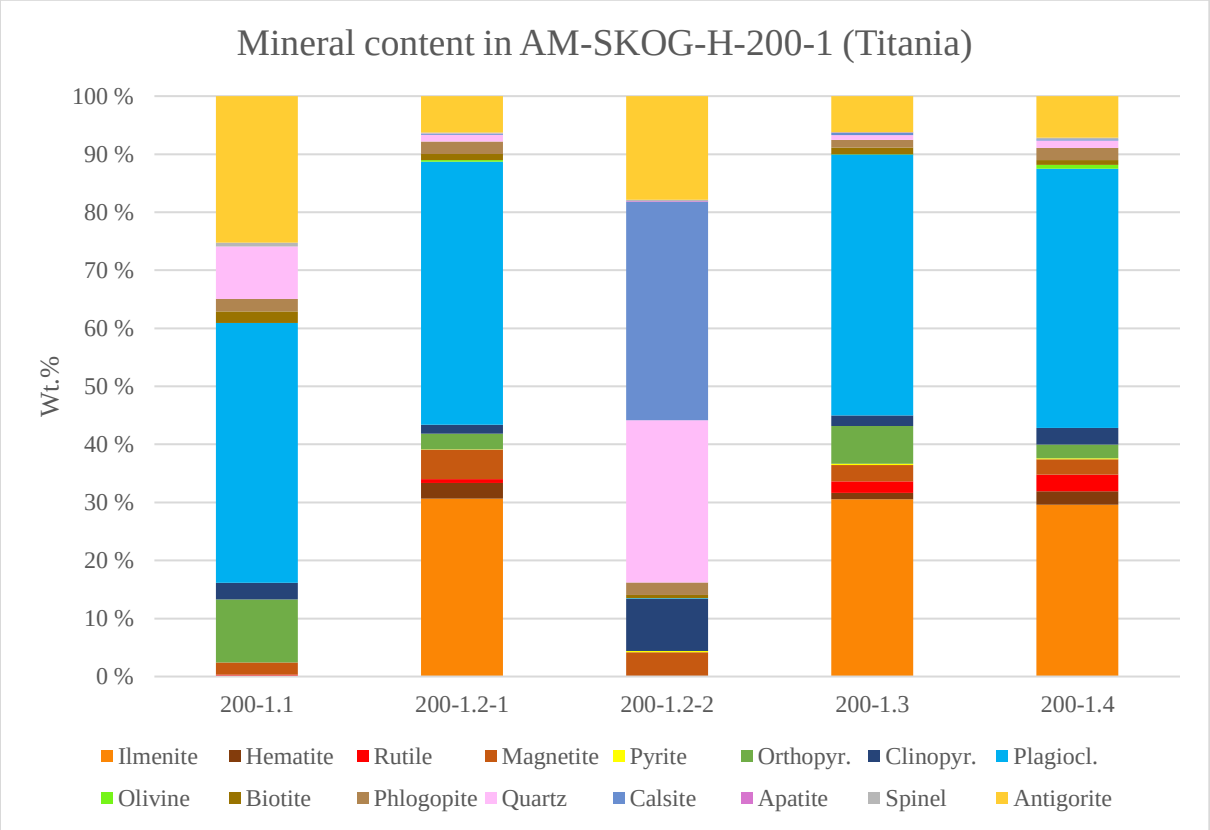

Figure 61: *The XRD analysis at Titania provided the following mineral identification and quantification for the samples in alteration zone 200-1. Mineral phases that were identified by XRD but not in the thin sections includes: olivine (0 – 0,69 Wt.%) and apatite (0 – 0,08 Wt.%).*

The XRD analysis at IGP identified and quantified the minerals shown in Figure 62. All mineral phases identified by the XRD analysis were identified in at least one of the sections during the optical investigation.

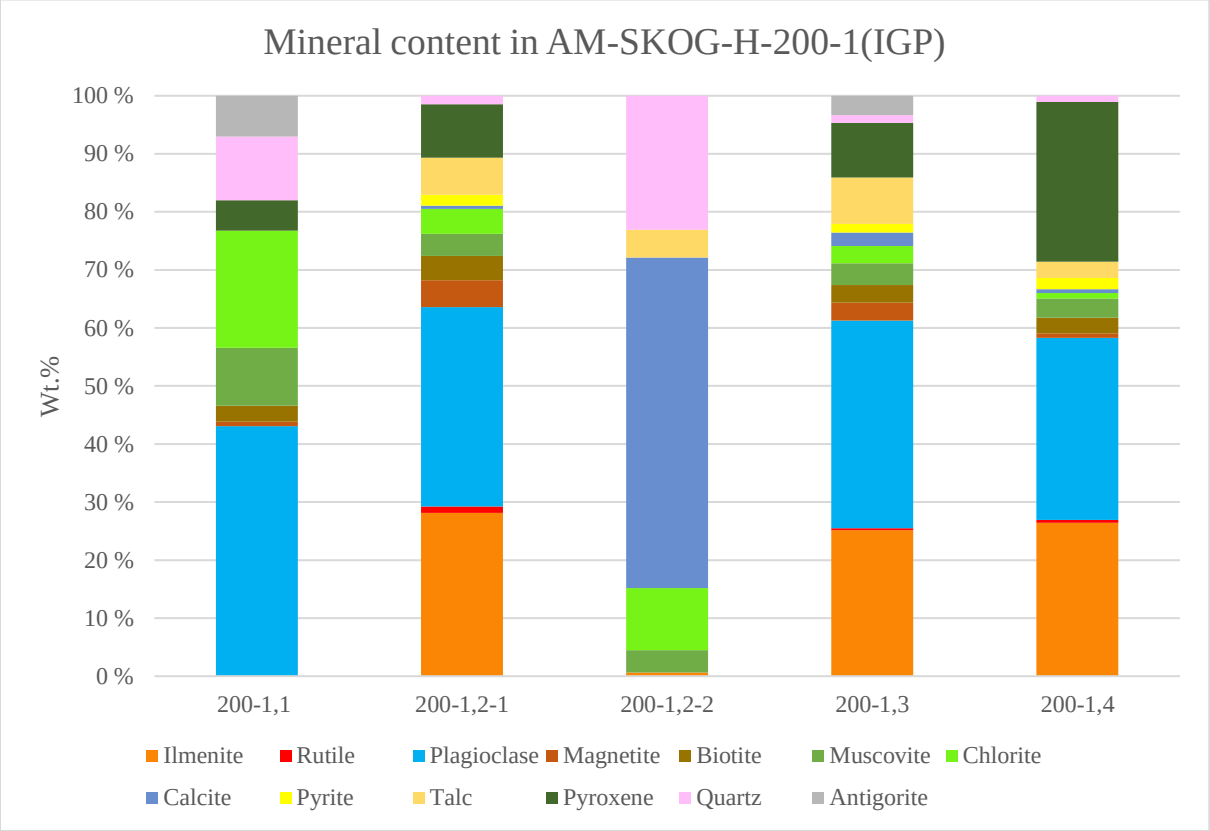

Figure 62: *The XRD analysis at IGP provided the following mineral identification and quantification for the samples in alteration zone 200-1.*

5.4.8 AM-TEL-H-155-2

5.4.8.1 Silicates

Plagioclase: Plagioclase is the most abundant mineral in all the sections at 155-2. The plagioclase is easily identified by distinct twinning features, with examples of albite-, pericline and Carlsbad twinning occurring in all sections. The plagioclase is affected by alteration by chlorite/serpentine, sericite and saussurite at varying degrees at 155-2. The grain size ranges from fine to medium grained with the dominant fraction being medium grained in all sections. At 155-2,1 the grains are euhedral to subhedral with tabular and equant shapes. The grains are heavily fractured and partially to heavily affected by alteration. At 155-2,2 the grains are subhedral to anhedral with tabular and equant shapes. The grains are partially fractured and partially to moderately affected by alteration. At 155-2,3 the grains are subhedral with tabular and equant shapes. The grains are partially fractured and little to partially affected by alteration. At 155-2,4 the grains are subhedral with tabular and equant shapes. The grains are partially fractured and heavily to moderately affected by alteration. At 155-2,5 the grains are euhedral to subhedral with tabular and equant shapes. The grains are partially fractured and little to partially affected by alteration. Grains have a mixture of straight and lobate boundaries and inclusions of ilmenite and biotite occur in some grains in all sections. The plagioclase content in the five samples at 155-2 is determined by the XRD analysis at IGP, and is given in Figure 63.

Orthopyroxene: Orthopyroxene is identified in all sections at 155-2. The orthopyroxene is altered and replaced by talc (except 155-2,1), chlorite/serpentine, clinopyroxene and quartz (only at 155-2,4) at varying degrees. The orthopyroxene contains Fe-Ti-oxide lamellas and inclusions of ilmenite, biotite and rutile. The boundaries vary from straight to lobate in all sections. At 155-2,1 the grain size is fine to medium grained with subhedral, tabular and equant shapes. The grains are partially to moderately fractured and moderately to very heavily affected by alteration. At 155-2,2 the grain size is fine grained with anhedral, equant grain shapes. The grains are partially fractured and heavily to very heavily affected by alteration. At 155-2,3 the grain size is fine grained with subhedral, equant shapes. The grains are partially to moderately fractured and are partially to very heavily affected by alteration, with most grains being pseudomorph. At 155-2,4 the grain size is fine to medium grained with subhedral to anhedral, equant shapes. The grains are moderately to very heavily fractured and moderately to very heavily affected by alteration. At 155-2,5 the grain size is fine to medium grained with subhedral to euhedral, prismatic/equant shapes. The grains are partially to moderately fractured and mostly partially affected by alteration. Some grains are pseudomorph. The orthopyroxene content in the five samples at 155-2 is determined by the XRD analysis at Titania, and is given in Figure 63.

Biotite: Biotite is present in all section at 155-2 and often occur in aggregates with ilmenite ± magnetite ± rutile, and as inclusions in plagioclase and pyroxene. The biotite is easily recognized by varying brown pleochroism with some featuring a greenish tint. At 155-2,1 the grains are fine grained with subhedral to anhedral, tabular, laths and equant grain shapes. Few to no fractures are found in the grains. At 155-2,2 the grain size is fine to medium with euhedral and subhedral, tabular and laths shapes. The grains are partially fractured. At 155-2,3 the grain size is fine with subhedral, tabular and laths shapes. The grains are partially fractured. At 155-2,4 the grain size is fine with euhedral to subhedral, tabular and laths shapes. The grains are moderately fractured. At 155-2,5 the grain size is fine to medium with euhedral to subhedral, tabular and laths shapes. The grains have few to no fractures. The boundaries are mostly straight and partially lobate in all sections. The biotite content in the five samples at 155-2 is determined by the XRD analysis at IGP, and is given in Figure 63.

Chlorite/Serpentine: Chlorite/serpentine is present in all 5 sections at 155-2. The grain size is indistinguishable making it difficult to separate the chlorite from the serpentine. It appears as an alteration product in altered plagioclase and orthopyroxene. The alteration of the plagioclase and orthopyroxene occurs along boundaries, in fractures, and in grain centres of heavily altered and pseudomorph grains. The chlorite/ serpentine content in the five samples at 155-2 is determined by the XRD analysis at IGP, and is given in Figure 63. Serpentine is identified as antigorite in the XRD analysis.

Talc: Talc is present in all sections except 155-2,1. The grain size is mainly indistinguishable, but some very fine grains are found at 155-2,4. The visible grains have a subhedral fibrous/laths grain shape with straight and lobate boundaries. The grains have few to no fractures. The talc appears as an alteration product in altered orthopyroxene often found with other alteration products such as chlorite/serpentine ± clinopyroxene ± quartz. The talc content in the five samples at 155-2 is determined by the XRD analysis at IGP, and is given in Figure 63.

Clinopyroxene: Clinopyroxene is identified in all sections at 155-2. The clinopyroxene occur as an alteration product of orthopyroxene and retains the Fe-Ti-oxide lamellas found in orthopyroxene. The boundaries vary between straight and lobate. At 155-2,1 the grain size is fine grained with anhedral equant shapes. The grains are moderately to heavily fractured. At 155-2,2 the grain size is fine to very fine grained with subhedral to anhedral, equant grain shapes. The grains are moderately fractured. At 155-2,3 the grain size is fine grained with subhedral to anhedral, equant grain shapes. The grains are partially fractured. At 155-2,4 the grain size is fine to very fine grained with anhedral, equant shapes. The grains are moderately to heavily fractured. At 155-2,5 the grain size is fine to medium grained with subhedral to anhedral, equant shapes. The grains are partially to moderately fractured. The clinopyroxene content in the five samples at 155-2 is determined by the XRD analysis at Titania, and is given in Figure 63.

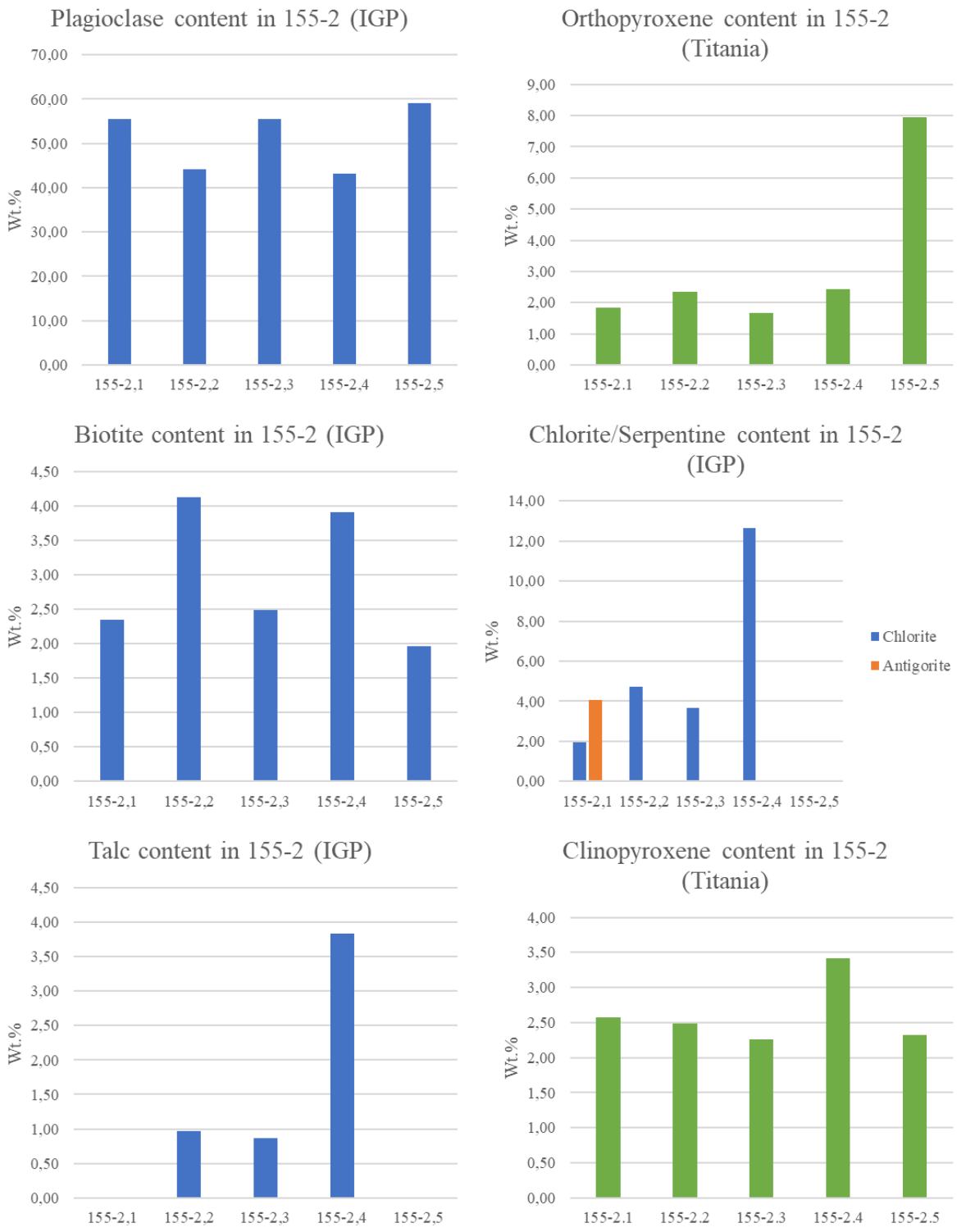

Figure 63: *The plagioclase, orthopyroxene, biotite, chlorite/serpentine, talc and clinopyroxene content in alteration zone 155-2 determined by the XRD analyses from IGP and Titania.*

Quartz: Quartz is identified in 155-2,1 and 155-2,4. The grain size is fine grained in 155-2,1 and very fine grained in 155-2,4. The grain shape is subhedral, equant and the boundaries are straight and lobate in both sections. There are a few fractures in the grains at 155-2,1 and no fractures in the grains at 155-2,4. The quartz appear primarily in 3 larger fractures in 155-2,1 together with calcite and chlorite/serpentine and in 155-2,4 it occurs as an alteration product in altered pyroxene. The quartz content in the five samples at 155-2 is determined by the XRD analysis at IGP, and is given in Figure 64.

Calcite: Calcite is only identified in section 155-2,1. The grain size is fine to very fine grained with subhedral equant grain shapes. The grains have straight and lobate borders, are moderately to heavily fractured and often lacks characteristic twinning. The appearance of the calcite is in 3 larger mineral filled fractures in association with quartz and chlorite/serpentine. The calcite content in the five samples at 155-2 is determined by the XRD analysis at IGP, and is given in Figure 64.

Muscovite: Muscovite occurs as alteration product of plagioclase in all sections at 155-2. The grain size is very fine grained with indistinguishable shapes. The muscovite is identified based on high interference colours. The muscovite content in the five samples at 155-2 is determined by the XRD analysis at IGP, and is given in Figure 64.

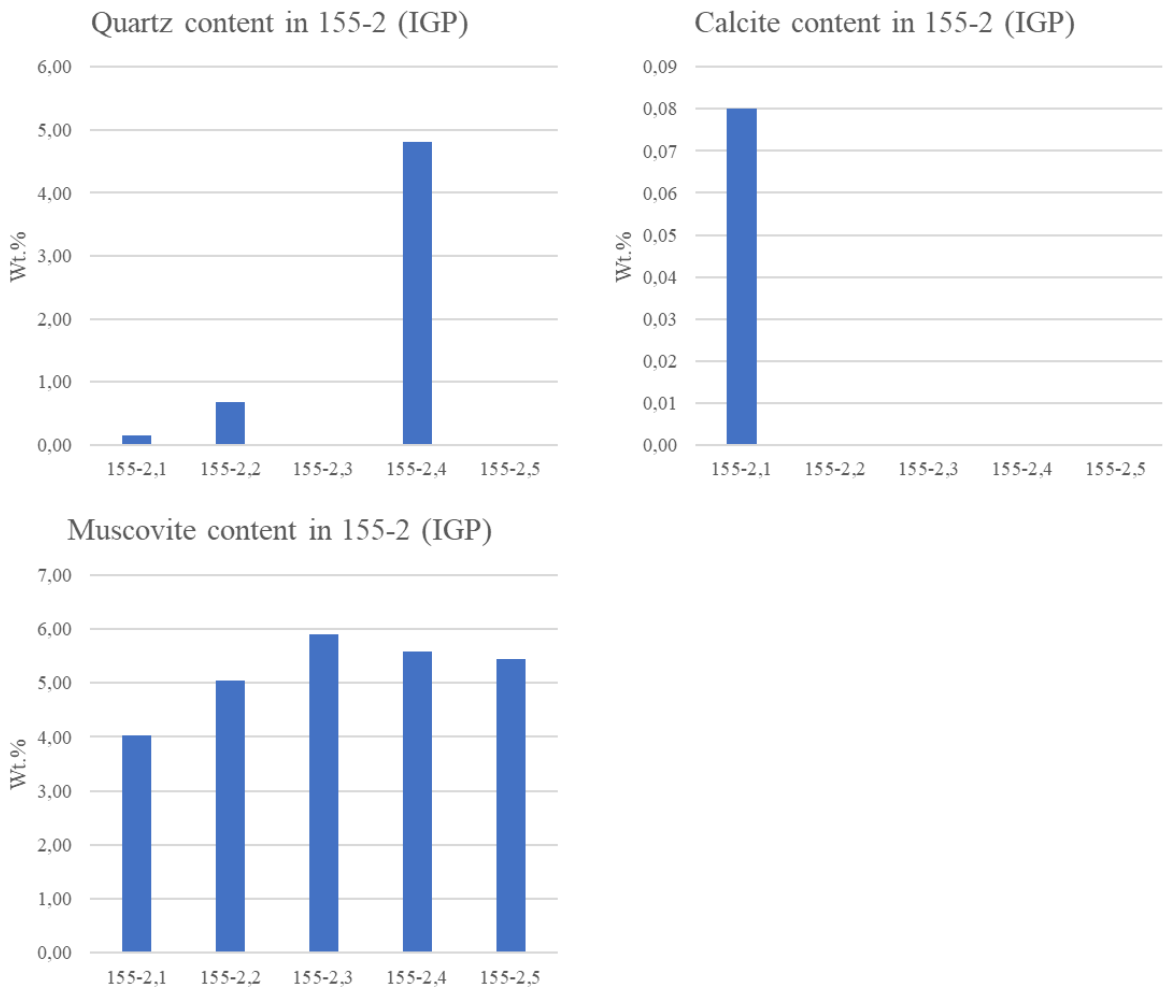

Figure 64: *The quartz, calcite and muscovite content in alteration zone 155-2 determined by the XRD analysis from IGP.*

5.4.8.2 Oxides

Ilmenite: Ilmenite occurs in all sections at 155-2. The grains have a subhedral to anhedral, equant grain shape in all sections, with straight and lobate borders. Alteration by rutile is present in all sections at varying degrees. The alteration occurs from fractures and boundaries inwards. At 155-2,1 the grain size is fine, with moderately fractured grains and are partially affected by alteration. At 155-2,2 the grain size is fine to medium, with partially fractured grains that are partially to moderately affected by alteration. At 155-2,3 the grain size is fine to medium, with partially fractured grains that are partially to moderately affected by alteration. At 155-2,4 the grain size is fine to medium, with partially to moderately fractured grains that are partially to moderately affected by alteration. At 155-2,5 the grain size is fine to medium, with partially fractured grains that are partially to moderately affected by alteration. The ilmenite occurs as inclusions in plagioclase, in aggregates with biotite and rutile, and as lamellas in orthopyroxene. The ilmenite grains contain hematite exsolution lamellas. The ilmenite content in the five samples at 155-2 is determined by the XRD analysis at IGP, and is given in Figure 65.

Rutile: Rutile is identified in all sections as an alteration product of ilmenite along grain boundaries, fractures and in grain centres. The boundaries vary between straight and lobate. The rutile occurs in aggregates with ilmenite ± biotite ± magnetite (at 155-2,4). At 155-2,1 the grain size is very fine grained with anhedral, equant grain shapes. The grains are partially fractured. At 155-2,2 the grain size is fine to very fine grained with subhedral to anhedral, equant shapes. The grains are partially fractured. At 155-2,3 the grain size is fine to very fine grained with subhedral to anhedral, equant grain shapes. The grains are partially fractured, and single grains of rutile are found sporadically throughout the section. At 155-2,4 the grain size is fine to medium grained with subhedral to anhedral, equant grain shapes. The grains are partially to moderately fractured and single grains of rutile are found sporadically throughout the section. At 155-2,5 the grain size is fine to medium grained with subhedral to anhedral, equant grain shapes. The grains are partially fractured, and single grains of rutile are found sporadically throughout the section. The rutile content in the five samples at 155-2 is determined by the XRD analysis at Titania, and is given in Figure 65.

Magnetite: Magnetite is only identified at 155-2,4 and have a fine grain size. The grains have subhedral to anhedral, equant grain shapes with boundaries that are straight and lobate. The degree of fracturing is moderate to heavy, and they often occur in aggregates with ilmenite, biotite and rutile. The magnetite content in the five samples at 155-2 is determined by the XRD analysis at IGP, and is given in Figure 65.

Hematite: Hematite occur as exsolution lamellas in ilmenite in all sections. The hematite content in the five samples at 155-2 is determined by the XRD analysis at Titania, and is given in Figure 65.

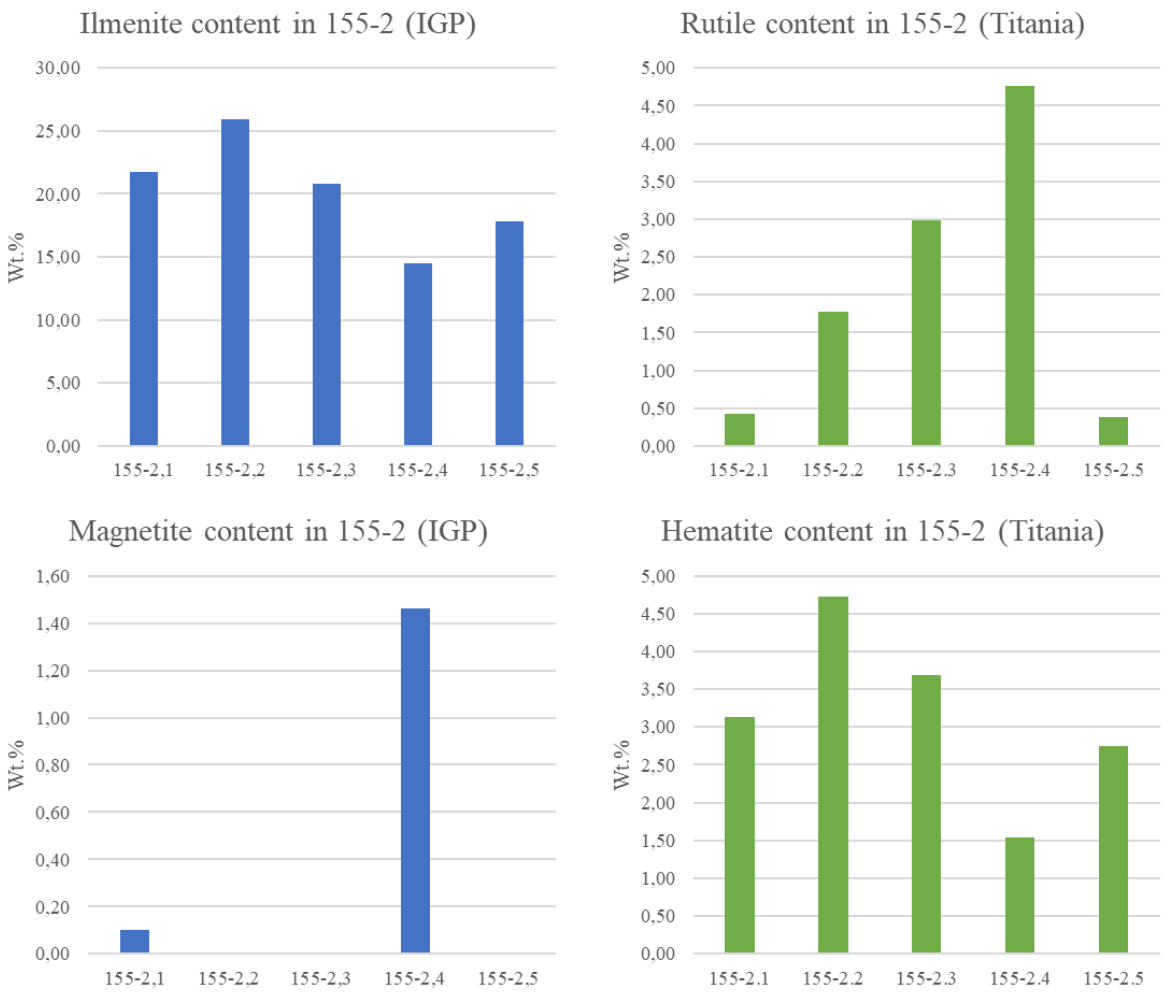

Figure 65: *The ilmenite, rutile, magnetite and hematite content in alteration zone 155-2 determined by the XRD analyses from IGP and Titania.*

5.4.8.3 Sulphides

The sulphides were not a main target during the investigation and a differentiation between different sulphide phases was not conducted. Sulphides are identified in section 155-2,2, 155-2,3 and 155-2,4. The sulphides are dominated by a pyrite phase and have a fine to very fine grain size. The grain shapes are subhedral to anhedral and equant and have straight and lobate borders. The grains are partially fractured and occurs sporadically throughout the sections. The pyrite content in the five samples at 155-2 is determined by the XRD analysis at IGP, and is given in Figure 66.

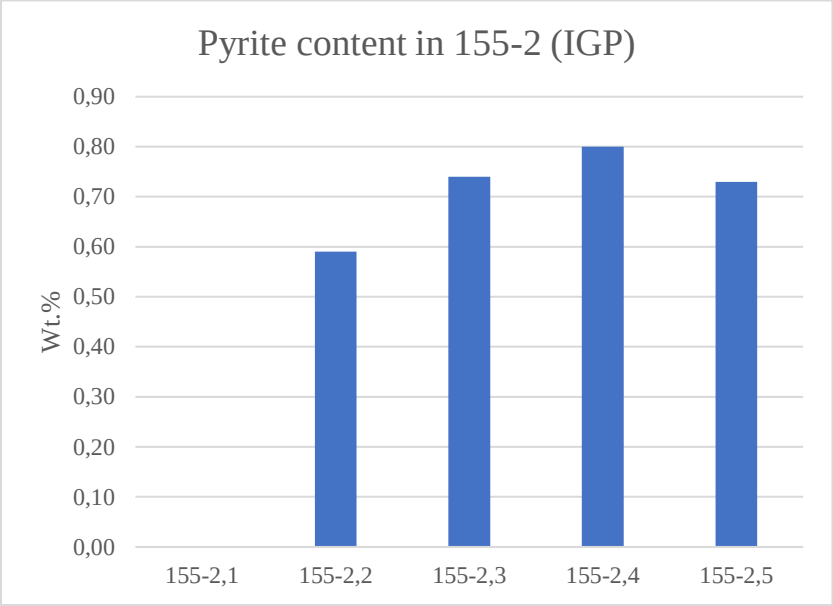

Figure 66: *The pyrite content in alteration zone 155-2. Pyrite is identified by XRD in all samples except 155-2,1 with a range from 0,59 – 0,80 Wt.%.*

5.4.8.4 Identification and quantification of additional mineral phases at AM-TEL-H-155-2

The XRD analysis at Titania identified and quantified the minerals shown in Figure 67. Some of the minerals identified by the XRD analysis were not identified in the thin sections during the optical investigation, and includes: olivine (0 – 0,23 Wt.%), apatite (0 – 0,10 Wt.%) and spinel (0,12 – 0,53 Wt.%).

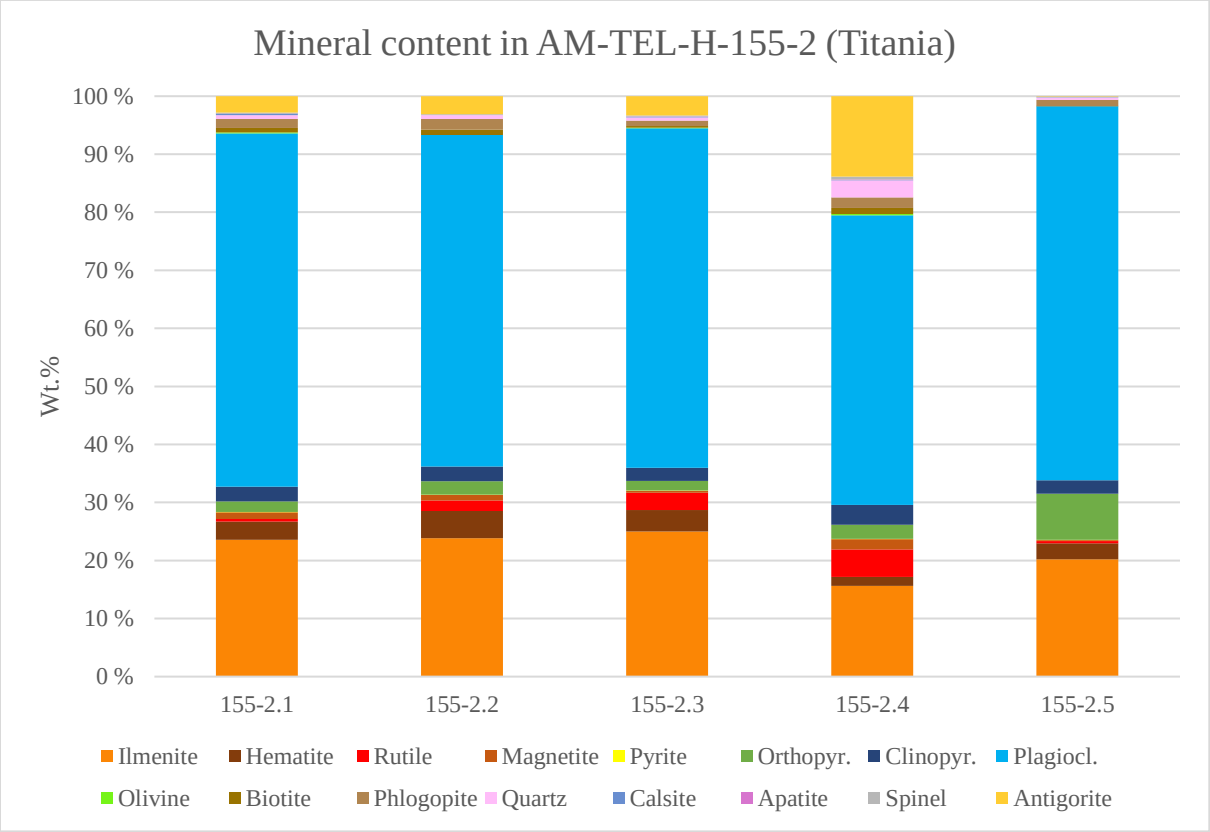

Figure 67: *The XRD analysis at Titania provided the following mineral identification and quantification for the samples in alteration zone 155-2. Mineral phases that were identified by XRD but not in the thin sections includes: olivine (0-0,23 Wt.%), apatite (0 – 0,10 Wt.%) and spinel (0,12 – 0,53 Wt.%).*

The XRD analysis at IGP identified and quantified the minerals shown in Figure 68. Mineral phases that were identified by XRD but not in the thin sections during the optical investigation includes: microcline (1,44 Wt.%) and stilbite (2,61 Wt.%). Both minerals were only identified in 155-2,1.

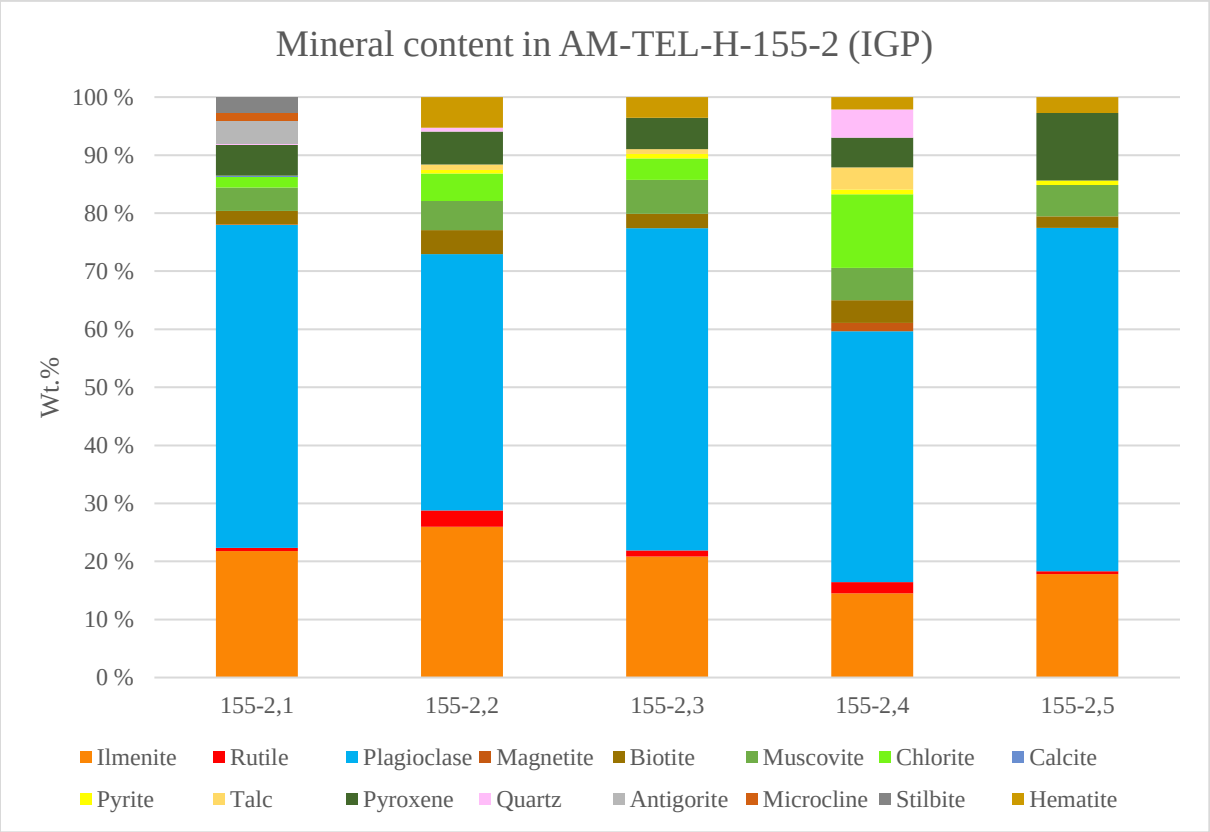

Figure 68: *The XRD analysis at IGP provided the following mineral identification and quantification for the samples in alteration zone 155-2. Mineral phases that were identified by XRD but not in thin section 155-2,1 includes: microcline (1,44 Wt.%) and stilbite (2,61 Wt.%).*

6. Discussion

6.1 Chemical content of alteration zones in the Skogestad- and Stabben area

The chemical contents of the alteration zones are, as presented in *5.2.1 Main elements (IGP)*, dominated by the main elements TiO_2, SiO_2, MgO, Na_2O, Al_2O_3, CaO and Fe_2O_3. A general description of the chemical content of alteration zones, based on the average chemical content for each main element, states that an alteration zone on average will contain 33,82 Wt.% SiO_2, 22,20 Wt.% Fe_2O_3, 14,39 Wt.% TiO_2, 11,46 Wt.% Al_2O_3, 6,60 Wt.% MgO, 4,82 Wt.% CaO and 2,02 Wt.% Na_2O.

The standard deviations for these averages give a good representation for which of the main elements that varies the most within the zones. The standard deviation establishes that the three elements that makes up most of the chemical content also have the greatest variation, with Fe_2O_3, SiO_2 and TiO_2 all having a standard deviation greater than 5 Wt.%. The elements CaO, Al_2O_3 and MgO show some variation with a standard deviation between 1,5 – 4,5 Wt.%, while the Na_2O content remains fairly stable with a standard deviation below 1 Wt.%.

Within the alteration zones the largest variation are generally observed within zones with distinct cores. This especially prominent in the zones 170-1, 185-1 and 200-1 which have the highest or among the highest standard deviations for all the main elements. This indicates a significant change in the chemical composition when moving from a core to the surrounding rock. The zones 155-1 and 170-3 which also contains distinct cores have variations comparable to the variations found in zones without distinct cores. When comparing the concentration range of TiO_2, SiO_2 and Fe_2O_3 in samples from cores with those from alteration zone centres, an interesting feature is discovered. The TiO_2 content ranges from 0,43 – 17,55 Wt.% in the cores compared to a range 11,07 – 17,50 Wt.% in the zone centres. The SiO_2 content ranges from 28,11 – 52,76 Wt.% in the cores compared to a range of 30,48 – 38,17 Wt.% in the centres. The Fe_2O_3 content ranges from 8,47 – 29,59 Wt.% in the cores compared to a range of 18,20 – 24,70 Wt.% in the centres. For the three elements the range of the samples from the centres lies within the range of the cores. This further indicates that the cores have a fairly irregular chemical composition compared to the centres which have a more stable chemical composition when moving outwards from the zone centre.

6.2 Classification of the alteration zones based on the TiO_2 content

The concentration of TiO_2 is the main controlling factor during the production of the ilmenite concentrate at Titania. When describing the ore quality, the TiO_2 concentration is prominent. Two cut-off values are prominent when classifying the ore quality: 15 Wt.% and 13 Wt.% TiO_2. The cut-off at 15 Wt.% TiO_2 is used as the lowest value for ore that enters the production line, while the cut-off at 13 Wt.% TiO_2 was established by Kullerud (2008) as the lowest TiO_2 content that is considered ore. The investigated alteration zones have a TiO_2 concentration ranging from 0,43 – 24,67 Wt.%. When comparing the investigated samples with the two cut-offs at 13 and 15 Wt.%

a classification system with three classes is established. The three classes are: (1) ore (above 15 Wt.% TiO_2), (2) ore with low potential (between 13 – 15 Wt.% TiO_2) and (3) not considered ore (below 13 Wt.% TiO_2). The 31 investigated samples classify as follows (Table 8):

Table 8: *Classification of the investigated samples based on the TiO_2 content. A sample is classified as ore when the TiO_2 content is above 15 Wt.%, a concentration between 13 and 15 Wt.% TiO_2 is classified ore with low potential, and a concentration below 13 Wt.% TiO_2 is not considered ore.*

Classification	Number of samples
Ore	18
Ore with low potential	3
Not considered ore	10

Out of the 31 investigated samples from the alteration zones 18/31 are classified as ore, 3/31 are classified as ore with low potential and 10/31 samples are not considered ore. The same classification system can be applied to the average TiO_2 content of each alteration zone giving the following classification (Table 9):

Table 9: *Classification of alteration zones based on average TiO_2 concentration. A sample is classified as ore when the TiO_2 content is above 15 Wt.% (green), a concentration between 13 and 15 Wt.% TiO_2 is classified ore with low potential (yellow), and a concentration below 13 Wt.% TiO_2 is not considered ore (red).*

	Average TiO_2 concentration (Wt.%)	Classification
AM-SKOG-H-155-1	17,33	Ore
AM-SKOG-H-170-1	12,31	Not considered ore
AM-SKOG-H-170-2	11,51	Not considered ore
AM-SKOG-H-170-3	15,27	Ore
AM-SKOG-H-185-1	13,07	Ore with low potential
AM-SKOG-H-185-2	19,27	Ore
AM-SKOG-H-200-1	10,15	Not considered ore
AM-TEL-H-155-2	13,85	Ore with low potential

Based on the classification for ore the alteration zones 155-1, 170-3 and 185-2 are classified as ore, the zones 185-1 and 155-2 are classified as ore with low potential and the alteration zones 170-1, 170-2 and 200-1 are not considered ore. The classification of the alteration zones based on requirements for TiO_2 content in ore classifies 5 out of 8 alteration zones as ore with potential for production.

6.3 Mineral characterization, content, and variation in and between alteration zones

6.3.1 Mineral characterisation, content, and variation of the primary ore minerals

Plagioclase is present in 30/31 samples from the alteration zones according to the XRD analysis at IGP, and is generally the most abundant mineral in the zones. The plagioclase contains characteristic twinning features, with examples of albite-, pericline and Carlsbad twinning occurring in most grains. Plagioclase appears primarily with four different textures: (1) medium grained, euhedral to subhedral, tabular and equant grains, (2) medium to fine grained, subhedral to anhedral, tabular and equant grains, (3) fine to medium grained, anhedral, equant grains, and (4) fine to very fine grained anhedral, equant grains. The plagioclase is affected chloritisation, serpentinisation, sericitisation, saussuritisation and kaolinisation at varying degrees altering along boundaries, fractures and within grains. The range of alteration is from none to pseudomorph. The boundaries vary from straight to lobate depending on the textural variation and the grains are often fractured at varying degrees. Some of the grains contains inclusions of ilmenite or biotite. The plagioclase content ranges from 0 – 70,40 Wt.% showing a great variation within alteration zones, but is generally between 30 – 55 Wt.%.

Ilmenite is present in 30/31 samples from the alteration zones according to the XRD analysis at IGP, often occurring in aggregates with magnetite and biotite. Ilmenite appears with three different textures: (1) fine to medium grained, subhedral to anhedral, equant grains, (2) fine to very fine grained, anhedral, equant grains, and (3) fine to medium grained, anhedral, equant grains. The grain boundaries vary from straight to lobate for all textural variations and are often fractured at varying degrees. The ilmenite is altered by rutile in most samples at varying degrees, and is altered from boundaries and fractures inwards. The alteration by rutile often forms partial or complete corona textures and in rare cases a finger like texture. The ilmenite grains appear interstitial to the other primary minerals and the grains contain acicular hematite exsolution lamellas in all sections except 185-2,3. The ilmenite content ranges from 0 – 46,73 Wt.% showing a great variation within alteration zones, but is generally between 20 – 30 Wt.%.

Orthopyroxene is present in 27/31 samples from the alteration zones according to the XRD analysis at Titania. The orthopyroxene appears primarily with four different textures: (1) near pseudomorph by alteration by talc, with very fine grained, anhedral, equant remains of orthopyroxene, (2) fine to medium grained, subhedral to anhedral, equant and tabular grains, (3) fine grained, anhedral, equant grains, and (4) fine to medium grained subhedral to euhedral, equant and prismatic grains. The orthopyroxene is often affected by alteration by talc, steatisation, and chlorite/serpentine along borders, fractures, and grain centres. Clinopyroxene grains can be found often replacing the orthopyroxene along boundaries, similarly to the clinopyroxene identified in healthy ore by Opsal (2015) and Eriksen Eia (2020). The orthopyroxene is often found with the Fe-oxide lamellas previously described by Eriksen Eia (2020). Quartz is present in grain centres of some heavily altered orthopyroxene grains. The orthopyroxene content ranges from 0 – 12,03 Wt.%, but is generally below 4 Wt.%.

Biotite is present in 30/31 samples from the alteration zones according to the XRD analysis at IGP, often occurring in aggregates with ilmenite. The biotite appears primarily with three textural variations: (1) fine grained, subhedral to anhedral, tabular, laths and equant grains, (2) fine to medium grained, euhedral to subhedral, laths, tabular and equant, and (3) fine grained, anhedral, laths and equant grains. The boundaries are mainly straight in all textural variations and the grains are generally partially fractured. The biotite appears unaltered. The biotite content ranges from 0 – 6,89 Wt.%.

Magnetite is present in 26/31 samples from the alteration zones according to the XRD analysis at IGP, often occurring in aggregates with ilmenite. The magnetite appears with two different textures: (1) fine to medium grained, subhedral to anhedral, equant grains, and (2) fine to very fine grained, anhedral, equant grains. The magnetite often has clear boundaries that varies from straight to lobate. The grains are often fractured varying from partially to very heavily fractured. The magnetite content ranges from 0 – 5,98 Wt.%.

6.3.2 Mineral characterization, content and variation of alteration minerals

Rutile is present in 30/31 samples according to the XRD analysis at Titania as the alteration product of ilmenite by rutilisation. The rutile appears with three different textures: (1) very fine to fine grained, anhedral, equant grains, (2) very fine to fine grained, anhedral to subhedral, equant grains, and (3) fine to medium grained, subhedral to anhedral, equant grains. The rutile alters the ilmenite from boundaries and fractures inwards, often forming corona like textures around the altered ilmenite (Figure 69). Rutile is also identified with a finger like texture altering into the ilmenite from fractures (Figure 69C). The rutile content ranges from 0 – 11,48 Wt.% but is generally below 3 Wt.%.

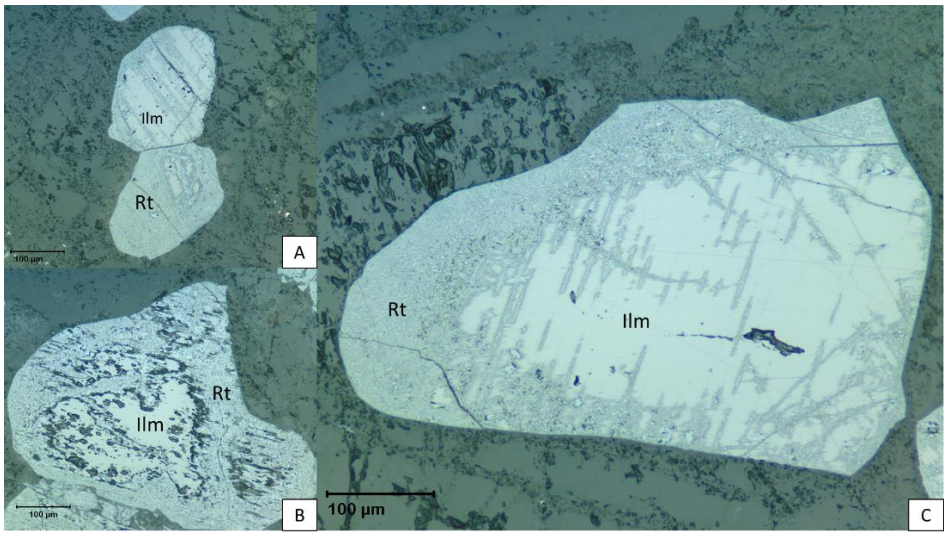

Figure 69: *Rutilisation alteration textures. (A & B) Partially and well-developed corona texture. (C) Partial corona texture and finger like textures stretching into the ilmenite from fractures and boundaries. Ilmenite (Ilm) and rutile (Rt).*

Chlorite and serpentine are occurring as alteration products of plagioclase and orthopyroxene. The chlorite and serpentine often occur in a mix where single grains are indistinguishable from each other resulting in uncertain grain size and grain shape. The mix also makes it near impossible to separate the two minerals with optical microscope. The XRD analysis at IGP managed to separate the two minerals and identified chlorite in 29/31 samples and serpentine in 15/31 samples. Some serpentine grains were identified with a fine grained, anhedral, equant/laths texture. The chlorite and serpentine have a range of 0 – 21,17 Wt.% for chlorite and 0 – 18,79 Wt.% for serpentine. Combined the two minerals make up 0 – 36,69 Wt.% of the mineral content in a sample. The presence of chlorite and serpentine confirms that chloritisation and serpentinization are alteration processes present in the alteration zones in the Skogestad- and Stabben area.

Talc is present in 27/31 samples according to the XRD analysis at IGP, and appears as one of the main alteration products of orthopyroxene. The talc appears with two textural variations: (1) very fine grained with subhedral, fibrous/laths shape, and (2) very fine to fine grained with euhedral to subhedral tabular/laths shape. The very fine-grained nature of the talc in the alteration zones often makes it difficult to distinguish single grains from each other and are therefore regarded as talc aggregates. The appearance of the talc is along boundaries, fractures and in grain centres of altered and pseudomorph orthopyroxene. The talc surrounds the Fe-oxide lamellas found in primary orthopyroxene. The mineral generally appears evenly throughout the sections with a slightly larger abundance along section cutting fractures. The talc content varies irregularly throughout the zones with a range from 0 – 17,26 Wt.%. As a result of the presence of talc in 27/31 samples, steatisation is confirmed as an alteration process in the alteration zones in the Skogestad- and Stabben area. The presence of steatisation also indicates hydrothermal conditions.

Muscovite is present in 31/31 samples according to the XRD analysis at IGP. The muscovite occurs as an alteration product of plagioclase altered by sericitisation and saussuritisation. The grain size is primarily very fine grained with indistinguishable grain shape. A few grains are identified with a fine-grained subhedral, tabular/laths texture. The muscovite is often found in cryptocrystalline aggregates formed by saussuritisation. The muscovite content ranges from 1,28 – 13,38 Wt.%, but is generally below 5 Wt.%.

Quartz is present in 27/31 samples according to the XRD analysis at IGP. The quartz appears with three textural variations: (1) fine to very fine grained, subhedral, equant grains, (2) very fine grained, anhedral, equant grains, and (3) fine grained anhedral to subhedral, equant grains. The grain boundaries vary from straight to lobate in all sections and the grains are not to partially fractured. The quartz has three ways of appearing in the sections: sporadically, as filling in larger section cutting fractures with vein texture, and in grain centres in some of the heavily altered orthopyroxene. The quartz content ranges from 0 – 23,06 Wt.%, but is generally below 3 Wt.%.

Calcite is present in 16/31 samples according to the XRD analysis at IGP. The calcite appears with three textural variations: (1) very fine to fine grained, anhedral, equant grains, (2) fine to very fine grained, subhedral, equant grains, and (3) fine grained, subhedral to anhedral, prismatic/equant grains. The boundaries vary between straight and lobate. The calcite has three ways of appearing in the sections: sporadically, as filling in larger section cutting fractures, and in thicker layers. The calcite content varies from 0 – 56,97 Wt.%, but is generally below 3 Wt.%.

Ankerite/dolomite is identified in 2/31 samples according to the XRD analysis at IGP. The ankerite/dolomite appear with two textural variations: (1) very fine grained, anhedral, equant grains, and (2) fine grained, subhedral, prismatic/equant grains. The boundaries are straight and lobate and contains few fractures. The ankerite/dolomite has two ways of appearing in the sections: sporadically, and as filling in fractures with vein like textures. The ankerite/dolomite is quantified to 1,14 Wt.% in one sample and to 19,33 Wt.% in the other sample.

Kaolinite is identified in the 7 samples analysed by AM and is not identified by the XRD due to the mineral being amorphous. The kaolinite occurs as an alteration product of plagioclase altering along boundaries, fractures and in grain centres. The kaolinite appears with one textural variation: very fine grained, anhedral, equant grains. The kaolinite content ranges from 1,15 – 21,18 Wt.% in the 7 samples, with all but one sample containing less than 4 Wt.%. The identification of kaolinite confirms that kaolinitisation occurs in the alteration zones in the Skogestad area.

6.3.3 Other minerals identified in the alteration zones

Other minerals identified in the alteration zones by optical microscope, XRD and AM include:

- Clinopyroxene
- Olivine
- Hematite
- Spinel
- Sulphides
- Hornblende
- Zoisite
- Microcline
- Siderite
- Apatite
- Stilbite
- Montmorillonite

Among these clinopyroxene, olivine, hematite, spinel and sulphides have been characterized in the results and in the optical microscope investigation, Appendix E.

6.4 Classification systems for degree of alteration

The establishment of a classification system for degree of alteration for the ore and the ilmenite are considered important steps in understanding and prevent the causes of changes in recovery during processing. The classification systems should be easily adoptable by the laboratory at Titania AS and are therefore designed to classify the ore and ilmenite based on data from the XRF- and XRD analysis.

It is important to emphasize that the suggested classification systems should be considered theoretical prototypes and should be developed further with assist from ore processing- and process mineralogy tests to enhance the practicality of the systems.

6.4.1 Classification system for degree of alteration for ore

6.4.1.1 The classification system for degree of alteration for ore

The classification system for degree of alteration for ore is designed is designed as a two-stage system. The first stage is consisting of an add-on to the TiO_2-content classification system used to determine if a rock sample is considered ore. The TiO_2- content classification system which was described in section *6.2 Classification of the alteration zones based on the TiO_2 content*, classifies samples by comparing the TiO_2 concentration in a sample to cut-off values at 13 and 15 Wt.% TiO_2, forming a system with three classes: 1) ore (above 15 Wt.% TiO_2), (2) ore with low potential (between 13 – 15 Wt.% TiO_2) and (3) not considered ore (below 13 Wt.% TiO_2).

Rutile has been identified as the main alteration product of ilmenite in the investigated alteration zones in the Skogestad- and Stabben area, similarly to the investigation of Malvik (1985) in the Tellnes area. Rutile is considered a loss to the customers, and elevated rutile levels in the concentrate will subsequently reduce the quality of the product. Ilmenite, with the ideal chemical formula $FeTiO_3$, and rutile, with the ideal chemical formula TiO_2, are the main TiO_2 consuming minerals in the ore. The amount of rutile in the ore will therefore directly impact the amount of TiO_2 which is available for ilmenite. The first stage of the classification system for alteration of ore determines if a sample is still ore after being affected by alteration. This is done by calculation the amount of TiO_2 which is available for ilmenite, and then compare the value to the cut-off values at 13 and 15 Wt.% TiO_2. The first factor is determined by subtracting the amount of rutile from the TiO_2 concentration in the ore, resulting in the following equation:

$$TiO_2\ (Wt.\%) - Rutile\ (Wt.\%) = Available\ TiO_2\ for\ ilmenite$$

The available TiO_2 for ilmenite is then compared with the cut-off values at 13 and 15 Wt.%. The samples which have more than 15 Wt.% available TiO_2 are considered ore with normal potential, the samples that contains 13 – 15 Wt.% available TiO_2 are considered ore with low potential, and the samples that contains less than 13 Wt.% available TiO_2 for ilmenite will not be considered ore.

The second stage of the classification system for alteration of ore is based on the amount of alteration products in the sample. The type of alteration mineral would also be of interest but will not be included in the system until ore processing- and process mineralogy tests are conducted to determine what/which of the alteration mineral(s) that are most crucial for the recovery of the ore.

The cut-off values of the second stage of the classification system are set at 10, 20, 30, 40 and 50 Wt.%. The cut-off values are set to give a wide description of altered ore. The decision to set the highest value at 50 Wt.% is based on the assumption that if more than 50 Wt.% of the sample is altered the quality of the ore will be too bad for production. This assumption will have to be tested with ore processing- and process mineralogy tests to ensure the validity of the assumption. From the five cut-off values a classification system with six classes of alteration is established (Table 10). The second stage of the classification system classifies the alteration of ore based on data provided by XRD analysis.

Table 10: *The classification system for degree of alteration for ore. The classification system consists of 6 classes of alteration based on the amount of alteration minerals in a sample. The cut-off values used to establish the system are set at 10, 20, 30, 40 and 50 Wt.%. Adverbs are added to describe the classes: Slightly altered (<10 Wt.%), partially altered (10-20 Wt.%), moderately altered (20-30 Wt.%), heavily altered (30-40 Wt.%), very heavily altered (40-50 Wt.%) and extremely altered (>50 Wt.%).*

<10 Wt.%	10 – 20 Wt.%	20 – 30 Wt.%	30 – 40 Wt.%	40 – 50 Wt.%	> 50 Wt.%
Slightly	Partially	Moderately	Heavily	Very heavily	Extremely

The two stages are then combined to provide a complete classification system for degree of alteration for ore.

6.4.1.2 The classification system for degree of alteration for ore applied to the investigated alteration zones

When applying the two-stage classification system for degree of alteration for ore the first stage will in this instance use the TiO_2 concentrations from the XRF analysis at IGP as this is the XRF analysis that provide the wider range and have been used previously in the project. The rutile content needed for the first stage is provided by the XRD analysis at Titania which utilizes a copper target material which was established in *3.4.1 X-ray diffraction (XRD)* as more accurate when analysing minerals that contain Ti, compared to the cobalt target material used in the analysis at IGP.

The calculations presented in Table 11 provides the first stage of the classification of the investigated samples giving the classification of the ore based on the available TiO_2 content for ilmenite. 10/31 samples are classified as ore, 5/31 are classified as ore with low potential and 16/31 samples are not considered to be ore. To determine the classification for an entire zone, the average TiO_2 and rutile values are put into the calculations. The classifications of the zones are presented in Table 12. Based on the classification only alteration zones 155-1 and 185-2 are considered ore, while the remaining six zones are not considered ore.

Table 11: *Classification of each sample based on the available TiO_2 content for ilmenite. The TiO_2 values are provided by the XRF analysis at IGP and the rutile content by the XRD analysis at Titania. Available TiO_2 content below 13 Wt.% (marked red) are not regarded as ore, available TiO_2 content between 13 and 15 Wt.% (marked yellow) are regarded as ore with low potential and available TiO_2 content above 15 Wt.% (marked green) are regarded as ore. 10/31 samples are considered ore, 5/31 are considered ore with low potential and 16/31 samples are not considered ore.*

	TiO_2 (Wt.%)	Rutile (Wt.%)	Available TiO_2 (Wt.%)	Classification
AM-SKOG-H-155-1,1	17,52	0,92	16,60	Ore
AM-SKOG-H-155-1,2	17,55	4,02	13,53	Ore with low potential
AM-SKOG-H-155-1,3	18,36	2,65	15,71	Ore
AM-SKOG-H-155-1,4	14,21	2,72	11,49	Not considered ore
AM-SKOG-H-155-1,5	19,16	0,15	19,01	Ore
AM-SKOG-H-155-1,6	17,17	0,22	16,95	Ore
AM-SKOG-H-170-1,1-1	15,43	0,40	15,03	Ore
AM-SKOG-H-170-1,1-2	6,63	2,19	4,44	Not considered ore
AM-SKOG-H-170-1,2	14,89	2,01	12,88	Not considered ore
AM-SKOG-H-170-2,1	11,07	2,05	9,02	Not considered ore
AM-SKOG-H-170-2,2	11,96	1,73	10,23	Not considered ore
AM-SKOG-H-170-3,1	12,79	11,48	1,31	Not considered ore
AM-SKOG-H-170-3,2	16,18	4,13	12,05	Not considered ore
AM-SKOG-H-170-3,3	16,84	1,83	15,01	Ore
AM-SKOG-H-185-1,1	16,48	6,56	9,92	Not considered ore
AM-SKOG-H-185-1,2	16,32	2,30	14,02	Ore with low potential
AM-SKOG-H-185-1,3	6,41	0,38	6,03	Not considered ore
AM-SKOG-H-185-2,1	19,27	4,51	14,76	Ore with low potential
AM-SKOG-H-185-2,2	17,50	1,20	16,30	Ore
AM-SKOG-H-185-2,3	15,64	9,01	6,63	Not considered ore
AM-SKOG-H-185-2,4	24,67	0,13	24,54	Ore
AM-SKOG-H-200-1,1	0,43	0,23	0,20	Not considered ore
AM-SKOG-H-200-1,2-1	17,21	0,65	16,56	Ore
AM-SKOG-H-200-1,2-2	0,69	0,00	0,69	Not considered ore
AM-SKOG-H-200-1,3	16,19	1,97	14,22	Ore with low potential
AM-SKOG-H-200-1,4	16,22	2,85	13,37	Ore with low potential
AM-TEL-H-155-2,1	12,52	0,43	12,09	Not considered ore
AM-TEL-H-155-2,2	17,26	1,78	15,48	Ore
AM-TEL-H-155-2,3	14,70	2,98	11,72	Not considered ore
AM-TEL-H-155-2,4	11,77	4,76	7,01	Not considered ore
AM-TEL-H-155-2,5	12,99	0,38	12,61	Not considered ore

Table 12: *Classification of each alteration zone based on the available TiO_2 content for ilmenite. The TiO_2 values are provided by the XRF analysis at IGP and the rutile content by the XRD analysis at Titania. Available TiO_2 content below 13 Wt.% (marked red) are not regarded as ore, available TiO_2 content between 13 and 15 Wt.% (marked yellow) are regarded as ore with low potential and available TiO_2 content above 15 Wt.% (marked green) are regarded as ore. 2/8 alteration zones are classified as ore, 0/8 alteration zones are classified as ore with low potential and 6/8 alteration zones are not considered ore.*

	Av. Rutile (Wt.%)	Av. TiO_2 (Wt.%)	Available TiO_2 (Wt.%)	Classification
AM-SKOG-H-155-1	1,78	17,33	15,55	Ore
AM-SKOG-H-170-1	1,53	12,32	10,78	Not considered ore
AM-SKOG-H-170-2	1,89	11,52	9,63	Not considered ore
AM-SKOG-H-170-3	5,81	15,27	9,46	Not considered ore
AM-SKOG-H-185-1	3,08	13,07	9,99	Not considered ore
AM-SKOG-H-185-2	3,71	19,27	15,56	Ore
AM-SKOG-H-200-1	1,14	10,15	9,01	Not considered ore
AM-TEL-H-155-2	2,07	13,85	11,78	Not considered ore

The second stage of the classification utilizes the data provided by the XRD analysis at IGP to classify the degree of alteration as this analysis has a wider mineral data base. This has resulted in a wider identification of the alteration products identified in the section and subsequently provides a more accurate quantification. The minerals that are regarded as alteration products are: rutile, muscovite, chlorite, calcite, dolomite, talc, quartz, antigorite and zoisite.

The second stage of the classification of the samples is presented in Table 13. The stage classifies 3/31 samples as slightly altered, 9/31 samples as partially altered, 9/31 samples as moderately altered, 4/31 samples as heavily altered, 2/31 samples as very heavily altered and 4/31 samples as extremely altered. To determine the classification for an entire zone, the average amount of alteration products where calculated. The classifications of the zones are presented in Table 14. Based on the classification alteration zone 155-2 is partially altered, the zones 155-1, 170-1, 170-2 and 185-2 are moderately altered, zones 185-1 and 200-1 are heavily altered and zone 170-3 is very heavily altered.

Table 13: *The second stage of the classification of degree of alteration for ore based on the amount of alteration products (Wt.%) provided by the XRD analysis at IGP. The samples are classified as slightly altered (<10 Wt.%), partially altered (10-20 Wt.%), moderately altered (20-30 Wt.%), heavily altered (30-40 Wt.%), very heavily altered (40-50 Wt.%), extremely altered (>50 Wt.%).*

	Amount of alteration products (Wt.%)	Classification
AM-SKOG-H-155-1,1	35,27	Heavily altered
AM-SKOG-H-155-1,2	35,93	Heavily altered
AM-SKOG-H-155-1,3	25,84	Moderately altered
AM-SKOG-H-155-1,4	24,86	Moderately altered
AM-SKOG-H-155-1,5	16,34	Partially altered
AM-SKOG-H-155-1,6	14,13	Partially altered
AM-SKOG-H-170-1,1-1	14,12	Partially altered
AM-SKOG-H-170-1,1-2	38,91	Heavily altered
AM-SKOG-H-170-1,2	22,36	Moderately altered
AM-SKOG-H-170-2,1	25,21	Moderately altered
AM-SKOG-H-170-2,2	22,32	Moderately altered
AM-SKOG-H-170-3,1	85,07	Extremely altered
AM-SKOG-H-170-3,2	30,51	Heavily altered
AM-SKOG-H-170-3,3	17,72	Partially altered
AM-SKOG-H-185-1,1	59,53	Extremely altered
AM-SKOG-H-185-1,2	41,37	Very heavily altered
AM-SKOG-H-185-1,3	11,36	Partially altered
AM-SKOG-H-185-2,1	27,04	Moderately altered
AM-SKOG-H-185-2,2	23,99	Moderately altered
AM-SKOG-H-185-2,3	55,69	Extremely altered
AM-SKOG-H-185-2,4	3,20	Slightly altered
AM-SKOG-H-200-1,1	48,14	Very heavily altered
AM-SKOG-H-200-1,2-1	17,66	Partially altered
AM-SKOG-H-200-1,2-2	99,39	Extremely altered
AM-SKOG-H-200-1,3	22,00	Moderately altered
AM-SKOG-H-200-1,4	9,24	Slightly altered
AM-TEL-H-155-2,1	12,27	Partially altered
AM-TEL-H-155-2,2	14,25	Partially altered
AM-TEL-H-155-2,3	11,49	Partially altered
AM-TEL-H-155-2,4	28,77	Moderately altered
AM-TEL-H-155-2,5	5,91	Slightly altered

Table 14: *The second stage of the classification of degree of alteration for ore for the investigated alteration zones. The classification is based on the average amount of alteration products (Wt.%) in the zones provided by the XRD analysis at IGP. The samples are classified as slightly altered (<10 Wt.%), partially altered (10-20 Wt.%), moderately altered (20-30 Wt.%), heavily altered (30-40 Wt.%), very heavily altered (40-50 Wt.%), extremely altered (>50 Wt.%).*

	Average amount of alteration products (Wt.%)	Classification
AM-SKOG-H-155-1	25,40	Moderately altered
AM-SKOG-H-170-1	25,13	Moderately altered
AM-SKOG-H-170-2	23,77	Moderately altered
AM-SKOG-H-170-3	44,43	Very heavily altered
AM-SKOG-H-185-1	37,42	Heavily altered
AM-SKOG-H-185-2	27,48	Moderately altered
AM-SKOG-H-200-1	39,29	Heavily altered
AM-TEL-H-155-2	14,54	Partially altered

The two classification stages are then combined to give a full assessment of the degree of alteration for the ore. The classification of degree of alteration for each sample is presented in Table 16 and the classification of degree of alteration for each zone is presented in Table 15.

Table 15: *The classification of degree of alteration for the investigated alteration zones. The classification is a combination of the two previous classification stages. The zones classified to not be considered ore in the first classification stage are reclassified as rock.*

	Classification of degree of alteration
AM-SKOG-H-155-1	Moderately altered ore
AM-SKOG-H-170-1	Moderately altered rock
AM-SKOG-H-170-2	Moderately altered rock
AM-SKOG-H-170-3	Very heavily altered rock
AM-SKOG-H-185-1	Heavily altered rock
AM-SKOG-H-185-2	Moderately altered ore
AM-SKOG-H-200-1	Heavily altered rock
AM-TEL-H-155-2	Partially altered rock

Table 16: *The classification of degree of alteration for the investigated samples. The classification is a combination of the two previous classification stages. The samples classified to not be considered ore in the first classification stage are reclassified as rock.*

	Classification of degree of alteration
AM-SKOG-H-155-1,1	Heavily altered ore
AM-SKOG-H-155-1,2	Heavily altered ore with low potential
AM-SKOG-H-155-1,3	Moderately altered ore
AM-SKOG-H-155-1,4	Moderately altered rock
AM-SKOG-H-155-1,5	Partially altered ore
AM-SKOG-H-155-1,6	Partially altered ore
AM-SKOG-H-170-1,1-1	Partially altered ore
AM-SKOG-H-170-1,1-2	Heavily altered rock
AM-SKOG-H-170-1,2	Moderately altered rock
AM-SKOG-H-170-2,1	Moderately altered rock
AM-SKOG-H-170-2,2	Moderately altered rock
AM-SKOG-H-170-3,1	Extremely altered rock
AM-SKOG-H-170-3,2	Heavily altered rock
AM-SKOG-H-170-3,3	Partially altered ore
AM-SKOG-H-185-1,1	Extremely altered rock
AM-SKOG-H-185-1,2	Very heavily altered ore with low potential
AM-SKOG-H-185-1,3	Partially altered rock
AM-SKOG-H-185-2,1	Moderately altered ore with low potential
AM-SKOG-H-185-2,2	Moderately altered ore
AM-SKOG-H-185-2,3	Extremely altered rock
AM-SKOG-H-185-2,4	Slightly altered ore
AM-SKOG-H-200-1,1	Very heavily altered rock
AM-SKOG-H-200-1,2-1	Partially altered ore
AM-SKOG-H-200-1,2-2	Extremely altered rock
AM-SKOG-H-200-1,3	Moderately altered ore with low potential
AM-SKOG-H-200-1,4	Slightly altered ore with low potential
AM-TEL-H-155-2,1	Partially altered rock
AM-TEL-H-155-2,2	Partially altered ore
AM-TEL-H-155-2,3	Partially altered rock
AM-TEL-H-155-2,4	Moderately altered rock
AM-TEL-H-155-2,5	Slightly altered rock

From the classification of degree of alteration for the samples, Table 16, the samples retrieved from the cores are classified as rock that is extremely, very heavily or heavily altered. There is one exception at 155-1,2 where the core is classified as a heavily altered ore with low potential. Moving outwards from the cores the degree of alteration gradually decrease. The state of the samples outside the cores are generally still affected to a degree that makes most of them classify as rock or ore with low potential. Alteration zone 155-1 differs from this trend and the samples retrieved just outside of the distinct cores are classified as moderately and partially altered ore. From the classification of degree of alteration for entire zones, Table 15, zone 155-1 is classified as moderately altered ore, 170-1 is classified as moderately altered rock, 170-3 is classified as very heavily altered rock, 185-1 is classified as heavily altered rock, and 200-1 is classified as heavily altered rock. This means that only 1/5 zones with distinct cores is considered interesting for production.

The zones without a distinct core show lower degrees of alteration with the zone centres classifying as moderately to partially altered with the exception of 185-2,3 which is extremely altered. Moving out from the centre the degree of alteration stays fairly stable as the degree of alteration remains at the same category or moves down one class. 185-2,3 is once again an exception as the degree of alteration goes from extremely altered rock to slightly altered ore. The minor change in the zones without cores does not necessarily mean that these zones are of higher production value as 7/11 samples in these zones are classified as rock. From the classification of degree of alteration for entire zones, Table 15, zone 170-2 is classified as moderately altered rock, 185-2 is classified as moderately altered ore, and 155-2 is classified as partially altered rock. This means that only 1/3 zones without distinct cores is considered interesting for production.

The evaluation of the alteration zones with regards to ore potential and degree of alteration classifies 2/8 zones as interesting for production. Both of these zones are classified as moderately altered ore meaning that the samples contain 20 – 30 Wt.% alteration products, but still contains enough TiO_2 to be considered interesting for production. The remaining 6 zones are altered to a degree where they only classify as rock and should not enter the production line.

6.4.2 Classification system for degree of alteration for ilmenite

6.4.2.1 Alteration of ilmenite and the classification system for degree of alteration for ilmenite

The quality of the ilmenite, and subsequently the ilmenite concentrate, depends on the degree of alteration for ilmenite. The investigations of the thin sections and XRD analyses of the alteration zones in the Skogestad- and Stabben area have found that rutile is the main alteration product of ilmenite. These results are similar to those found by Malvik (1985) in the Tellnes area. Rutile is considered a loss to the customers, and elevated rutile levels in the concentrate will subsequently reduce the quality of the product.

As the microprobe analysis of the ilmenite became limited, a detailed mapping of changes in mineral chemistry as ilmenite alters has not been conducted. The alteration of ilmenite by rutile has been identified by optical microscope and AM to occur from boundaries and fractures inwards, at times forming finger like textures that stretches into the ilmenite grains. As the alteration progresses, corona textures form around the ilmenite grains and the alteration continues inwards until the ilmenite is completely replaced by rutile. When the ilmenite alters to rutile the rutile content in the ore will gradually increase as alteration progresses. As the rutile content increases, the alteration process develops forming corona and complete replacement textures. The ratio between the two minerals could therefore give an indication for the degree of alteration for ilmenite. The quantification of the two minerals can be provided by XRD and subsequently an indicator for degree of alteration for ilmenite can be provided quickly during the mining operation.

The uppermost cut-off value is sat at a ratio of 0,2 as the rutilisation is considered to be well developed beyond this point. This is determined by the observation of well-developed corona textures and presence of singular rutile grains when the rutile/ilmenite ratio passes 0,2. Further cut-off values are set at a ratio of 0,15, 0,1 and 0,05 to provide a gradual classification system up till the critical value at 0,2. The four cut-off values provides a 5-class classification system (Table 17). The cut-off values for the rutile/ilmenite ratio is considered to be speculative and the values might be adjusted after processing- and process mineralogy tests are conducted to obtain data on the rutile content that enters the ilmenite concentrate.

Table 17: *The classification system for degree of alteration for ilmenite. The classification system consists of 5 classes of alteration based on the rutile/ilmenite ratio. The cut-off values used to establish the system are set at a ratio of 0,05, 0,1, 0,15 and 0,2. Adverbs are added to describe the classes: Slightly altered (ratio <0,05), partially altered (ratio of 0,05 – 0,1), moderately altered (ratio of 0,1 – 0,15), heavily altered (ratio of 0,15 – 0,2) and very heavily altered (ratio >0,2).*

<0,05	0,05 – 0,1	0,1 – 0,15	0,15 – 0,2	>0,2
Slightly	Partially	Moderately	Heavily	Very heavily

6.4.2.2 The classification system for degree of alteration for ilmenite applied to the investigated samples

When applying the classification system for degree of alteration to the investigated samples the XRD analysis at IGP provides the ilmenite content and the XRD analysis at Titania provides the rutile content. The classification of degree of alteration for ilmenite is calculated in Table 18.

Table 18: *The classification of degree of alteration for ilmenite in the investigated samples. The classification is based on the rutile/ilmenite ratio and the cut-off values established in Table 17.*

	Rutile/Ilmenite	Classification of degree of alteration for ilmenite
AM-SKOG-H-155-1.1	0,03	Slightly altered
AM-SKOG-H-155-1.2	0,11	Moderately altered
AM-SKOG-H-155-1.3	0,08	Partially altered
AM-SKOG-H-155-1.4	0,10	Partially altered
AM-SKOG-H-155-1.5	0,00	Slightly altered
AM-SKOG-H-155-1.6	0,01	Slightly altered
AM-SKOG-H-170-1.1-1	0,01	Slightly altered
AM-SKOG-H-170-1.1-2	0,22	Very heavily altered
AM-SKOG-H-170-1.2	0,07	Partially altered
AM-SKOG-H-170-2.1	0,09	Partially altered
AM-SKOG-H-170-2.2	0,07	Partially altered
AM-SKOG-H-170-3.1	3,84	Very heavily altered
AM-SKOG-H-170-3.2	0,13	Moderately altered
AM-SKOG-H-170-3.3	0,06	Partially altered
AM-SKOG-H-185-1.1	0,31	Very heavily altered
AM-SKOG-H-185-1.2	0,08	Partially altered
AM-SKOG-H-185-1.3	0,05	Partially altered
AM-SKOG-H-185-2.1	0,14	Moderately altered
AM-SKOG-H-185-2.2	0,04	Slightly altered
AM-SKOG-H-185-2.3	1,70	Very heavily altered
AM-SKOG-H-185-2.4	0,00	Slightly altered
AM-SKOG-H-200-1.1	N/A	Very heavily altered
AM-SKOG-H-200-1.2-1	0,02	Slightly altered
AM-SKOG-H-200-1.2-2	0,00	Slightly altered
AM-SKOG-H-200-1.3	0,06	Partially altered
AM-SKOG-H-200-1.4	0,10	Partially altered
AM-TEL-H-155-2.1	0,02	Slightly altered
AM-TEL-H-155-2.2	0,07	Partially altered
AM-TEL-H-155-2.3	0,12	Moderately altered
AM-TEL-H-155-2.4	0,30	Very heavily altered
AM-TEL-H-155-2.5	0,02	Slightly altered

Out of the 31 investigated samples, 10 are classified as slightly altered, 11 are classified as partially altered, 4 are classified as moderately altered and 6 are classified as very heavily altered. None of the samples are classified as heavily altered. At sample 200-1,1 no ilmenite is detected while the rutile is detected at 0,23 Wt.% causing a lack of a ratio. The sample is classified as very heavily altered as 100% of the Ti- oxides in the sample is rutile.

Based on this classification, the alteration zones generally contain slightly and partially altered ilmenite. The cores and zone centres are the areas that contains the ilmenite with the highest degree of alteration. The cores and zone centres contain all of the samples classified to contain very heavily altered ilmenite. The moderately altered ilmenite is also found in the cores, zone centres or in the samples right next to a core classified as very heavily altered.

6.4.3 Limitations when applying the classification systems to the investigated samples

When the classification systems have been applied to the investigated samples the classification of the individual samples are seen as a good evaluation and provides good evaluations of trends when moving from cores/centres outwards. The classification of entire zones based on average chemical and mineralogical concentrations is limited by the sampling method. It is important to emphasize that the samples are retrieved directly from mining faces, and therefore only represents the alteration zones in two dimensions. The lack of a third dimension means that no estimations of volume have been conducted. The samples are weighted equally in all calculations due to the lack of volume estimations meaning that the evaluations of the alteration zones that are based on averages are likely to overestimate reality as extreme values will have a great effect on the averages. The evaluations of ore quality of entire zones provided by this study should therefore be used as indicators rather than absolutes.

When the mining operation moves to the areas with the identified alteration zones extensive analysis of shavings from drilling should be conducted. This will provide a three-dimensional view of the extent of the alteration, and a better basis for evaluation of ore quality of the entire alteration zones.

6.5 Comparison of alteration

6.5.1 Comparison to previous investigations at Tellnes

Previous investigations of the alteration zones in the Tellnes area by Malvik (1978, 1985), Schenk (1987), Hagen (1995), and Karlsen (1997) have found multiple secondary minerals and associated alteration processes. The minerals found in the investigated alteration zones in the Skogestad- and Stabben area only contains one mineral not previously identified in the alteration zones in the Tellnes area: ankerite. Ankerite is formed during carbonate precipitation in fractures and fissures which is an alteration process previously identified in the Tellnes area. Ankerite is therefore added as one of the carbonate minerals formed during the carbonate precipitation.

Malvik (1978, 1985), Schenk (1987), Hagen (1995), and Karlsen (1997) identified saussuritisation, uralisation, sericitisation, kaolinization, steatisation, chloritisation, biotitisation, rutilisation, carbonate and quartz precipitation, alteration to clay minerals and sulphide enrichment in the alteration zones in the Tellnes area. The investigation of the alteration zones in the Skogestad- and Stabben area identified the following alteration processes: saussuritisation, sericitisation, kaolinization, steatisation, chloritisation, rutilisation, carbonate and quartz precipitation and serpentinization.

The alteration zones in the Skogestad- and Stabben area differs from the Tellnes area by the lack of uralisation and biotitisation. Biotite is identified in the alteration zones in the Skogestad- and Stabben area without showing any signs of alteration textures. The lack of evidence means that biotitisation is currently neglected as an alteration process in the investigated zones. Serpentinization has been confirmed as an alteration process in the in investigated zones unlike the zones in the Tellnes area. This might be a result of serpentines being overprinted by chlorite and talc in the Tellnes area, during chloritisation and/or steatisation, causing a camouflage effect for the evidence of serpentinisation.

The alteration zones in the Skogestad- and Stabben area does not seem to differ much from the zones previously investigated in the Tellnes area. The minerals identified in the Skogestad area, have previously been identified in the Tellnes area, with only the carbonate mineral ankerite being a new addition. With regards to alteration processes serpentinization is added as an alteration process found in the Tellnes deposit.

As the alteration zones have a similar mineralogic content to the alteration zones that previously have caused reduced recovery, the previously experienced changes in recovery when processing ore/rock from alteration zones would be expected to continue.

6.5.2 Comparison to other norite and ilmenite deposits

The altered norite found in the Skogestad- and Stabben area of the Tellnes deposit have similarities and differences to the norite found in the Sudbury Igneous Complex located in Ontario, Canada, the Archan Mayurbhanj Mafic Complex in Singhbhum Craton, India, and the Lac Des Iles Palladium Deposit in Ontario, Canada. The major difference between the alteration in the Skogestad- and Stabben area compared to the three norite complexes are the lack of uralitisation. Uralitisation is found in all three norite complexes (Bhattacharjee & Mondal, 2021; Boudreau et al., 2014; Oliver, 1951), but has not been identified as an alteration process in the Skogestad- and Stabben area. The plagioclase in the Skogestad- and Stabben area are affected by sericitisation, saussuritisation, kaolinitisation, chloritisation and serpentinisation. This is more diverse than the alteration found in the plagioclase in the other norite complexes where the Lac Des Iles Paladium deposit is the nearest with plagioclase altering from sericitisation, through saussuritisation to an almost complete replacement by choritisation (Boudreau et al., 2014). In comparison the Sudbury Igneous Complex only show saussuritisation of the plagioclase (Oliver, 1951), and the Archan Mayurbhanj Mafic Complex contains sericitisation and small amounts of chloritization (Bhattacharjee & Mondal, 2021).

The alteration of ilmenite in the Skogestad- and Stabben area of the Tellnes deposit have similarities and differences to the Lac Tio Orebody and the Manavalakurichi beach placer. The rutilisation in the Skogestad- and Stabben area are more extensive than the rutilisation found in the Lac Tio orebody where the rutile is only found as a trace mineral (Bergeron, 1980). The rutile content in the Manavalakurichi beach placer is higher on average, but local concentrations in the cores in the Skogestad area, up to 11,48 Wt.%, are higher than the 8 Wt.% found in the beach placer (Bhaskar et al., 2005). The rutile in the Lac Tio deposit is located near a main fault (Bergeron, 1980), similarly to the rutile found in the Skogestad- and Stabben area which are found near or in fractures and cores. As the Manavalakurichi beach placer is a sedimentary deposit, the appearance is incomparable to the Skogestad- and Stabben area.

The alteration zones in the Skogestad- and Stabben area have a more complex and diverse alteration content compared to the other three norite complexes indicating a more complex alteration history, but lacks evidence of uralitization. The rutile content in the alteration zones is comparable to the rutile content found in the Manavalakurichi beach placer and is more extensive than the Lac Tio deposit. The rutile appears near or in fractures in both the Lac Tio and in the Skogestad- and Stabben area.

7. Conclusions

The investigated alteration zones in the Skogestad area have a prevalence of up to ~20 m in width and are found at multiple bench levels in the open pit. The alteration zone found in the Stabben area is greater in size reaching a width of 40-50 m. A map of the alteration zones is found in Appendix G.

The mineralogical content in the alteration zones in the Skogestad- and Stabben area share many similarities with previously investigated alteration zones in the Tellnes area, with the carbonate mineral ankerite being the only new mineral identified. Alteration processes identified in the Skogestad- and Stabben area includes: sericitisation, saussuritisation, kaolinisation, steatisation, chloritisation, rutilisation, carbonate and quartz precipitation and serpentinisation, indicating a complex alteration history. The lack of evidence for uralitisation and biotitisation is the primary difference between the alteration zones in the Skogestad- and Stabben area compared to the previously investigated zones in the Tellnes area.

Among the primary ore minerals plagioclase has been identified with four textural variations, ilmenite appear with three textural variations, orthopyroxene appear with four textural variations, biotite appears with two textural variations, and magnetite appears with two textural variations. The secondary alteration minerals identified as the most prominent in the alteration zones are rutile, chlorite, serpentine, talc, muscovite, kaolinite, quartz and calcite.

Two classification systems for degree of alteration have been established, one for the degree of alteration for ore, which classifies the ore based on the amount of TiO_2 that is available for ilmenite and the amount of secondary alteration minerals in the samples, and one for the degree of alteration for ilmenite, which classifies the ilmenite based on the rutile/ilmenite ratio. The classification of the investigated alteration zones has concluded that 2 out of the 8 alteration zones can be classified as ore of interest for production, while the remaining 6 zones are altered to a state where they no longer are classified as ore.

The classification of the samples and zones have found that the degree of alteration is highest in distinct cores/fractures, and gradually decreases when moving outwards from these distinct cores. The alteration zones without such cores have a more stable degree of alteration from zone centres outwards, but the alteration is still regularly of a degree that makes the rock uninteresting for production. Rutile is confirmed to be the main alteration product of ilmenite by rutilisation. The alteration of ilmenite follows the same trend as the ore, with the highest degree of alteration being located in the cores and some zone centres while most samples found outside of these cores and centres are of a lower degree of alteration. The ilmenite in the investigated zones are generally classified as slightly – partially altered by rutile.

8. Annotations for further work

- The mineral identification library for the XRD at Titania should be expanded to include the alteration minerals identified in the alteration zones in the Skogestad- and Stabben area to provide an on-site classification of the ore during production.

- Processing tests and process mineralogy tests should be conducted on the collected material from the alteration zones to determine which of the minerals that affect the recovery, and these results should be incorporated into the systems for degree of alteration.

- As the EPMA analyses of ilmenite, talc and serpentine became limited in this study, a study which specifically targets mineral chemistry is advised.

- Further investigation of the thin sections that have not been analysed by automated mineralogy. The automated mineralogy has provided the best identification of kaolinite and the extent of kaolinitisation in the remaining samples could be of interest for Titania.

- The mapped alteration zones should be added to the modelling programs used at Titania to provide the information needed during planning of future mining operations.

- As the mining operations advance both deeper and further east in the orebody follow up mapping of the alteration zones are advised to keep the maps and models up to date.

- The alteration zones in the Tellnes deposit contains multiple alteration types and investigations with a more geological focus on origin and alteration history could be a possibility

9. References

Barstad, Å. E. E. (2020). Personal Communications on production numbers and reserves. In A. Mong (Ed.). Unpublished, E-mail communication: Barstad, Åsa E. E. (TITANIA AS Mine Geologist).

Bergeron, M. (1980). *A MINERALOGICAL STUDY OF THE HEMO-ILMENITE ORE FROM LAC TIO, QUEBEC*. É. e. R. n. Québec.

Bernhard, S., Dirk, S., & Sabine, G. (2020). SEM-Based Automated Mineralogy and Its Application in Geo- and Material Sciences. *Minerals (Basel)*, *10*(11), 1004. https://doi.org/10.3390/min10111004

Bhaskar, R. G., Rao, D. S., Vijaya Kumar, T. V., Subba Rao, S., & Prabhakar, S. (2005). Alteration characteristics of the Manavalakurichi beach placer ilmenite, Tamilnadu. *Journal of Applied Geochemistry, Vol. 7*, 195-200.

Bhattacharjee, C., & Mondal, S. K. (2021). Geochemistry of Fe-Ti oxide and sulfide minerals in gabbroic rocks and magnetitite of the Archean Mayurbhanj mafic complex (eastern India): Magma fractionation, thermometry and oxygen fugacity of re-equilibration, and implications for Ni-Cu mineralization. *Ore geology reviews*, *131*, 104005. https://doi.org/10.1016/j.oregeorev.2021.104005

Boudreau, A., Djon, L., Tchalikian, A., & Corkery, J. (2014). The Lac Des Iles Palladium Deposit, Ontario, Canada part I. The effect of variable alteration on the Offset Zone. *Mineralium deposita*, *49*(5), 625-654. https://doi.org/10.1007/s00126-014-0510-y

Carstens, H. (2002). *TITANIA i 100! Jubileumsbok for Titania A/S* (2. opplag ed.). Skipnes AS.

Charlier, B., Duchesne, J.-C., & Vander Auwera, J. (2006). Magma chamber processes in the Tellnes ilmenite deposit (Rogaland Anorthosite Province, SW Norway) and the formation of Fe–Ti ores in massif-type anorthosites. *Chemical Geology*, *234*(3-4), 264-290.

Charlier, B., Skår, Ø., Korneliussen, A., Duchesne, J.-C., & Vander Auwera, J. (2007). Ilmenite composition in the Tellnes Fe–Ti deposit, SW Norway: fractional crystallization, postcumulus evolution and ilmenite–zircon relation. *Contributions to mineralogy and petrology*, *154*(2), 119-134. https://doi.org/10.1007/s00410-007-0186-8

Demaiffe, D., & Hertogen, J. (1981). Rare earth element geochemistry and strontium isotopic composition of a massif-type anorthositic-charnockitic body: the Hidra Massif (Rogaland, SW Norway). *Geochimica et cosmochimica acta*, *45*(9), 1545,1553-1551,1561. https://doi.org/10.1016/0016-7037(81)90284-2

Diot, H., Bolle, O., Lambert, J.-M., Launeau, P., & Duchesne, J.-C. (2003). The Tellnes ilmenite deposit (Rogaland, South Norway): magnetic and petrofabric evidence for emplacement of a Ti-enriched noritic crystal mush in a fracture zone. *Journal of structural geology*, *25*(4), 481-501. https://doi.org/10.1016/S0191-8141(02)00050-0

DMF. (2021). *Kart - Aktsomhetskart, Bergrettigheter, Rapporter, Uttaksregister*. https://minit.dirmin.no/kart/, Direktoratet for Mineralforvaltning.Retrieved 04.05.2021 from https://minit.dirmin.no/kart/

Duchesne, J.-C. (2001). *The Rogaland intrusive massifs: an excursion guide*. Norway, Trondheim : NGU.

Duchesne, J. C. (1999). Fe-Ti deposits in Rogaland anorthosites (South Norway): geochemical characteristics and problems of interpretation. *Mineralium Deposita*, *34*(2), 182-198. https://doi.org/10.1007/s001260050195

Duchesne, J. C., Wilmart, E., Demaiffe, D., & Hertogen, J. (1989). Monzonorites from Rogaland (Southwest Norway): a series of rocks coeval but not comagmatic with massif-type anorthosites. *Precambrian research*, *45*(1), 111-128. https://doi.org/10.1016/0301-9268(89)90034-X

Dutrow, B. L., & Clark, C. M. (n.d.). *X-ray Powder Diffraction (XRD)*. The Science Education Resource Center. Retrieved 24.03.2021 from https://serc.carleton.edu/research_education/geochemsheets/techniques/XRD.html

Dybdahl, I. (1960). Ilmenite deposits of the Egersund anorthosite complex, in Mines in south and central Norway. *Int. Geol. Congr, 21st*(Guidebook Field Excursion C-10), 48-53.
Eriksen Eia, K. (2020). *Characterisation of pyroxene and olivine in the Tellnes deposit*

With focus on types, occurances and physical properties for separation Norwegian University of Science and Technology].
Gierth, E., & Krause, H. (1973). *Die Ilmenitlagerstätte Tellnes (Süd-Norwegen). Norsk Geologisk Tidsskrift, 53*, 359-402.
Gray, I. E., & Reid, A. F. (1975). The Structure of Pseudorutile and Its Role in

The Natural Alteration of llmenite. *American Mineralogist, 60*, 898-906.
Hagen, R. (1995). *Tellnesmalmen - en geologisk vurdering av omvandlinger og utvinning.*
Harlov, D. (2013). *Metasomatism and the Chemical Transformation of Rock : The Role of Fluids in Terrestrial and Extraterrestrial Processes* (H. Austrheim, Ed. 1st ed. 2013. ed.). Springer Berlin Heidelberg : Imprint: Springer.
Hékinian, R. (1982). Chapter 11 Deuteric Alteration. *Petrology of the ocean floor, 33*, 329-331. https://doi.org/10.1016/S0422-9894(08)70953-X

info:doi/10.1016/S0422-9894(08)70953-X (Petrology of the Ocean Floor)
Janssen, A., Geisler-Wierwille, T., Putins, A., & Putins, C. V. (2010). The experimental replacement of ilmenite by rutile in HCl solutions. *Mineralogical Magazine, 74*, 633-644.
Karlsen, T. A. (1997). *Geometry of fracture zones and their influence on the ore quality at the Tellnes ilmenite mine, Rogaland*. (Unpublished report for Titania AS)
Karlsen, T. A., Furuhaug, L., & Korneliussen, A. (2000). *Oppfølgende struktur-målinger i Tellnes-bruddet, Rogaland*. (Unpublished report for Titania AS)
King, H. M. (n.d). *Ilmenite. A black iron titanium oxide mineral. The primary ore of titanium, source of titanium dioxide.* Geology.com Geoscience News and Information. Retrieved 15.02.2021 from https://geology.com/minerals/ilmenite.shtml
Kovalev, A. A., Tishchenko, L. A., Shashurin, V. D., & Galinovskii, A. L. (2017). Application of X-ray Diffraction Methods to Studying Materials. *Russian metallurgy Metally, 2017*(13), 1186-1193. https://doi.org/10.1134/S0036029517130110
Krause, H., Gierth, E., & Schott, W. (1985). *Ti-Fe Deposits in the South Rogaland Igneous Complex, with Special Reference to the Åna-Sira Anorthosite Massif. Norges geologiske undersøkelse Bulletin, 402*, 25-37.
Krause, H., & Pedall, G. (1980). *Fe-Ti-Mineralizations in the Åna-Sira Anorthosite, Southern Norway* (1547).
Krause, H., & Zeino-Mahmalat, R. (1970). *Untersuchungen an erz und Nebengestein der Grube Blåfjell in SW-Norwegen*. *Norsk Geologisk Tidsskrift, 50*(1), 45-88.
Kullerud, K. (2003). *Geochemistry and mineralogy of the Tellnes ilmenite ore body*. *Norges geologiske undersøkelse, Special publication 9*, 70.
Kullerud, K. (2005). *Cr2O3 og MgO-innhold i ilmenitt fra Tellnesmalmen - oppfølging av tidligere arbeider*. (Unpublished report for Titania AS)
Kullerud, K. (2007). *Compositional variations of the Tellnes ore in the Skogestad area*. (Unpublished report for Titania AS)
Kullerud, K. (2008). *Kjemiske variasjoner i malmen i Skogestadområdet*. (Unpublished report for Titania AS)
Maijer, C., Padget, P., & Provinces, N. A. S. I. o. t. D. P. C. t. N. A. (1987). *The Geology of southernmost Norway : an excursion guide : a geological excursion guide with thematic articles prepared for the NATO Advanced Study Institute Meeting held at Moi, Norway, 1984* (Vol. 1).
Malvik, T. (1978). *Investigation of minerals in filled joints and zones of weakness in the Telnes ore*. (Unpublished report for Titania AS)

Malvik, T. (1985). *Rutilization of ilmenite. Microscopic investigation.* (Unpublished report for Titania AS)
Mos, Y. M., Vermeulen, A. C., Buisman, C. J. N., & Weijma, J. (2018). X-Ray Diffraction of Iron Containing Samples: The Importance of a Suitable Configuration. *Geomicrobiology journal*, *35*(6), 511-517. https://doi.org/10.1080/01490451.2017.1401183
Mücke, A., & Bhadra Chaudhuri, J. N. (1991). The continuous alteration of ilmenite through pseudorutile to leucoxene. *Ore geology reviews*, *6*(1), 25-44. https://doi.org/10.1016/0169-1368(91)90030-B
Nesse, W. D. (2012a). *Introduction to mineralogy* (Second edition ed.). Oxford University Press.
Nesse, W. D. (2012b). Talc. In *Introduction to mineralogy* (Second edition ed., pp. 273-274). Oxford University Press.
Oliver, T. A. (1951). The effect of uralitization upon the chemical composition of the Sudbury norite. *American Mineralogist*, *36*, 421-429.
Opsal, E. (2015). *Sammenheng mellom kjemiske variasjoner hos malm og mineraler i Skogestadmalmen, Tellnes* UiT - Norges Arktiske Univeristet].
Pedro, W., William, R. H., Jonas, T., Julie, A. H., Christopher, L. K., Carson, K., Chris, Y., Nicholas, J. G., David, Z., Hugo, K. H. O., Peter, C. L., & Kristoffer, S. (2020). Geodynamic Implications of Synchronous Norite and TTG Formation in the 3 Ga Maniitsoq Norite Belt, West Greenland. *Frontiers in earth science (Lausanne)*, *8*. https://doi.org/10.3389/feart.2020.562062
Pinti, D. L. (2011). Serpentinization. *Encyclopedia of Astrobiology*, 1504-1504. https://doi.org/https://doi.org/10.1007/978-3-642-11274-4_1430
Proto. (2021). *Unmasking Microabsorption: Why Fluorescence Suppression in Powder XRD Does More Harm Than Good*. AZoM. Retrieved 03.05.2021 from https://www.azom.com/article.aspx?ArticleID=20003
Schenk, M. (1987). *Alteration effects on ilmenite-norite along faults and fracture zones in the Tellnes open pit area*. (Unpublished report for Titania AS)
Schiellerup, H., Korneliussen, A., Heldal, T., Marker, M., Bjerkgård, T., & Nilsson, L.-p. (2003). *Mineral resources in the Rogaland Anorthosite Province, South Norway: origins, history and recent developments*. *Norges geologiske undersøkelse, Special Publication 9*, 117-122.
Schärer, U., Wilmart, E., & Duchesne, J.-C. (1996). The short duration and anorogenic character of anorthosite magmatism: U Pb dating of the Rogaland complex, Norway. *Earth and planetary science letters*, *139*(3), 335-350. https://doi.org/10.1016/0012-821X(96)00033-7
Streckeisen, A. (1974). Classification and nomenclature of plutonic rocks recommendations of the IUGS subcommission on the systematics of Igneous Rocks. *Geologische Rundschau*, *63*, 773-786. https://doi.org/https://doi.org/10.1007/BF01820841
Strekeisen, A. (n.d-a). *Norite*. Retrieved 12.02.2021 from http://www.alexstrekeisen.it/english/pluto/norite.php
Strekeisen, A. (n.d-b). *Talc - $Mg_3Si_4O_{10}(OH)_2$*. Alex Strekeisen. Retrieved 25.06.21 from https://www.alexstrekeisen.it/english/meta/talc.php
Temple, A. K. (1966). Alteration of ilmenite. *Economic geology and the bulletin of the Society of Economic Geologists*, *61*(4), 695-714. https://doi.org/10.2113/gsecongeo.61.4.695
Wengorsch, T., Beinlich, A., Grguric, B., & Puntis, A. (2019). *Experimental Alteration in Composite Mineral Systems: Mg-silicates, Fe-Ni-sulphides and Fe-Ti-oxides* Curtin University]. Perth.
Wilmart, E., Demaiffe, D., & Duchesne, J. C. (1989). Geochemical constraints on the genesis of the Tellnes ilmenite deposit, Southwest Norway. *Economic geology and the bulletin of the Society of Economic Geologists*, *84*(5), 1047-1056. https://doi.org/10.2113/gsecongeo.84.5.1047
Winter, J. D. (2010). *An introduction to igneous and metamorphic petrology* (2nd ed. ed.). Prentice Hall.
Zeino-Mahmalat, R., & Krause, H. (1976). *Plagioklase im anorthosit-komplex von Åna-Sira, SW-Norwegen. Petrologische und chemische untersuchungen*. *Norsk Geologisk Tidsskrift*, *56*, 51-94.

10. Appendixes

The appendixes are provided in a separate folder delivered together with the thesis. The appendixes are named and organized as follows:

Appendix A Thin section scans

Appendix B XRF analyses

Appendix C XRD analyses

Appendix D Automated mineralogy

Appendix E Optical thin section description

Appendix F EPMA data

Appendix G Map of the investigated alteration zones

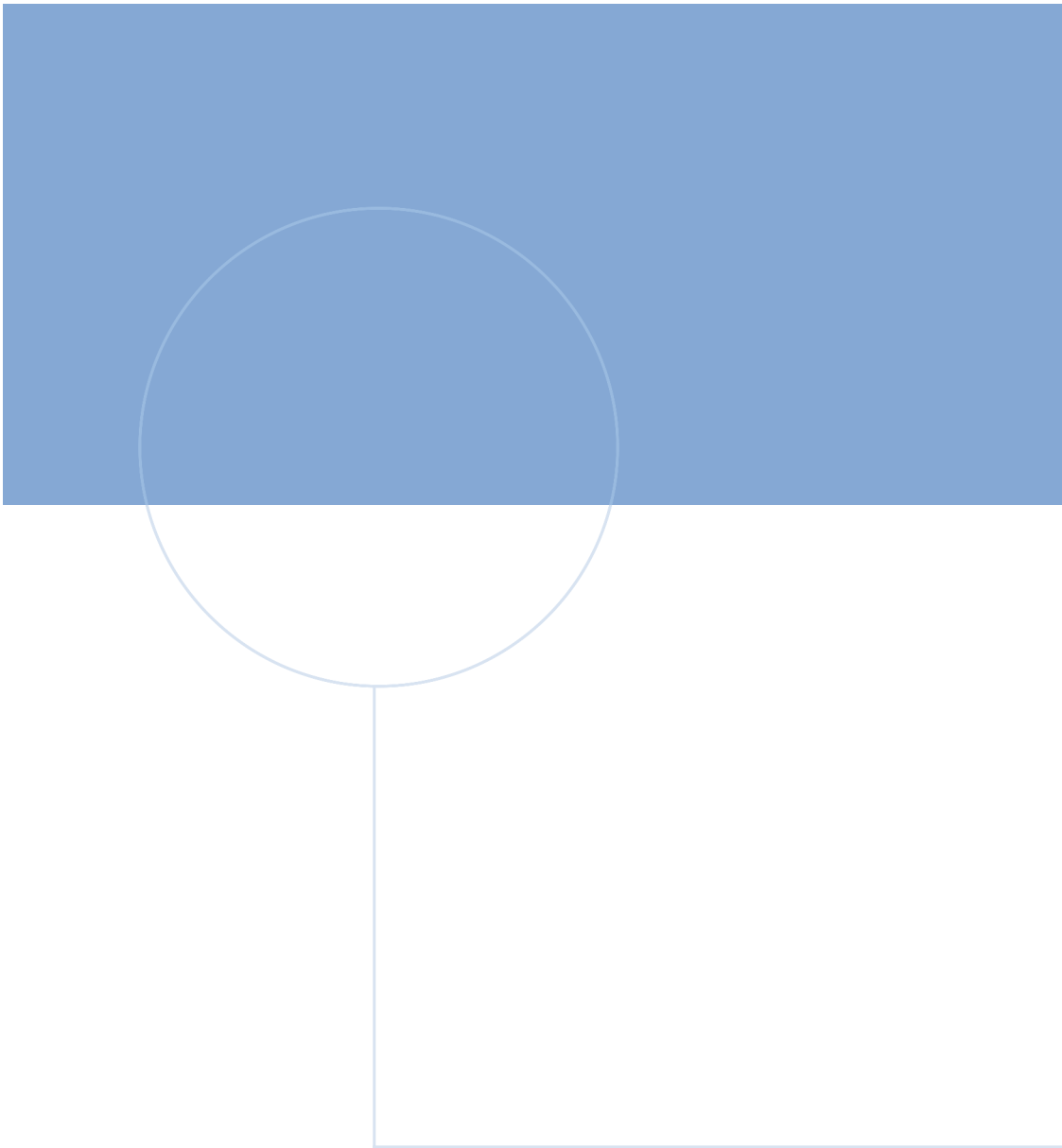

NTNU
Norwegian University of
Science and Technology

TITANIA
- a KRONOS Company